Synthesis of ganglioside and lysoganglioside lipoforms as internal standards for MS quantification

---

Dissertation

zur

Erlangung des Doktorgrades (Dr. rer. nat.)

der

Mathematisch-Naturwissenschaftlichen Fakultät

der

Rheinischen Friedrich-Wilhelms-Universität Bonn

vorgelegt

von

Dipl.-Chem. Martin Gantner

aus

Eckenhagen

Bonn, September 2014

Die vorliegende Arbeit wurde in der Zeit von September 2010 bis September 2014 unter der Leitung von Priv.-Doz. Dr. Thomas Kolter am Kekulé-Institut für Organische Chemie und Biochemie der Universität Bonn angefertigt.

Angefertigt mit Genehmigung der Mathematisch-Naturwissenschaftlichen Fakultät der Rheinischen Friedrich-Wilhelms-Universität Bonn

1. Referent: Priv.-Doz. Dr. Thomas Kolter
2. Referent: Prof. Dr. Dirk Menche
3. Referent: Prof. Dr. Ulrich Kubitscheck
4. Referent: Priv.-Doz. Dr. Gerhild van Echten-Deckert

Tag der Promotion: 10.12.2014

Erscheinungsjahr: 2015

Mein besonderer Dank geht an Herrn *Privatdozent Dr. Thomas Kolter* für die Ermöglichung, Förderung und angenehme Betreuung der Arbeit.

Herrn *Professor Dr. Konrad Sandhoff* danke ich für die Förderung und freundliche Unterstützung der Arbeit.

Herrn *Dr. Günter Schwarzmann* danke ich für seine freundliche Unterstützung der Arbeit und für viele anregende Fachgespräche.

Frau *Dr. Bernadette Breiden* danke ich für ihre freundliche Unterstützung der Arbeit und für viele anregende Fachgespräche.

Herrn *Professor Dr. Christoph Thiele* und der NRW International Graduate Research School LIMES Chemical Biology danke ich für die finanzielle Förderung der Arbeit

Folgenden Mitarbeitern danke ich herzlich für ihre Beiträge zu dieser Arbeit:

NMR-Spektroskopie:	*Herr Claus Schmidt, Frau Karin Prochnicki*
Massenspektrometrie:	*Frau Dipl.-Ing. Heike Hupfer*
Elementaranalyse:	*Frau Anne Martens*
GC-MS-Analyse:	*Frau Lilly Hofmann*
FID-Analysen:	*Frau M. Sc. Katharina vom Dorp, Herr B. Sc. Adrian Semeniuk*
CerS4-*(-/-)*-Mäuse:	*Frau Dr. Christina Ginkel, Herr M. Sc. Andreas Bickert, Herr M. Sc. Philipp Ebel*

Allen Laborkollegen und Mitarbeitern des Arbeitskreises Sandhoff, insbesondere *Herrn Dr. Radwan Hameed*, *Herrn Dipl.-Chem. Vincent Oninla* und *Frau Dr. Heike Schulze*, danke ich für das angenehme Arbeitsklima und so manchen Ratschlag.

Weiterhin danke ich meiner Familie und meinen Freunden, insbesondere *Peter Gantner*, *Marta Gantner*, *Julia Gantner*, *Rosemarie Gantner, Siegmund Hering*, *Ella Kempel, Thorsten Röser*, *Dipl.-Phys. Henning Schories* und *Diplom Japanologin Gudrun Franzen*.

Publications:

Gantner M., Schwarzmann G., Sandhoff K., and Kolter T. 2014. Partial synthesis of ganglioside and lysoganglioside lipoforms as internal standards for MS quantification. (J. Lip. Res., submitted).

List of abbreviations

ABC	ATP binding cassette
ATP	adenosine triphosphate
BMP	bis(monoacylglycero)phosphate
BODIPY	boron dipyrromethene
Cer	ceramide
CerS	ceramide synthase
CERT	ceramide transfer protein
CID	collision-induced dissociation
CMP	cytidine monophosphate
CNS	central nervous system
CoA	coenzyme A
CV	column volume
DCC	*N,N'*-dicyclohexylcarbodiimide
DEAE-	diethylaminoethyl-
Des1	dihydroceramide desaturase
DESI	desorption electrospray ionization
DKO	double knockout
DPH	diphenyl-1,3,5-hexatrienyl
EGFR	epidermal growth factor receptor
ER	endoplasmic reticulum
ESI	electrospray ionization
Fig	figure
Fmoc	9-fluorenylmethoxycarbonyl
FRET	Förster resonance energy transfer
GalCer	galactosylceramide
GalNAcT	*N*-acetylgalactosaminyltransferase
GalT	galactosyltransferase
GC-FID	gas chromatography with flame ionization detector
GC-MS	gas chromatography-mass spectrometry
Gg	Gal*β*1-3GalNAc*β*1-4Gal*β*1-4-Glc-
GlcCer	glucosylceramide

GPI	glycosylphosphatidylinositol
GSL	glycosphingolipid
HDL	high density lipoprotein
HIV	human immunodeficiency virus
HPLC	high-performance liquid chromatography
HSAN	hereditary sensory and autonomic neuropathy
IR	insulin receptor
IUPAC-IUBMB	international union of pure and applied chemistry and international union of biochemistry and molecular biology
Kdn	2-keto-3-deoxy-nononic acid
KO	knockout
LacCer	lactosylceramide
LBSA	lipid-bound sialic acid
LC-MS	liquid chromatography-mass spectrometry
LDL	low density lipoprotein
MAG	myelin-associated glycoprotein
MALDI	matrix-assisted laser desorption/ionization
MRM	multiple reaction monitoring
MS	mass spectrometer, mass spectrometry
NADPH	nicotinamide adenine dinucleotide phosphate, reduced form
NANA	*N*-acetylneuraminic acid
NBD	7-nitro-2,1,3-benzooxadiazol-4-yl
NCX	Na^+/Ca^{2+}-exchanger
NE	nuclear envelope
Neu1	*N*-acetyl-alpha-neuraminidase-1
Neu5Ac	*N*-acetylneuraminic acid
Neu5Gc	*N*-glycolylneuraminic acid
NGNA	*N*-glycolylneuraminic acid
NP	normal-phase
NPC1	Niemann-Pick C1
NR	Nile Red

RP	reversed-phase
RT	room temperature
Sap	saposin
SCDase	sphingolipid ceramide *N*-deacylase
Siglec	sialic-acid-binding immunoglobulin-like lectin
SIM	selected ion monitoring
SIMS	secondary ion mass spectrometry
SM	sphingomyelin
SPTLC1	serine palmitoyltransferase, long chain base subunit 1
SRM	selected reaction monitoring
ST	sialyltransferase
STED	stimulated emission depletion far-field fluorescence nanoscopy
TLC	thin layer chromatography
TNF-α	tumor necrosis factor alpha
TUP	theoretical upper phase
UDP	uridine diphosphate
v/v	volume ratio
VEGF	vascular endothelial growth factor
VLDL	very low density lipoprotein
wt%	weight percent

Table of Contents

1 Summary

Gangliosides are sialic acid-containing glycosphingolipids (GSLs), which are especially abundant in the brain of vertebrates. The precise function of the complex patterns of brain gangliosides including the role of different alkyl chain lengths within the lipid part is not known.

Quantification of gangliosides is usually achieved by staining after chromatographic separation, most often by thin layer chromatography and subsequent densitometric analysis (1, 2). These procedures are usually not suitable for the determination of different lipoforms of a given ganglioside.

Within recent years, ganglioside patterns have been increasingly analyzed by mass spectrometry (section 2.2.3). Due to the lack of suitable standard substances for internal calibration, MS gives no reliable information on the amount of complex gangliosides in samples of biological origin: Standard substances are only available for gangliosides GM1, GM2, and GM3 (Fig. 1.1).

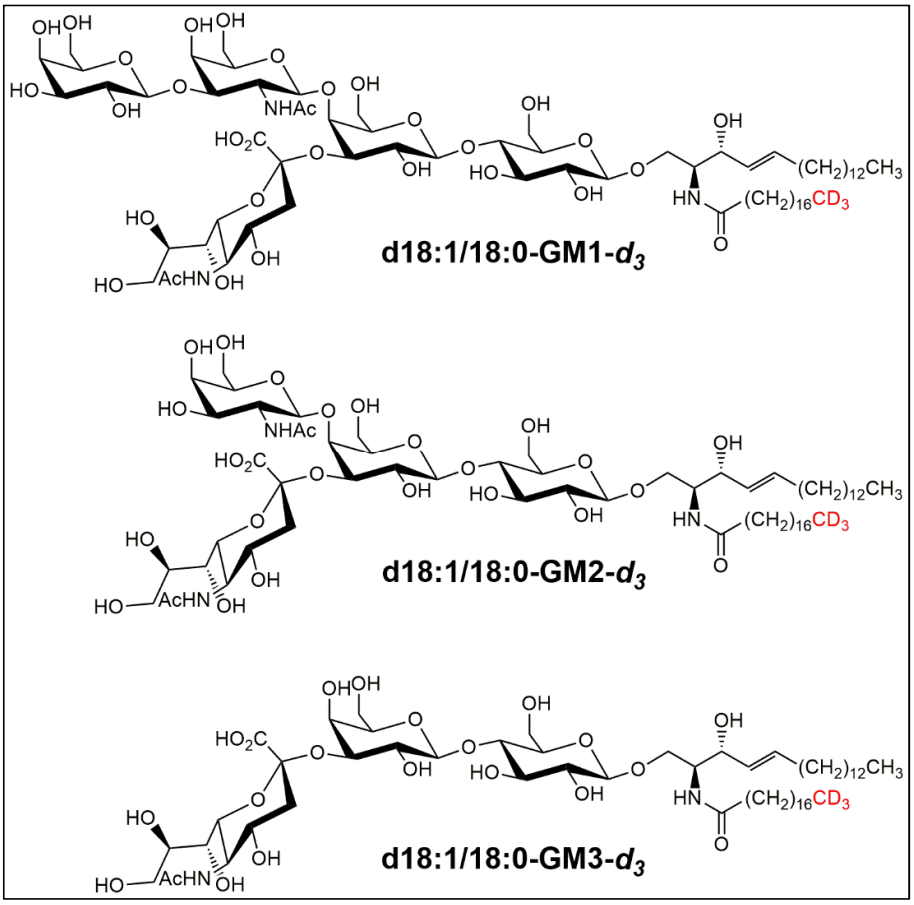

Fig. 1.1: *Internal ganglioside standards that are commercially available (3).*

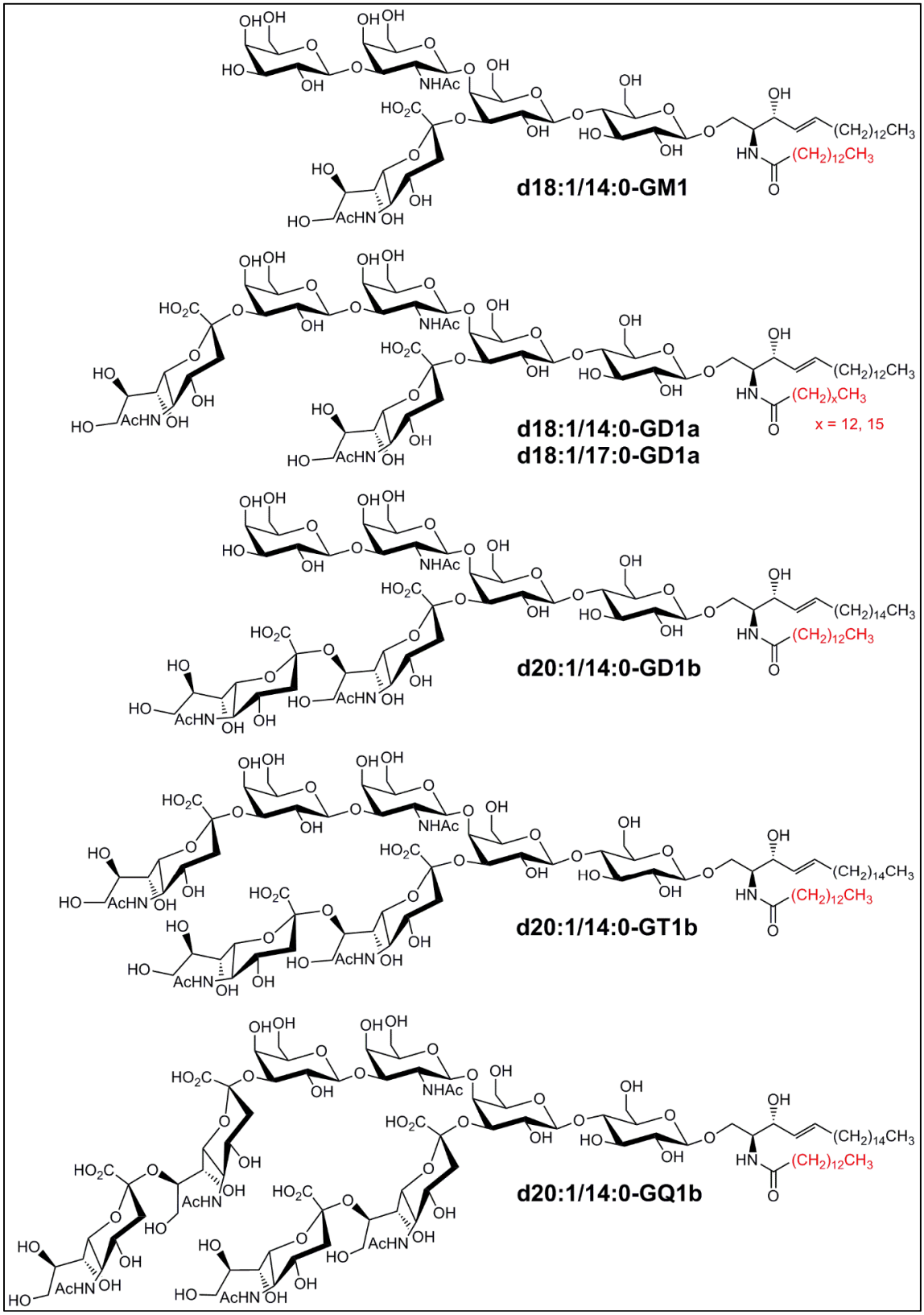

Fig. 1.2: *Internal ganglioside standards of the major brain gangliosides.*

The goal of this work was to establish methods for the synthesis of modified gangliosides that are suitable as internal standards for mass spectrometry. During this work the following structural analogs of brain gangliosides have been prepared from mixtures of bovine brain gangliosides (Fig. 1.2).

Also standard substances for the tumor-associated gangliosides GM2 and GD2 have been prepared (Fig. 1.3). They are important targets for immunotherapy because they are highly expressed on human tumors of neuroectodermal origin while they are only minor gangliosides in healthy tissue (4, 5). Furthermore, the quantification of GM2 is of interest in lysosomal storage diseases (section 2.2.3).

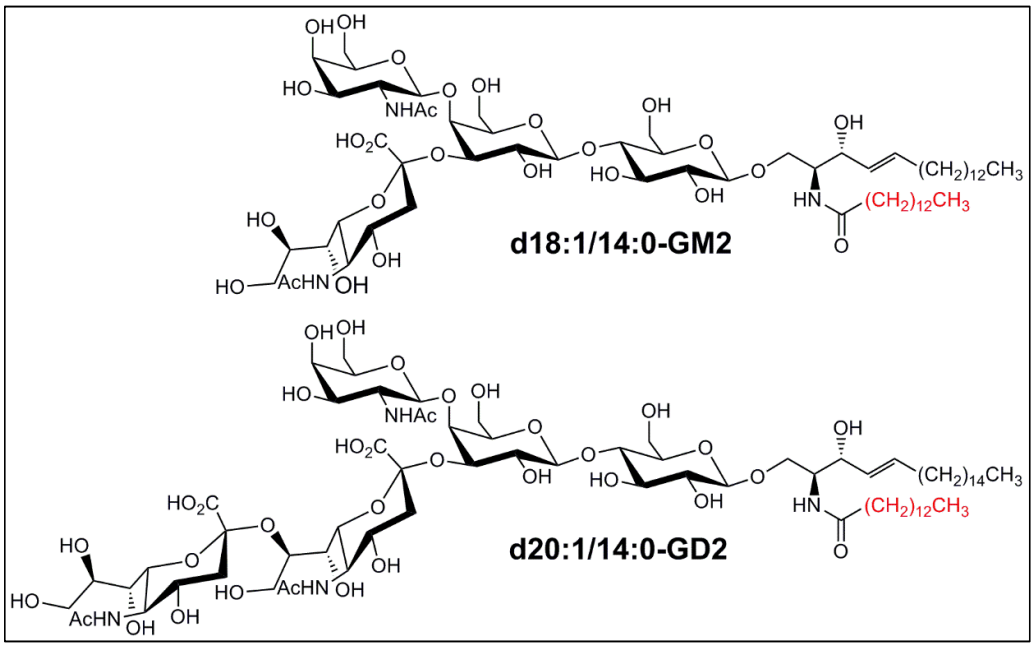

Fig. 1.3: *Internal standards of GM2 and GD2.*

In addition, a method based on an olefin metathesis has been established that is suitable for the synthesis of modified lysogangliosides. By this, non-natural lipoforms have been prepared that are suitable as internal standards for lyso-GM1 and lyso-GM2.

Currently, the standard substances are applied for the analysis of the brains of genetically engineered mice with deficiency of ceramide synthase 4 (CerS4).

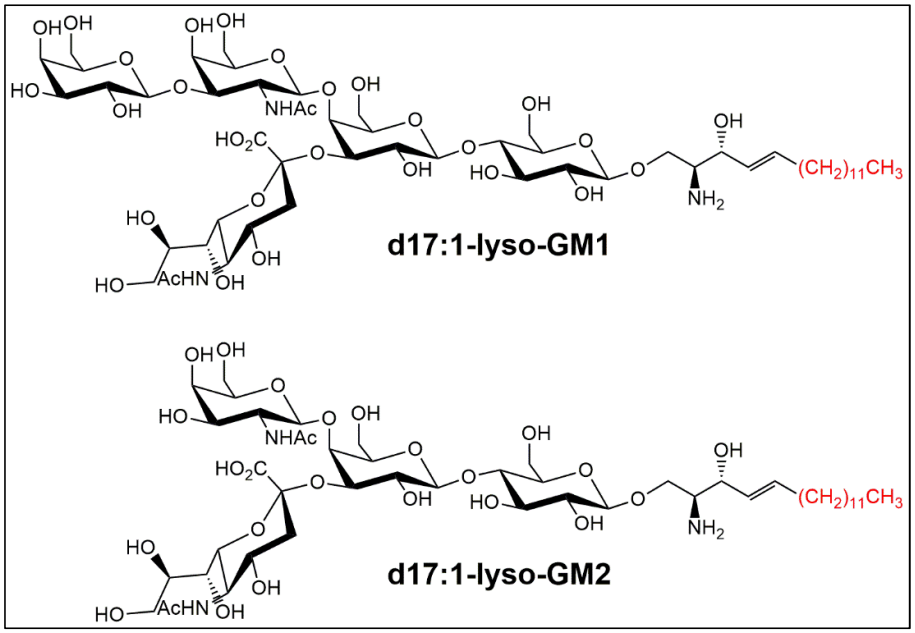

Fig. 1.4: *Internal standards of lyso-GM1 and lyso-GM2.*

2 Introduction

2.1 Gangliosides

2.1.1 Structure

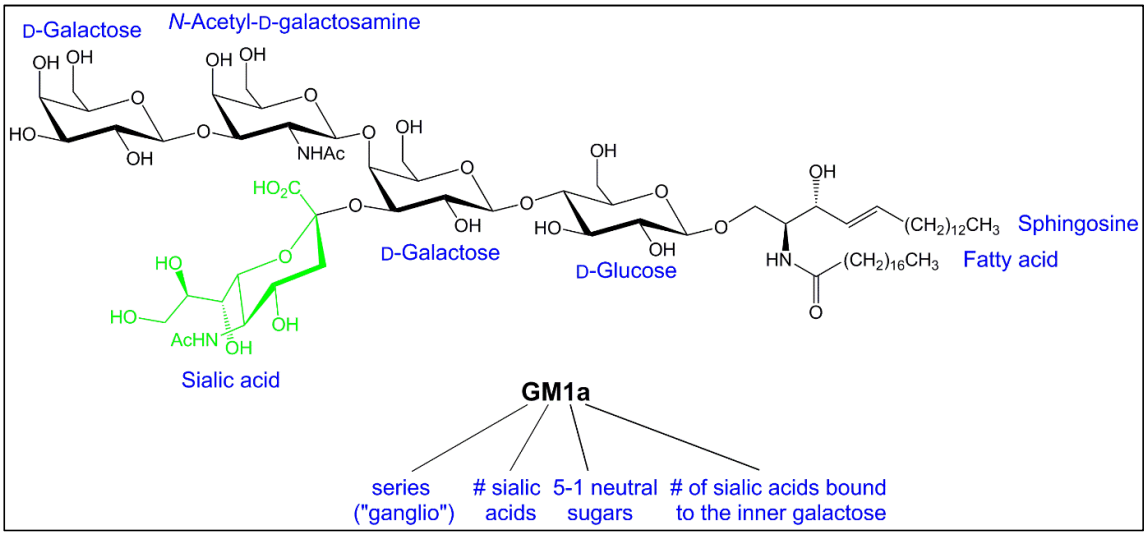

Fig. 2.1.1: Structure of one lipoform of ganglioside GM1a.

Gangliosides are sialic acid-containing glycosphingolipids (6). Most glycosphingolipids consist of a ceramide moiety attached to one or more sugar units. Ceramide consists of a sphingoid base, often C_{18}-sphingosine ((2*S*,3*R*,*E*)-2-aminooctadec-4-ene-1,3-diol) acylated by a fatty acid. In lysoglycosphingolipids the sugars are attached to a sphingoid base. The gangliosides of mammals contain mostly C_{18}- and C_{20}-sphingosine acylated by stearic acid, which constitute more than 80 % of the total ganglioside fatty acid content in the nervous system (7). C_{18}-sphingosine-containing gangliosides are present in all tissues while C_{20}-sphingosine-containing gangliosides can only be found in the nervous system of mammals in significant amounts (8). In human skin fibroblasts, where GM3 and GD3 (Fig. 2.1.4) are the major gangliosides, C_{18}-sphingosine and C_{18}-sphinganine (dihydrosphingosine) are the major sphingoid bases of gangliosides, and the major fatty acids are behenic acid ($C_{22:0}$) and lignoceric acid ($C_{24:0}$) (9). There is also a spatial distribution of the C_{18}/C_{20}-sphingosine ratio in mouse brain, and an increase of the C_{20}-sphingosine content has been observed during ageing. The function of this is not fully understood but it is

known that C_{20}-sphingosine-containing gangliosides are more effective in reducing membrane fluidity (7, 8). An accumulation of C_{20}-sphingosine-containing gangliosides might increase the risk for neuronal diseases like Alzheimer disease because these species preferentially accumulate in the entorhinal cortex, which is severely affected in Alzheimer disease (8, 10). Changes in the fatty acid composition of gangliosides were not investigated in the study of Sugiura et al. In humans it is reported that the fatty acid content in the brain gangliosides changes for $C_{18:0}$ from 95 % to 78 % and for $C_{20:0}$ from 2.7 % to 9.5 % during ageing (11).

Glycosphingolipids show characteristic carbohydrate sequences, linkages, and anomeric configurations. They can be divided into so called series. The ganglio series is characterized by the sequence Gal*β*1-3GalNAc*β*1-4Gal*β*1-4-Glc*β*1-1'Cer. Sialic acids are frequently occurring terminal sugars in glycoconjugates on the plasma membrane of eukaryotic cells (12). They are primarily found in the deuterostome lineage of animals. There are more than 50 kinds of sialic acids known in nature. All of them are derivatives of neuraminic acid, which is the 5-amino derivative of 2-keto-3-deoxy-nononic acid (Kdn) (13). The most abundant sialic acids in gangliosides are *N*-acetylneuraminic acid and *N*-glycolylneuraminic acid (14), but other modifications like *O*-acetylation in position 4, 7 or 9 or *N*-deacetylation, *O*-methylation, sulfatation, and lactonization can occur. In humans *N*-glycolylneuraminic acid can only be found in traces, which is explained by inactivation of the CMP-*N*-acetylneuraminic acid hydroxylase gene during evolution (12). Exceptions are human cancers and fetal tissues. In nonhuman mammals *N*-glycolylneuraminic acid can be found in every tissue except the brain where the levels are very low, for instance 1-2 % in the gangliosides in the grey matter of bovine brain (15) or 3 % in the gangliosides of whole equine brain (16). *N*-glycolylneuraminic acid is absent with a few exceptions in sauropsides (birds and reptiles) and monostremes (platypus) (17).

2.1.2 Nomenclature

For the nomenclature of gangliosides, the Svennerholm system is most frequently applied (18). It consists of four signs: The first sign describes the series, where G indicates the ganglio-series (Gal*β*1-3GalNAc*β*1-4Gal*β*1-4-Glc*β*1-1'Cer). The second sign specifies the number of the sialic acids in the ganglioside, where M means one, D means two, T means three, and so on. The third sign indicates the number (5 – n)

of neutral sugar residues. For example, ganglioside GM1 contains 5 – 1 = 4 neutral sugar residues. In the ganglio series the fourth sign indicates the number of sialic acids that are attached to the inner galactosyl residue (a = 1, b = 2, etc.). Exceptions of this rule are the gangliosides GM1b and GD1c of the 0-series (Fig. 2.1.4). In addition, gangliosides containing a sialic acid residue in *α*2-6 linkage at the inner *N*-acetylgalactosamine residue are called α-series gangliosides (19). The IUPAC-IUBMB suggests a nomenclature where the series is abbreviated (for instance Gg for ganglio) and the number of neutral sugars is subscripted behind the symbol. The position of the sialic acids is described by roman numbers which describe the number of the sugar they are attached to. The number of the hydroxyl group they are bound to is described by a superscripted Arabic number behind the Roman number. For instance, the name of GD1a (NeuAc*α*2-3Gal*β*1-3GalNAc*β*1-4(NeuAc*α*2-3)Gal*β*1-4-Glc*β*1-1'Cer (Fig. 1.2)) is IV^3-*α*-NeuAc,II^3-*α*-NeuAc-Gg_4Cer (20). When lipoforms are specified, the ceramide part is designated as d18:1/18:0, where the first part characterizes the sphingoid base by the number of hydroxyl groups (m = mono, d = di, t = tri) and the number of carbon atoms:double bonds (21). The same applies to the remaining numbers, which describe the fatty acid chain.

2.1.3 Occurrence

Gangliosides can be found in vertebrates and, with few exceptions, not in invertebrates. They occur in all tissues and are especially abundant in neuronal tissues, where their content is one to two orders of magnitude higher than in extraneural tissues (22). In the brain they are five times more abundant in the grey matter than in the white matter (14). The main gangliosides in the brain of mammals are GM1, GD1a, GD1b, GT1b, 9-*O*-Ac-GT1b, and GQ1b (7). Here, they contribute to 10-12 % of the total lipid content. Gangliosides can also be found in serum, where they occur mainly on serum lipoproteins, predominantly LDL (66 %), HDL (25 %) and VLDL (7 %) (14). The main gangliosides in serum are GM3, GM2, GD3, GD1a, GD1b, GT1b, GQ1b and sialylneolactotetraosylceramide. Subcellularly, the majority of gangliosides can be found in the plasma membrane. Additionally, GD3 can be found in the mitochondria, but only during apoptosis. In response to cell dead signals like TNF-α GD3 is transported from the plasma membrane to the membranes of mitochondria. It is assumed that GD3 contributes to mitochondrial fission, which is

associated with apoptosis execution (23). Furthermore, gangliosides GM1 and GD1a occur in the outer and inner membrane of the nuclear envelope. GM1 on the inner nuclear membrane forms a complex with the Na^{+}/Ca^{2+}-exchanger (NCX) that meditates the Ca^{2+} transport from the nucleoplasm to the nuclear envelope (NE) lumen and hence to the ER, which serves as a major storage site for cellular Ca^{2+} (24). The Ca^{2+} concentration of the nucleoplasm and the cytosol are in a homeostatic equilibrium via nuclear pores. GD1a has no proven function in the nucleus and apparently serves only as precursor of GM1. The conversion of GD1a to GM1 is catalyzed by Neu1 in the outer membrane of the nuclear envelope and by a Neu3 isoform in the inner membrane (24). Gangliosides are also able to form lactones, for instance GD1b-lactone I, which can contribute up to 3.5 % of total lipid bound sialic acid in human brain (25), and GM3-lactone, which occurs on tumor cells like melanoma (26). GD1b-lactone is termed I if only the terminal sialic acid is lactonized, and termed II if both sialic acids are lactonized (27). The biological function of ganglioside lactones is mostly uninvestigated, but it is known that GM3-lactone, which occurs on tumor cells in much higher concentration than on normal cells, is much more immunogenic than GM3 (26).

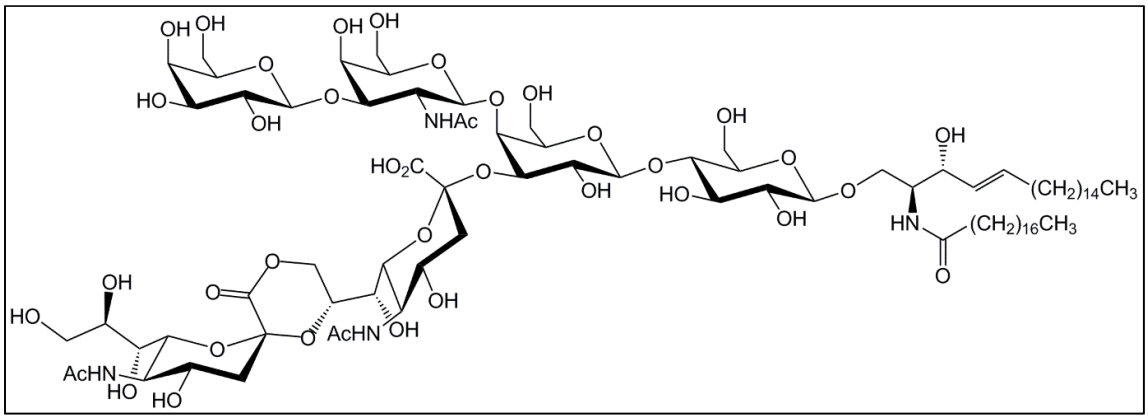

Fig. 2.1.2: Structure of GD1b-lactone I

2.1.4 Biosynthesis

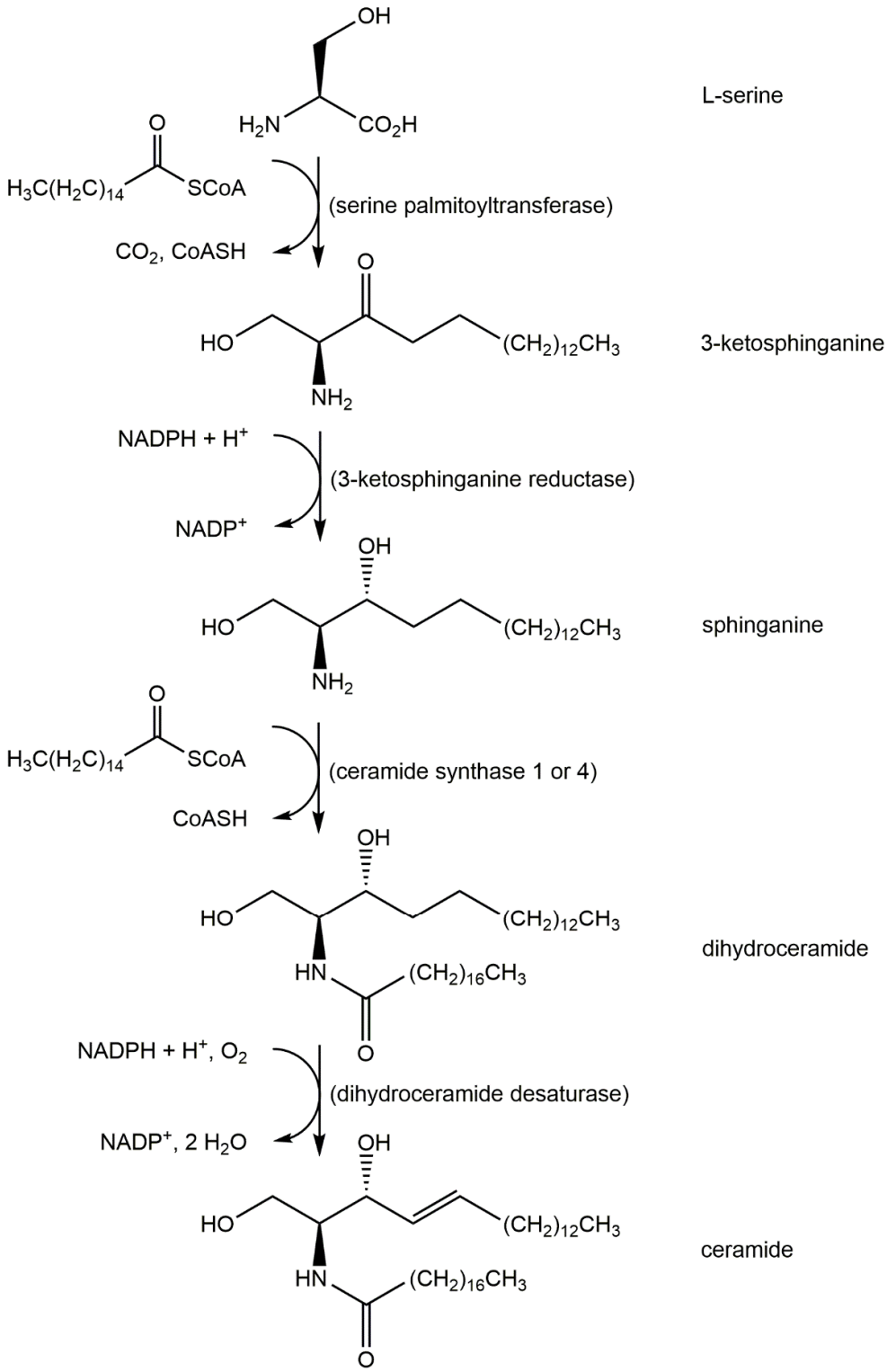

Fig. 2.1.3: Biosynthesis of d18:1/18:0-ceramide as a precursor of gangliosides.

In eukaryotic cells gangliosides can be synthesized *de novo* or within a salvage pathway, where the building blocks of gangliosides are recycled. The *de novo* biosynthesis starts with the formation of ceramide at the cytoplasmic leaflet of the ER membrane. The first and rate-determining step is the condensation of L-serine and palmitoyl CoA, resp. stearoyl CoA, catalyzed by serine palmitoyltransferase (7). The resulting 3-ketosphinganine is reduced to sphinganine by 3-ketosphinganine reductase using NADPH + H^+ as co-substrate. In the case of ceramides with stearoyl moiety sphinganine is acylated with stearoyl CoA to dihydroceramide catalyzed by CerS1 or CerS4. Synthesis of ceramides with other acyl chain lengths is catalyzed by other ceramide synthases (28). The last step is the dehydrogenation of dihydroceramide to ceramide catalyzed by dihydroceramide desaturase des1 using NADPH + H^+ and O_2 as co-substrates (29). Then, ceramide, the common precursor of ganglioside biosynthesis, is transported to the Golgi apparatus by the transport protein CERT (14). The next step in the biosynthesis of most gangliosides is the glycosylation of ceramide with UDP-glucose catalyzed by UDP-glucose ceramide glucosyltransferase, which occurs at the cytoplasmic face of the Golgi membrane. GlcCer is then translocated across the membrane to the luminal face of the Golgi apparatus, at least in vitro, mediated by ABC transporters. In the next step GlcCer is glycosylated with UDP-galactose to LacCer catalyzed by beta-1,3-galactosyltransferase I. All gangliosides except GM4, which is synthesized from GalCer, are synthesized from LacCer. In the following steps the sialyl-donor is always CMP-sialic acid. First, GM3 is synthesized by the addition of sialic acid to LacCer catalyzed by LacCer alpha-2,3-sialyltransferase I (ST-I or GM3 synthase) (14, 19). Then, GD3 is synthesized by addition of another sialic acid residue to GM3 catalyzed by GM3 alpha-2,8-sialyltransferase (ST-II or GD3 synthase). Subsequently, GT3 can be synthesized by addition of a further sialic acid residue to GD3 catalyzed by GD3 alpha-2,8-sialyltransferase (ST-III or GT3 synthase). LacCer, GM3, GD3, and GT3 serve as precursors for higher gangliosides of the 0-, a-, b- and c-series. They are substrates of beta-1,4-*N*-acetylgalactosaminyltransferase I (GalNAcT I or GA2/GM2/GD2/GT2 synthase) in order to get GA2, GM2, GD2, and GT2. These products are accepted by beta-1,3-galactosyltransferase II (GalT II or GA1/GM1/GD1b/GT1c synthase) in order to get GA1, GM1, GD1b, and GT1c. Then, they can be sialylated by alpha-2,3-sialyltransferase IV (ST-IV or GM1b/GD1a/GT1b/GQ1c synthase) to GM1b, GD1a, GT1b, and GQ1c. These

products can be further sialylated by alpha-2,3-sialyltransferase V (ST-V or GD1c/GT1a/GQ1b/GP1c synthase) to GD1c, GT1a, GQ1b, and GP1c. An alternative pathway is the sialylation of GM1b, GD1a, GT1b, and GQ1c in position 6 of the *N*-acetylgalactosamine residue, which is catalyzed by alpha-2,6-sialyltransferase VII (ST-VII or GD1aα/GT1aα/GQ1bα/GP1cα synthase) in order to get GD1aα, GT1aα, GQ1bα, and GP1cα. The anabolic pathway for lysogangliosides has not been investigated, yet. It is hypothesized that they are synthesized by the same enzymes like gangliosides by starting from sphingosine instead of ceramide (30).

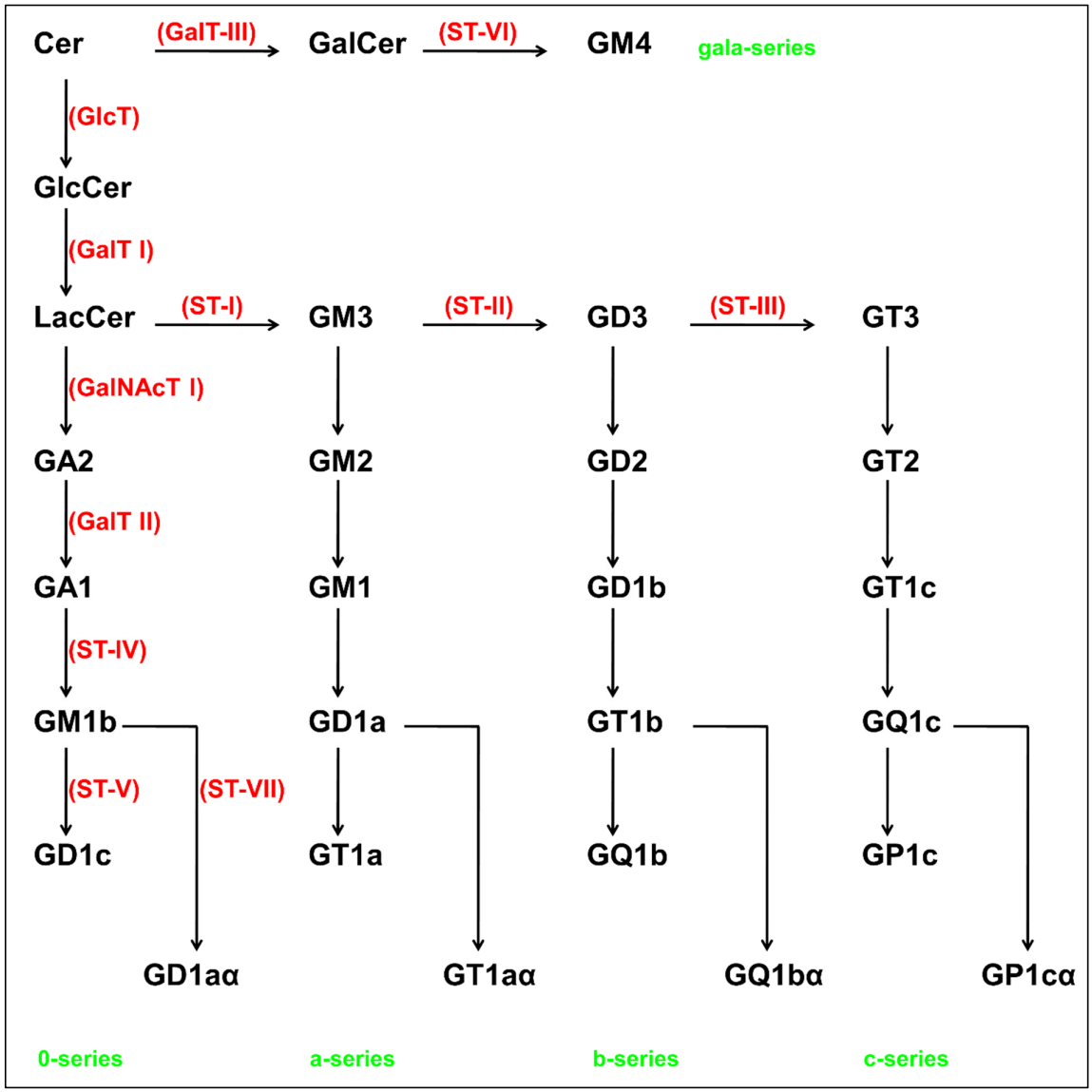

Fig. 2.1.4: Biosynthesis of gangliosides starting from ceramide at the Golgi apparatus. The enzymes are highlighted in red (modified from: (31)).

These glycosyltransferases are also described as an assembly line because they have a broad specificity and accept a member of every sub-series as a substrate (31). In contrast, the enzymes catalyzing the first steps are highly specific for their substrates. Therefore, the amounts of LacCer, GM3, GD3, and GT3 determine the amounts of 0-, a-, b-, and c-series gangliosides.

2.1.5 Biological function of gangliosides

Major advances in the analysis of the biological function of gangliosides became possible with the aid of genetically engineered mice. In 1996, mice were engineered that were disrupted in their *GalNAcT I* gene so that they could not synthesize gangliosides beyond GM3, GD3, and GT3. These *GalNAcT*-(*-/-*)-mice were viable with a normal life span and a mainly intact CNS, but they showed a decreased neural conduction velocity in the somatosensory cortex (32) and an age-related CNS- and peripheral nerves dysmyelination process (33) resulting in motor defects at the age of 12 month (34). Furthermore, male *GalNAcT-(-/-)*-mice are infertile (35). These results suggested that higher gangliosides are not essential for survival in mammals but for reproduction of males. Also a mouse model with disrupted *ST-II* gene, which could not synthesize b- and c-series gangliosides, showed no phenotype different from normal mice (36). DKO (double knock out) mice (*GalNAcT/ST-II*-(*-/-*)) are unable to synthesize gangliosides except GM3. These GM3-only mice showed a sudden death phenotype and lethal seizures induced by sound stimuli (36). In 2003, mice were engineered that were disrupted in their *ST I* gene so that only the 0-series gangliosides were present. Gangliosides of this series are usually only present in traces in adult mammalian brain (14). These *ST I-(-/-)*-mice were also viable and apparently showed no abnormalities in any tissue. The only difference to wild type mice was an enhanced insulin signaling response in skeletal muscle, which is the major site of glucose uptake, which suggests that gangliosides are involved in the regulation of the insulin receptor response (37). Additionally, it was reported that *ST I-(-/-)*-mice completely loose hearing 17 days after birth and show a complete loss of the organ of Corti 2 month after birth. In wild type mice gangliosides, especially GM3, are expressed in all regions of the cochlea in the early phase of hearing maturation, which suggests an important role of them in the functional organization of this organ (38). In 2005, DKO mice (*ST-I/GalNAcT-I-(-/-)*) were engineered that showed a

complete absence of gangliosides (39). These mice form sulfate-containing GSLs instead of gangliosides and show neurologic abnormalities like tremors and weakened hind limbs soon after birth and also shrinking and degeneration of the brain and the axons, leading usually to death soon after weaning. In humans a very rare disruption of the *ST I* gene and hence a lack of gangliosides beyond the 0-series leads to an autosomal recessive infantile-onset symptomatic epilepsy with development stagnation, blindness and mental retardation (40). In 2013, also an upregulation of the globoside pathway and a secondary dysfunction of the respiratory chain could be observed in human *ST I-(-/-)*-patients (41). Furthermore, these patients were deaf. In 2013, also patients with disrupted *GalNAcT I* gene were identified. They developed early onset and slowly progressing spastic paraparesis, cognitive impairment, and cerebellar ataxia (42). Another disease with impaired sphingolipid biosynthesis is HSAN1 (Hereditary sensory and autonomic neuropathy type 1), which is caused by mutations in a serine palmitoyltransferase subunit. In human patients, there are no differences in the total levels of sphingolipids (43), but the mutation in the *SPTLC1* gene causes a substrate specificity shift of the enzyme leading to synthesis and accumulation of toxic sphingolipid metabolites, which cause neuropathies. Up to now, these are the only anabolic diseases known for gangliosides.

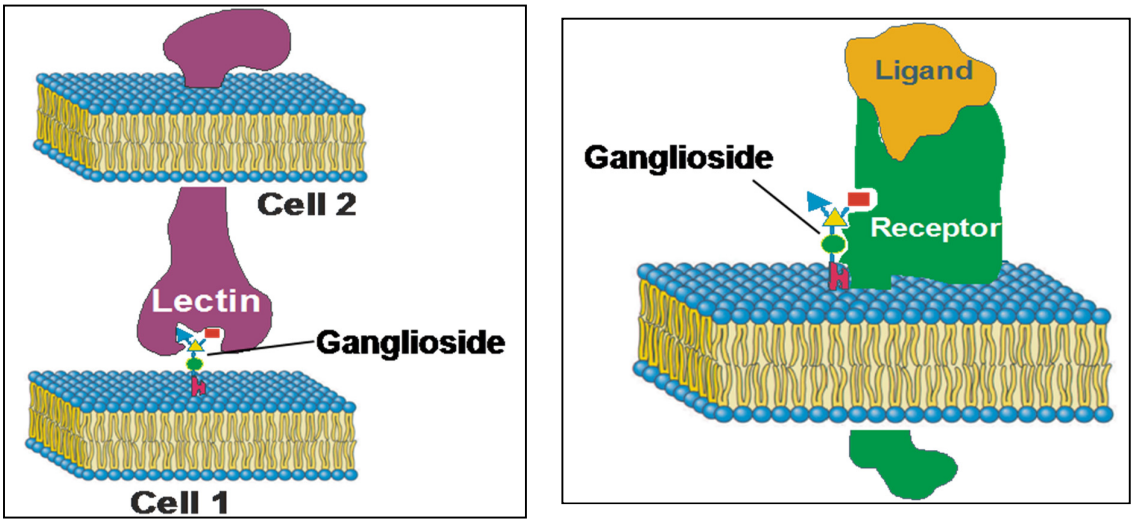

Fig. 2.1.5: Left figure: Trans interaction of gangliosides and binding proteins. Right figure: Cis interaction of gangliosides and binding proteins (modified from: (44)).

In the plasma membrane one biological function of gangliosides is the interaction with sialic acid binding proteins. This is one example of a so called “trans” interaction with

carbohydrate binding proteins outside the cell. Another possibility is a “cis” interaction with molecules within the same membrane (45). Hereby, it is assumed that gangliosides are part of microdomains in the membrane which, when occurring at nerve endings, were called glycosynapses (46). Three types have been distinguished: GSL clusters organized with signal transducers, *O*-linked mucin-type adhesion epitopes organized with signal transducers in a cholesterol-rich lipid microdomain, and adhesion receptors with *N*-glycosylation complexed with tetraspanin and gangliosides in microdomains. In another concept, microdomains on membranes have been called lipid rafts, which are defined as dynamic, nanoscale, sterol-sphingolipid-enriched, ordered assemblies of proteins and lipids. They can also be stimulated to merge into larger, more stable rafts (47). The existence of lipid rafts was investigated by microscopy techniques like stimulated emission depletion far-field fluorescence nanoscopy (STED), by mass spectrometry of membrane compositions, and by constructing membrane model systems (47). STED nanoscopy showed that the free diffusion of sphingolipids and GPI-anchored proteins on the plasma membrane in living mammal cell is hindered by transient trapping in cholesterol mediated complexes (48). The upper limit for size and life time of these complexes is 20 nm and 20 ms. It is assumed that lipid rafts have a functional role in membrane-associated processes like T cell signalling, virus budding of HIV and influenza, post-Golgi traffic to the cell surface, and glycosphingolipid-mediated endocytosis (47).

In “trans” interactions, gangliosides act as receptors for glycan binding proteins (lectins) in cell-cell recognition events. They modulate the cytotoxity of natural killer cells by interacting with Siglec-7, an inhibitory receptor on these cells. Siglec-7 prefers sialic acids in *α*2-8 linkage, which is rare on glycoproteins but common on b-series gangliosides (45). Furthermore, gangliosides bind to Siglec-4 (MAG), which is expressed in nerve tissue, functions in stabilizing myelin-axon interactions, and limits axon regeneration after injury. Siglec-4 recognizes the terminal glycan sequence NeuAc*α*2-3Gal*β*1-3GalNAc, which is found on GD1a and GT1b. This explains the age-related dysmyelination process observed in *GalNAcT*-(-/-)-mice. Gangliosides are also the receptors for E-selectin on neutrophils, which together with P-selectin initiates the binding of neutrophils to blood vessels in response to infection or injury (45). For this process, neutrophils express special gangliosides of the neolacto series

containing long chains of multiple LacNAc (Galβ1-4GlcNAc) units, which contain one or more fucosyl residues and one terminal sialic acid residue.

In “cis” interactions, gangliosides modulate the responsiveness of insulin receptors. According to a hypothesis, IRs are usually associated with caveolin-1 in caveolae and are immobile, which is necessary for their insulin metabolic signaling. If GM3 binds to an IR, it becomes mobile and is released from the association with caveolin-1 which hinders insulin signaling (49). The influence of other gangliosides was not investigated, yet. Another example is the regulatory inhibition of the epidermal growth factor receptor (EGFR) by GM3, but not by other gangliosides. For activation of EGFR, a dimerization is necessary and GM3 stabilizes the inactive monomeric form. *In vitro*, the inhibition could only be observed in liquid ordered phases, which suggests an important role of membrane microdomains for this process (50). Third, gangliosides are regulators of angiogenesis. Angiogenesis is induced by release of vascular endothelial growth factor (VEGF) which binds to VEGF-receptors and induces the proliferation of vascular endothelial cells. GD1a and other higher gangliosides enhance the effect of VEGF while GM3 suppresses it (51).

2.1.6 Lysosomal degradation

The degradation of gangliosides mainly takes place in endosomes and lysosomes. Gangliosides from the plasma membrane reach the lysosomes via endocytosis. At the stage of late endosomes gangliosides and other membrane components that are designated for degradation are sorted from the perimeter membrane into luminal membranes. The lipid composition of both membrane pools is adjusted in a way that the perimeter membrane is stabilized while the luminal membranes become degradable (52). A lipid that is crucial for endosomal and lysosomal membrane degradation is bis(monoacylglycero)phosphate (BMP). The BMP content of the luminal membrane increases up to 70 % of total phospholipid content (53) while membrane stabilizing lipids like cholesterol and other sterols are transported out of the inner membrane (52).

Lysosomal ganglioside degradation takes place in a sequential manner, in which the sialic acid- and monosaccharide units are cleaved from the non-reducing end of the glycan chain catalyzed by different glycosidases (Fig. 2.1.7) (14).

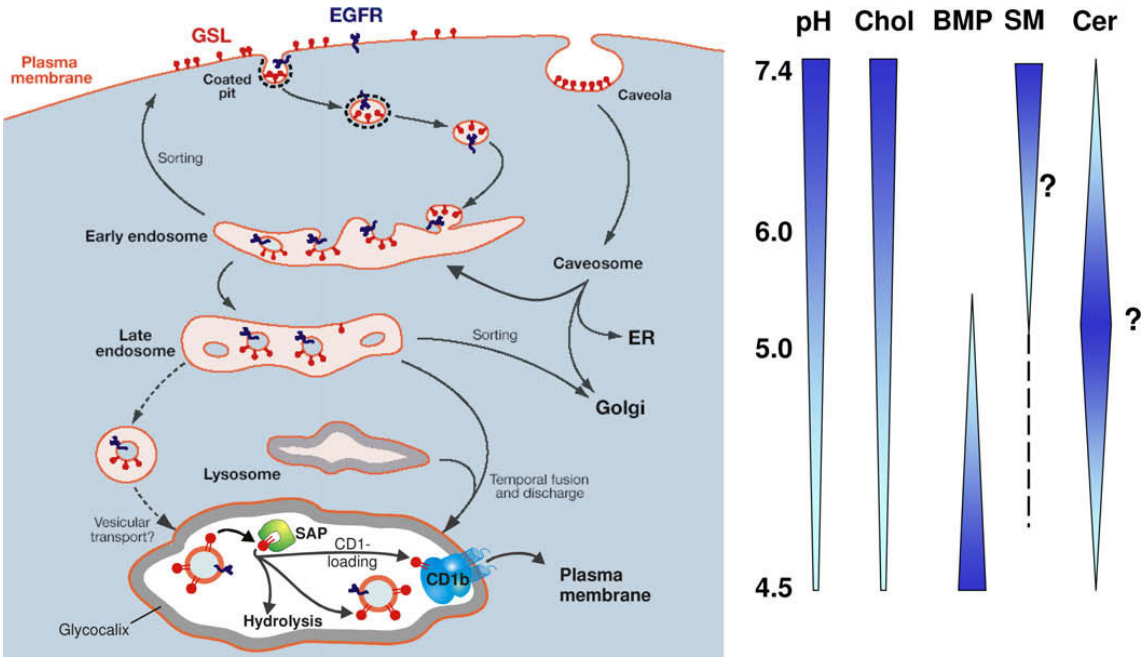

Fig. 2.1.6: Model of lysosomal degradation of glycosphingolipids. Gradients of pH-value, cholesterol, BMP, sphingomyelin (SM) and ceramide (Cer) are shown (modified from: (52)).

In the first step, terminal sialic acid residues are cleaved by sialidase Neu1. Together with carboxypeptidase A, GM1 beta-galactosidase, and *N*-acetylaminogalactose-6-sulfate sulfatase Neu1 is part of a lysosomal multienzyme complex (54). The degradation of GM1 to GM2 and of GA1 to GA2 is catalyzed by GM1 beta-galactosidase, which requires saposin-B or the GM2-activator as cofactor (14). Then, GM2 is degraded to GM3 and GA2 to LacCer by one of the beta-hexosaminidase isoenzymes, which require the GM2-activator as a cofactor. GM3 is subsequently degraded to LacCer by Neu1. LacCer is degraded to GlcCer by GalCer beta-galactosidase using the cofactor saposin-C or by GM1 beta-galactosidase using the cofactor saposin-B. Then, GlcCer is degraded to ceramide catalyzed by glucosylceramide-beta-glucosidase using saposin-C as a cofactor. Ceramide is degraded to sphingosine by acid ceramidase using Saposin-D as a cofactor. The final degradation products are able to leave the lysosome (55).

Defects in enzymes and cofactors involved in the degradation of gangliosides and also of other GSLs can lead to inherited diseases, the lysosomal storage diseases (56). They are all inherited autosomal recessive except Fabry disease (55). Defects in the *Neu1* gene lead to the very rare disorder sialidosis. The stored substances are mainly sialyloligosaccharides and sialylglycoproteins. The storage of gangliosides is

increased in visceral organs, but not in the brain (57). The reasons for this have not been investigated, yet. A defect in the GM1 beta-galactosidase gene leads to GM1 gangliosidosis, which is also called Landing disease (14). Here, the stored substances are GM1 and GA1. A defect in the beta-hexosaminidase gene leads to GM2 gangliosidosis. The enzyme beta-hexosaminidase consists of two subunits, which can be an α- or a β-subunit. beta-Hexosaminidase A consists of an α- and a β-subunit, beta-hexosaminidase B consists of two β-subunits, and beta-hexosaminidase S consists of two α-subunits. A defect in the α-subunit leading to deficient beta-hexosaminidase A and S is called Tay-Sachs disease or B-variant, and the stored substance is mainly GM2. A defect in the β-subunit leading to deficient beta-hexosaminidase A and B is called Sandhoff disease or 0-variant, and the stored substances are mainly GM2, GA2, globotetraosylceramides, and oliogosaccharides (55). Also a variant with deficient GM2 activator is known which is called AB-variant. A defect in the glucosylceramide beta-glucosidase gene leads to storage of GlcCer. This disease is called Gaucher disease, which is the most common sphingolipidosis (56). A variant of Gaucher disease can also be caused by a deficiency in saposin-C. A deficiency in the acid ceramidase leads to Farber disease. Here, the stored substance is ceramide. Gaucher disease and Farber disease are not referred to as gangliosidoses.

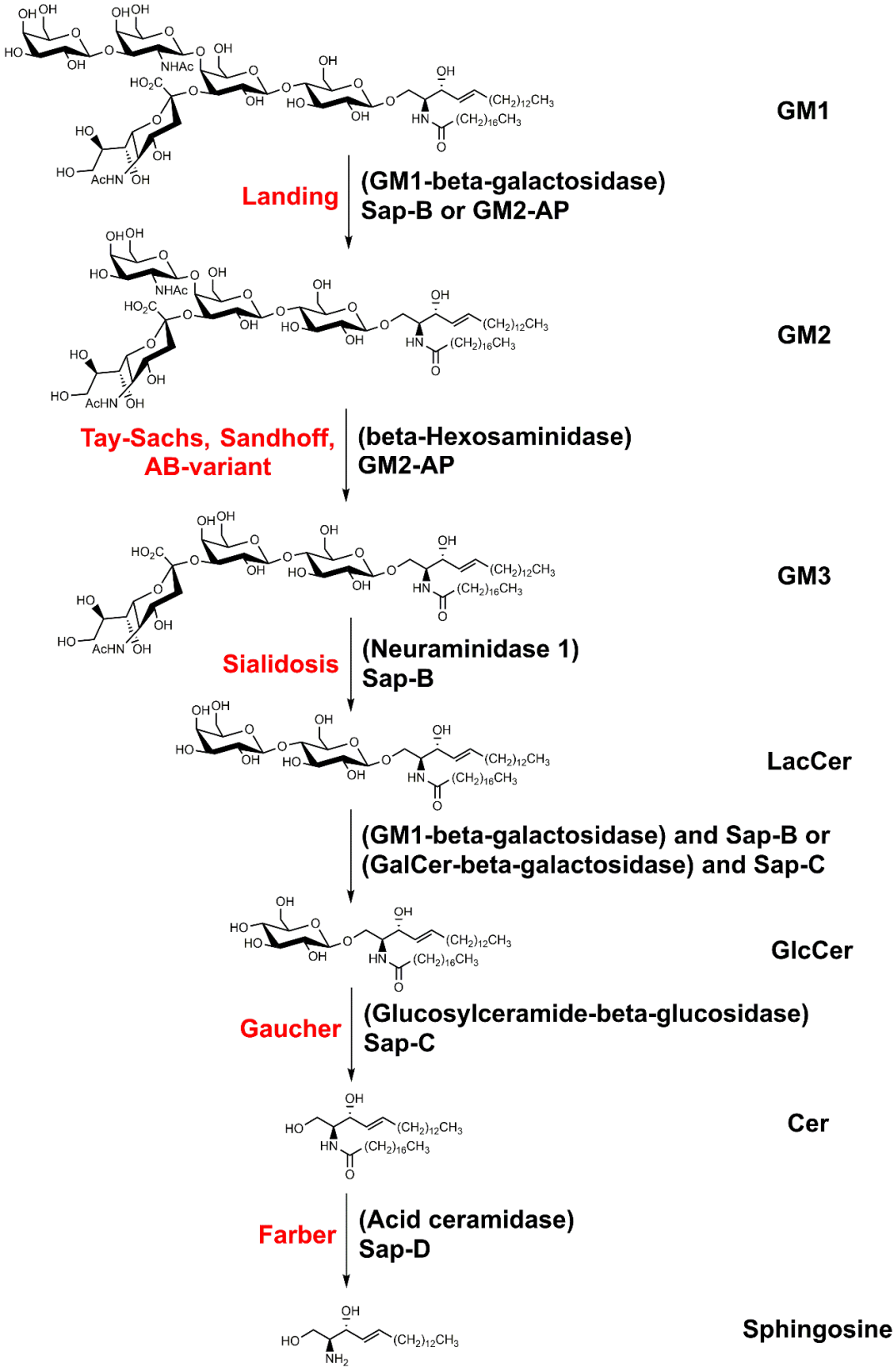

Fig. 2.1.7: Lysosomal degradation of gangliosides. The storage diseases of each step are highlighted in red (modified from:(56)).

2.2 Internal standards for mass spectrometric quantification of gangliosides

2.2.1 Mass spectrometric quantification

The goal of quantification is to measure the amount of an analyte in absolute terms (absolute quantification) or relative to another analyte (relative quantification) (58). Mass spectrometry is applicable to most type of biomolecules, shows high sensitivity, high specificity, is suitable for coupling to chromatographic methods, and has a wide dynamic range and a high speed of analysis. Special mass spectrometers are needed for quantification. Mostly, electrospray ionization (ESI) is used, which is a mild ionization technique where no or only very little fragmentation of the analyte is possible. For many applications, the mass spectrometer is preferably a tandem mass spectrometer because detection sensitivity and specificity can be enhanced by special operating modes. In general, the analyzing steps of a tandem mass spectrometer can be performed tandem in space or tandem in time (59). A tandem in space MS contains three structurally separated analyzers, for example a triple quadrupole. A tandem in time MS contains an ion trap analyzer, which can perform multiple analyzing steps successively at the same place, for example as a Q-Trap MS.

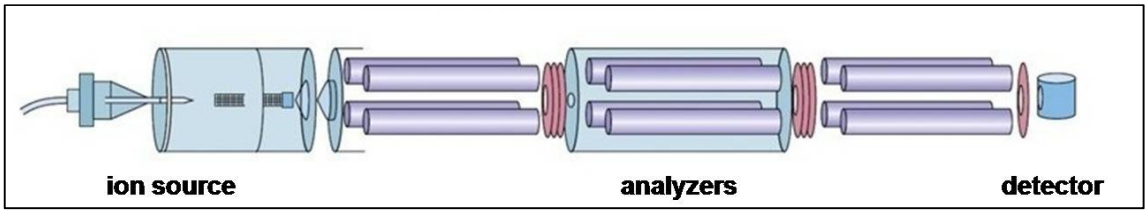

Fig. 2.2.1: Schematic structure of a triple-quadrupole mass spectrometer (modified from: (60)).

An appropriate mode for quantification is selected ion monitoring (SIM), where only a particular mass instead of the whole mass spectrum is measured, which results in a 1000-fold gain in detection sensitivity (58). A disadvantage of this method is the lack of specificity, because isobaric compounds of the analyte cannot be distinguished. Another approach is the parent ion scan, where the first analyzer is in scan mode, the second analyzer is in CID (collision-induced dissociation) mode, and the third

analyzer is in SIM mode. All masses are measured by the first analyzer and are fragmented by the second analyzer. The third analyzer is measuring only one particular fragment.

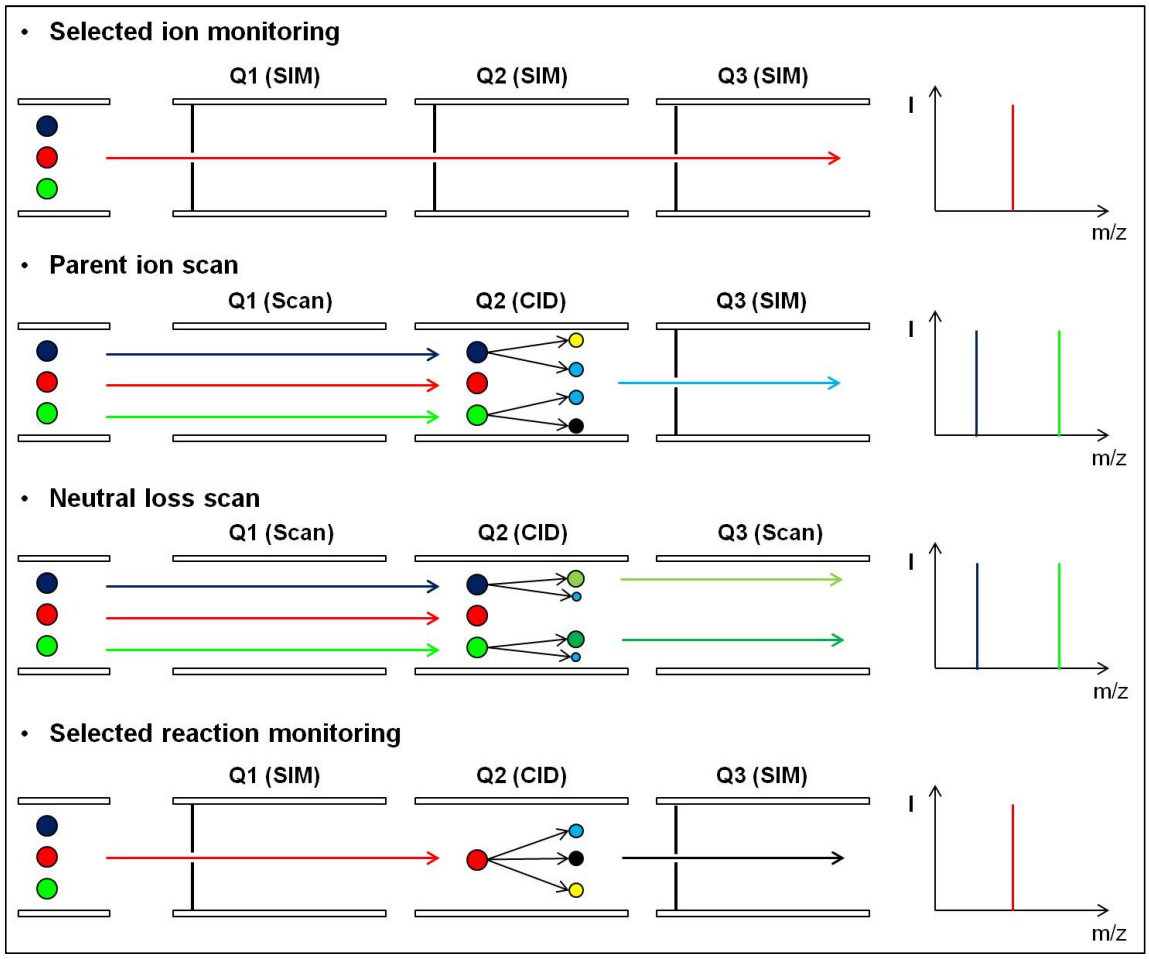

Fig. 2.2.2: Schematic view of MS modes which are suited for MS quantification (modified from: (61)).

If a characteristic fragment of the analyte is uncharged, the neutral loss scan technique can be used in which analyzer 1 and 3 are in a synchronized scan mode. The first analyzer scans the whole spectrum, the second analyzer is in CID mode, and the third analyzer scans the masses that lost a particular uncharged mass (61). The highest specificity, but not the highest sensitivity, can be achieved by selected reaction monitoring (SRM) and multiple reaction monitoring (MRM). Here, the first analyzer is in SIM mode, the second analyzer is in CID mode, and the third analyzer is in SIM mode. The first analyzer measures only a particular mass, which is then

fragmented, and the third analyzer measures only a particular fragment ion. The measuring of more than one reaction at the same time is termed multiple reaction monitoring (MRM).

2.2.2 Calibration

For quantification, calibration of the instrument has to be performed, which is here defined as the determination of a correlation between analyte concentration and mass spectrometer response (58). Three principle methods can be distinguished. In external calibration the standard used is identical to the analyte. Approximately five different concentrations are measured and the intensity of the response is plotted against the concentration. The calibration curve obtained after linear regression can be described by the following equation (62):

$$I_{i,std} = a_{EC} \cdot c_{i,std} + b_{EC}$$

($I_{i,std}$: intensity measured for calibration standard, $c_{i,std}$: concentration of calibration standard, a_{EC}: slope of external calibration, b_{EC}: y-axis intercept of external calibration)

Then, the analyte is measured and its concentration is calculated from the regression line. Accuracy and precision of the calibration are limited because analyte and standard are measured in different sample matrices at different times. An advance is the standard addition method. Here, the standard used is also identical to the analyte. First, the analyte is measured alone. Then, a defined amount of standard is added and the response of the whole amount is measured. This is repeated for several different standard concentrations and the intensity is plotted against the standard concentration. The calibration curve can be described by the following equation:

$$I_{i,an+added} = a_{SAC} \cdot c_{i,added} + b_{SAC}$$

($I_{i,an+added}$: intensity measured for analyte and added standard, $c_{i,added}$: concentration of added calibration standard, a_{SAC}: slope of standard addition calibration, b_{SAC}: y-axis intercept of standard addition calibration)

The x-axis intercept provides the concentration of the analyte. Accuracy and precision of the method are higher because analyte and standard are measured in the same sample matrix at the same time. However, this method cannot compensate analyte losses during purifications steps of the sample. Another problem are fluctuations in the mass spectrometer response, which are also not compensated. These problems can be overcome by the internal standard method, in which the standard used is a chemically and physically similar but non-isobaric derivative of the analyte. The standard is added in a defined amount to the sample at an early stage of sample handling. After purification of the sample, the ratio of the mass spectrometric response of analyte and standard are measured. The concentration of the analyte can be calculated by the following equation (62):

$$c_{an} = \frac{I_{an}}{I_{IS}} \cdot c_{IS} = CF_{IS} \cdot I_{an}$$

(I: intensity measured for internal standard respectively analyte, c: concentration of internal standard respectively analyte, CF_{IS}: calibration factor)

One advantage of internal standard calibration is a reduced analysis time because it is a one point calibration (62). Furthermore, accuracy and precision of the method are high because the internal standard acts as a self correcting system for analyte losses during purification steps and for fluctuations in mass spectrometer response.

There are five criteria for a good internal standard. First, its chemical and physical properties should match those of the analyte as closely as possible. Second, its chromatographic behavior should be similar so that standard and analyte elute close to each other if LC-MS is used. Third, the molecular mass of the standard must be distinct from that of the analyte. Fourth, its mass spectrometric behavior must be similar to that of the analyte. Fifth, it should not be a constituent of the sample which is measured.

In general, there are three types of internal standards (58). The first type is any compound that has similar physical and chemical properties to those of the analyte and that is not isobaric. Usually accuracy and precision of such standards are low.

The second type are homologous compounds of the analyte. The third type are isotope labeled versions of the analyte and often ^{2}H and ^{13}C are used. Second and third types of internal standards have very similar chemical and physical properties to the analyte and thus show high accuracy and precision.

2.2.3 Ganglioside quantification

One goal of ganglioside quantification is ganglioside pattern investigation. In 2009, Fong et al. quantified the ganglioside levels of GM1, GM2, GM3, GD3, GD1a, GD1b, GT1b, and GQ1b in the brains of 2-day-old and 80-day-old Wistar rats by using an external standard calibration. They found an increase of the total ganglioside levels of more than two-fold by ageing. In two day old rats GD1a (28 % of lipid bound sialic acid) and GQ1b (28 %) were the most abundant gangliosides while at the age of 80 d GM1 (25 %), GD1a (28 %), GD1b (17 %), and GT1b (17 %) were more frequent (63). GQ1b decreased to 9 % at the age of 80 d. In 2011, the same group quantified GM3 and GD3 in dairy milk products, where GM3 and GD3 are the main gangliosides (80 % of total ganglioside content in bovine milk) (64). They used an external standard method and a standard addition method as a control. The measured values for GD3 in different dairy milk products were in the range of 120 µg/g to 15000 µg/g based on dry weight. The GM3 levels were only in the range of less than 1 % of the GD3 levels in most products, but 5-10 % in G600 milkfat extract. In 2013, Lee et al. quantified GD3 and GM3 in bovine milk during different lactation periods (65). They found GD3 values of 15.2 mg/L and GM3 values of 0.98 mg/L in colostrums, which decreased to 2.4 mg/L and 0.15 mg/L, respectively, 90 days after calving.

Second, ganglioside quantification can also be used in the field of quantitative imaging mass spectrometry. MS methods applied are MALDI-MS, secondary ion MS (SIMS), and desorption electrospray ionization (DESI) (59). If internal standard are used, they have to be added uniformly to the tissue by microspotting or spray coating (66). There are few applications for gangliosides, yet. In 2013, NanoSIMS was used to image the phase separation of 18-F-GM1 (contains one fluorine atom at position 18 of the fatty acid part) into lipid rafts in a model membrane system. It was synthesized from lyso-GM1 and activated 18-F-stearic acid. The 18-F-GM1 served as analyte as well as an internal standard for quantitative analysis (67).

Another goal is the quantification of stored substances in lysosomal storage diseases, where GM1, GM2, lyso-GM1, and lyso-GM2 are of relevance as primary storage substances in GM1- and GM2 gangliosidosis. Furthermore, gangliosides also play a role as secondary storage substances in various lysosomal storage diseases. In Niemann-Pick disease type C1 and C2, in which the cholesterol transport proteins NPC1 resp. NPC2 are deficient (68), secondary storage of GM1 is observed (57). NPC1 and NPC2 are responsible for the efflux of cholesterol from the luminal membrane of the late endosomes to the perimeter membrane. Hereby, NPC2 transports cholesterol from the luminal membrane to NPC1, which is an integral protein of the perimeter membrane. Subsequently, NPC1 inserts cholesterol into the perimeter membrane (52). Mutations of these proteins lead to accumulation of cholesterol in the luminal membrane and hence to their stabilization against degradation (68). Therefore, lipids like cholesterol, GM1, GM2, GM3, and others are stored. Secondary storage was also reported for galactosialidosis (GD1a, GM1, GM2, and GM3 are stored), Gaucher disease (GD3, GM1, GM2, and GM3 are stored), GM1 gangliosidosis (GM2 and GM3 are stored), for various forms of mucopolysaccharidoses (mostly GM2 and GM3 are stored), and α-mannosidosis (GM2 and GM3 are stored) (57). There are few reports on the MS-determination of gangliosides, yet. In 2008, Gu et al. quantified GM1 and GM2 in human cerebrospinal fluid samples of infantile Tay Sachs patients by using d18:1/C18:0-GM1-d_3 and d18:1/C18:0-GM2-d_3 as internal standards. They compared the GM1 and GM2 levels of these patients with those of healthy controls. Furthermore, they tested the clinical effectiveness of bone marrow transplantation over a period of one year (69).

Up to now, standards of type 2 or type 3 for GM1, GM2 and GM3 have been synthesized and are commercially available (3). Standards for GD1a, GD1b, GT1b and GQ1b have not been synthesized yet and are not commercially available (59).

2.2.4 Application of the standards to CerS1- and CerS4-deficient mice

The acylation of sphinganine with stearoyl CoA to d18:0/18:0-dihydroceramide catalyzed by CerS1, which is mainly expressed in brain and skeletal muscle, and CerS4, which is expressed in leukocytes, skin, heart, spleen, but also in brain (28), is

a crucial step in the biosynthesis of gangliosides, and a deficiency of these enzymes can also affect ganglioside levels. In 2012, Ginkel et al. reported that 18 month old *CerS1-/-* mice show decreased ganglioside levels in cerebellum (GM1, 36 %; GD1a, 30 %; GD1b, 19 %; GT1b, 56 %) and forebrain (GM1, 55 %; GD1a, 72 %; GD1b, 59 %; GT1b, 37 %) compared to wild type mice (70). The ganglioside levels were quantified by TLC and densitometry. Also a decrease of the expression of MAG, which prefers GD1a and GT1b as ligands, down to 40 % was measured in both tissues, which suggests that a particular ganglioside concentration is necessary for myelin stabilization by MAG. Furthermore, the size of the cerebellum was reduced by 40 % and the mice showed altered behavior like decreased exploration of novel objects, locomotion, and running speed. Naturally occurring mutations in the *lass1* gene, which encodes CerS1, are associated with Purkinje cell degeneration and lipofuscin accumulation, but do not lead to differences in lifespan (71). CerS4 is the least studied ceramide synthase and *CerS4-(-/-)*-mice have not been reported (72), but have been created in the workgroup Willecke. Besides CerS1, CerS4 is the only ceramide synthase that accepts stearoyl CoA as substrate and is also expressed in the brain. The application of the synthesized internal standards is planned for the quantification of the ganglioside levels in the brain of *CerS4-(-/-)*-mice. Also the determination of ganglioside levels in *CerS1-(-/-)*-mice by MS methods and comparison to those in *CerS4-(-/-)*- and wild type mice is planned with the aid of the standard substances prepared in this work.

2.3 The olefin cross-metathesis

2.3.1 General considerations

In this work olefin metathesis is applied as the key step to the synthesis of artificial lysoganglioside lipoforms. The olefin metathesis, for which the Nobel Prize in chemistry was awarded in 2005, is a reorganization of C-C double bonds (73). It allows access to olefins that are cumbersome to prepare from olefins that are easy to prepare. The olefin metathesis can be classified into three categories: cross metathesis, ring-closing metathesis, and ring opening metathesis. The catalysts used are Schrock carbenes with molybdenum or ruthenium as central atom. Mo catalysts

are more active, sensitive to hard nucleophils and electrophils like water, alcohols, carboxylic acids, and carbonyls, and insensitive to soft ones like amines and phosphanes. The reverse holds for Ru catalysts which are less active, sensitive to amines and phosphanes, and insensitive to alcohols, carboxylic acids or carbonyls and also water (73). The structures of some of the most important achiral catalysts are shown in fig. 2.3.1. The advantages of the Hoveyda-Grubbs catalysts over the Grubbs catalysts are a higher thermal stability and a higher oxygen- and moisture tolerance (74).

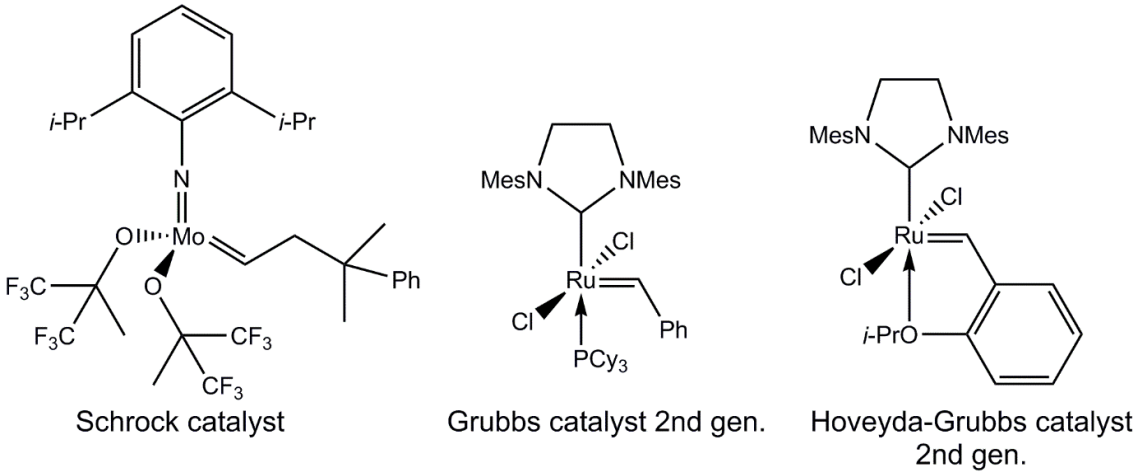

Schrock catalyst | Grubbs catalyst 2nd gen. | Hoveyda-Grubbs catalyst 2nd gen.

Fig. 2.3.1: Important achiral olefin metathesis catalysts
(Cy = cyclohexyl, Mes = mesityl)

The mechanism of the olefin metathesis consists of two steps: catalyst's initiation to generate the active catalyst and catalyst's propagation, where the active catalyst promotes additional cycles (Fig. 2.3.2) (75).

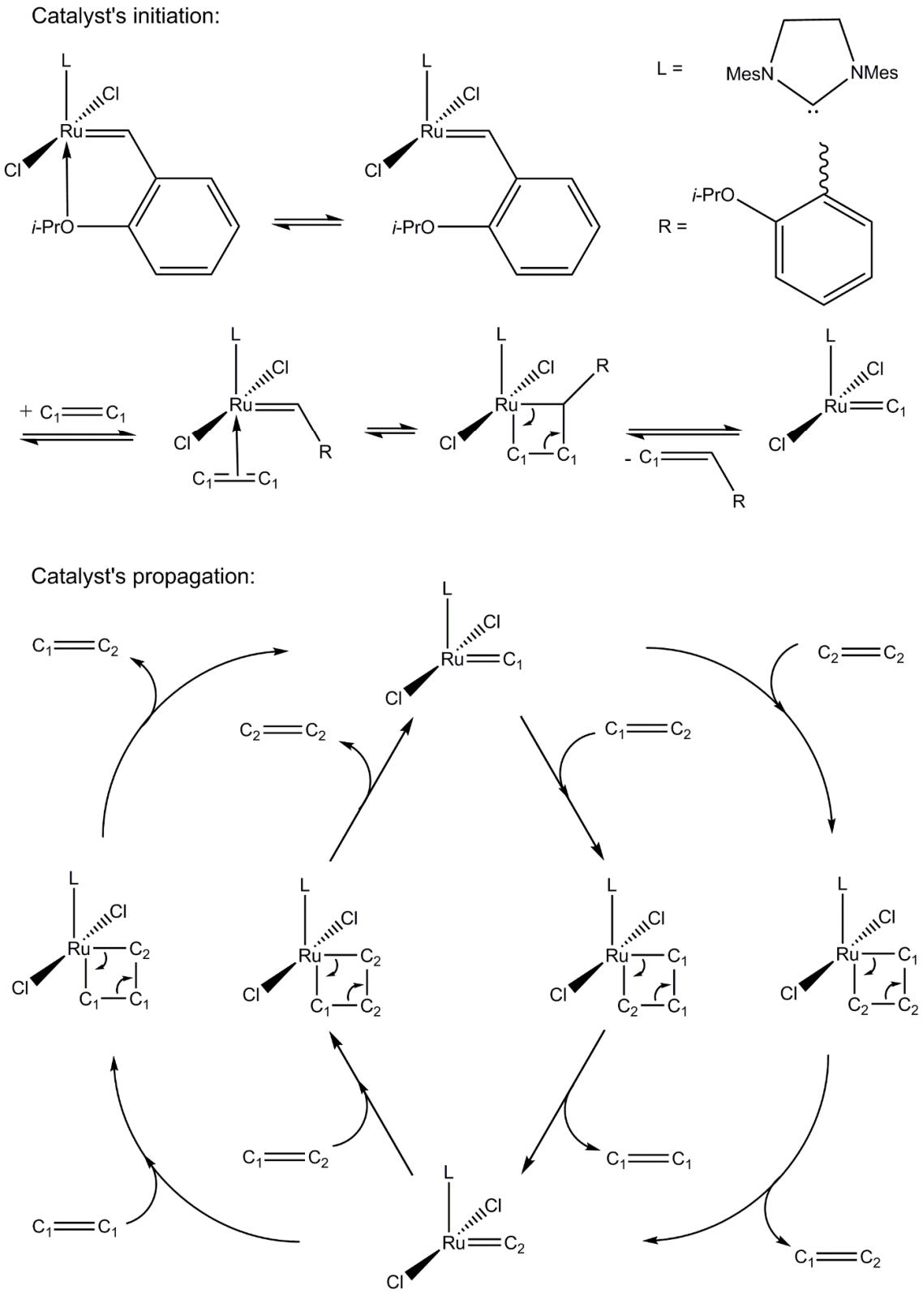

Fig. 2.3.2: Mechanism of olefin cross metathesis (modified from: (75)).

In the first step for Ru catalysts a phosphane ligand or the *iso*-propoxystyrene ligand is dissociated to form a 14-electron species that subsequently coordinates an olefin ligand, which acts primarily as a π-acid (73). For Hoveyda-Grubbs catalysts, this step is interchange rather than dissociative (74). The next step is a [2 + 2] cycloadditon to form a metallacyclobutane followed by a [2 + 2] cycloreversion to release a different olefin and regeneration of the active catalyst. For first generation catalysts, the metallacyclobutane formation is the rate-determining step while for second generation catalyst it is the dissociation step (76). In the propagation steps the active catalyst reacts with every available olefin in the same manner to get different olefins until the catalyst is deactivated. Every reaction step is reversible so that the driving force for olefin cross metathesis is the entropy of mixing. If terminal olefins are used, the equilibrium can be moved to the product side by removal of ethylene.

2.3.2 Product selectivity and *E*/*Z*-stereoselectivity of olefin cross metathesis

The product selectivity of olefin cross metathesis depends on the reactivity of the cross partners (77). Grubbs et al. subdivided terminal olefins into four categories dependent on their reactivity towards the applied catalyst. Type 1 olefins show rapid homodimerization and the homodimers are consumable. Type 2 olefins show slow homodimerization and the homodimers are sparingly consumable. Type 3 olefins show no homodimerization and can only react with type 1 or type 2 olefins. Type 4 olefins are inert to cross metathesis, but do not deactivate the catalyst. In general, if two olefins of the same type are crossed, a nonselective cross metathesis will result because parts of the educts are wasted as homodimers. In this case, an excess of one partner is necessary to provide a high yield of the cross product. High product selectivity can be obtained if two olefins of different types are crossed because the less reactive olefin will not make homodimers and the reaction product will not undergo secondary metathesis.

The *E*/*Z*-stereoselectivity of an olefin cross metathesis depends mainly on the steric bulkiness of the residues on the olefins, which favors the *E*-product (78). Also a redistribution of the products by secondary metathesis favors the thermodynamically more stable *E*-product (78).

2.3.3 Isomerization

Olefin isomerization along an alkyl chain is a side reaction in olefin metathesis that can significantly decrease the yield and hamper product purification. Factors that promote isomerization are high temperatures, high dilution, long reaction times, and high catalyst loadings (79). Isomerizations are caused by ruthenium hydride complexes (Fig. 2.3.3), which are formed by decomposition of two catalyst molecules (80). The isomerization of olefins could proceed by insertion of the olefin into the Ru-H bond and subsequent β-hydride elimination, but the exact mechanism is unknown. Isomerizations can be prevented by addition of hydride scavengers which do not reduce catalyst activity like acetic acid or *p*-benzoquinone. *p*-Benzoquinone is a Michael acceptor and also a type 4 olefin. In many cases, *p*-benzoquinone is more effective than acetic acid due to his twofold acceptor groups. Electron deficient benzoquinones like tetrafluoro-1,4-benzoquinone are even more effective than the parent compound.

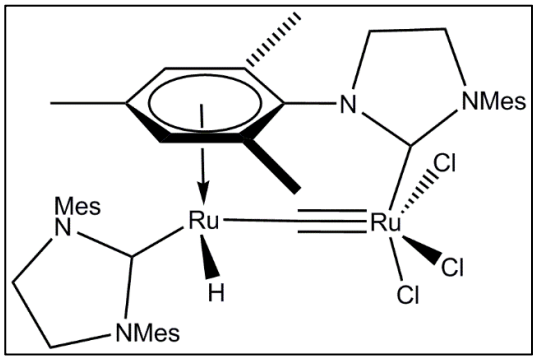

Fig. 2.3.3: Main product which is formed by decomposition of two catalyst molecules

2.4 Aims

2.4.1 Partial synthesis of homologous ganglioside standards

Internal ganglioside standards can be prepared by total synthesis (81) or by partial synthesis starting from natural gangliosides. Until today, total syntheses have been developed for the most common gangliosides with major contributions by the group

of Richard R. Schmidt (82-84). GQ1b, for instance, can be synthesized in a convergent synthesis in 26 steps starting from methyl [phenyl 5-acetamido-8-*O*-(5-acetamido-4,7,8,9-tetra-*O*-acetyl-3,5-dideoxy-D-*glycero*-*α*-D-*galacto*-2-nonulopyranosylono-1,9-lactone)-4,7-di-*O*-acetyl-3,5-dideoxy-2-thio-D-*glycero*-D-*galacto*-2-nonulopyranosid]-onate **a**, (2-trimethylsilyl)-ethyl 3,6-di-*O*-benzyl-*β*-D-galactopyranoside **b**, phenyl 2-deoxy-2-*N*-(2,2,2-trifluoroethoxy)carbonylamido-1-thio-*β*-D-galactopyranoside **c**, allyl 4,6-*O*-(4-methoxybenzylidene)-*β*-D-glucopyranoside **d**, and 3-*O*-benzoylceramide **e** (85) (Fig. 2.4.1). The synthesis of these building blocks requires additional 3 steps for the synthesis of **a** from colominic acid (86, 87), which is a commercially available *α*2-8 polymer of *N*-acetylneuraminic acid from *Escheria coli* K235 (88). Furthermore, it requires 4 steps for the synthesis of **b** from D-galactose (89-91), 3 steps for the synthesis of **c** from D-galactosamine (92, 93), 3 steps for the synthesis of **d** from 2,3,4,6-tetra-*O*-acetyl-*α*-D-glycopyranosyl bromide (94, 95), and 10 steps for the synthesis of **e** from D-xylose (96-98).

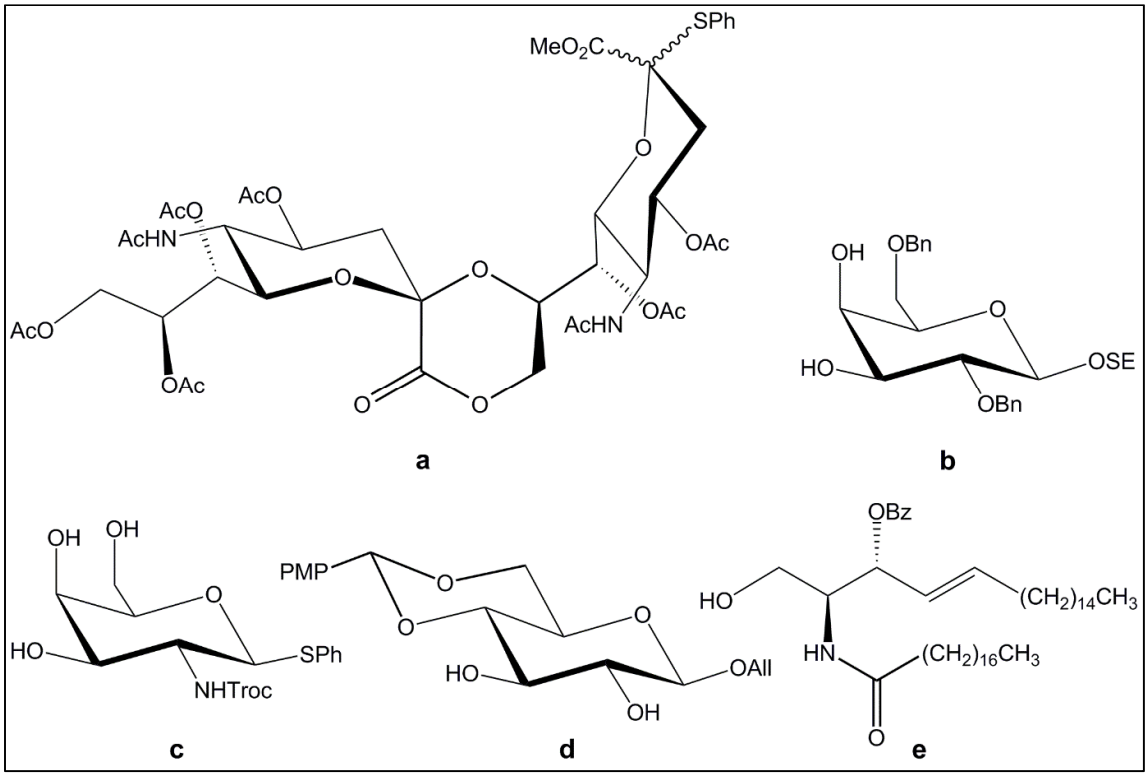

Fig. 2.4.1: *Common building blocks for the total synthesis of gangliosides (85)* (SE = 2-(trimethylsilyl)-ethyl, Troc = 2,2,2-trichloroethoxycarbonyl, PMP = *p*-methoxyphenyl)

In an alternative approach 3-benzoyl-2-azidosphingosine has been used instead of **e** because it has yields in the range of 80 % (98) in glycosylations with trichloroacetimidate-activated glycosyl donors compared to 48 % (85) reported for **e**. Another advantage of the use of protected azidosphingosine as glycosyl acceptor is its applicability for the total synthesis of lysogangliosides, which can be obtained by reduction of the azido group after the glycosylation step.

Due to the high effort required for total syntheses we chose partial syntheses of the title compounds. A partial synthesis of gangliosides was, for instance, described by Clasen for ganglioside GM3. He purified 3'-sialyl lactose from bovine colostrum and activated it as a trichloroacetimidate. Then, it was coupled to (2*S*,3*R*,*E*)-2-azido-1-hydroxyoctadec-4-en-3-yl benzoate by the method of Schmidt et al (98). After reduction, acylation, and removal of the protective groups he obtained GM3 in 7 steps (99). In another example Schwarzmann et al. synthesized ^{14}C-labeled GM1 containing a thioglycosidic bond to the ceramide part starting from natural GM1 (100). Thioglycosidic bonds are not cleavable by catabolic enzymes and thus can be used for metabolic studies of glycosphingolipids (101). First, the ganglioside sugar was isolated by the method of Wiegandt et al (102). Then, it was peracetylated and converted into an *α*-glycosyl bromide, which was treated with thioacetate in the next step. Conversion with an 1-Iodo-2-dichloroacetamido derivative of protected ceramide under weak alkaline conditions, removal of the protecting groups, and introduction of a labeled fatty acid lead to labeled SGM1 (Fig. 2.4.2).

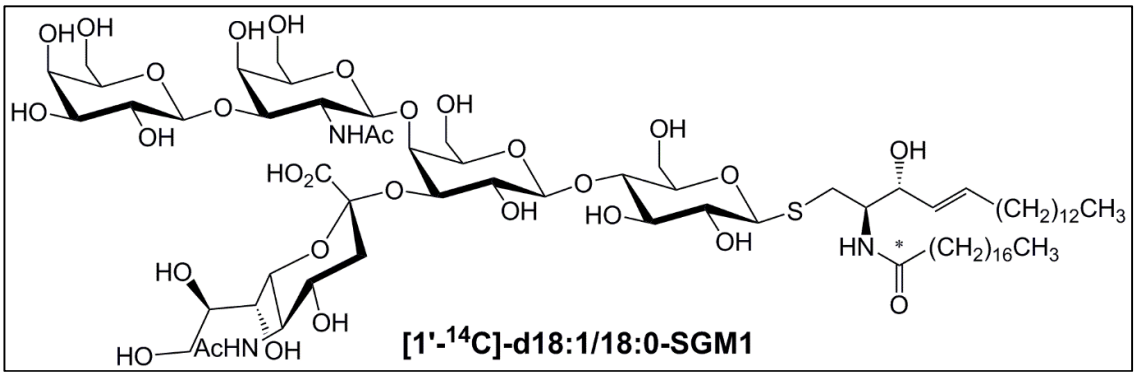

Fig. 2.4.2: ^{14}C-labeled thio-GM1 synthesized by partial synthesis starting from natural GM1 (100)

One concept for the synthesis of pure ganglioside lipoforms is the modification of the fatty acid residue. A new concept is the modification of the sphingosine part, which has only been applied to ceramides, yet (103).

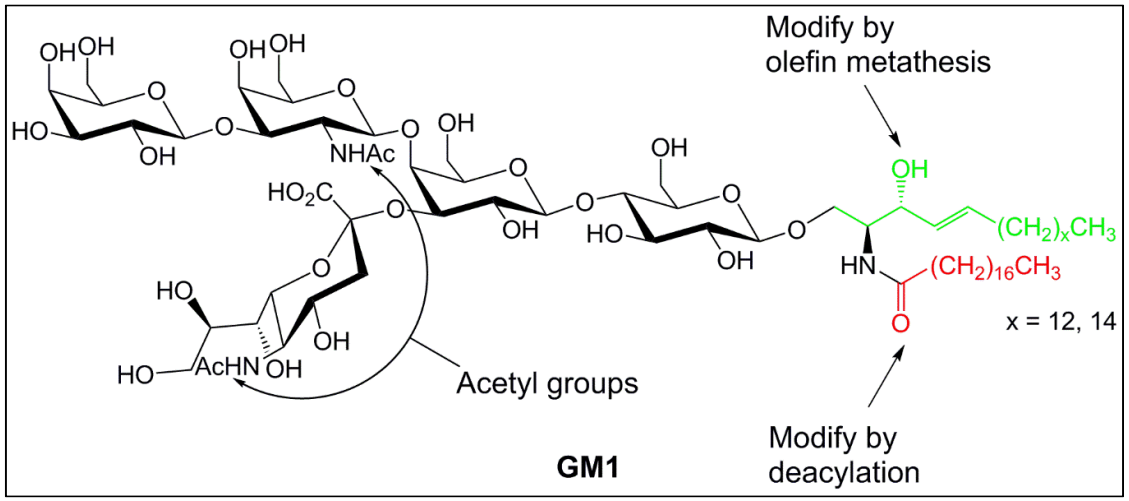

Fig. 2.4.3: Concepts for the partial synthesis of ganglioside lipoforms

The fatty acid part of gangliosides can be modified by deacylation to lysogangliosides and subsequent reacylation by an activated fatty acid (104). Up to now, three methods have been reported for the first step (Fig. 2.4.4). The first method is a chemical deacylation under alkaline conditions (105). As a reason for the regioselectivity in the deacylation of ganglioside GM1 to lyso-GM1 (105) it can be assumed that the negative charge of the sialic acid group repels the attacking hydroxide ion. If this assumption is correct, the method should also be applicable to the regioselective deacylation of oligosialogangliosides. The second method is a three-step synthesis in which gangliosides are completely deacylated except on their *N*-acetylgalactosamine residue in the first step (Fig. 2.4.5). Then, the amino group in the sphingosine part is regioselectively protected by an Fmoc-group. Subsequently, the remaining amino groups are reacetylated and the protecting group is removed. The overall yield is 30 % for GM1, GM2, GM3, and GD1a (106). The third method is an enzymatic deacylation by using sphingolipid ceramide *N*-deacylase (SCDase), which is reported to be regioselective for GM1 (107), GM2, GM3, GD3, GD1a, and GQ1b (108). In the work of Kurita et al (107). and Ito et al (108) the extent of hydrolysis for the mentioned gangliosides was determined by densitometry. The products were not purified and the yields were not determined. The next step in this work should be a reacylation by activated myristic acid or heptadecanoic acid, which

could be activated as *N*-hydroxysuccinimide esters (104). This method should be applied to lyso-GM1, lyso-GD1a, lyso-GD1b, lyso-GT1b, and lyso-GQ1b.

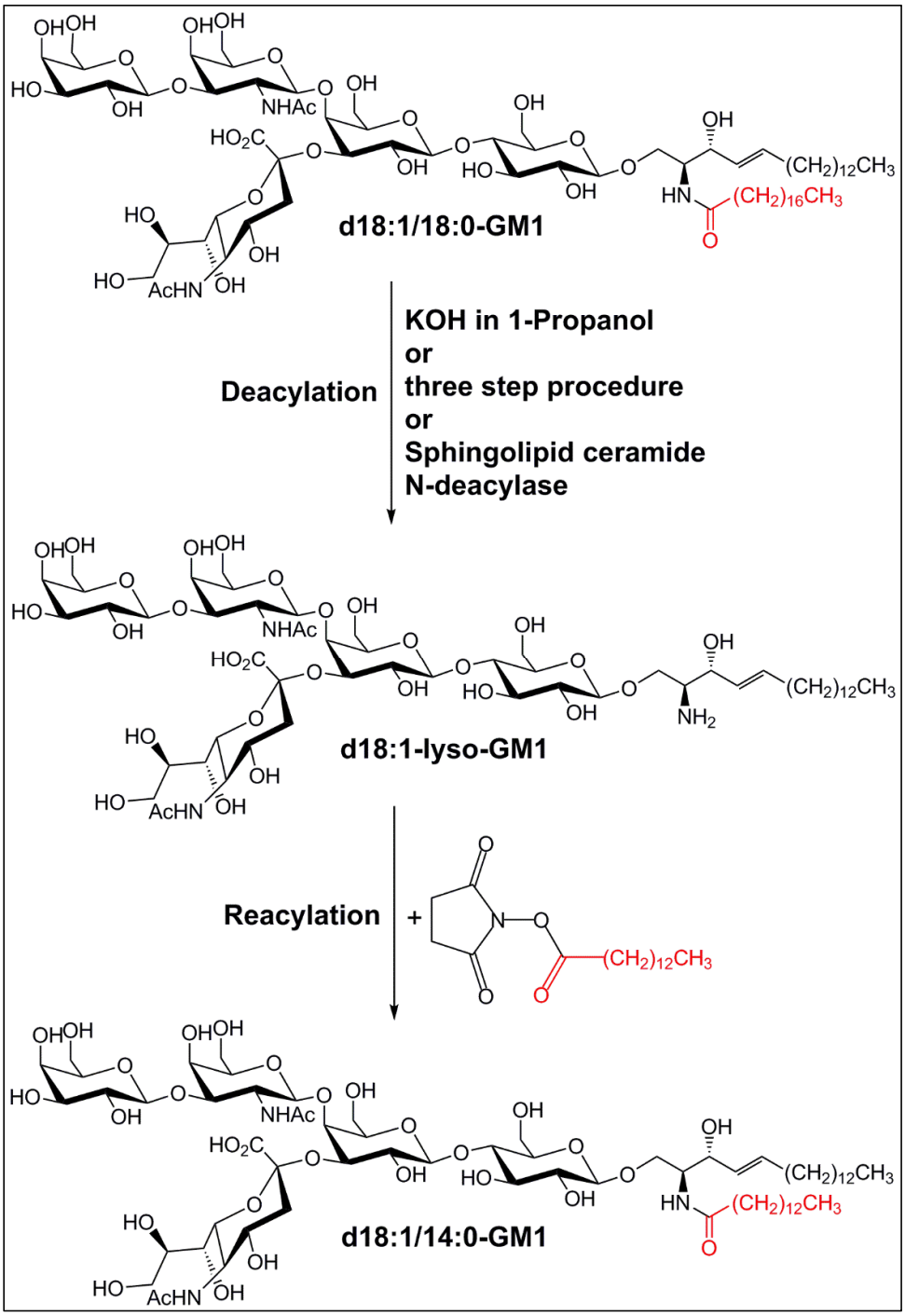

Fig. 2.4.4: Modification of the acyl chain of gangliosides

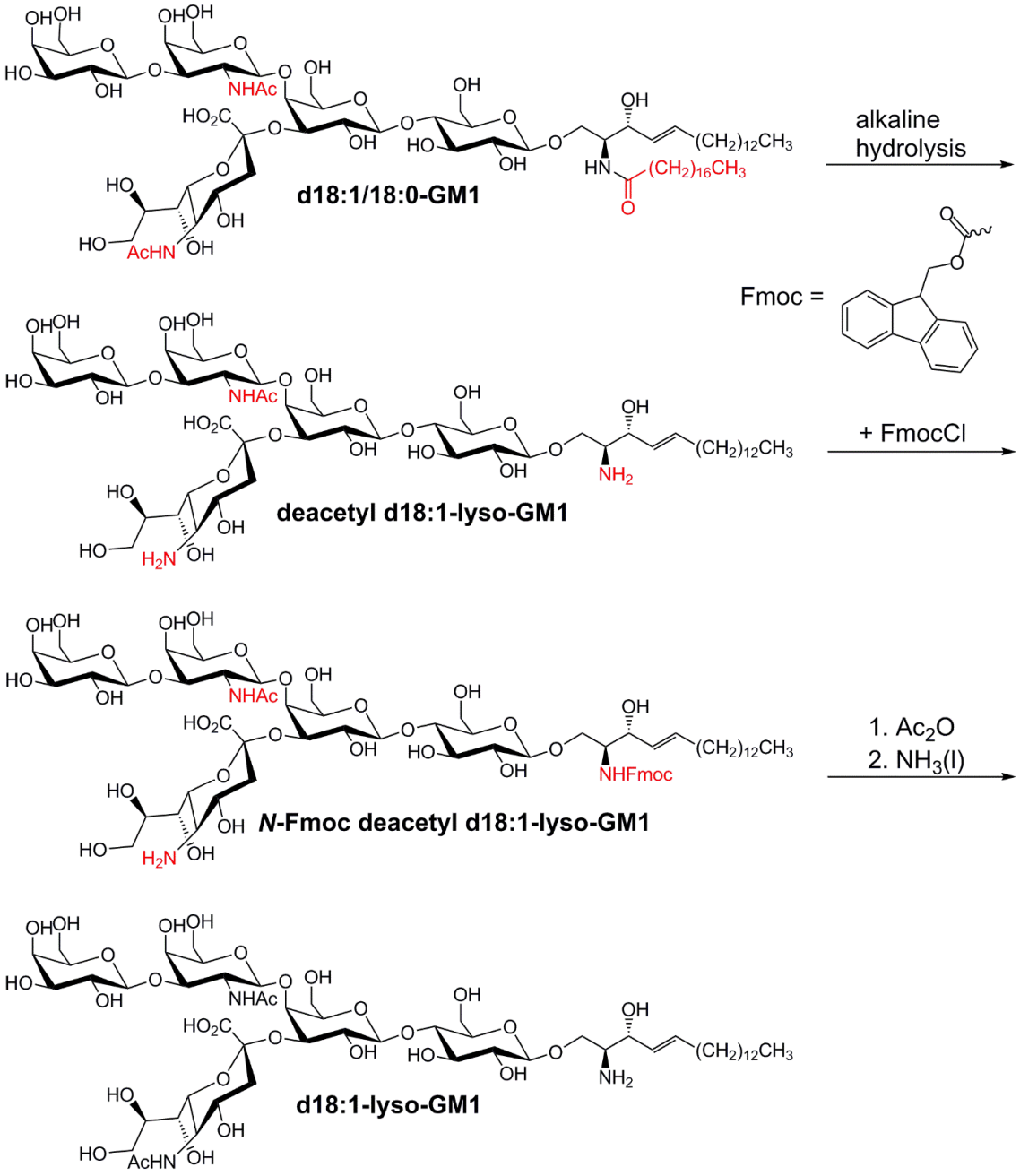

Fig. 2.4.5: Three step procedure for the preparation of lysogangliosides

2.4.2 Purification of the educts

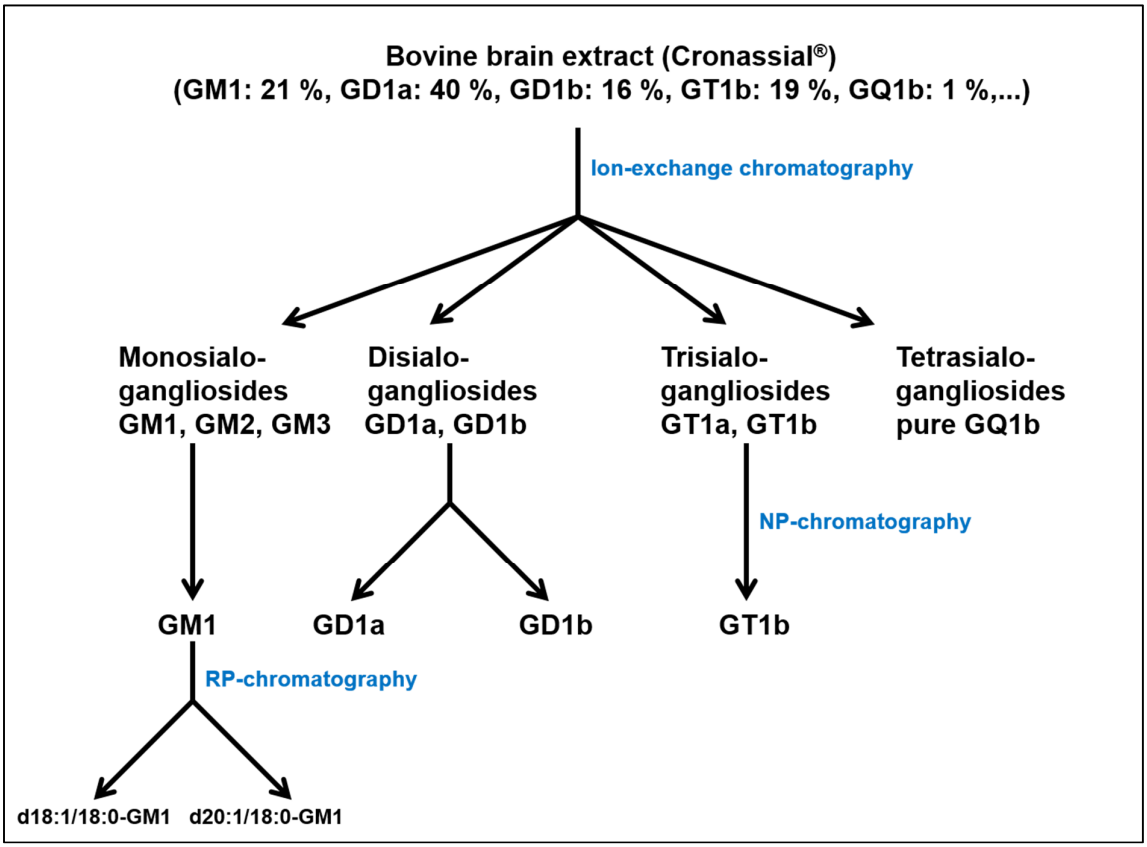

Fig. 2.4.6: Plan for the separation of the ganglioside mixture Cronassial®. The RP chromatography step is shown only for GM1, but was also applied to the other gangliosides.

For the partial synthesis planned in this work, a sufficient amount of starting material was required. A source that was available to us is a commercial mixture of gangliosides purified from bovine brain for pharmaceutical purposes (Cronassial®). It consists of 21 % of GM1, 40 % of GD1a, 16 % of GD1b, 19 % of GT1b, and 4 % of other gangliosides (109). As the first purification step we decided to use a separation into mono-, di-, tri- and tetrasialogangliosides by anion-exchange chromatography using a modified method of Momoi et al (110). The next step was a further purification of these ganglioside classes by NP-chromatography to get GM1, GD1a, GD1b, and GT1b. Then, the C_{18}- and C_{20}-sphingosine homologs of each ganglioside were separated by RP-chromatography.

2.4.3 Preparation of ganglioside standards by degradation of other standards

Another approach to prepare ganglioside standards is the enzymatic degradation of already prepared ganglioside standards with modified lipid part. We used a beta-galactosidase from bovine testes, an exoglycosidase, which can hydrolyze terminal galactosyl residues in β1-3, β1-4, and β1-6 linkage from saccharides, glycosaminoglycans, glycoproteins, and glycolipids (111).

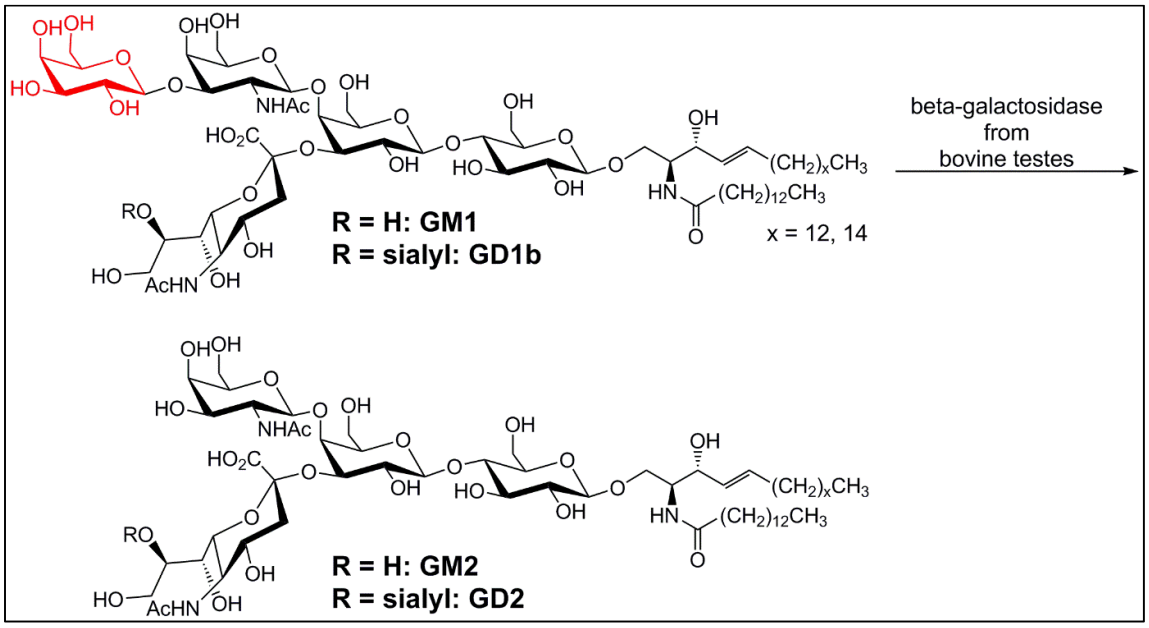

Fig. 2.4.7: Plan for the enzymatic degalactosylation of already synthesized ganglioside standards

The degradation of GM1 to GM2 by this enzyme has been reported by Larsson et al. for fluorescence labeled GM1 in a yield of 54 % and for fluorescence labeled asialo-GM1 in a yield of 58 % (112). Therefore, it should be possible to prepare a GM2-standard from the GM1-standard and, as a new approach, a GD2-standard from the GD1b-standard.

2.4.4 Development of a new synthetic method to modify the sphingosine chain of gangliosides

An alternative method for the synthesis of artificial ganglioside lipoforms can be a modification of the sphingosine chain. One appropriate reaction sequence might be an ozonolysis to a ganglioside aldehyde followed by a Wittig reaction.

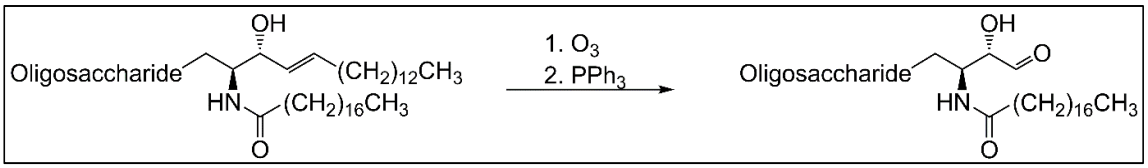

Fig. 2.4.8: Synthesis of ganglioside aldehydes

Ozonolysis was rarely used for the synthesis of ganglioside aldehydes because of fragmentation under alkaline conditions and formation of a side product by isomerization of the allyl alcohol, which was reported by Wiegandt et al (113). In 2009, aldehydes of GM1 and GM3 obtained after ozonolysis have been used for reductive amination reactions (114). Yields for the ozonolysis reaction were not reported in this study. Usually, ozonolysis has been used to isolate the oligosaccharide part of glycosphingolipids after subsequent alkaline fragmentation of the aldehyde (115). The overall yield for ozonolysis and alkaline fragmentation was reported to be 60 % (100). A procedure to obtain protected ganglioside aldehydes after dihydroxylation and periodate cleavage has been reported by Hakomori et al (116). But this method was also just used to isolate the oligosaccharide part of gangliosides and not to isolate the aldehyde.

An alternative approach can be an olefin cross metathesis. The first step would be a peracetylation of the ganglioside in order to make it soluble in unpolar solvents. The second step can be an ethenolysis in order to get gangliosides bearing terminal olefin groups. However, ethenolysis (tested by the model methyl oleate using standard Ru-based catalysts) has yields only in the range of 13 to 57 % (117) resp. 13 to 24 % (118). In the recent years, more effective catalysts for ethenolysis have been developed, which give yields up to 95 % (119) resp. 80 % (120), but only for (*Z*)-olefins. These catalysts are much more reactive towards (*Z*)-olefins than towards (*E*)-olefins because the residues of the olefin are forced into the same direction in the metallacyclobutane formation by bulky ligands (78). Presumably, these catalysts

cannot be applied to gangliosides, which contain (*E*)-double bonds. In 2006, Patel et al. suggested a 2-butenolysis instead of an ethenolysis. They could achieve a yield of 96 % in the 2-butenolysis of methyl oleate (121). Based on this approach, we investigated a stilbenolysis for the modification of the sphingosine chain of gangliosides (Fig. 2.4.9).

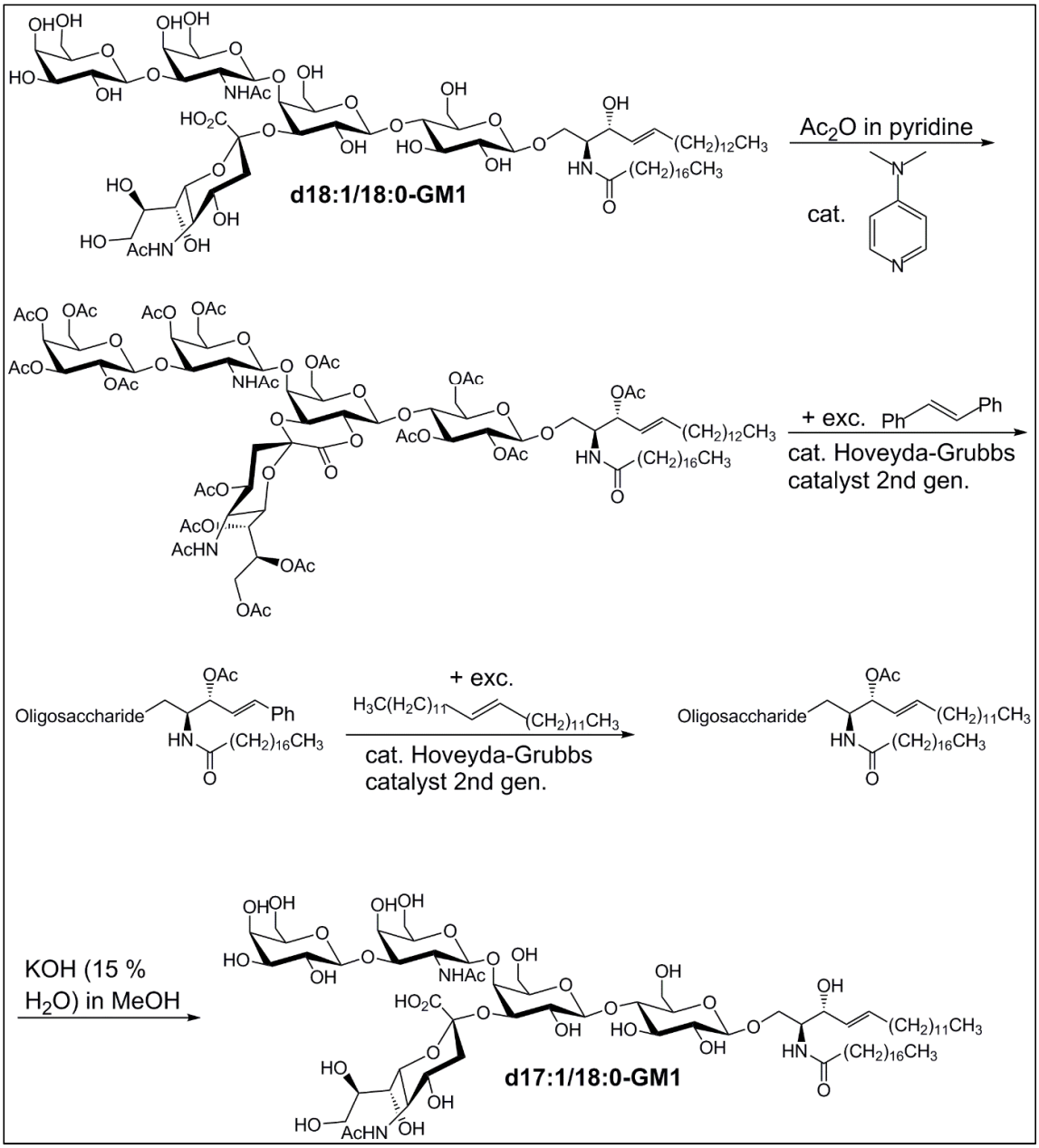

Fig. 2.4.9: Plan of synthesis for the modification of the sphingosine chain of gangliosides

The concept has three advantages: First, the phenyl group facilitates the chromatographic purification because it is more polar than the alkyl group, which is a

key requirement for the preparation of ganglioside standards. Second, the phenyl group serves as an UV-probe. Third, stilbene is not prone to isomerizations because the phenyl group stops the migration of the double bond. The next step should be another olefin metathesis in which an excess of hexacos-13-ene is used. A direct reaction of a peracetylated ganglioside lactone is impracticable because of separation problems. In the last step, the protecting groups should be cleaved by alkaline hydrolysis.

3 Results

3.1 Purification of gangliosides

3.1.1 Purification of GM1, GD1a, GD1b, GT1b, and GQ1b from Cronassial®

An attempt was made to separate Cronassial® by isocratic NP column chromatography using $CHCl_3$/MeOH/0.2 % aq. $CaCl_2$ 60:35:8 v/v/v as eluent. Salts like $CaCl_2$ are used because they improve the separation of gangliosides (122), which is explained by an association of strongly ionized cations with the gangliosides to ion pairs, which can be better separated (123). By this, GM1 and GD1a were obtained in pure form. GD1b could not be separated from GD1a and GT1b could not be separated from GQ1b by this method. From 1.02 g of Cronassial® 135 mg of GM1 and 246 mg of GD1a were obtained after desalting.

In another approach, Cronassial® was separated into mono-, di-, tri-, and tetrasialogangliosides by anion-exchange chromatography using the weak anion exchanger DEAE-sephadex® (diethylaminoethyl-sephadex). In contrast to Momoi et al. (110), a step gradient instead of a linear gradient was applied. The monosialogangliosides did not adsorb completely so they were partially eluted by pure $CHCl_3$/MeOH/H_2O 30:60:8 v/v/v. The reason for this could be a slightly overloading of the column, but it did not disturb the separation. Another part was eluted by an NH_4OAc-concentration of 0.05 mol/L. The disialogangliosides and also the trisialogangliosides were successively eluted by an NH_4OAc-concentration of

0.15 mol/L and could be separated without overlap. The tetrasialogangliosides, which consisted only of GQ1b, were eluted by an NH_4OAc-concentration of 0.45 mol/L. The ganglioside classes were analyzed by HPTLC (Fig. 5.2.1). From 5.03 g of Cronassial 4.79 g of gangliosides (27 % monosialogangliosides, 58 % disialogangliosides, 14 % trisialogangliosides and 0.88 % tetrasialogangliosides) were obtained after desalting (95 % recovery) (Tab. 5.2.1).

In the next step the ganglioside classes were separated by NP column chromatography using different techniques and different solvent systems. From 1.28 g of monosialogangliosides only 300 mg GM1 were obtained in pure form because of impurities migrating close to GM1 like GM2 and GM3, which could only partially be separated. It was observed that GD1a and GD1b, which make up the greater part of the disialogangliosides, cannot be separated well by isocratic elution. This problem was overcome by using a step gradient of $CHCl_3$/MeOH/2.5 M NH_3 60:35:6 v/v/v for the elution of GD1a and $CHCl_3$/MeOH/2.5 M NH_3 60:35:8 v/v/v for the elution of GD1b. From 1.00 g of disialogangliosides 472 mg of GD1a and 158 mg of GD1b were obtained. GT1b makes up the greater part of the trisialogangliosides. From 672 mg of trisialogangliosides 382 mg of pure GT1b were obtained. GQ1b was already obtained in pure form after anion-exchange chromatography and subsequent desalting. From 5.03 g of Cronassial 41.5 mg of GQ1b were obtained.

Ganglioside	Amount (mg)
GM1	300
GD1a	472
GD1b	158
GT1b	382
GQ1b	41.5

Tab. 3.1.1: Gangliosides that were obtained by purification of Cronassial®

The purified gangliosides were analyzed by HPTLC, ESI-MS and ESI-MS/MS. The NP-HPTLCs showed only one band for each ganglioside (Fig. 3.1.1). The RP-TLCs showed two distinct bands for each ganglioside (Fig. 3.1.2, presented for GQ1b). Hereby, the upper band corresponds to the more polar d18:1/18:0-lipoform and the lower band to the less polar d20:1/18:0-lipoform.

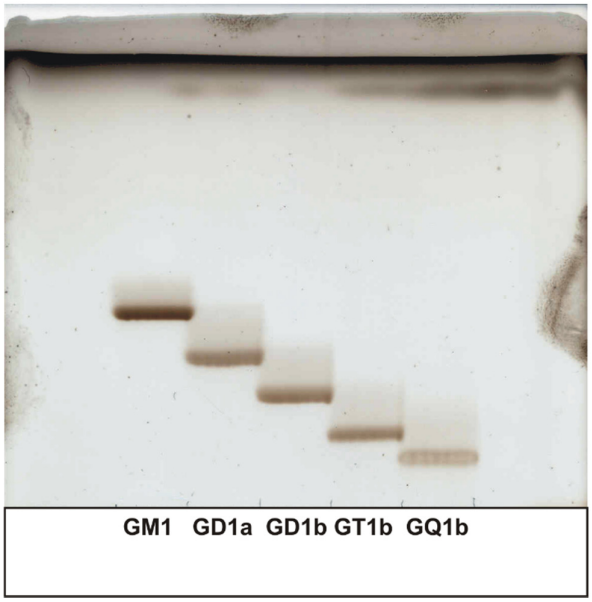

Fig. 3.1.1: *NP HPTLC of the purified gangliosides.* Solvent system: $CHCl_3$/MeOH/0.2 % aq. $CaCl_2$ 45:55:10 v/v/v.

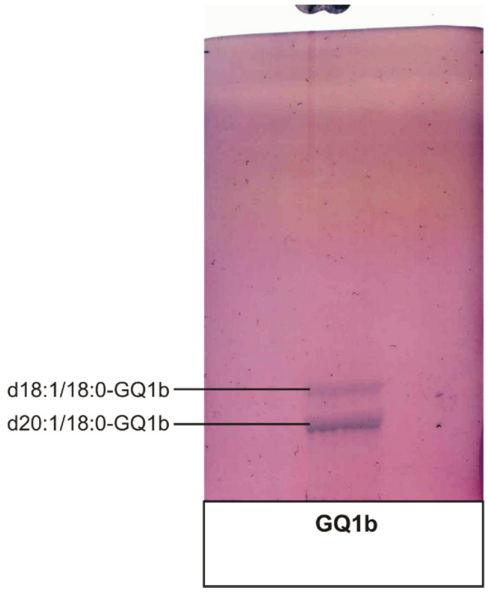

Fig. 3.1.2: *RP HPTLC of GQ1b.* Solvent system: MeOH/H_2O 90:20 v/v.

By ESI-MS, it was demonstrated that GM1, GD1a, GD1b, and GQ1b consist mainly of d18:1/18:0- and d20:1/18:0-ceramide. For GT1b, also the occurrence of a d20:1/20:0-species, which made up to 11 % of the total GT1b content, was measured (Fig. 3.1.3).

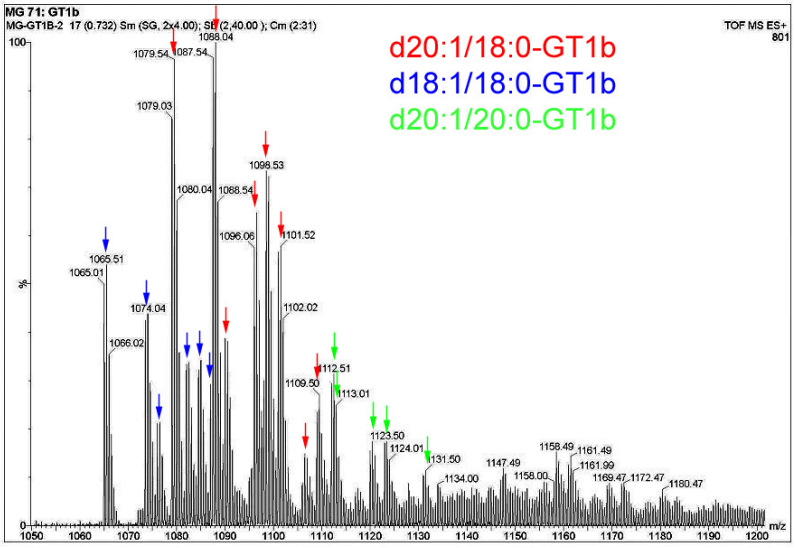

Fig. 3.1.3: *ESI-MS of GT1b*

This species could not be measured in the other gangliosides, so it might have been separated in previous chromatography steps. The structure of the ganglioside species was analyzed by ESI-MS/MS of the most intensive peaks. Hereby, the structure of the oligosaccharide chain is derived from B- and C-series fragments while the structure of the ceramide base is derived from Z- and Y-series fragments. The gangliosides analyzed contained exclusively d18:1/18:0-ceramide species resp. d20:0/18:0-ceramide species. But isobaric d20:1/18:0- and d18:1/20:0-ceramide species, which can occur in traces, could not be differentiated by ESI-MS and also not by RP-TLC.

3.1.2 Purification of ganglioside lipoforms by RP column chromatography

In the next step the gangliosides were separated isocratically by RP column chromatography using MeOH/H_2O in different compositions as eluent. The results are given in Table 3.1.2. After separation, the obtained ganglioside lipoforms were purified from column material (section 5.1.8) by NP-chromatography. Every ganglioside fraction contained significantly more d20:1/18:0-lipoform than d18:1/18:0-lipoform. Beside these lipoforms, also compounds were observed that migrated in-between the main lipoforms on RP-TLC (Fig. 3.1.4), but they could not be separated and analyzed.

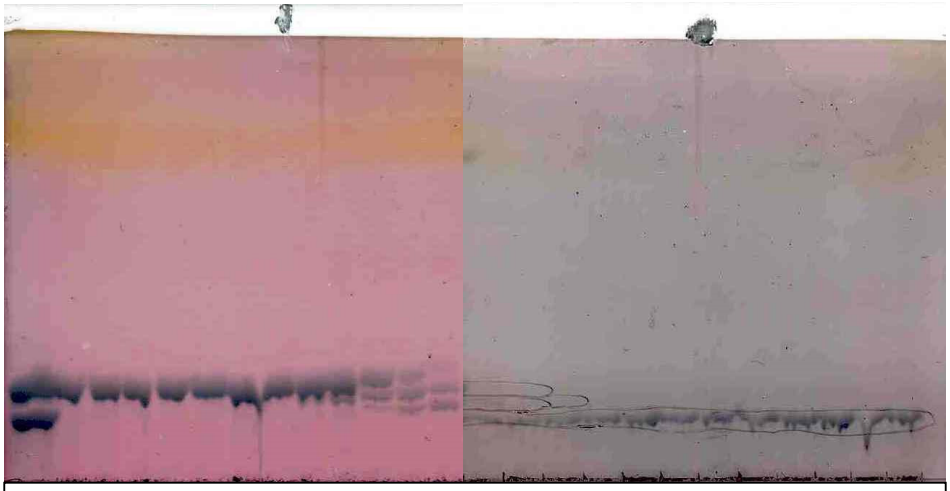

Fig. 3.1.4: *RP HPTLCs of the separation of GM1 by RP column chromatography.*
Solvent system: MeOH/H_2O 90:10 v/v.
Visualization: Kägi-Miescher reagent

Gang-lioside	m (input) (mg)	m (d18:1/18:0-lipoform) (mg)	m (d20:1/18:0-lipoform) (mg)	Solvent system
GM1	300	64.8	100	MeOH/H_2O 90:25 v/v
GD1a	472	89.5	not determined	MeOH/H_2O 90:49 v/v
GD1b	76	not determined	19.1	MeOH/H_2O 90:40 v/v
GT1b	382	not determined	40.4	MeOH/H_2O 90:40 v/v
GQ1b	125	not determined	55.3	MeOH/H_2O 90:50 v/v

Tab. 3.1.2: *Results of the purification of the gangliosides GM1, GD1a, GD1b, GT1b, and GQ1b by RP column chromatography. The purified amounts of the ganglioside lipoforms are given in column 3 and 4.*

Pure ganglioside lipoforms were obtained in amounts of 19.1 mg to 100 mg (Tab. 3.1.2). They were analyzed by RP TLC (Fig. 3.1.6), ESI-MS, ESI-MS/MS, ^{1}H-NMR, and CHN analysis. ESI-MS demonstrated a clear separation of the d18:1- and d20:1 lipoforms. The ESI-MS of d20:1/18:0-GT1b·3NH_3 showed traces of d20:1/20:0-GT1b·3NH_3 in a quantity of 6.0 % (Fig. 3.1.5). The fragments in the ESI-MS/MS spectra could clearly be correlated to the structure of the lipoforms on the basis of the Z- and Y-series fragments. In the ^{1}H-NMR spectra, the olefinic protons, the anomeric protons, the acetyl protons, and the methyl and methylene protons of the ceramide

part could be assigned. Other assignments were made by comparison to literature (124, 125)

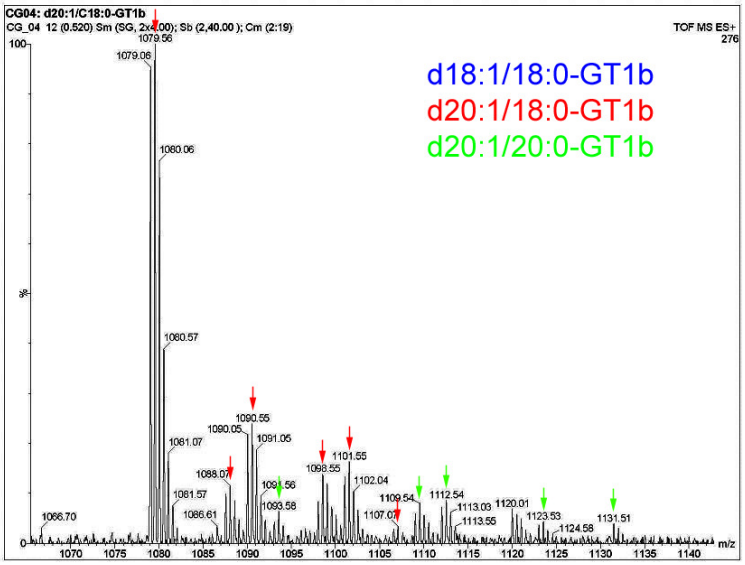

Fig. 3.1.5: *ESI-MS of d20:1/18:0-GT1b·3NH$_3$*

Fig. 3.1.6: *RP HPTLC of d20:1/18:0-GT1b.*
Solvent system: MeOH/H_2O 90:9 v/v.

The signal at 1.98 ppm was correlated to H-6 of the ceramide part also by comparison to literature (105). The ^{1}H-NMR spectra of GD1b, GT1b, and GQ1b were assigned by comparison to the spectra of GM1 and GD1a. The signal at 1.88 ppm indicated the presence of further acetyl groups in the spectra of GD1a, GD1b, GT1b, and GQ1b. The integral of the multiplet at 1.22 ppm indicated the lengths of the alkyl chains.

Quantification of gangliosides by sialic acid determination is necessary because weighing is inaccurate due to residual water content and residual column material. The usage of pure Neu5Ac and α_1-acid glycoprotein, which contains 12.6 wt% Neu5Ac (106), as external were tested for d18:1/18:0-GM1·NH_3 (**1**) and d18:1/18:0-GD1a·2NH_3 (**3**), but gave deviant results. Hence, we decided to analyze the purity of the ganglioside lipoforms by elemental analysis and to use these substances as calibration standards for other probes. The purity of the obtained ganglioside lipoforms was 86-95 % (Tab. 3.1.3). The discrepancy of the values is due to residual water content as it is observed in monosaccharides.

Ganglioside	Purity (wt%)
d18:1/18:0-GM1·NH_3 (**1**)	88.5
d20:1/18:0-GM1·NH_3 (**2**)	94.8
d18:1/18:0-GD1a·$2NH_3$ (**3**)	90.4
d20:1/18:0-GD1b·$2NH_3$ (**4**)	90.1
d20:1/18:0-GT1b·$3NH_3$ (**5**)	86.9
d20:1/18:0-GQ1b·$4NH_3$ (**6**)	85.7

Tab. 3.1.3: *Results of the elemental analysis of the purified ganglioside lipoforms*

Although the two GM1 lipoforms were purified by the same procedure, **2** was more anhydrous than **1**. The reason is that it was dried *in vacuum* instead of lyophilization. The water content of gangliosides was also demonstrated by ^{1}H-NMR of d18:1/18:0-GD1a·$2NH_3$ (**3**) (Fig. 3.1.7).

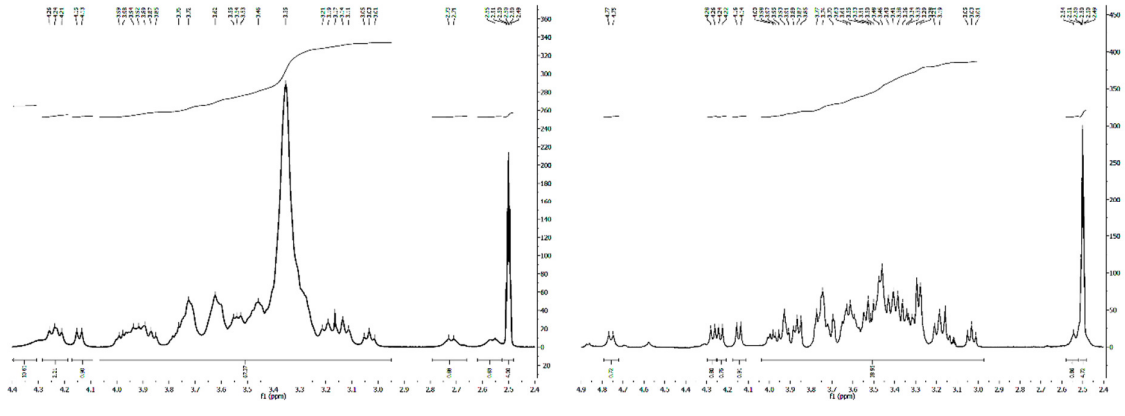

Fig. 3.1.7: *Comparison of ^{1}H-NMR spectra of d18:1/C18:0-GD1a·$2NH_3$ (**3**).The range from 2.4 to 4.9 ppm is shown.*

Left figure: ^{1}H-NMR spectrum without exchanging of exchangeable protons. The water signal can be seen at 3.35 ppm. Right figure: ^{1}H-NMR spectrum after exchanging all exchangeable protons by deuterium. The water signal has vanished.

3.2 Preparation of lysogangliosides

3.2.1 Chemical preparation of lysogangliosides

This part of the work was focused on one step preparations of lysogangliosides. In the chemical deacylation potassium hydroxide in an alcohol was used. The reaction is an amide hydrolysis under alkaline conditions.

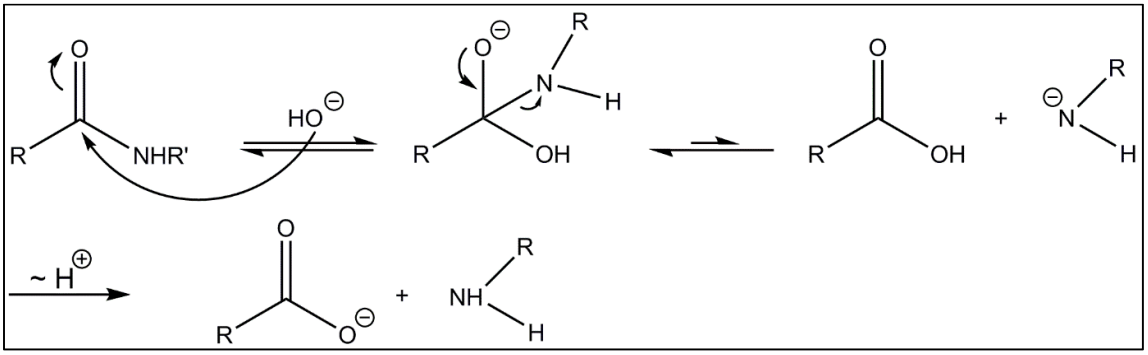

Fig. 3.2.1: *Mechanism of the amide hydrolysis under alkaline conditions (126)*

The reaction is reported to be regioselective for the preparation of lyso-GM1 in a yield of 54 % (105). For the preparation of lyso-GM3 from GM3, a yield of 36-40 % by using sodium *tert*-butoxide in MeOH has been reported, which is more a statistical deacylation rather than a regioselective deacylation (127). In this work, KOH in 1-propanol was applied to d18:1/18:0-GM1·NH_3 and d18:1/18:0-GD1a·2NH_3 (Tab. 3.2.1).

Lysoganglioside	Amount (mg)	Yield (%)
d18:1-lyso-GM1·NH_3 (**7**)	8.69	52
d18:1-lyso-GD1a·2 NH_3 (**8**)	1.23	4.8

Tab. 3.2.1: *Results of the chemical preparation of lyso-gangliosides*

d18:1-Lyso-GM1·NH_3 was obtained in a yield of 52 %. In the case of GD1a, however, the yield of lyso-GD1a dropped to 4.8 % due to the formation of other deacylation products. The ESI-MS spectra of the products showed no impurities of other ganglioside lipoforms. Sialic acid determination demonstrated a product content of

97.5 % resp. 80.2 % compared to the weighed quantity. Two experiments were performed in order to increase the yield of the chemical preparation of lyso-GD1a. First, the reaction was performed anhydrously by using potassium *tert*-butoxide instead of KOH, which contains a residual water content of 15 %. After a reaction time of 12 h, TLC-analysis revealed no increase in the regioselectivity. In a second experiment the reaction temperature was reduced to 80 °C and the quantity of educt and product were analyzed after different reaction times. After 12 h reaction time, six compounds were present in the reaction medium in both experiments. Densitometric analysis of a 4 µL aliquot of the reaction mixtures revealed the following distribution:

Band	**R_f**	**Ganglioside**	**Quantity (%) (Exp. 1)**	**Quantity (%) (Exp. 2)**
1	0.38	d18:1/18:0-GD1a	25.1	64.1
2	0.31	Byproduct 1	23.3	23.9
3	0.27	d18:1-lyso-GD1a	14.7	12.0
4	0.22	Byproduct 2	10.0	0.0
5	0.18	Byproduct 3	17.4	0.0
6	0.11	Byproduct 4	9.4	0.0

Tab. 3.2.2: Densitometric analysis of the chemical deacylation of d18:1/18:0-GD1a· 2 NH_3 after 12 h reaction time. Quantities were calculated by the following equation:

$$\text{quantitiy} = \frac{A_i}{\sum A_i} \cdot$$

These results demonstrate that after 12 h at 90 °C approximately 60 % of the educt is converted to byproducts while only 14.7 % is converted to product. After 12 h at 80 °C only 12 % of the educt is converted to product whereas 23.9 % is converted to a byproduct migrating slightly faster on NP-TLC. This product could be monodeacetyl-GD1a. The quantity of the educt and the product were also analyzed at different reaction times. 4 µL of the reaction mixture was taken each time and quantified by HPTLC followed by densitometry (Fig. 3.2.2).

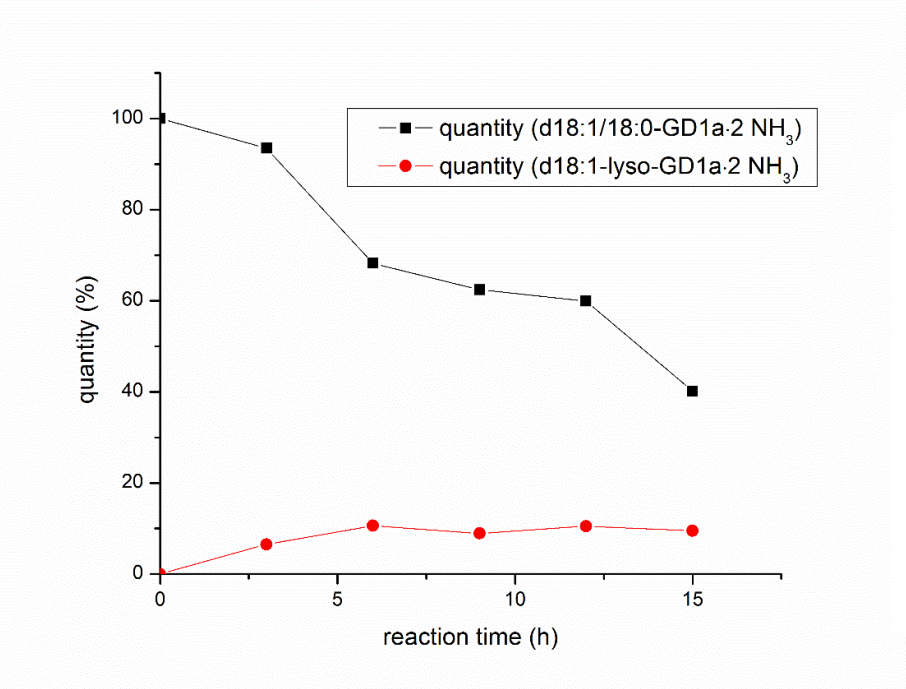

Fig. 3.2.2: *Densitometric analysis of d18:1/18:0-GD1a·2NH$_3$ and d18:1-lyso-GD1a·2NH$_3$ in the chemical deacylation at different reaction times*

The results demonstrated that after 6 h a minor amount of 10-15 % is converted to lyso-GD1a. In the following 9 h of reaction time the amount of lyso-GD1a remained constant while further amounts of educt were converted to byproducts.

3.2.2 Enzymatic preparation of lysogangliosides

The enzyme sphingolipid ceramide *N*-deacylase (SCDase) catalyzes the hydrolysis and also the reverse reaction of various glycosphingolipids, but not ceramides, in a reversible manner (128). Its enzyme classification number is EC 3.5.1.69, which means it is a hydrolase that acts on amide bonds other than peptide bonds in linear amides (129).

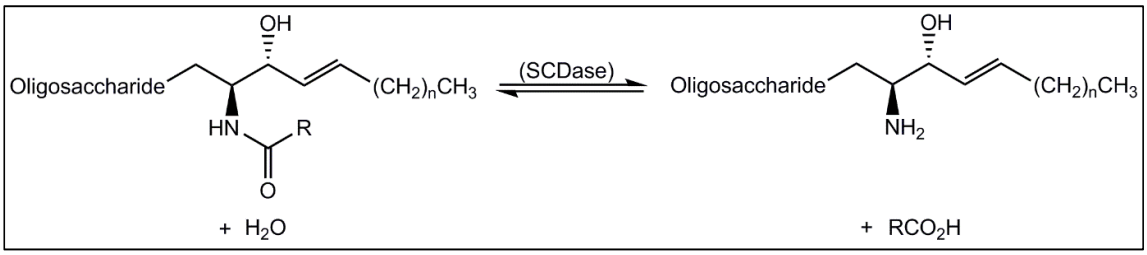

Fig. 3.2.3: *Reaction catalyzed by the enzyme sphingolipid ceramide N-deacylase*

The site of the equilibrium depends mainly on the reaction conditions. A pH value of 5-6 favors the hydrolysis while a pH value of 7 favors the condensation. A high detergent concentration favors the hydrolysis while a low detergent concentration favors the condensation. In general, the v_{max} value but also the K_m value of the condensation reaction is one order of magnitude higher than for the hydrolysis reaction so that the catalytic efficacy k ($k = \frac{v_{max}}{K_m}$) is comparable (128). The reaction mechanism of SCDase is unknown. But it could be demonstrated that Trp- and Arg residues are essential and that hydrolysis and condensation are catalyzed by the same active site (128). The method was applied to d18:1/18:0-GD1a·2NH_3, d20:1/18:0-GD1b·2NH_3, d20:1/18:0-GT1b·3NH_3, and d20:1/18:0-GQ1b·4NH_3 (Tab. 3.2.3).

Lysoganglioside	**$n_{SCDASE}/n_{substrate}$ (mU/µmol)**	**Amount of Lyso-ganglioside (mg)**	**Yield (%)**
d18:1-lyso-GD1a·2NH_3 (**8**)	110	0.74	47
d20:1-lyso-GD1b·2NH_3 (**9**)	110	1.72	53
d20:1-lyso-GT1b·3NH_3 (**10**)	73.6	1.16	60
d20:1-lyso-GQ1b·4NH_3 (**11**)	74.3	0.97	44

Tab. 3.2.3: *Results of the enzymatic preparation of lysogangliosides*

Yields were in the range of 44 to 60 %. The ESI-MS spectrum of d18:1-lyso-GD1a·2NH_3 showed no impurities of other ganglioside lipoforms. By comparing the $[M + 2H]^{2+}$ peaks, it was found that d20:1-lyso-GD1b·2NH_3 contained an impurity of 3.1 % of d18:1-lyso-GD1b·2NH_3, which is due to traces of d18:1/20:0-GD1b·2NH_3 in the precursor, which could not be separated by RP column chromatography. Also, d20:1-lyso-GT1b·3NH_3 contained 4.7 % of d18:1-lyso-GT1b·3NH_3. For d20:1-lyso-GQ1b·4NH_3 no other GQ1b-lipoforms could be detected. The fragments in the ESI-MS/MS spectra could clearly be correlated to the structure of the lysoganglioside lipoforms.

3.3 Reacylation of lysogangliosides

Tetradecanoic acid and heptadecanoic acid were activated as *N*-hydroxysuccinimide esters by a modified method of Lapidot et al (130).

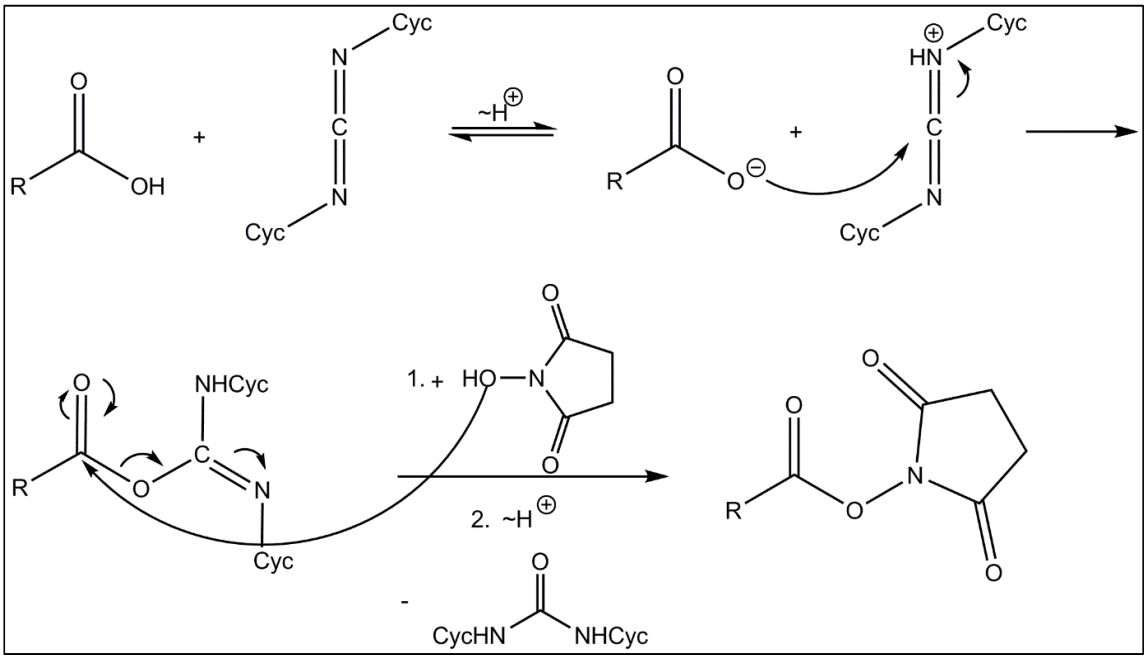

Fig. 3.3.1: *Mechanism of carboxylic acid activation by DCC and N-hydroxysuccinimide (131)*

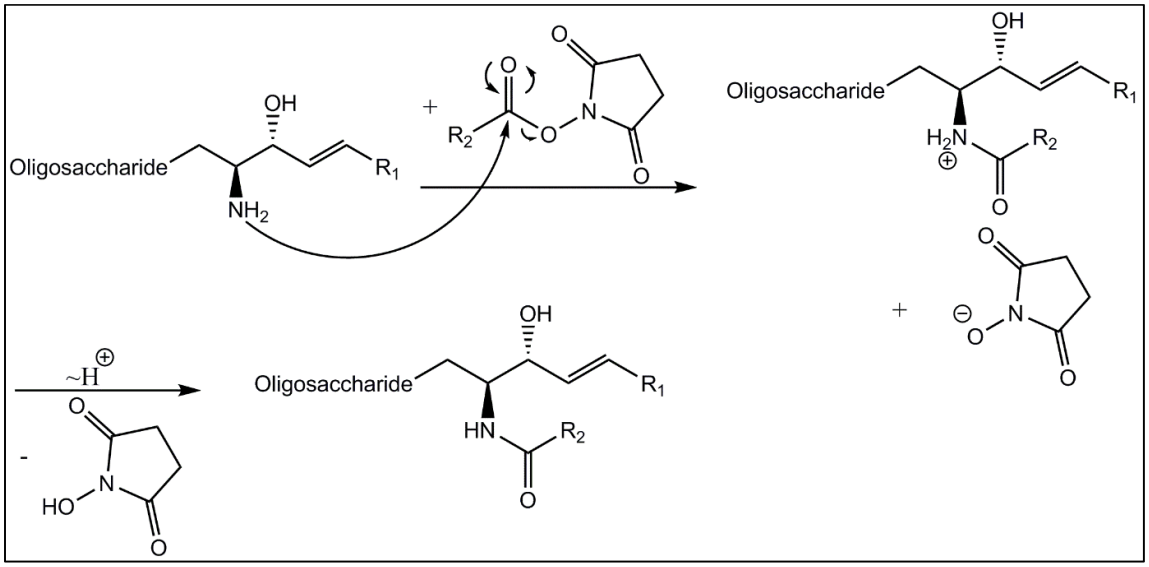

Fig. 3.3.2: *Reacylation of lysogangliosides by N-hydroxysuccinimide esters*

N-Hydroxysuccinimide esters do not react with hard nucleophils like carboxyl groups or hydroxyl groups but with softer ones like amino groups (130). The activation of tetradecanoic acid and heptadecanoic acid was performed in a yield of 72 % resp. 66 %. The products were characterized by ^{1}H-NMR, ^{13}C-NMR, EI-MS, and CHN-analysis. In the next step, the lysogangliosides were reacylated by a method of Schwarzmann and Sandhoff (104). An excess of the non-nucleophilic Hünig's base was applied for two reasons. First, amino groups are better nucleophils than hydroxyl groups under weak alkaline conditions. Second, the zwitterionic form of the lysogangliosides has to be deprotonated. The reaction was applied to d18:1-lyso-GM1·NH_3, d18:1-lyso-GD1a·$2NH_3$, d20:1-lyso-GD1b·$2NH_3$, d20:1-lyso-GT1b·$3NH_3$, and d20:1-lyso-GQ1b·$4NH_3$ (Tab. 3.3.1).

Ganglioside standard	Amount (mg)	Yield (%)
d18:1/14:0-GM1·NH_3 (**14**)	6.32	28
d18:1/14:0-GD1a·$2NH_3$ (**15**)	0.88	42
d18:1/17:0-GD1a·$2NH_3$ (**16**)	0.98	86
d20:1/14:0-GD1b·$2NH_3$ (**17**)	1.28	70
d20:1/14:0-GT1b·$3NH_3$ (**18**)	0.40	34
d20:1/14:0-GQ1b·4 NH_3 (**19**)	0.19	19

Tab. 3.3.1: *Ganglioside standards that were synthesized by modification of the fatty acid part*

Yields were in the range of 19 to 86 %. The ESI-MS of **14**, **15**, **16**, and **19** showed no traces of other ganglioside lipoforms than the desired products. The ESI-MS of d20:1/14:0-GD1b·$2NH_3$ (**17**) showed an impurity of 3.4 % of d18:1/14:0-GD1b·$2NH_3$ and the ESI-MS of d20:1/14:0-GT1b·$3NH_3$ **18** showed an impurity of 4.8 % of d18:1/14:0-GT1b·$3NH_3$ as it was observed in their precursors. The fragments in the ESI-MS/MS spectra could clearly be correlated to the structure of the ganglioside lipoforms. Yields were estimated by weighing followed by sialic acid determination. For d18:1/14:0-GM1·NH_3 also densitometry was applied. The deviation between the value obtained by densitometry and the one determined by sialic acid determination was -8.4 %. Densitometric quantification bears some inaccuracies because the regression line is measured by only 3 values and also different lipoforms have different absorption coefficients. So this method was not further applied in this work. The values obtained by weighing were always higher than the values obtained by

sialic acid determination and the deviation became higher for amounts much smaller than 1 mg because the weighing error increased. In table 3.3.1, the corrected amounts of the synthesized standards are given.

3.4 Preparation of ganglioside standards by degradation of other standards

Glycosidases are subdivided into enzymes that catalyze glycoside hydrolysis with retention of the configuration of the anomeric center and enzymes that catalyze with inversion (132).

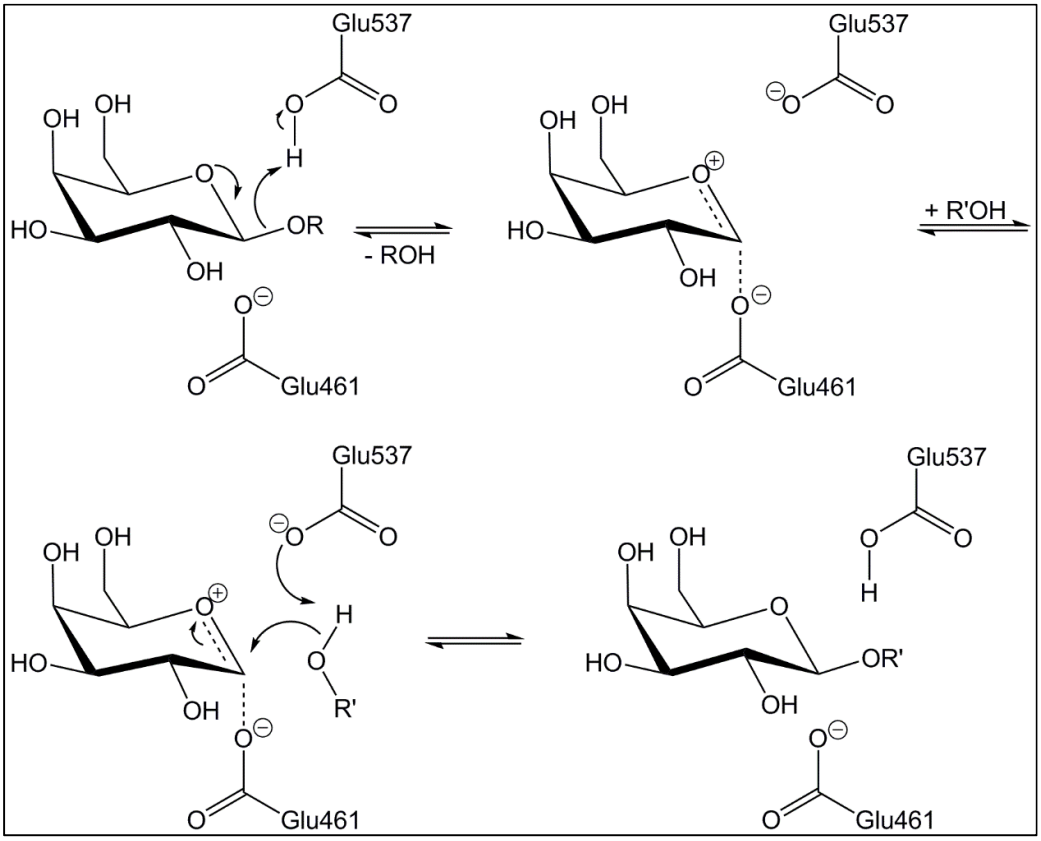

Fig. 3.4.1: *Mechanism for retaining glycosidases.* The amino acid numbering refers to beta-galactosidase from Escheria coli (132).

Beta-galactosidases belong to the first category. Their enzyme classification number is EC 3.2.1.23, which means they are hydrolases, subclass glycosylases, and sub-subclass glycosidases (129). In the first step the alkoxy group of the glycosidic bond is cleaved by the assistance of two glutamic acid residues, which reside in the active

site of the enzyme (Fig. 3.4.1). Glu537 activates the alkoxy leaving group by donating a proton while Glu461 stabilizes the arising carboxonium ion intermediate. A hydrogen bond between the carboxyl group and the hydroxyl group in position 2 stabilizes the transition state of the deglycosylation step as well as the one for the glycosylation step (133). In the next step a nucleophil which is usually water or an alcohol attacks on the same face resulting in retention of the anomeric configuration. The deprotonated Glu537 accepts a proton from the nucleophil, which facilitates the nucleophilic addition. The reaction is thermodynamically controlled so every step is reversible (132). If the reaction is carried out in an aqueous solvent, the equilibrium is shifted to the product site.

In this work the commercially available enzyme beta-galactosidase from bovine testes was chosen because it preferentially cleaves terminal galactose residues in *β*1-3 linkage (111). The reaction was applied to the preparation of d18:1/14:0-GM2·NH_3 and d20:1/14:0-GD1b·2NH_3.

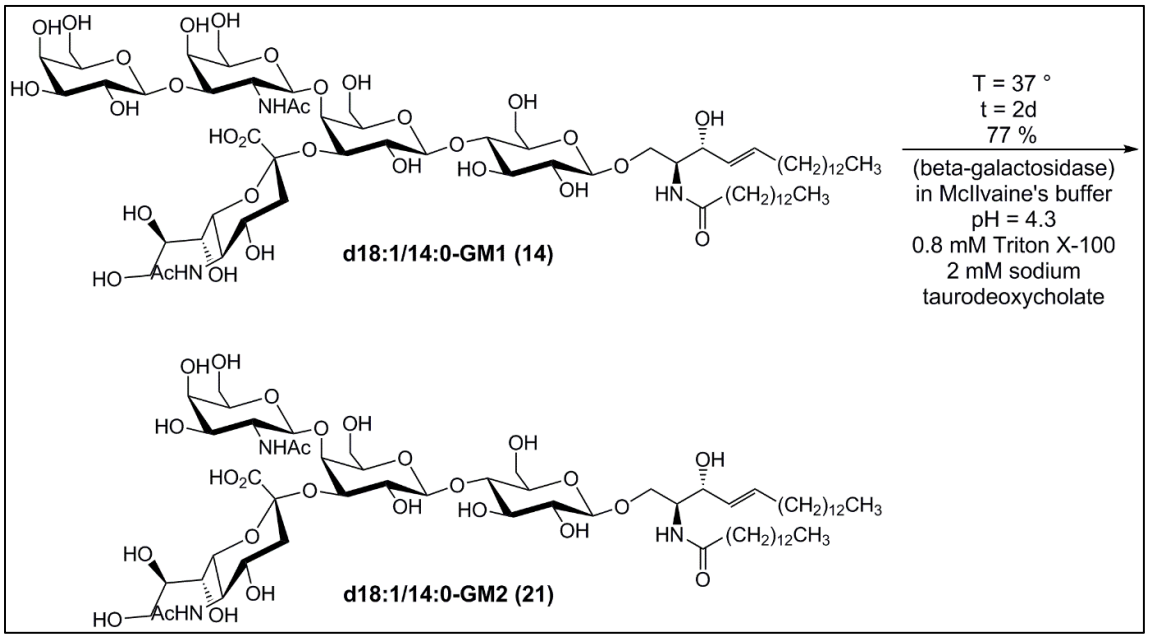

Fig. 3.4.2: *Preparation of d18:1/14:0-GM2*

The optimal reaction conditions were investigated by preparation of d18:1/18:0-GM2·NH_3 and d20:1/18:0-GD1b·2NH_3. The applicability of the method to lyso-gangliosides was tested by the preparation of d18:1-lyso-GM2·NH_3. The results are given in table 3.4.1.

Product	$n_{enzyme}/n_{substrate}$ (mU/µmol)	Amount of ganglioside (mg)	Yield (%)
d18:1/18:0-GM2·NH_3 (**20**)	306	0.22	36
d18:1/14:0-GM2·NH_3 (**21**)	300	1.84	77
d20:1/18:0-GD2·$2NH_3$ (**22**)	530	0.28	60
d20:1/14:0-GD2·$2NH_3$ (**23**)	359	0.25	61
d18:1-lyso-GM1·NH_3 (**24**)	277	0.41	78

Tab. 3.4.1: *Results of the degalactosylation of ganglioside derivatives*

The yields of the preparation of GM2 derivatives are in the range of 75-80 %. In contrast, the yields of the preparation of GD2 derivatives are in the range of 60 %. This is due to a slight desialylation of GD1b, which occurs at the applied pH value of 4.5. This could be demonstrated by a control experiment, in which the reaction conditions described in section 5.5.3 were applied but without enzyme. By TLC analysis, it could be demonstrated that GD1b is slightly converted to GM1 (Fig. 3.4.3). In order to reduce the reaction time for the preparation of GD1b derivatives, the concentration of enzyme and detergents were doubled.

Fig. 3.4.3: *HPTLC analysis of the control experiment for the degalactosylation of d20:1/C18:0-GD1b.*
Lane 1: d20:1/18:0-GD1b.
Lane 2: Reaction mixture after 21 h.
Lane 3: d20:1/18:0-GM1
Lane 4: d18:1/18:0-GM2
Solvent system: $CHCl_3$/MeOH/2.5 M NH_3 60:44:12 v/v/v.

The ESI-MS of **20**, **21**, **22** and **24** showed no traces of other ganglioside lipoforms than the desired products. The ESI-MS of **23** showed an impurity of 3.2 % of d18:1/14:0-GD2·$2NH_3$ as it was observed in the precursor.

3.5 Development of a new synthetic method to modify the sphingosine chain of gangliosides

3.5.1 Synthesis of a model compound

It was planned to apply an olefin cross metathesis to peracetylated GM1 for a modification of the sphingosine chain. To test the reaction conditions, methyl oleate was chosen as a model compound (Fig. 3.5.1). In the first step (*E*)-stilbene was applied in a tenfold excess. Methyl (*E*)-10-phenyldec-9-enoate (**25**) was obtained in a yield of 84 %. It was analyzed by ^{1}H-NMR, ^{13}C-NMR, and GC-MS. The ^{1}H-NMR did not show a triplet of the terminal methyl group in the range of 0.9 ppm, which indicates that the product was free of educt.

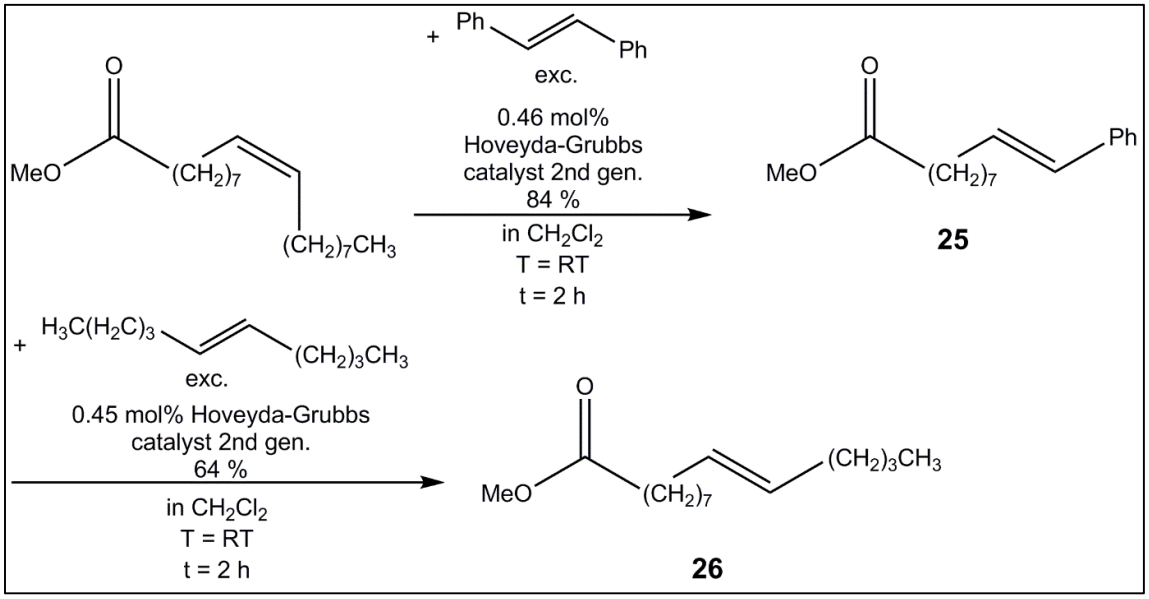

Fig. 3.5.1: *Synthesis of methyl (E)-tetradec-9-enoate*

For the olefinic protons, a doublet at 6.37 ppm and a doublet of triplets at 6.21 ppm were found. The coupling constant was 15.8 Hz, which demonstrates an E-configuration of the double bond. In the GC-MS chromatogram two peaks with very similar retention times were found. The mass spectra proved that these compounds had the same mass. It can be concluded that the first compound (proportion 0.75 %) is methyl (*Z*)-10-phenyldec-9-enoate and the second compound (proportion 99.25 %) is methyl (*E*)-10-phenyldec-9-enoate.

In the second step, **25** was converted to methyl (*E*)-tetradec-9-enoate (**26**) by using an tenfold excess of (*E*)-5-decene under the same reaction conditions. A yield of 64 % was obtained. The ^{1}H-NMR spectrum showed a triplet at 0.89 ppm and no signals of the phenyl group anymore. For the olefinic protons, only a broad triplet was found which should be a non-resolved triplet of triplets. The coupling of the olefinic protons could not be measured because they are chemically equivalent. GC-MS analysis revealed 3 peaks. The mass spectra demonstrated that peak 1 (proportion 2.91 %) is methyl tridecenoate, peak 2 (proportion 91.54 %) is methyl tetradec-9-enoate, and peak 3 (proportion 5.55 %) is methyl pentadecenoate. These results demonstrated that the method in principle works but isomerization occurs in a proportion of 8.5 % if no hydride scavengers are used.

3.5.2 Application of the method to d20:1/18:0-GM1 (2)

In the first step (*E*)-hexacos-13-ene was synthesized because it is commercially not available.

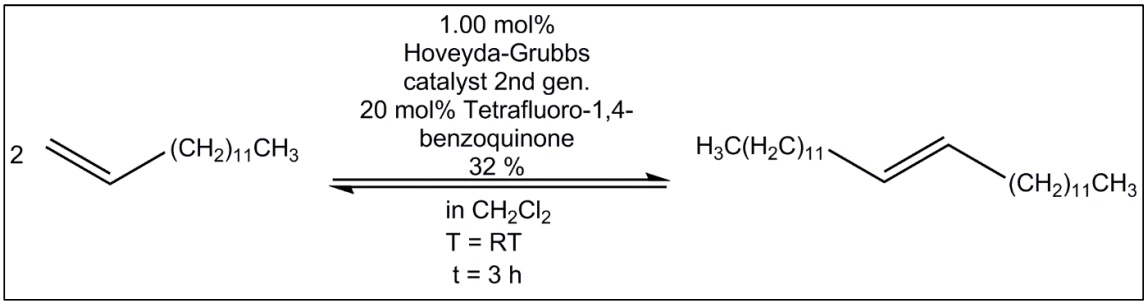

Fig. 3.5.2: *Synthesis of (E)-hexacos-13-ene*

Previous attempts for the synthesis of this compound demonstrated that only a statistical mixture of isomers of hexacos-13-ene is obtained if no hydride scavenger is used. By using 20 mol% of *p*-benzoquinone an isomeric purity of the synthesized product of 98.21 % was obtained. GC-MS analysis revealed four peaks. The mass spectra demonstrated that peak 1 (proportion 0.45 %) was tetracosene, peak 2 (proportion 0.49 %) was pentacosene, peak 3 (proportion 98.21 %) was hexacos-13-ene, and peak 4 (proportion 0.84 %) was octacosene. The yield was 30 %. The E/Z-configuration of the product could not be analyzed due to the chemical equivalence of the olefinic protons. Since they showed only one signal in the ^{1}H-NMR- and ^{13}C-

NMR spectra, it was concluded that selectively the E-isomer was formed. In a second experiment, the purity of the product could be enhanced to 100 % by using tetrafluoro-1,4-benzoquinone as hydride scavenger. The yield was 32 %.

In the next step, d20:1/18:0-GM1 (**2**) was peracetylated by a modified method of Schwarzmann et al (100). Under these reaction conditions the formation of a lactone was observed, which is explained by activation of the carboxylic acid to a mixed anhydride and subsequent lactone formation to a six-membered ring (Fig. 3.5.3). A yield of 62 % was obtained. The product was analyzed by ^{1}H-NMR, ESI-MS, and ESI-MS/MS. The peracetylation of GM1 leads to a low field shift of the sugar protons. The olefinic proton H-5 was assigned to a doublet of triplets. The E-configuration of the product was demonstrated by a coupling constant of 15.1 Hz. The anomeric protons of GalNAc, of one Gal residue, and of the Glc residue were assigned. Because of their coupling constants, also H-4, H-5, and H-3e of the NeuAc residue could be assigned. The singlets of the 51 acetyl protons were found in the range of 2.0 ppm. For the ceramide part, a multiplet assigned to H-3', a broad multiplet assigned to 54 CH_2 protons, and a triplet assigned to the two methyl groups were found. In the ESI-MS spectrum only peaks of the product and a methyl ester of the product were found. The formation of the methyl ester is explained by opening of the lactone ring by methanol, which is used as solvent in the measurement. The fragments in the ESI-MS/MS spectra could be correlated to the desired product. The observed fragment $[Y_0 + 2H - \text{stearic acid} - H_3CCO_2H]^+$ at 292.30 demonstrated the composition of the fatty acid part of the product. In the next step, **28** was converted by a tenfold excess of stilbene and 14 mol% of Grubbs catalyst 2nd gen. to **29** in a yield of 68 %. In the ^{1}H-NMR the signals of the phenyl group were found in the range of 7.1 to 7.4 ppm. The olefinic proton H-5 showed a doublet at 6.65 ppm while H-4 showed a doublet of doublets at 6.09 ppm. The coupling constant was 15.9 Hz indicating the E-configuration of the product. The loss of 14 CH_2 groups and one methyl group was demonstrated by the integral of the broad multiplet at 1.2 ppm and of the triplet at 0.86 ppm.

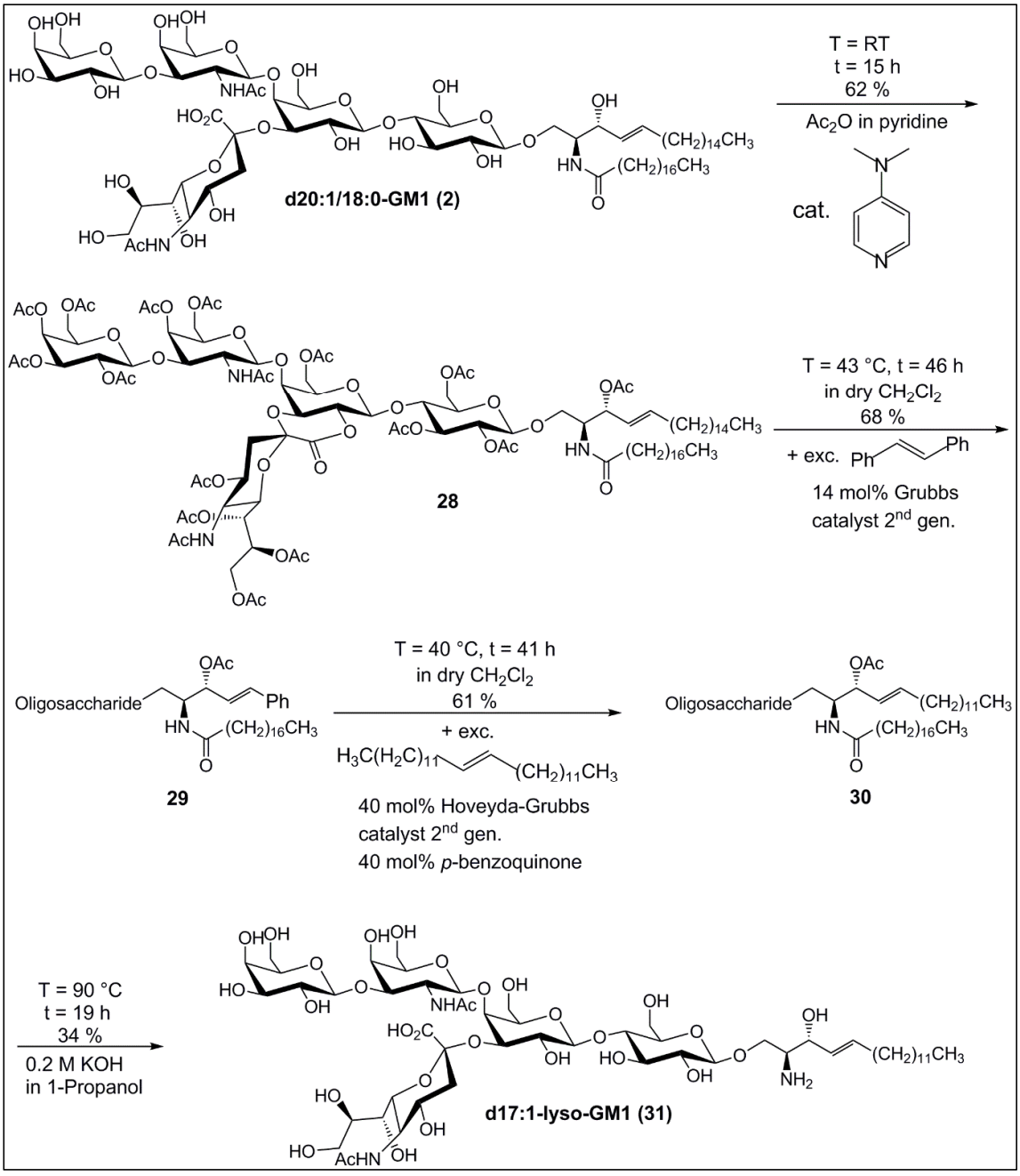

Fig. 3.5.3: *Summary of the synthetic steps of the synthesis of d17:1-lyso-GM1*

In the ESI-MS only peaks of the product and the methyl ester of the product were found. In the next step, **29** was converted to **30** by a twentyfold excess of (*E*)-hexacos-13-ene (**27**) under the reaction conditions described in fig. 3.5.3. The yield was 61 %. Some attempts were made to optimize the reaction conditions. First, the more effective hydride scavengers tetrafluoro-1,4-benzoquinone and 2,6-dichloro-1,4-benzoquinone were tested. Second, the Stewart-Grubbs catalyst, which contains

N-tolyl groups instead of *N*-mesityl groups in the *N*-heterocyclic carbene ligand, was tested. This catalyst is reported to be more active in cross metatheses of sterically challenging olefines (134).

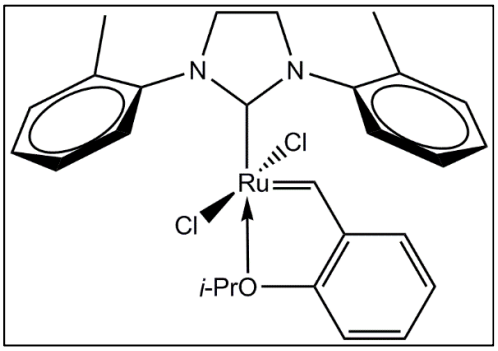

Fig. 3.5.4: Stewart-Grubbs catalyst

Catalyst (20 mol%)	Hydride Scavenger	Conversion (%)
Hoveyda-Grubbs cat. 2nd gen.	*p*-benzoquinone (40 mol%)	30
Hoveyda-Grubbs cat. 2nd gen.	*p*-benzoquinone (20 mol%)	60
Hoveyda-Grubbs cat. 2nd gen.	tetrafluoro-1,4-benzoquinone (40 mol%)	< 5
Hoveyda-Grubbs cat. 2nd gen.	tetrafluoro-1,4-benzoquinone (20 mol%)	< 5
Hoveyda-Grubbs cat. 2nd gen.	tetrafluoro-1,4-benzoquinone (1 mol%)	< 5
Hoveyda-Grubbs cat. 2nd gen.	2,6-dichloro-1,4-benzoquinone (20 mol%)	< 5
Hoveyda-Grubbs cat. 2nd gen.	2,6-dichloro-1,4-benzoquinone (5 mol%)	< 5
Hoveyda-Grubbs cat. 2nd gen.	2,6-dichloro-1,4-benzoquinone (1 mol%)	< 5
Stewart-Grubbs. cat.	*p*-benzoquinone (20 mol%)	0
Stewart-Grubbs. cat.	tetrafluoro-1,4-benzoquinone (20 mol%)	0
Stewart-Grubbs. cat.	2,6-dichloro-1,4-benzoquinone (20 mol%)	0

Tab. 3.5.1: *Results for the synthesis of **30** under different reaction conditions.* Conversions were estimated by TLC analysis after a reaction time of 1 d.

The results are given in table 3.5.1. Unexpectedly, the more active hydride scavengers tetrafluoro-1,4-benzoquinone and 2,6-dichloro-1,4-benzoquinone suppressed the catalyst activity even when they were added in low amounts. Furthermore, the Stewart-Grubbs catalyst showed no activity towards **29** regardless of the hydride scavenger tested. So the most effective reaction conditions are 20 mol% of Hoveyda-Grubbs cat. 2nd gen. and 20 mol% of *p*-benzoquinone.

The ^{1}H-NMR spectrum of **30** was similar to that of **28**. The coupling constant of the olefinic protons was 15.2 Hz. The loss of 3 CH_2 groups was indicated by the integral

of the broad multiplet at 1.25 ppm. The ESI-MS showed only peaks of the desired product. In the last step, the protecting groups and also the acyl chain were removed from **30** by alkaline hydrolysis to get d17:1-lyso-GM1·NH_3 (**31**). The yield was 34 %. The ESI-MS showed that the product contained 4.8 % of d16:1-lyso-GM1, which indicates that isomerizations on the second olefin metathesis step could not be completely suppressed. Other isomers were not found. This isomer was removed by isocratic RP-column chromatography. The ESI-MS/MS confirmed the structure of the product. A proportion of **31** was used for the preparation of d17:1-lyso-GM2·NH_3 (**32**) by enzymatic degalactosylation. The yield was 69 %.

3.5.3 Validation of the lysoganglioside lipoforms as calibrators

As a proof of principle, the synthesized lysoganglioside standards **31** and **32** were tested for the quantification of pure d18:1-lyso-GM1·NH_3 (**7**) and d18:1-lyso-GM2·NH_3 (**24**) (Fig. 3.5.5). Good linearity of I_{an}/I_{IS} and c_{an} was obtained for both compounds in the applied concentration range. As expected, quantification of pure substances is possible in the full scan mode but for biological samples MS/MS modes have to be applied.

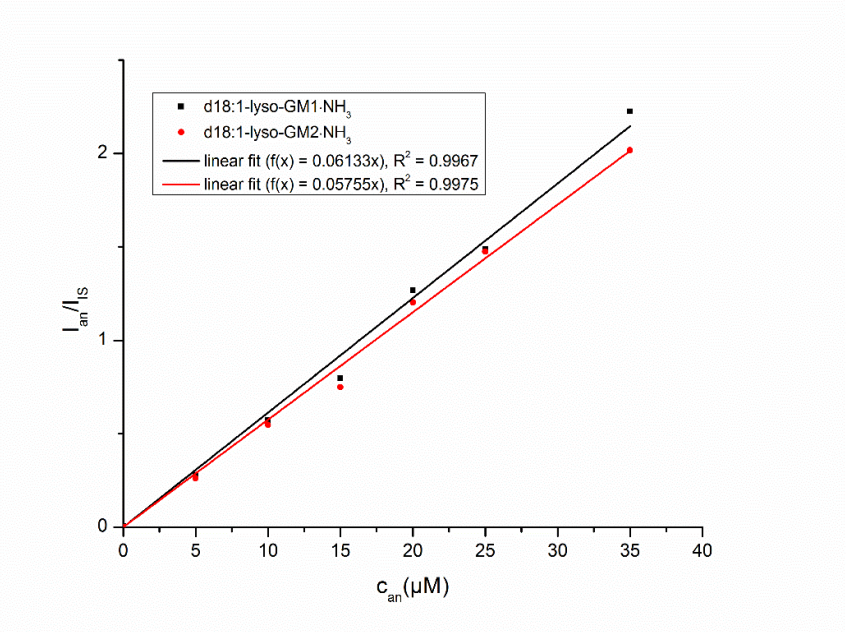

Fig. 3.5.5: *Quantification of pure lyso-GM1·NH_3 and lyso-GM2·NH_3.* A concentration series of pure d18:1-lyso-GM1 (**7**) and d18:1-lyso-GM2 (**24**) was quantified by using the internal standards d17:1-lyso-GM1·NH_3 (**31**) and d17:1-lyso-GM2·NH_3 (**32**).

4 Discussion

4.1 Purification of gangliosides

For the synthesis of non-natural ganglioside lipoforms suitable as MS-standards, we chose a partial synthesis rather than a total synthesis (section 2.4.1) because of the high effort necessary for the latter. The first part was a chromatographic separation of a ganglioside mixture from bovine brain to isolate homologous pure ganglioside lipoforms. Conditions for isocratic NP column chromatography were found to obtain pure GM1 and GD1a in sufficient amounts from Cronassial®. This was not successful for GD1b, GT1b, and GQ1b. By using anion-exchange chromatography, all the mentioned ganglioside classes were separated without overlap. Momoi reported that NH_4OAc in MeOH leads to a better separation than NH_4OAc in $CHCl_3$/MeOH/H_2O 30:60:8 v/v/v (110)., but we found them to be equally suitable. The quantities of ganglioside classes obtained were mainly in accordance with those reported by Zamfir et al. (109). We obtained 27 % of monosialogangliosides and 14 % of trisialogangliosides while they reported quantities of 21 % and 19 % of the mentioned ganglioside classes. In the next step, the major bovine brain gangliosides and also GQ1b were obtained by isocratic or step gradient NP column chromatography. In order to modify the fatty acid part (section 2.4.1), gangliosides with homogenous sphingoid bases as educts were necessary, which were obtained by RP column chromatography of the purified gangliosides. In general, this method worked sufficiently for every ganglioside. It was confirmed that bovine brain gangliosides mainly contain d18:1/18:0- and d20:1/18:0-lipoforms. In the case of GT1b, also the existence of a d20:1/20:0-lipoform was demonstrated by ESI-MS. For other gangliosides, it has to be concluded that the corresponding d20:1/20:0 species were separated in the NP column chromatography step. We found no indication for the presence of *N*-glycolylneuraminic acid in the title compounds. Usually, the purity of gangliosides is analyzed by fluorimetric (135) or photometric (136, 137) sialic acid determination, sphingoid base determination by HPLC (138), GC-FID (110) or densitometry (139). Initially, we used photometric sialic acid determination with pure Neu5Ac or α_1-acid glycoprotein as external standards. Since we obtained deviating results (section 5.2.12), we concluded that these standards were not appropriate. Hence, we decided to use elemental analysis to analyze the purified ganglioside

lipoforms and to use these compounds as external standards for the analysis of compounds derived from them. The results of the elemental analysis demonstrated that there is residual water content of 10-15 % in the gangliosides after lyophilization. By drying in vacuum, this can be reduced to 5 % (Tab. 3.1.3).

4.2 Preparation of lysogangliosides

In this work lysogangliosides have been prepared by chemical and enzymatical deacylation. The yield of 52 % for the preparation of lyso-GM1 demonstrated that this method is regioselective for the deacylation of GM1. But the yield of 4.8 % for the preparation of lyso-GD1a demonstrated no regioselectivity for the deacylation of GD1a. Additionally, Sonnino et al. reported yields of 36-40 % for the chemical deacylation of GM3, which also demonstrates no regioselectivity (127). From these three results it can be concluded that the *N*-Acetyl groups of the NeuAc residue at the inner galactose are protected against nucleophilic attacks, but only when the Gal*β*1-3GalNAc*β*1-4 residue is present. In this case the *N*-Acetyl group of the GalNAc residue is also protected. It can be assumed that in the deacylation of GA1 also no regioselectivity would be observed.

The enzymatic deacylation of gangliosides turned out to be more appropriate: yields were in the range of 44 to 60 % for lyso-GD1a, lyso-GD1b, lyso-GT1b, and lyso-GQ1b. This is comparable to the results of Ando et al. They prepared lyso-GM1 and lyso-GM2 from GM1 and GM2 in order to test the applicability of SCDase. They obtained yields of 62 % resp. 52 % for lyso-GM1 and lyso-GM2 (140). Oligosialogangliosides were not investigated in their study.

The prepared d20:1-lyso-GD1b·2NH_3 and d20:1-lyso-GT1b·3NH_3 contained 3.1 % resp. 4.7 % of their d18:1-lipoform, which we decided not to remove by RP column chromatography because it does not disturb the mass spectrometric application of the standards. These residues must originate from d18:1/20:0-lipoforms, which could not be separated by RP-column-chromatography before because they have the same chromatographic properties like the d20:1/18:0-lipoforms. The presence of d18:1/20:0-lipoforms could not be verified at the ganglioside stage because neither RP-TLC nor ESI-MS/MS can differentiate between those isobaric lipoforms. Hereby, MS^3 of the Z_0 fragments could have been a useful method (141) but could not be performed with the mass spectrometer available to us. Taken together, enzymatic

deacylation using SCDase is a very selective and reliable method for the preparation of complex lysogangliosides. The disadvantage of the method are the high costs for the enzyme (≈ 820 €/250 mU). A regeneration of the enzyme after the preparation has not been described, yet. Fluorimetric sialic acid determination was used for the analysis of the lysogangliosides because of its higher sensitivity compared to photometric sialic acid determination. The required amount of sialic acid was in the range of 2 µg per measurement while photometric sialic acid determination requires approximately 20 µg. The deviance of both methods was 0.3 %, which was estimated for d18:1-lyso-GD1a·2 NH_3 **8**. The disadvantage of the method is the high price for the assay kit. The amount of sialic acid required for photometric sialic acid determination was reduced fourfold from 20 µg to 5 µg in this work by using Eppendorf tubes and only the minimal volume which is required for photometry (section 5.1.9.6). Lysogangliosides can also be analyzed by derivatization with *o*-phtalaldehyde, ethanethiol and subsequent HPLC analysis (138). But we were not able to reproduce the results reported by Kobayashi et al. Presumably, this was due to the lack of an appropriate HPLC-column.

4.3 Reacylation of lysogangliosides

The activation of the fatty acids as succinimide esters was carried out in yields of around 70 %. This is comparable to the results of Georgiades et al. who obtained 2,5-dioxopyrrolidin-1-yl tridecanoate in a yield of 76 % (142). Succinimde esters were chosen because they selectively react with amino groups in the presence of hydroxyl groups (130). The reacylation of the lysogangliosides was carried out in yields in the range of 19 to 86 %. In general, the reaction worked accurate for monosialolysogangliosides and disialolysogangliosides giving yields in the range of 70 to 86 %. This is comparable to the yields of 80 % obtained by Schwarzmann et al. for reacylation of lyso-GM1 (104). The yield of 28 % for the reacylation of lyso-GM1 obtained by us is due to a loss of substance during the chromatographic purification, so this value is not optimized. For lyso-GT1b and lyso-GQ1b the yields dropped to 34 % and 19 %, respectively. This can be explained by the greater number of carboxylic acid groups, which hamper the deprotonation of the protonated amino group. Additionally, the greater ammonium ion content destroys a greater part of the acylating agent. An optimization of the reaction conditions for these substrates

should be performed in the future. Additionally, the crude product could be treated with methanolic KOH in order to convert putative ester- or anhydride like byproducts which could have arisen in this reaction to the desired product, although we could not detect any byproducts by TLC during the reaction.

4.4 Preparation of ganglioside standards by enzymatic degalactosylation

The commercially available enzyme beta-galactosidase from bovine testes was chosen because of its preference in cleaving terminal *β*-1,3 linked galactose residues and its acceptable price (300 €/500 mU). For the degradation of GM1 to GM2, a yield of 77 % was obtained under optimized reaction conditions, which is higher than the yield of 54 % obtained by Larsson et al (112). For the degradation of lyso-GM1 derivatives, comparable yields of 69 % resp. 78 % were obtained. The method is also applicable to GD1b derivatives although we observed a slight degradation to GM1 due to the applied pH-value. Hereby, sufficient yields in the range of 60 % were obtained. As far as we know this method has not been applied to lyso-GM1- and GD1b derivatives in the literature.

4.5 Modification of the sphingosine chain of gangliosides

The preparation of the required starting materials for the regioselective deacylation of gangliosides which are homologous in their sphingosine parts requires tedious chromatographic steps. As an alternative, we developed a synthetic method for the preparation of gangliosides with homogenous (and, if required, artificial) sphingoid bases. An ozonolysis followed by Wittig reaction is a problematic concept because of isomerizations of the allyl alcohol, alkaline fragmentation, and the need for separation of E/Z-mixtures. The Schlosser modification is less helpful because the alkaline conditions required are incompatible with hydroxyl groups and carboxylic acid groups (143).

Hence, the olefin metathesis seems to be a suitable reaction for this purpose because it is performed under neutral conditions and tolerates hard nucleophils. Ethenolysis has only been carried out for Z-olefins in sufficient yields therefore we investigated a stilbenolysis. As a model compound methyl (*E*)-tetradec-9-enoate **26** was synthesized from methyl oleate in two steps in a total yield of 54 %. By GC-MS, it was proven that the stilbenolysis step is not prone to isomerizations. However, in the exchange of the phenyl group for a pentyl group in the second step isomerizations in a proportion of 8.5 % occurred. So we decided to use *p*-benzoquinone derivatives as hydride scavengers.

First, (*E*)-hexacos-13-ene was synthesized in a yield of 32 %. *p*-Benzoquinone turned out to be a sufficient hydride scavenger because isomerizations occurred only in a proportion of 1.8 %. A complete suppression of isomerizations was achieved by using tetrafluoro-1,4-benzoquinone. Then, d20:1/18:0-GM1·NH_3 was peracetylated in a yield of 62 %, which is slightly less than the yield of 72 % obtained by Schwarzmann et al. for the peracetylation of II^3-*α*-NeuAcGg$_4$ (100). In the future, it should be tested if an extension of the reaction time increases the yield because as a side product incompletely peracetylated d20:1/C18:0-GM1 sialoyl-II^2-lactone lacking only one acetyl group was obtained. In the next step, a phenyl group was introduced into the sphingosine part by an olefin metathesis in a sufficient yield of 68 %. Isomerizations were not observed. The exchange of the phenyl group for a dodecyl group by an excess of (*E*)-hexacos-13-ene was performed in a sufficient yield of 61 %. Hereby, a larger amount of catalyst was required. An improvement of the reactions conditions by using more efficient hydride scavengers or the Stewart-Grubbs catalyst, which is reported to be more active towards sterically hindered olefins, was not successful. Electron deficient benzoquinone derivatives suppress the catalytic activity of the Hoveyda-Grubbs catalyst 2nd gen. even when they are added in low amounts. The Stewart-Grubbs catalyst shows no activity towards **29** regardless of the hydride scavenger. This is a surprising result because the catalyst is reported to be more active in the cross metathesis of sterically hindered olefins than the Hoveyda-Grubbs catalyst 2nd gen. It can be explained by the preference of an unproductive pathway during the metallacyclobutane formation (Fig. 4.5.1). But this pathway is usually only preferred in the cross metathesis of 1,1-disubstituted olefins.

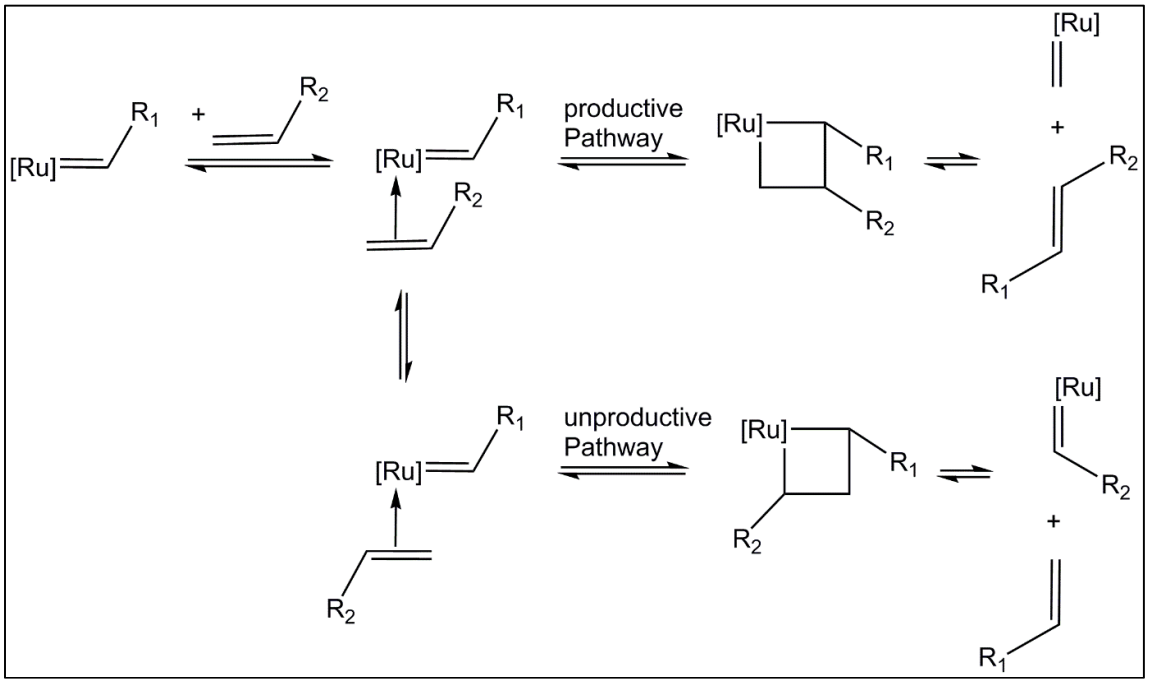

Fig. 4.5.1: Productive and unproductive pathways in olefin cross metathesis (134).

In the next step, the protective groups and also the acyl group were removed by alkaline hydrolysis in a yield of 34 % (105). This result is slightly less than the yield of 52 % which was obtained by us for the chemical preparation of d18:1-lyso-GM1. So the total yield for the synthesis of d17:1-lyso-GM1 is 8.7 %. If the yield for the removal of the acetyl groups is estimated to be 90 %, the total yield for the synthesis of d17:1/18:0-GM1 from d20:1/18:0-GM1 would be 23 %. In comparison, the method of Neuenhofer et al. has a total yield of 29 % for the synthesis of, for example, d18:1/17:0-GM1 from d18:1/18:0-GM1 (104, 106). The enzymatic preparation has the highest overall yield of approx. 42 % for the same product (Fig. 4.5.2). The disadvantage of this method is the high price of SCDase. But in contrast to our method, the other methods require homologous pure gangliosides as starting materials.

The position of the unnatural alkyl chain in the fatty acid part or the sphingosine part should not influence the mass spectrometric quantification because usually the transition $[Ganglioside - H]^-/[Neu5Ac - H]^-$ is monitored if MRM is used. The reason is that these peaks usually show the greatest intensities (69, 144). If neutral loss scan is used, the loss of sialic acid would be monitored and if parent ion scan is used, the

parent ions of [Neu5Ac – H]$^-$ would be scanned because these transitions show the greatest intensities.

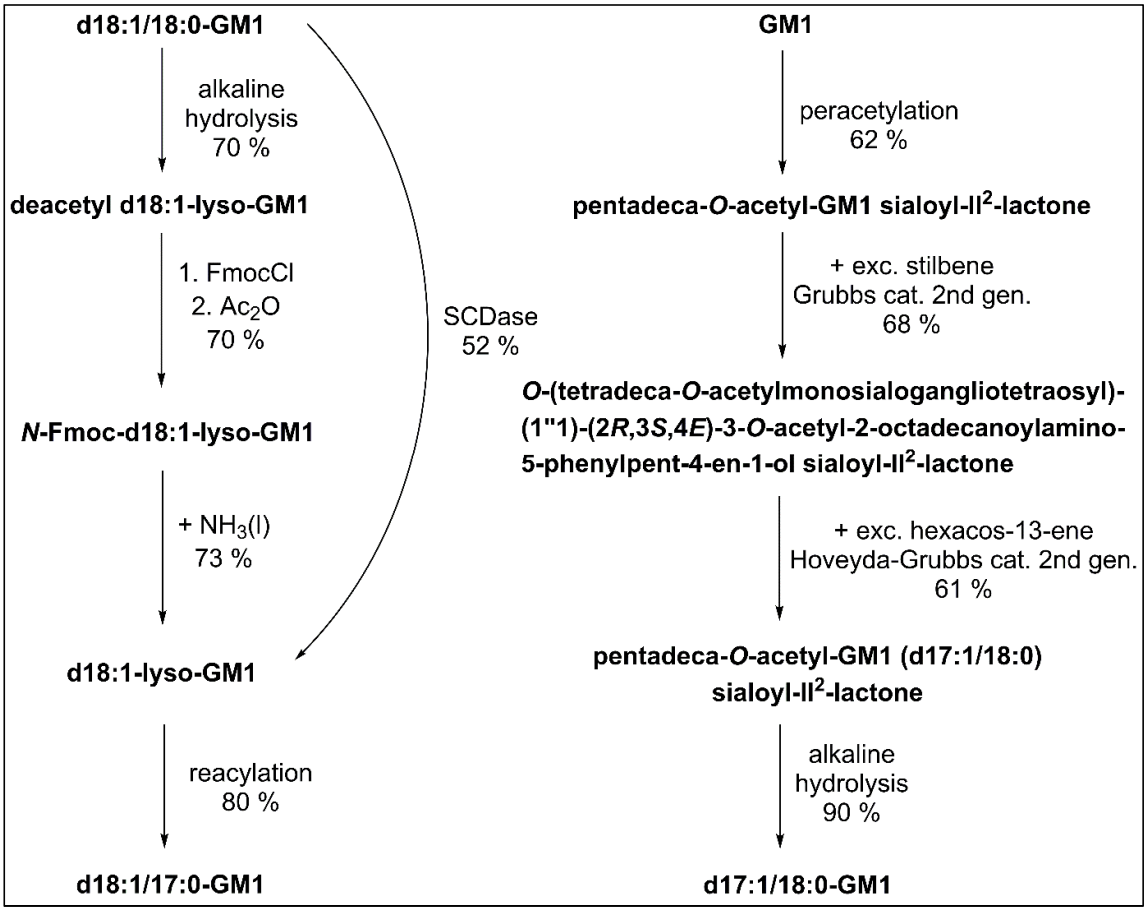

Fig. 4.5.2: *Comparison of the published methods for the synthesis of ganglioside standards to the new method developed in this work.*
Left: Method of Neuenhofer et al. Center: Enzymatic method. Right: Olefin metathesis method.

During the second olefin metathesis step isomerizations occurred in a proportion of 4.8 %. This result demonstrates that *p*-benzoquinone cannot suppress isomerizations completely but to an extent of greater than 90 %.

The method developed by us has a wide scope: First, it should be applicable not only to gangliosides, but also to other sphingolipids and glycosphingolipids like ceramides, neutral glycosphingolipids, sphingomyelins, and sulfatides. Second, isotope labeling of the sphingosine part can also be achieved because the phenyl group facilitates the chromatographic separation of educts and products. Third, the method might be used to incorporate fluorescent dyes into the sphingosine part of sphingolipids. In the

literature, the introduction of fluorescent dyes into the sphingosine part by an olefin metathesis was only applied to sphingosines and ceramides yet. In 2005, Nussbaumer et al. (145) inserted the fluorescent dye NBD (7-nitro-2,1,3-benzooxadiazol-4-yl) in the sphingosine part of commercially available ceramide in yields of 14 to 71 %.

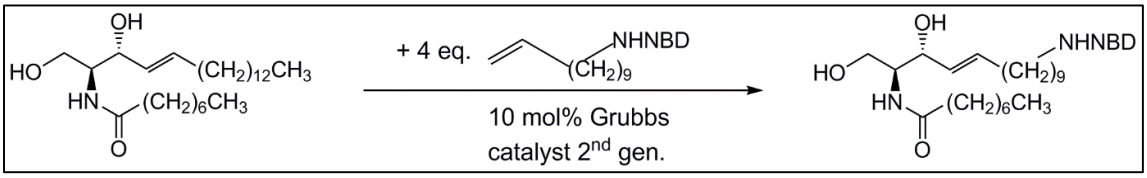

Fig. 4.5.3: *Partial synthesis of fluorescence labeled ceramide by using an olefin cross metathesis (145)*

It would be difficult to apply this method to the introduction of non-functionalized alkyl chains because the products would not be easily separable from the educts. In the recent years, an olefin metathesis method has been used for the total synthesis of fluorescence labeled sphingosines and ceramides. It starts from commercially available Garner aldehyde (146). In the first step, Garner aldehyde is converted to *anti*-Garner allylic alcohol by addition of vinyl lithium (147). Then, various olefinic groups can be inserted by an olefin cross metathesis. After deprotection, fluorescence labeled sphingosine is obtained.

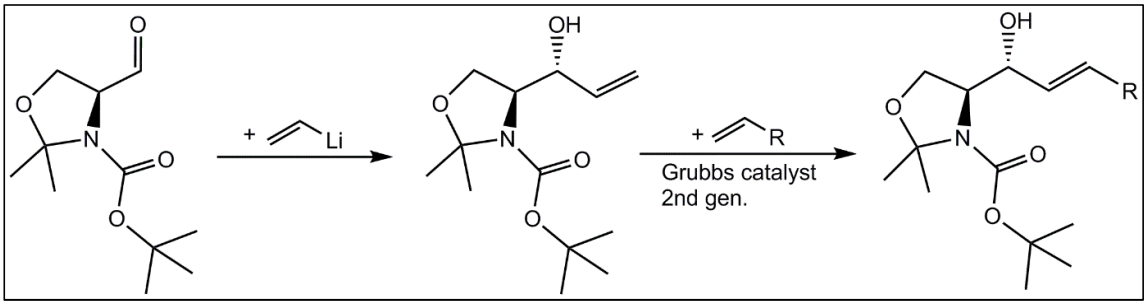

Fig. 4.5.4: *Synthesis of fluorescence labeled ceramide starting from Garner aldehyde.*

Peters et al. used this method for the synthesis of NBD- and BODIPY (borondipyrromethene, 4,4-difluoro-4-bora-3a,4a-diaza-*s*-indacene)-labeled sphingosines (146). Fluorescent labeled sphingosines and ceramides are typically used to study uptake, metabolism, intracellular transport, and distribution of sphingolipids in

cells. In 1992, Schwarzmann et al. used DPH-sphingosine (diphenyl-1,3,5-hexatrienyl) to investigate the metabolism of this lipid in human fibroblasts (148).

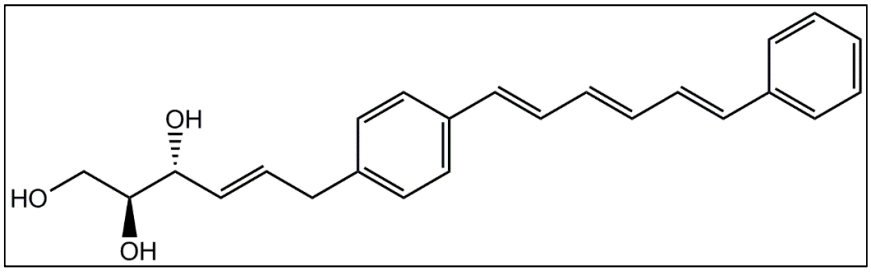

Fig. 4.5.5: *DHP-sphingosine*

DHP-sphingosine was synthesized in a convergent synthesis starting from cinnamaldehyde and 2,4-*O*-benzylidene-D-threose.

The method of Peters et al. was used in 2011 by Bhabak et al. for the synthesis of Sph-NR-Cer (Nile Red) and Sph-NBD-Cer in order to compare their suitability as substrates for neutral and acid ceramidase to common Acyl-NR-Cer and Acyl-NBD-Cer. Unexpectedly, it was found that the more hydrophilic NBD-tagged ceramides shows in general a higher cleavage rate than the NR-tagged ceramides (149).

Up to now, fluorescence labeled gangliosides have been prepared by modification of the fatty acid part, for instance, by acylation with 12-(pyren-1-yl)dodecanoic acid (104), 6-Tetramethylrhodamine-(β-alanine)-amide (112), or 2-NBD-stearic acid (101). Our method enables the possibility of synthesizing double fluorescence labeled gangliosides with one label in the sphingosine part and another in the fatty acid part as FRET (Förster resonance energy transfer) probes. This concept has been realized only for ceramides by Arenz et al (150), yet. In addition, our method provides access to pure ganglioside lipoforms that allow functional studies *in vitro*.

5 Experimental Part

5.1 Materials and methods

5.1.1 Devices

Device	Model, manufacturer and place of business
Centrifuges	Rotina 48 R, Hettich, Mühlheim a. d. Ruhr, Ger; MiniSpin, Eppendorf, Hamburg, Ger
Densitometer	TLC Scanner 3, CAMAG, Muttenz, Sui
Evaporator	Reacti-Varp lll, Pierce/Perbio Science, Rockford, IL, USA
Fraction collector	Microcol TDC 80, Gilson Medical Electronics, Villiers-le-Bel, France
Heating and stirring module	Reacti-Therm lll, Pierce/Perbio Science, Rockford, IL, USA
Horizontal developing TLC-chamber	Camag, Berlin, Ger
HPLC-System	CMB-101 with LC-10AT VP pump and RF-10AXL detector Shimadzu, Kyoto, Jpn; Model AS-100 HPLC automatic sampling system, Bio-Rad, Berkeley, USA
LC pump	Latek-P 402, Latek Labortechnik Geräte GmbH & Co. Analysensysteme KG, Eppelheim, Ger
Micropipettes	Eppendorf Research®, Eppendorf, Hamburg, Ger
Microplate Fluorometer	Fluoroscan ll, Labsystems Oy, Helsinki, Fin

Nano-ESI-QTOF mass spectrometer	QTOF-2 hybrid quadrupole mass spectrometer with nanoflow-interface, Micromass, Manchester, UK
pH meter	pH 537, WTW, Weilheim, Ger
Photometer	Ultrospec III, Pharmacia Biotech, Uppsala, Swe
Shaking water bath	1083, Gesellschaft für Labortechnik, Burgwedel, Ger
Thermomixer	Comfort, Eppendorf, Hamburg, Ger
TLC plate heater	TLC plate heater lll, CAMAG, Muttenz, Sui
Ultrapure water system	EASYpure UV/UF D8612, Werner Reinstwassersysteme, Leverkusen, Ger
Ultrasonic bath	Sonorex RK 100, Bandelin, Berlin, Ger
Ultrasonic device	Sonifier 250, Branson, Danbury, USA
UV lamp	MinUVis, Desaga, Heidelber, Ger
Vacuum pump	Rotary vane pump RZ 6, Vacuum-Brand GmbH & Co. KG, Wertheim, Ger
Vortexer	Vibrofix VF1 electronic, Janke & Kunkel IKA-Werk, Staufen, Ger
Weighing instruments	BP 210 D, Sartorius, Göttingen, Ger; Explorer, Ohaus, Gießen, Ger

5.1.2 Chemicals

All chemicals were – unless otherwise indicated – of highest purity available. Water used for buffers and solutions was purified by an ultrapure water system. Reactions using oxygen- and moisture sensitive reagents were handled by standard Schlenk techniques. The native mixture of bovine brain gangliosides Cronassial® was available in our lab. Sphingolipid ceramide N-deacylase (SCDase) and beta-galactosidase from bovine testes were from Sigma Aldrich (Schnelldorf, Ger).

Triton™ X-100, sodium taurodeoxycholate, Grubbs catalyst 2nd gen., Hoveyda-Grubbs cat. 2nd gen., and Stewart-Grubbs catalyst were also from Sigma Aldrich. For anion-exchange chromatography, DEAE Sephadex™ A-25 from Amersham Pharmacia Biotech AB (Uppsala, Swe) was used.

5.1.3 Anhydrous solvents

Solvents used in reactions of oxygen- and moisture sensitive compounds were in anhydrous form. 1-Propanol, methanol, pyridine, and acetic anhydride were degassed before use.

5.1.4 NP-column chromatography

For NP-column chromatography, silica gel from Merck (Darmstadt, Ger) (0.040-0.063 mm or 0.015-0.040 mm) was used.

5.1.5 Preparative TLC

For preparative TLC, Kieselgel 60 plates (10 × 10 cm or 20 × 20 cm) manufactured by Merck were used. After developing, bands were made temporarily visible by spraying with MeOH/H_2O 90:50 v/v. Bands of interest were scraped out with a spatula. The scraped out silica gel was collected in a frit and extracted. After evaporation of the solvent, residues of silica gel were removed by the method described in section 5.1.8.

5.1.6 Desalting

For RP-column chromatography and desalting, filtration columns from Supelco (Bellefonte, USA) were used. The stationary phase was LiChroprep RP-18 (0.040-0.063 mm) from Merck. For desalting, a slightly modified method of Wiliams and McCluer was used (151). The LiChroprep RP-18 powder was suspended in MeOH and left for 5 h. The supernatant was decanted and the procedure was repeated with $CHCl_3$/MeOH 1:1 v/v, then with $CHCl_3$/MeOH 2:1 v/v, and again with MeOH. The

suspension was introduced into a filtration column. The column was washed with 3 column volumes (CVs) of MeOH, 3 CVs of $CHCl_3$/MeOH 1:1 v/v, 2 CVs of MeOH, 2 CVs of H_2O, and 2 CVs of theoretical upper phase (TUP), which is $CHCl_3$/MeOH/0.1 M aq. KCl 3:48:47 v/v/v (151). Gangliosides were dissolved in TUP in a concentration of approx. 1 mg/mL and applied to the column. Then, the column was washed with 6 CVs of water to remove salts. Afterwards, gangliosides were eluted by MeOH.

5.1.7 RP-column chromatography

Columns were prepared in the same way like for desalting. Gangliosides were dissolved in TUP and applied to the column. Then, the column was washed with 6 CVs of H_2O to remove salts. In contrast, lysogangliosides were dissolved and applied in water. Subsequently, the substances were separated isocratically by the eluent MeOH/H_2O in different compositions.

5.1.8 Removal of column material

If polar eluents are used in column chromatography, the purified substances contain significant amounts of column material. The following method was used to minimize the amount of column material. NP columns of a very small column volume were prepared in filtration columns from Supelco using a mobile phase in which the substance is retained. The substance was applied to the column and washed with three column volumes. Then, the substance is eluted by an appropriate solvent of higher polarity.

5.1.9 Analytical methods

5.1.9.1 TLC

For thin layer chromatography, HPTLC Kieselgel 60 F_{254}- and HPTLC Kieselgel 60 RP-18 plates (10 × 5 cm, 10 × 10 cm, 20 × 10 cm or 20 × 20 cm) manufactured by Merck were used. NP-HPTLC plates were developed either by dipping in copper sulfate reagent (10 % $CuSO_4 \cdot 5H_2O$ in 8 % aq. H_3PO_4) (152) and subsequent heating to 190 °C for a few minutes or by dipping in Kägi-Miescher reagent (EtOH/conc.

H_2SO_4/4-anisaldehyde 18:1:1 v/v/v) (153) and subsequent heating to 136 °C for a few minutes. RP-HPTLC plates were developed with Kägi-Miescher reagent in the same way.

5.1.9.2 NMR-spectroscopy

For ^1H- and ^{13}C-NMR-spectroscopy, Bruker Avance 300, 400, or 500 instruments (Billerica, USA) were used. Chemical shifts were indicated in parts per million (ppm) and coupling constants (*J*) were indicated in Hertz (Hz). Spin multiplicities were abbreviated as follows: s: singlet, d: doublet, t: triplet, ps-t: pseudo-triplet, dd: doublet of doublets, dt: doublet of triplets, m: multiplet, etc. In order to exchange exchangeable protons by deuterium, analytes were dissolved in CD_3OD and the solvent was removed in a nitrogen stream. This process was repeated three times before measurement.

5.1.9.3 Mass spectrometry

For EI-MS, a MAT 95 XL sector field instrument (Thermo Finnigan MAT GmbH, Bremen, Ger) or a MAT 90 sector field instrument (Thermo Finnigan MAT GmbH) were used. For ESI-MS and ESI-MS/MS, a nano-ESI-QTOF mass spectrometer (Micromass, Manchester, UK) was used. In general, the positive ion mode was used because it showed a higher sensitivity towards gangliosides than the negative ion mode. For interpretation of the ESI-MS/MS spectra, the nomenclature for carbohydrate fragments by Domon et al. was applied (154). The major part of fragments in the CID of gangliosides results from heterolytic cleavage of glycosidic- and interglycosidic bonds. If a glycosidic bond is cleaved, the fragments are termed B_i and Y_j. If an interglycosidic bond is cleaved, the fragments are termed C_i and Z_j. B and C fragments contain a reducing end and Y and Z fragments contain a non-reducing end. The subscripts i and j indicate the bond which was cleaved, counting for B and C fragments from the non-reducing end and for Z and Y fragments from the aglycon bond, which is termed 0. If a sugar ring is fragmented, the fragments are termed $^{k,l}A_i$ and $^{k,l}X_j$. The superscripts k and l indicate the two bonds of the sugar which were cleaved. The A fragment contains a non-reducing end while the X fragment contain a reducing end. If a glycoconjugate is branched, the “antennas” are described by subscripted Greek letters, where α indicates the antenna with the largest molecular weight, β indicates the antenna with the second largest molecular

weight, etc. If second generation fragmentation occurs, the resulting fragment is indicated by the first-order fragment, a slash, and the fragment which was lost by second order cleavage (109), for example $Y_{2\alpha}/B_{1\beta}$.

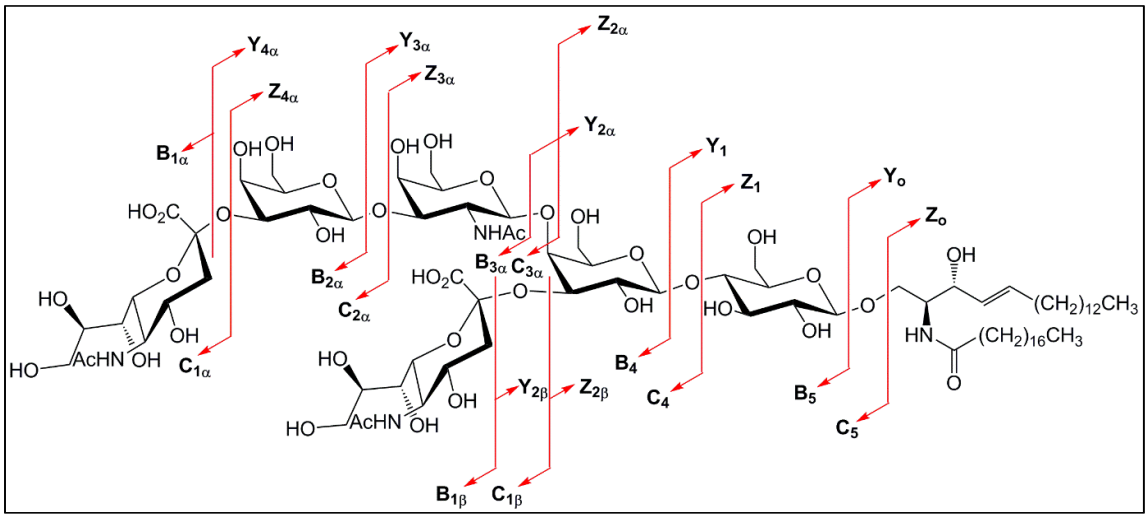

Fig. 5.1.1: Nomenclature of ganglioside ESI-MS/MS fragments presented for d18:1/18:0-GD1a

5.1.9.4 GC-MS

For GC-MS, a GCMS-QP2010 Ultra (Shimadzu, Kyoto, Jpn) was used. It was equipped with a ZB-5MSi column (l = 30 m, Ø = 0.25 mm, df (film thickness) = 0.25 µm) containing a 5 % phenyl and 95 % dimethylpolysiloxane stationary phase.

5.1.9.5 CHN-microanalysis

For CHN-microanalysis, a vario EL cube (Elementar Analysensysteme GmbH, Hanau, Ger) was used.

5.1.9.6 Photometric sialic acid determination

In general, ganglioside yields were calculated by weighing, dissolving in a defined volume of methanol and subsequent sialic acid determination.

Photometric sialic acid determination was performed by the resorcinol method by Svennerholm et al. (137) modified by Miettinen et al (136). All standards and analytes were measured in duplicate. Standard curves were measured by five different concentrations of sialic acid (0 µg/mL, 2.5 µg/mL, 5.0 µg/mL, 10 µg/mL, 15 µg/mL, and 20 µg/mL). Resorcinol reagent was prepared by adding 20 mL of an aq.

10 mg/mL resorcinol solution to 80 mL of 37 % aq. HCl and 0.25 mL of an aq. 25 mg/mL $CuSO_4 \cdot 5\ H_2O$ solution. 250 µL of a sample containing 1 to 10 µg of sialic acid were applied to an Eppendorf tube. 250 µL of resorcinol reagent were added, the tube was vortexed, and heated for 20 min at 100 °C. The mixture was cooled on a water/ice bath and 500 µL of *n*-butyl acetate/*n*-butanol 85:15 v/v were added. After vortexing, 370 µL of the upper phase were measured photometrically at 580 nm.

5.1.9.7 Fluorimetric sialic acid determination

The sialic acid assay kit EnzyChrom™ ESLA-100 of BioAssay Systems (Hayward, USA) was used. All standards and analytes were measured in duplicate. Standard curves were measured by five different concentrations of sialic acid (0 mM, 0.02 mM, 0.04 mM, 0.06 mM, 0.08 mM, and 0.1 mM). 20 µL of a sample containing a sialic acid concentration of 0.06-0.6 mM were mixed with 80 µL of hydrolysis reagent and incubated at 80 °C for 60 min. The mixture was cooled to RT and 20 µL of neutralization reagent were added. After vortexing, 10 µL of each standard and each sample were applied to black 96-well-plate and 90 µL of working reagent were added. Working reagent contains NANA-aldolase activity, pyruvate oxidase activity to produce hydrogen peroxide, *p*-chlorophenol, and 4-aminoantipyrine (135). After incubation at RT for 60 min, the fluorescence was read at λ_{ex} = 544 nm and λ_{em} = 590 nm.

5.1.9.8 Densitometry

For densitometry, HPTLC Kieselgel 60 plates (10x10 cm) manufactured by Merck were used. After development with Kägi-Miescher reagent, the TLC plates were densitometrically scanned at a wavelength of 595 nm. For densitometric quantification, the analyte was applied to one lane. A calibration curve was obtained by applying 1 µg, 3 µg, and 5 µg of standard to three other lanes. The analyte mass was plotted against the absorption in order to simplify the evaluation. The data were polynomial evaluated and the analyte concentration was calculated from the regression curve.

5.2 Purification of gangliosides

5.2.1 Separation of Cronassial© by NP column chromatography

Experimental procedure:

1.02 g of Cronassial® were separated by NP column chromatography on silica gel (Merck-silica gel 60/40-63 µm, 3.0 × 52 cm, isocratic, eluent: $CHCl_3$/MeOH/0.2 % $CaCl_2$ 60:35:8 v/v/v). By this, fractions of pure GM1 and GD1a were obtained. After desalting, evaporation, and drying in vacuum GM1 (135 mg) and GD1a (246 mg) were obtained as colorless solids.

Analytics:

The analytics of GM1 are described in section 5.2.3. The analytics of GD1a are described in section 5.2.4.

5.2.2 Separation of Cronassial® by anion-exchange chromatography

Experimental procedure:

15 g of DEAE Sephadex® A-25 were suspended in 150 mL of $CHCl_3$/MeOH/0.8 M NaOAc 30:60:8 v/v/v, left for 30 min and decanted. The procedure was repeated 4 times and the anion-exchanger was left in the same solvent overnight. Afterwards, it was washed four times with 150 mL of $CHCl_3$/MeOH/H_2O 30:60:8 v/v/v and introduced into a column (2.2 × 22.2 cm). Then, 5.03 g of Cronassial were dissolved in 400 mL of the same solvent and applied to the column (v ≤ 1 mL/min). The column was washed with $CHCl_3$/MeOH/H_2O 30:60:8 v/v/v until all not adsorbed gangliosides were eluted. Then, a step gradient of different NH_4OAc-concentrations in MeOH was used to elute the different ganglioside classes. Subsequently, each ganglioside class was desalted. After evaporation and drying in vacuum, the ganglioside classes were obtained as colorless solids in amounts ranging from 41.5 mg to 2.80 g (Tab. 5.2.1).

Ganglioside class	c(NH_4OAc) (mol/L)	Amount (g)
Monosialogangliosides	0.05	1.28
Disialogangliosides	0.15	2.80
Trisialogangliosides	0.15	0.674
Tetrasialogangliosides	0.45	0.0415

Tab. 5.2.1: Results of the anion-exchange chromatography of Cronassial®

The procedure was repeated one time under slightly modified conditions in order to obtain more GQ1b. DEAE-sephadex was swollen in water. Then it was introduced into a column and washed by 30 column volumes 1 M aq. NaOAc. The eluate showed no Cl^- content in an AgCl precipitation test. The column material was suspended in $CHCl_3$/MeOH/H_2O 30:60:8 v/v/v and introduced into a column (Ø = 2.2 cm, h = 37.5 cm). Then, 10.0 g of Cronassial were applied. The procedure was the same like described above. This time a step gradient of different NH_4OAc-concentrations in $CHCl_3$/MeOH/H_2O 30:60:8 v/v/v was used. Monosialogangliosides were obtained at c (NH_4OAc) = 0.02 mol/L, disialogangliosides at c (NH_4OAc) = 0.04 mol/L, trisialogangliosides at c (NH_4OAc) = 0.05 mol/L, and GQ1b at c (NH_4OAc) = 0.08 mol/L. Yields were not estimated for this elution system because the only purpose of this experiment was to obtain more GQ1b.

Analytics:

HPTLC:

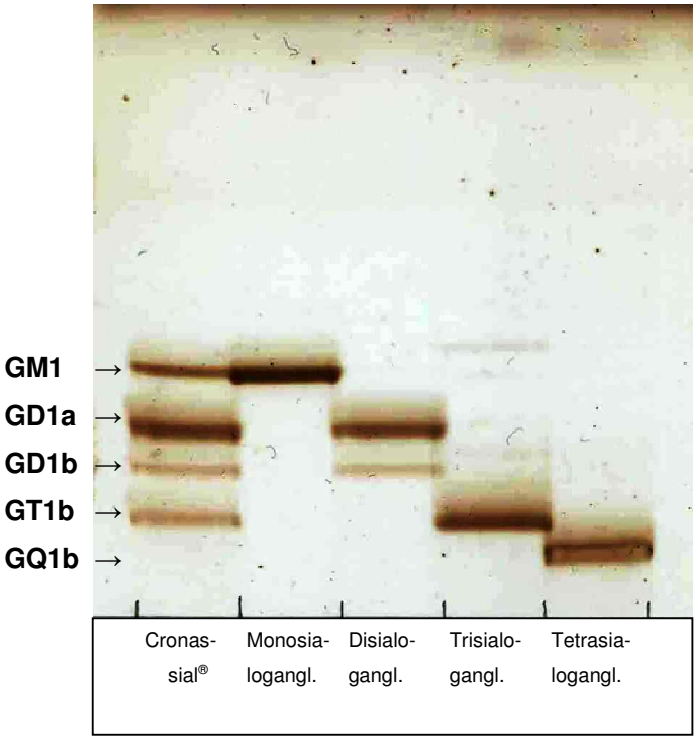

Fig. 5.2.1: *NP HPTLC of the isolated ganglioside classes.* Solvent system: $CHCl_3$/MeOH/0.2 % $CaCl_2$ 50:42:11 v/v/v.

5.2.3 Separation of monosialogangliosides

Experimental procedure:

1.28 g of monosialogangliosides were separated by NP chromatography on silica gel (Merck-silica gel 60/15-40 µm, 3.5 × 25 cm, isocratic, eluent: $CHCl_3$/MeOH/0.2 % $CaCl_2$ 60:35:8 v/v/v). After desalting, GM1 was obtained as a colorless solid (300 mg).

Analytics:

Ganglioside	Molecular Formula	Molecular Weight (g/mol)	R_f (RP TLC, MeOH/ H_2O 90:9 v/v)
d18:1/18:0-GM1	$C_{73}H_{131}N_3O_{31}$	1546.84	0.24
d20:1/18:0-GM1	$C_{75}H_{135}N_3O_{31}$	1574.90	0.18

Tab. 5.2.2: Physical properties of GM1

MS (ESI, pos. Mode, MeOH, M_1 = 1545.88, M_2 = 1573.91): m/z (%) = 1591.91 (1.5) $[M_2 + NH_4]^+$, 1577.90 (1.1) $[M_1 + M_2 + 2NH_4]^{2+}$, 1574.86 (0.50) $[M_2 + H]^+$, 1057.95 (2.0) $[M_1 + M_2 + 3NH_4]^{3+}$, 815.45 (7.6) $[M_2 + K + NH_4]^{2+}$, 807.46 (15) $[M_2 + Na + NH_4]^{2+}$, 798.96 (7.0) $[M_2 + Na + H]^{2+}$, 804.98 (100) $[M_2 + 2NH_4]^{2+}$, 796.46 (49) $[M_2 + NH_4 + H]^{2+}$, 787.95 (11) $[M_2 + 2H]^{2+}$, 1584.88 (0.46) $[M_1 + K]^+$, 1563.88 (1.2) $[M_1 + NH_4]^+$, 801.43 (6.7) $[M_1 + K + NH_4]^+$, 793.44 (13) $[M_1 + Na + NH_4]^{2+}$, 784.94 (3.6) $[M_1 + Na + H]^{2+}$, 790.96 (87) $[M_1 + 2NH_4]^{2+}$, 782.45 (41) $[M_1 + NH_4 + H]^{2+}$, 773.94 (10) $[M_1 + 2H]^{2+}$.

MS/MS (m/z = 804.98): m/z (%) = 1265.79 (3.4) $[Z_{2\beta}]^+$, 1191.76 (14) $[Z_{2\alpha}]^+$, 1103.72 (7.3) $[Z_{2\beta}/B_{1\alpha} + H]^+$, 900.67 (25) $[Z_{2\beta}/B_{2\alpha} + H]^+$, 804.89 (3.5) $[M_2 + 2NH_4]^{2+}$, 738.61 (32) $[Z_1]^+$, 594.57 (6.0) $[Y_0 + 2H]^+$, 576.56 (65) $[Z_0]^+$, 558.55 (14) $[Z_0 - H_2O]^+$, 366.14 (100) $[B_{2\alpha}]^+$, 292.29 (36) $[B_{1\beta}]^+$, 274.08 (48) $[B_{1\beta} - H_2O]^+$, 204.06 (93) $[B_{2\alpha}/B_{1\alpha} + H]^+$, 186.04 (35) $[B_{2\alpha}/B_{1\alpha} + H - H_2O]^+$.

MS/MS (m/z = 790.96): m/z (%) = 1237.74 (2.8) $[Z_{2\beta}]^+$, 1163.70 (10) $[Z_{2\alpha}]^+$, 1075.71 (9.5) $[Z_{2\beta}/B_{1\alpha} + H]^+$, 872.63 (30) $[Z_{2\beta}/B_{2\alpha} + H]^+$, 710.59 (32) $[Z_1]^+$, 566.54 (2.8) $[Y_0 + 2H]^+$, 548.53 (70) $[Z_0]^+$, 530.52 (17) $[Z_0 - H_2O]^+$, 366.14 (100) $[B_{2\alpha}]^+$, 292.09 (20)

$[B_{1\beta}]^+$, 274.08 (53) $[B_{1\beta} - H_2O]^+$, 204.06 (100) $[B_{2\alpha}/B_{1\alpha} + H]^+$, 186.04 (36) $[B_{2\alpha}/B_{1\alpha} + H - H_2O]^+$.

5.2.4 Separation of disialogangliosides

Experimental procedure:

1.00 g of disialogangliosides were separated by NP column chromatography on silica gel (Merck-silica gel 60/40-63 µm, 2.5 × 21.0 cm, step gradient). The gangliosides were applied to the column in $CHCl_3$/MeOH/2.5 M NH_3 60:35:4 v/v/v. GD1a was eluted by $CHCl_3$/MeOH/2.5 M NH_3 60:35:6 v/v/v while GD1b was eluted by $CHCl_3$/MeOH/2.5 M NH_3 60:35:8 v/v/v. After evaporation and drying in vacuum, the disialogangliosides were obtained as colorless solids (GD1a: 472 mg, GD1b: 158 mg).

Analytics:

Ganglioside	Molecular Formula	Molecular Weight (g/mol)	R_f (RP TLC, MeOH/ H_2O 90:10 v/v)
d18:1/18:0-GD1a·2NH_3	$C_{84}H_{154}N_6O_{39}$	1872.16	0.32
d20:1/18:0-GD1a·2NH_3	$C_{86}H_{158}N_6O_{39}$	1900.21	0.23
d18:1/18:0-GD1b·2NH_3	$C_{84}H_{154}N_6O_{39}$	1872.16	0.19
d20:1/18:0-GD1b·2NH_3	$C_{86}H_{158}N_6O_{39}$	1900.21	0.13

Tab. 5.2.3: *Physical properties of GD1a and GD1b.* The ammonium salts resulted from the last purification step in which an ammonia containing eluent was used.

MS (ESI, pos. Mode, MeOH, M_1 = 1836.97, M_2 = 1865.00): m/z (%) = 1882.81 (0.53) $[M_2 + NH_4]^+$, 1866.93 (0.60) $[M_2 + H]^+$, 971.46 (7.3) $[M_2 + 2K]^{2+}$, 963.48 (14) $[M_2 + K + Na]^{2+}$, 961.00 (21) $[M_2 + K + NH_4]^{2+}$, 953.00 (30) $[M_2 + Na + NH_4]^{2+}$, 950.53 (100) $[M_2 + 2NH_4]^{2+}$, 942.01 (33) $[M_2 + NH_4 + H]^{2+}$, 933.50 (23) $[M_2 + 2H]^{2+}$, 946.98 (12) $[M_1 + K + NH_4]^{2+}$, 936.52 (62) $[M_1 + 2NH_4]^{2+}$, 928.00 (21) $[M_1 + NH_4 + H]^{2+}$, 919.49 (16) $[M_1 + 2H]^{2+}$.

MS/MS (m/z = 950.53): m/z (%) = 1866.98 (7.1) $[M_2 + H]^+$, 1394.83 (5.5) $[Z_{3\alpha}]^+$, 1191.77 (13) $[Z_{2\alpha}]^+$, 1103.76 (4.3) $[Z_{3\alpha}/B_{1\beta} + H]^+$, 950.45 (5.6) $[M + 2NH_4]^{2+}$, 900.67

(13) $[Z_{2\alpha}/B_{1\beta} + H]^+$, 756.63 (8.8) $[Y_1 + 2H]^+$, 738.62 (31) $[Z_1]^+$, 657.23 (63) $[B_{3\alpha}]^+$, 594.59 (8.3) $[Y_0 + 2H]^+$, 576.57 (62) $[Z_0]^+$, 558.57 (8.4) $[Z_0 - H_2O]^+$, 454.15 (13) $[B_{2\alpha}]^+$, 366.14 (30) $[B_{3\alpha}/B_{1\alpha} + H]^+$, 292.09 (100) $[B_{1\alpha}$ o. $B_{1\beta}]^+$, 274.08 (92) $[B_{1\alpha}$ o. $B_{1\beta} - H_2O]^+$, 204.06 (55) $[B_{3\alpha}/B_{2\alpha} + H]^+$, 186.04 (7.4) $[B_{3\alpha}/B_{2\alpha} + H - H_2O]^+$.

MS/MS (m/z = 936.52): m/z (%) = 1866.98 (12) $[M_2 + H]^+$, 1366.86 (6.1) $[Z_{3\alpha}]^+$, 1181.73 (6.1) $[Y_{2\alpha} + 2H]^+$, 1163.74 (19) $[Z_{2\alpha}]^+$, 1075.71 (4.4) $[Z_{3\alpha}/B_{1\beta} + H]^+$, 872.64 (13) $[Z_{2\alpha}/B_{1\beta} + H]^+$, 728.60 (13) $[Y_1 + 2H]^+$, 710.59 (31) $[Z_1]^+$, 657.23 (76) $[B_{3\alpha}]^+$, 566.57 (9.0) $[Y_0 + 2H]^+$, 548.54 (53) $[Z_0]^+$, 454.15 (18) $[B_{2\alpha}]^+$, 366.14 (30) $[B_{3\alpha}/B_{1\alpha} + H]^+$, 292.10 (100) $[B_{1\alpha}$ o. $B_{1\beta}]^+$, 274.08 (98) $[B_{1\alpha}$ o. $B_{1\beta} - H_2O]^+$, 204.06 (47) $[B_{3\alpha}/B_{2\alpha} + H]^+$, 186.05 (5.8) $[B_{3\alpha}/B_{2\alpha} + H - H_2O]^+$.

MS (ESI, pos. Mode, MeOH, M_1 = 1836.97, M_2 = 1865.00): m/z (%) = 1882.87 (2.2) $[M_2 + NH_4]^+$, 1866.90 (2.9) $[M_2 + H]^+$, 963.46 (4.0) $[M_2 + K + Na]^{2+}$, 960.99 (5.2) $[M_2 + K + NH_4]^{2+}$, 955.48 (5.0) $[M_2 + 2Na]^{2+}$, 952.99 (13) $[M_2 + Na + NH_4]^{2+}$, 944.49 (19) $[M_2 + Na + H]^{2+}$, 950.51 (27) $[M_2 + 2NH_4]^{2+}$, 942.00 (72) $[M_2 + NH_4 + H]^{2+}$, 933.49 (100) $[M_2 + 2H]^{2+}$, 930.47 (12) $[M_1 + Na + H]^{2+}$, 936.51 (17) $[M_1 + 2NH_4]^{2+}$, 927.99 (43) $[M_1 + NH_4 + H]^{2+}$, 919.48 (62) $[M_1 + 2H]^{2+}$.

MS/MS (m/z = 933.49): m/z (%) = 1866.98 (2.4) $[M_2 + H]^+$, 1265.80 (3.5) $[Z_{2\alpha}]^+$, 1191.77 (6.3) $[Z_{2\beta}/B_{1\alpha} + H]^+$, 1103.75 (6.9) $[Z_{3\beta}/B_{2\alpha} + H]^+$, 900.67 (16) $[Z_{2\beta}/B_{2\alpha} + H]^+$, 738.62 (19) $[Z_1]^+$, 576.56 (53) $[Z_0]^+$, 558.56 (12) $[Z_0 - H_2O]^+$, 454.15 (3,6) $[Z_{2\beta}/B_{1\alpha}/Z_1 + 2H]^+$, 366.14 (92) $[B_{2\beta}]^+$, 292.09 (58) $[B_{1\alpha}]^+$, 274.08 (100) $[B_{1\alpha} - H_2O]^+$, 204.06 (67) $[B_{1\beta}/B_{1\beta} + H]^+$, 186.04 (23) $[B_{1\beta}/B_{1\beta} + H - H_2O]^+$.

MS/MS (m/z = 919.48): m/z (%) = 1866.98 (3.0) $[M_2 + H]^+$, 1366.80 (3.2) $[Z_{3\beta}/B_{1\alpha} + H]^+$, 1237.77 (5.2) $[Z_{2\alpha}]^+$, 1163.74 (8.6) $[Z_{2\beta}/B_{1\alpha} + H]^+$, 1075.72 (8.0) $[Z_{3\beta}/B_{2\alpha} + H]^+$, 872.63 (16) $[Z_{2\beta}/B_{2\alpha} + H]^+$, 728.59 (3.1) $[Y_1 + 2H]^+$, 710.59 (17) $[Z_1]^+$, 566.55 (4.5) $[Y_0 + 2H]^+$, 548.54 (40) $[Z_0]^+$, 530.53 (6.7) $[Z_0 - H_2O]^+$, 454.15 (4.5) $[Z_{2\beta}/B_{1\alpha}/Z_1 + 2H]^+$, 366.14 (100) $[B_{2\beta}]^+$, 292.09 (67) $[B_{1\alpha}]^+$, 274.08 (80) $[B_{1\alpha} - H_2O]^+$, 204.06 (44) $[B_{1\beta}/B_{1\beta} + H]^+$, 186.04 (12) $[B_{1\beta}/B_{1\beta} + H - H_2O]^+$.

5.2.5 Separation of trisialogangliosides

Experimental procedure:

0.674 g of trisialogangliosides were separated by NP column chromatography on silica gel (Merck-silica gel 60/40-63 µm, 3.5 × 53 cm, isocratic, eluent: $CHCl_3$/MeOH/H_2O 50:42:11 v/v/v). After evaporation and drying in vacuum, GT1b was obtained as a colorless solid (382 mg).

Analytics:

Ganglioside	Molecular Formula	Molecular Weight (g/mol)	R_f (RP TLC, MeOH/ H_2O 90:10 v/v)
d18:1/18:0-GT1b	$C_{95}H_{165}N_5O_{47}$	2129.35	0.39
d20:1/18:0-GT1b	$C_{97}H_{169}N_5O_{47}$	2157.41	0.29

Tab. 5.2.4: Physical properties of GT1b

MS (ESI, pos. Mode, MeOH, M_1 = 2129.07, M_2 = 2157.10, M_3 = 2185.13): m/z (%) = 1866.90 (3.0) $[Y_{3\beta} + 2H]^+$, 1459.01 (6.6) $[2M_2 + K + Na + H]^{3+}$, 1109.50 (27) $[M_2 + K + Na]^{2+}$, 1107.01 (14) $[M_2 + K + NH_4]^{2+}$, 1098.53 (73) $[M_2 + K + H]^{2+}$, 1101.52 (58) $[M_2 + 2Na]^{2+}$, 1090.52 (38) $[M_2 + Na + H]^{2+}$, 1096.57 (63) $[M_2 + 2NH_4]^{2+}$, 1088.04 (100) $[M_2 + NH_4 + H]^{2+}$, 1079.54 (96) $[M_2 + 2H]^{2+}$, 1084.52 (32) $[M_1 + K + H]^{2+}$, 1087.54 (97) $[M_1 + 2Na]^{2+}$, 1085.02 (34) $[M_1 + Na + NH_4]^{2+}$, 1076.51 (21) $[M_1 + Na + H]^{2+}$, 1082.55 (34) $[M_1 + 2NH_4]^{2+}$, 1074.04 (44) $[M_1 + NH_4 + H]^{2+}$, 1065.51 (54) $[M_1 + 2H]^{2+}$, 1131.50 (11) $[M_3 + 2K]^{2+}$, 1123.50 (17) $[M_3 + K + Na]^{2+}$, 1121.00 (15) $[M_3 + K + NH_4]^{2+}$, 1112.51 (31) $[M_3 + K + H]^{2+}$, 1113.01 (25) $[M_3 + Na + NH_4]^{2+}$.

MS/MS (m/z = 1088.04): m/z (%) = 1482.89 (3.7) $[Z_{2\alpha}]^+$, 1191.79 (4.5) $[Z_{2\alpha}/B_{1\beta} + H]^+$, 1088.04 (11) $[M_2 + NH_4 + H]^{2+}$, 941.99 (8.7) $[Y_{3\beta} + 2H + NH_4]^{2+}$, 900.69 (8.2) $[Z_{2\alpha}/B_{2\beta} + H]^+$, 738.64 (9.5) $[Z_1]^+$, 657.25 (72) $[B_{3\alpha}]^+$, 576.59 (29) $[Z_0]^+$, 454.17 (20) $[B_{2\alpha}]^+$, 366.15 (17) $[B_{3\alpha}/B_{1\alpha} + H]^+$, 292.10 (100) $[B_{1\alpha}$ o. $B_{1\beta}]^+$, 274.09 (58) $[B_{1\alpha}$ o. $B_{1\beta} - H_2O]^+$, 204.06 (19) $[B_{3\alpha}/B_{2\alpha} + H]^+$.

MS/MS (m/z = 1065.51): m/z (%) = 1163.73 (5.1) $[Z_{2\alpha}/B_{1\beta} + H]^+$, 1065.56 (6.9) $[M_1 + 2H]^{2+}$, 872.65 (7.8) $[Z_{2\alpha}/B_{2\beta} + H]^+$, 710.64 (6.6) $[Z_1]^+$, 657.24 (52) $[B_{3\alpha}]^+$, 548.55 (29) $[Z_0]^+$, 454.17 (21) $[B_{2\alpha}]^+$, 366.15 (16) $[B_{3\alpha}/B_{1\alpha} + H]^+$, 292.10 (100) $[B_{1\alpha}$ o. $B_{1\beta}]^+$, 274.08 (64) $[B_{1\alpha}$ o. $B_{1\beta} - H_2O]^+$, 204.06 (26) $[B_{3\alpha}/B_{2\alpha} + H]^+$.

5.2.6 Analytics of GQ1b

GQ1b was already obtained in pure form after anion-exchange chromatography and subsequent desalting.

Analytics:

Ganglioside	Molecular Formula	Molecular Weight (g/mol)	R_f (RP TLC, MeOH/ H_2O 90:20 v/v)
d18:1/18:0-GQ1b	$C_{106}H_{182}N_6O_{55}$	2420.59	0.24
d20:1/18:0-GQ1b	$C_{108}H_{186}N_6O_{55}$	2448.64	0.16

Tab. 5.2.5: Physical properties of GQ1b

MS (ESI, pos. Mode, MeOH, M_1 = 2420.17, M_2 = 2448.20): m/z (%) = 1657.15 (2.0) $[2M_2 + K + 2NH_4]^{3+}$, 1263.10 (15) $[M_2 + 2K]^{2+}$, 1252.62 (59) $[M_2 + K + NH_4]^{2+}$, 1244.13 (42) $[M_2 + K + H]^{2+}$, 1244.62 (34) $[M_2 + Na + NH_4]^{2+}$, 1242.16 (100) $[M_2 + 2NH_4]^{2+}$, 1233.65 (67) $[M_2 + NH_4 + H]^{2+}$, 1225.14 (30) $[M_2 + 2H]^{2+}$, 1249.10 (7.9) $[M_1 + 2K]^{2+}$, 1238.61 (23) $[M_1 + K + NH_4]^{2+}$, 1230.61 (13) $[M_1 + Na + NH_4]^{2+}$, 1228.15 (41) $[M_1 + 2NH_4]^{2+}$, 1219.63 (28) $[M_2 + NH_4 + H]^{2+}$, 1211.12 (13) $[M_2 + 2H]^{2+}$.

MS/MS (m/z = 1242.16): m/z (%) = 1483.88 (4.7) $[Z_{2\alpha}]^+$, 1191.81 (5.0) $[Z_{2\alpha}/B_{1\beta} + H]^+$, 948.35 (38) $[B_{4\alpha}]^+$, 918.71 (6.6) $[Y_{2\alpha}/B_{2\beta} + 3H]^+$, 900.70 (6.8) $[Z_{2\alpha}/B_{2\beta} + H]^+$, 756.65 (6.9) $[Y_1 + 2H]^+$, 745.27 (11) $[B_{3\alpha}]^+$, 657.25 (20) $[B_{4\alpha}/B_{1\alpha} + H]^+$, 594.59 (12) $[Y_0 + 2H]^+$, 583.21 (25) [$B_{2\alpha}$ o. $B_{2\beta}$], 576.59 (26) $[Z_0]^+$, 454.17 (33) $[B_{3\alpha}/B_{1\alpha} + H]^+$, 366.15 (11) $[B_{4\alpha}/B_{2\alpha} + H]^+$, 292.11 (100) $[B_{1\alpha}$ o. $B_{1\beta}]^+$, 274.09 (36) $[B_{1\alpha}$ o. $B_{1\beta} - H_2O]^+$, 204.07 (4.6) $[B_{4\alpha}/B_{3\alpha} + H]^+$.

MS/MS (m/z = 1228.15): m/z (%) = 1454.87 (6.5) $[Z_{2\alpha}]^+$, 1228.15 (3.9) $[M_1 + 2NH_4]^{2+}$, 1163.77 (6.6) $[Z_{2\alpha}/B_{1\beta} + H]^+$, 948.35 (43) $[B_{4\alpha}]^+$, 890.66 (7.4) $[Y_{2\alpha}/B_{2\beta} + 3H]^+$, 872.67 (7.1) $[Z_{2\alpha}/B_{2\beta} + H]^+$, 745.27 (14) $[B_{3\alpha}]^+$, 728.62 (9.2) $[Y_1 + 2H]^+$, 710.61 (9.4) $[Z_1]^+$, 657.25 (21) $[B_{4\alpha}/B_{1\alpha} + H]^+$, 583.21 (20) $[B_{2\alpha}$ o. $B_{2\beta}]$, 548.55 (26) $[Z_0]^+$, 454.17 (26) $[B_{3\alpha}/B_{1\alpha} + H]^+$, 366.14 (12) $[B_{4\alpha}/B_{2\alpha} + H]^+$, 292.10 (100) $[B_{1\alpha}$ o. $B_{1\beta}]^+$, 274.09 (37) $[B_{1\alpha}$ o. $B_{1\beta} - H_2O]^+$, 204.06 (5.7) $[B_{4\alpha}/B_{3\alpha} + H]^+$.

5.2.7 Separation of d20:1/18:0-GM1·NH_3 and d18:1/18:0-GM1·NH_3

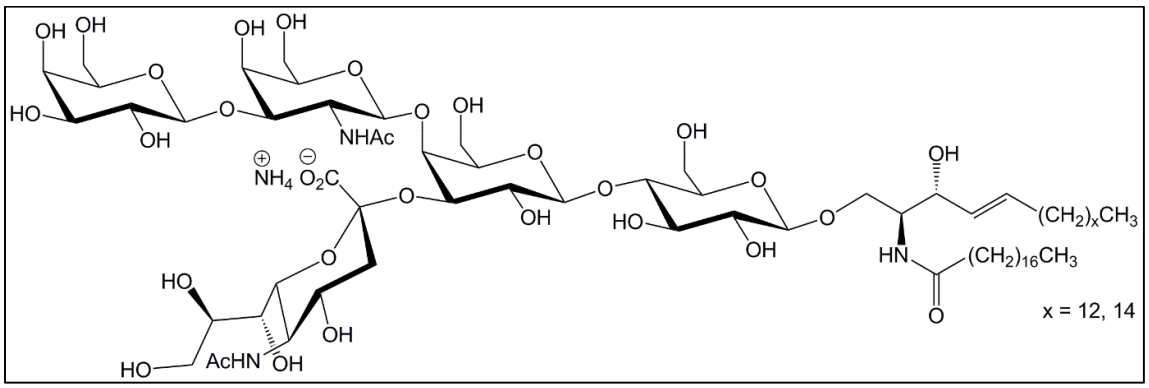

Experimental procedure:

GM1 (300 mg) was separated into its lipoforms by RP column chromatography (Merck-LiChroprep RP-18/40-63 µm, 2.0 × 3.5 cm, isocratic, eluent: MeOH/H_2O 90:25 v/v). Column material was removed from both fractions by NP column chromatography (Merck-silica gel 60/40-63 µm, 2.0 cm × 3.5 cm, step gradient, application: $CHCl_3$/MeOH/2.5 M NH_3 60:35:2 v/v/v, elution: $CHCl_3$/MeOH/2.5 M NH_3 60:40:10 v/v/v). After lyophilization, d18:1/18:0-GM1·NH_3 (**1**) (64.8 mg) and d20:1/18:0-GM1·NH_3 (**2**) (100 mg) were obtained as colorless powders.

Analytics of d18:1/18:0-GM1·NH_3 (1):

Molecular Formula: $C_{73}H_{134}N_4O_{31}$

Molecular Weight: 1563.87 g/mol

R_f = 0.20 ($CHCl_3$/MeOH/2.5 M NH_3 60:40:9 v/v/v)

^{1}H NMR (500 MHz, DMF-d_7, RT): δ [ppm] = 8.55 (s, 1H, GalNAc, NH), 7.67 (d, 1H, $^{3}J_{NH\text{-}H5}$ = 5,5 Hz, NeuAc, NH), 7.44 (s, 1H, Cer, NH), 5.89 (s, OH), 5.69 – 5.59 (m, 1H, Cer, H-5), 5.50 (dd, 1H, $^{3}J_{H4\text{-}H5,\ trans}$ = 15.3 Hz, $^{3}J_{H4\text{-}H3}$ = 7.1 Hz, Cer, H-4), 5.06 (bs, OH), 4.51 (d, 1H, $^{3}J_{H1\text{-}H2}$ = 7.4 Hz, Gal, H-1), 4.40 (m, 1H, Gal, H-1), 4.30 (d, 1H, $^{3}J_{H1\text{-}H2}$ = 7.7 Hz, Glc, H-1), 4.22 – 3.16 (m, 35H), 2.74 – 2.69 (m, 1H, NeuAc, H-3e), 2.16 (t, 2H, $^{3}J_{H2'\text{-}H3'}$ = 7.2 Hz, Cer, H-2'), 2.03 (s, 3H, NeuAc, C$\underline{H}_3CO_2R$), 1.99 (dt, 2H, $^{3}J_{H6\text{-}H5}$ = 6,9 Hz, $^{3}J_{H6\text{-}H7}$ = 6.9 Hz, Cer, H-6), 1.94 – 1.83 (m, 4H, GalNAc (C$\underline{H}_3CO_2R$), NeuAc (H-3a)), 1.63 – 1.49 (m, 2H, Cer, H-3'), 1.43 – 1.20 (m, 50H), 0.88 (t, 6H, $^{3}J_{H18\text{-}H17}$ = 6.1 Hz, $^{3}J_{H18'\text{-}H17'}$ = 6,1 Hz, Cer, H-18, H-18').

^{1}H NMR (500 MHz, DMF-d_7, RT, exchangeable Protons were exchanged by deuterium prior to measurement): δ [ppm] = 5.70 – 5.58 (m, 1H, Cer, H-5), 5.50 (dd, 1H, $^{3}J_{H4\text{-}H5,\ trans}$ = 15.4 Hz, $^{3}J_{H4\text{-}H3}$ = 6.9 Hz, Cer, H-4), 5.02 (d, 1H, $^{3}J_{H1\text{-}H2}$ = 8.7 Hz, GalNAc, H-1), 4.52 (d, 1H, $^{3}J_{H1\text{-}H2}$ = 7.9 Hz, Gal, H-1), 4.41 (m, 1H, Gal, H-1), 4.31 (d, 1H, $^{3}J_{H1\text{-}H2}$ = 7.8 Hz, Glc, H-1), 4.22 – 3.14 (m, 35H), 2.73 – 2.68 (m, 1H, NeuAc, H-3e), 2.16 (t, 2H, $^{3}J_{H2'\text{-}H3'}$ = 7.2 Hz, Cer, H-2'), 2.02 (s, 3H, NeuAc, C$\underline{H}_3CO_2R$), 1.98 (m, 2H, Cer, H-6), 1.87 (s, 3H, GalNAc, C$\underline{H}_3CO_2R$), 1.54 (m, 2H, Cer, H-3'), 1.29 (m, 50H), 0.88 (t, 6H, $^{3}J_{H18\text{-}H17}$ = 6.7 Hz, $^{3}J_{H18'\text{-}H17'}$ = 6,7 Hz, Cer, H-18, H18').

MS (ESI, pos. Mode, MeOH): m/z (%) = 1568.83 (1.1) $[M + Na]^+$, 1563.86 (3.3) $[M + NH_4]^+$, 1555.35 (1.3) $[2M + NH_4 + H]^{2+}$, 1546.84 (1.7) $[M + H]^+$, 1181.71 (7.7) $[Y_{2\alpha} + 2H]^+$, 793.40 (4.4) $[M + Na + NH_4]^{2+}$, 790.94 (2.1) $[M + 2NH_4]^{2+}$, 784.91 (6.6) $[M + Na + H]^{2+}$, 782.43 (12) $[M + NH_4 + H]^{2+}$, 773.92 (100) $[M + 2H]^{2+}$.

MS/MS (m/z = 773.92): m/z (%) = 1237.73 (4.2) $[Z_{2\beta}]^+$, 1163.70 (15) $[Z_{2\alpha}]^+$, 1075.69 (7.3) $[Z_{3\alpha}/B_{1\beta} + H]^+$, 890.63 (3.8) $[Y_{2\alpha}/B_{1\beta} + 3H]^+$, 872.62 (17) $[Z_{2\alpha}/B_{1\beta} + H]^+$, 728.59 (7.6) $[Y_1 + 2H]^+$, 710.58 (19) $[Z_1]^+$, 566.54 (5.9) $[Y_0 + 2H]^+$, 548.53 (37) $[Z_0]^+$, 530.52 (9,1) $[Z_0 - H_2O]^+$, 366.14 (100) $[B_{2\alpha}]^+$, 292.10 (28) $[B_{1\beta}]^+$, 274.10 (39) $[B_{1\beta} - H_2O]^+$, 204.10 (69) $[B_{2\alpha}/B_{1\alpha} + H]^+$, 186.10 (22) $[B_{2\alpha}/B_{1\alpha} + H - H_2O]^+$.

CHN-Analysis:

Theoretical (wt %):	C: 56.07	H: 8.64	N: 3.58
Measured (wt %):	C: 49.61	H: 8.51	N: 3.93

Analytics of d20:1/18:0-GM1·NH_3 (2):

Molecular Formula: $C_{75}H_{138}N_4O_{31}$

Molecular Weight: 1591.93 g/mol

R_f = 0.21 ($CHCl_3$/MeOH/2.5 M NH_3 60:40:9 v/v/v)

MS (ESI, pos. Mode, MeOH): m/z (%) = 1596.88 (2.2) $[M + Na]^+$, 1591.92 (10) $[M + NH_4]^+$, 1583.40 (1.5) $[2M + NH_4 + H]^{2+}$, 1574.88 (1.3) $[M + H]^+$, 1209.76 (4.5) $[Y_{2\alpha} + 2H]^+$, 809.92 (4.1) $[M + 2Na]^{2+}$, 807.43 (7.2) $[M + Na + NH_4]^{2+}$, 804.97 (18) $[M + 2NH_4]^{2+}$, 798.93 (11) $[M + Na + H]^{2+}$, 796.46 (41) $[M + NH_4 + H]^{2+}$, 787.94 (100) $[M + 2H]^{2+}$.

MS/MS (m/z = 773,92): m/z (%) = 1265.78 (2.8) $[Z_{2\beta}]^+$, 1191.75 (11) $[Z_{2\alpha}]^+$, 1103.74 (7.1) $[Z_{3\alpha}/B_{1\beta} + H]^+$, 900.66 (22) $[Z_{2\alpha}/B_{1\beta} + H]^+$, 738.62 (25) $[Z_1]^+$, 594.57 (3.6) $[Y_0 + 2H]^+$, 576.57 (55) $[Z_0]^+$, 558.56 (16) $[Z_0 - H_2O]^+$, 366.14 (82) $[B_{2\alpha}]^+$, 292.31 (75) $[B_{1\beta}]^+$, 274.10 (55) $[B_{1\beta} - H_2O]^+$, 204.10 (100) $[B_{2\alpha}/B_{1\alpha} + H]^+$, 186,09 (47) $[B_{2\alpha}/B_{1\alpha} + H - H_2O]^+$, 126.09 (18) [acetamidopentenylium]$^+$.

CHN-Analysis:

Theoretical (wt %):	C: 56.59	H: 8.74	N: 3.52
Measured (wt %):	C: 53.63	H: 8.70	N: 3.51

5.2.8 Separation of d20:1/18:0-GD1a·$2NH_3$ and d18:1/18:0-GD1a·$2NH_3$ to obtain d18:1/18:0-GD1a·$2NH_3$ (3)

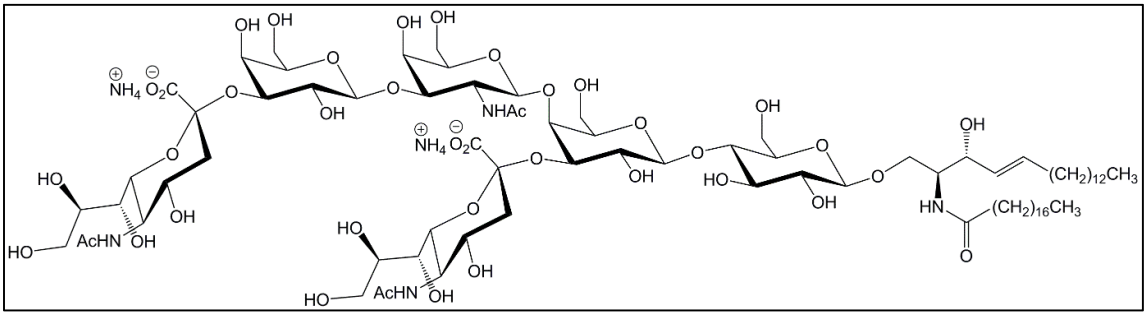

Experimental procedure:

GD1a (472 mg) was separated into its lipoforms by RP column chromatography (Merck-LiChroprep RP-18/40-63 µm, 2.7 × 4.0 cm, isocratic, eluent: MeOH/H_2O 90:49 v/v). Column material was removed by NP column chromatography (Merck-silica gel 60/40-63 µm, 2.0 × 3.5 cm, step gradient, application: $CHCl_3$/MeOH/2.5 M NH_3 60:35:5 v/v/v, elution: $CHCl_3$/MeOH/2.5 M NH_3 60:44:12 v/v/v). After lyophilization, d18:1/18:0-GD1a·2NH_3 was obtained as a colorless powder (89.5 mg).

Analytics:

Molecular Formula: $C_{84}H_{154}N_6O_{39}$

Molecular Weight: 1872.16 g/mol

R_f = 0.18 ($CHCl_3$/MeOH/2.5 M NH_3 60:40:10 v/v/v)

^{1}H-NMR (400 MHz, DMSO-d_6, RT): δ [ppm] = 8.13 (bs, 1H, GalNAc, NH), 7.50 (d, 1H, $^3J_{NH-H5}$ = 8.9 Hz, NeuAc, NH), 7.20 (bs, 1H, NeuAc , NH), 7.07 (d, 1H, $^3J_{NH-H2}$ = 7.1 Hz, Cer, NH), 5.89 (bs, OH), 5.61 – 5.45 (m, 1H, Cer, H-5), 5.34 (dd, 1H, $^3J_{H4-H5,\ trans}$ = 15.2 Hz, $^3J_{H4-H3}$ = 7.1 Hz, Cer, H-4), 5.21 – 4.36 (m, 16H, OH), 4,24 (m, 2H, Gal (II) H-1, Gal (IV) H-1), 4,14 (d, 1H, $^3J_{H1-H2}$ = 7,6 Hz, Glc, H-1), 4.05 – 2.96 (m, 42H), 2.55 (m, 2H, NeuAc A and B, H-3e), 2.02 (t, 2H, $^3J_{H2'-H3'}$ = 7.3 Hz, Cer, H-2'), 1.92 (m, 2H, Cer, H-6), 1.88 (s, 3H, NeuAc, C<u>H</u>$_3$CO$_2$R), 1.88 (s, 3H, NeuAc, C<u>H</u>$_3$CO$_2$R), 1.74 (s, 3H, GalNAc, C<u>H</u>$_3$CO$_2$R), 1.60 (m, 2H, NeuAc A and B, H-3a), 1.41 (m, 2H, Cer, H-3'), 1.23 (m, 50H), 0.85 (t, 6H, $^3J_{H18'-H17'}$ = 6.8 Hz, $^3J_{H18-H17}$ = 6,8 Hz, Cer, H18, H-18').

^{1}H NMR (400 MHz, DMSO-d_6, RT) (exchangeable Protons were exchanged by deuterium prior to measurement): δ [ppm] = 5.58 – 5.48 (m, 1H, Cer, H-5), 5.34 (dd, 1H, $^3J_{H4-H5,\ trans}$ = 15.3 Hz, $^3J_{H4-H3}$ = 7.2 Hz, Cer, H-4), 4.76 (d, 1H, $^3J_{H1-H2}$ = 8.0 Hz, GalNAc, H-1), 4.27 (d, $^3J_{H1-H2}$ = 7.9 Hz, Gal, H-1), 4.23 (d, 1H, $^3J_{H1-H2}$ = 7.6 Hz, Gal, H-1), 4.15 (d, 1H, $^3J_{H1-H2}$ = 7.7 Hz, Glc, H-1), 4.04 – 2.97 (m, 42H), 2.54 (m, 2H, NeuAc A and B, H-3e), 2.02 (t, $^3J_{H2'-H3'}$ = 7.3 Hz, Cer, H-2'), 1.92 (m, 2H, Cer, H-6), 1.87 (s, 3H, NeuAc, C<u>H</u>$_3$CO$_2$R), 1.85 (s, 3H, NeuAc, C<u>H</u>$_3$CO$_2$R), 1.77 (s, 3H, GalNAc, C<u>H</u>$_3$CO$_2$R), 1.65 (m, 2H, NeuAc A and B, H-3a), 1.50 – 1.37 (m, 2H, Cer, H-3'), 1.23 (m, 50H), 0.85 (t, $^3J_{H18'-H17'}$ = 6.8 Hz, $^3J_{H18-H17}$ = 6.8 Hz, H-18, H-18').

MS (ESI, pos. Mode, MeOH): m/z (%) = 1859.92 (2.0) $[M + Na]^+$, 1854.98 (1.5) $[M + NH_4]^+$, 1837.98 (0.43) $[M + H]^+$, 1181.71 (20) $[Y_{2\alpha} + 2H]^+$, 957.41 (7.3) $[M + 2K]^{2+}$, 949.43 (37) $[M + K + Na]^{2+}$, 946.95 (12) $[M + K + NH_4]^{2+}$, 938.44 (32) $[M + K + H]^{2+}$, 941.44 (45) $[M + 2Na]^{2+}$, 938.95 (72) $[M + Na + NH_4]^{2+}$, 930.45 (32) $[M + Na + H]^{2+}$, 936.48 (56) $[M + 2NH_4]^{2+}$, 927.97 (34) $[M + NH_4 + H]^{2+}$, 919.46 (100) $[M + 2H]^{2+}$.

MS/MS (m/z = 919.46): m/z (%) = 1366.77 (5.6) $[Z_{3\alpha}]^+$, 1181.71 (13) $[Y_{2\alpha} + 2H]^+$, 1163.70 (15) $[Z_{2\alpha}]^+$, 1075.69 (3.0) $[Z_{3\alpha}/B_{1\beta} + H]^+$, 919.46 (10) $[M + 2H]^{2+}$, 890.62 (4.3) $[Y_{2\alpha}/B_{1\beta} + 3H]^+$, 872.62 (8.8) $[Z_{2\alpha}/B_{1\beta} + H]^+$, 819.26 (3.5) $[B_4/B_{1\beta} + H]^+$, 728.59 (15) $[Y_1 + 2H]^+$, 710.58 (18) $[Z_1]^+$, 657.22 (99) $[B_{3\alpha}]^+$, 566.54 (10) $[Y_0 + 2H]^+$, 548.53 (43) $[Z_0]^+$, 454.15 (22) $[B_{2\alpha}]^+$, 366.14 (24) $[B_{3\alpha}/B_{1\alpha} + H]^+$, 292.10 (100) $[B_{1\alpha}$ o. $B_{1\beta}]^+$, 274.10 (87) $[B_{1\alpha} - H_2O$ o. $B_{1\beta} - H_2O]^+$, 204.10 (45) $[B_{3\alpha}/B_{2\alpha} + H]^+$, 186.10 (8.0) $[B_{3\alpha}/B_{2\alpha} + H - H_2O]^+$.

CHN-Analysis:

Theoretical (wt %):	C: 53.89	H: 8.29	N: 4.49
Measured (wt %):	C: 48.71	H: 8.43	N: 4.45

5.2.9 Separation of d20:1/18:0-GD1b·2NH$_3$ and d18:1/18:0-GD1b·2NH$_3$ to obtain d20:1/18:0-GD1b·2NH$_3$ (4)

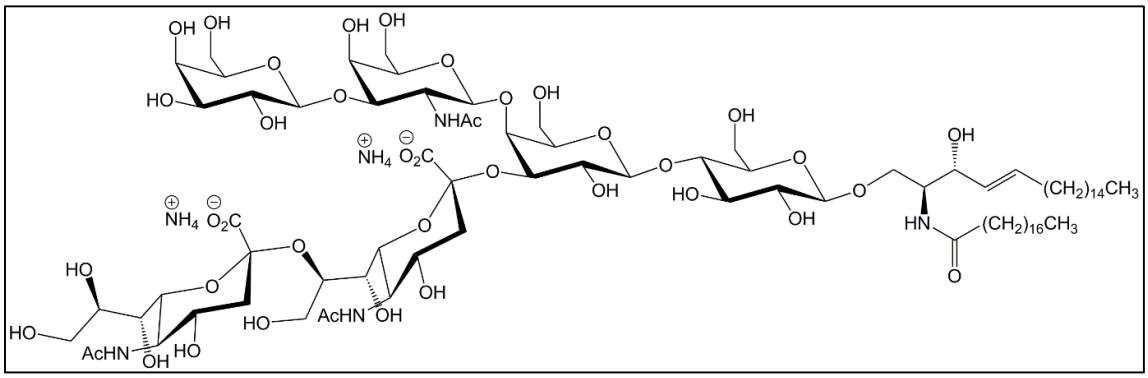

Experimental procedure:

GD1b (76 mg) was separated into its lipoforms by RP column chromatography (Merck-LiChroprep RP-18/40-63 µm, 2.0 × 4.0 cm, isocratic, eluent: MeOH/H_2O 90:40 v/v). Column material was removed by NP column chromatography on silica gel (Merck-silica gel 60/40-63 µm, 2.0 × 3.5 cm, step gradient, application: $CHCl_3$/MeOH/2.5 M NH_3 60:35:6 v/v/v, elution: $CHCl_3$/MeOH/2.5 M NH_3 60:44:12 v/v/v) again. After lyophilization, d20:1/18:0-GD1b·2NH$_3$ was obtained as a colorless powder (19.1 mg).

Analytics:

Molecular Formula: $C_{86}H_{158}N_6O_{39}$

Molecular Weight: 1900.21 g/mol

R_f = 0.19 ($CHCl_3$/MeOH/2.5 M NH_3 60:44:12 v/v/v)

^{1}H-NMR (400 MHz, DMSO-d$_6$, RT): δ [ppm] = 7.99 (m, 2H, NH), 7.50 (d, 1H, $^3J_{NH-H5}$ = 9.0 Hz, NeuAc, NH), 5.51 (dt, 1H, $^3J_{H5-H4,\ trans}$ = 15.4 Hz, $^3J_{H5-H6}$ = 6.6 Hz, Cer, H-5), 5.33 (dd, 1H, $^3J_{H4-H5,\ trans}$ = 15.3 Hz, $^3J_{H4-H3}$ = 7.1 Hz, Cer, H-4), 4.87 (d, 1H, $^3J_{H1-H2}$ = 8.6 Hz, GalNAc, H-1), 4.29 (d, 2H, $^3J_{H1-H2}$ = 8.0 Hz, Gal, H-1), 4.13 (d, 1H, $^3J_{H1-H2}$ = 7.6 Hz, Glc, H-1), 4.00 – 2.90 (m, 42H), 2.84 (m, 1H, NeuAc, H-3e), 2.07 (s, 1H, OH), 2.00 (t, 2H, $^3J_{H2'-H3'}$ = 7.3 Hz, Cer, H-2'), 1.92 (m, 2H, Cer, H-6), 1.86 (s, 6H, NeuAc,

C<u>H</u>$_3$CO$_2$R), 1.74 (s, 3H, GalNAc, C<u>H</u>$_3$CO$_2$R), 1.42 (m, 2H, Cer, H-3'), 1.22 (m, 54H), 0.88 – 0.79 (t, 6H, $^3J_{H18'-H17'}$ = 6,8 Hz, $^3J_{H20-H19}$ = 6.8 Hz, H-18', H-20).

^{1}H NMR (400 MHz, DMSO-d$_6$, RT) (exchangeable Protons were exchanged by deuterium prior to measurement): δ [ppm] = 5.51 (dt, 1H, $^3J_{H5-H4,\ trans}$ = 15.2 Hz, $^3J_{H5-H6}$ = 6.8 Hz, Cer, H-5), 5.33 (dd, 1H, $^3J_{H4-H5,\ trans}$ = 15.2 Hz, $^3J_{H4-H3}$ = 7.1 Hz, Cer, H-4), 4.31 (d, 1H, $^3J_{H1-H2}$ = 7.6 Hz, Gal, H-1), 4.27 (d, $^3J_{H1-H2}$ = 6.8 Hz, Gal, H-1), 4.13 (d, 1H, $^3J_{H1-H2}$ = 7.8 Hz, Glc, H-1), 4.04 – 2.98 (m, 42H), 2.77 (m, 1H, NeuAc, H-3e), 2.59 (m, 1H, NeuAc, H-3e), 2.00 (t, 2H, $^3J_{H2'-H3'}$ = 7.3 Hz, Cer, H-2'), 1,91 (m, 2H, Cer, H-6), 1,86 (s, 6H, NeuAc, C<u>H</u>$_3$CO$_2$R), 1.76 (s, 3H, GalNAc, C<u>H</u>$_3$CO$_2$R), 1.42 (m, 2H, Cer, H-3'), 1.22 (m, 54H), 0.91 – 0.76 (t, 6H, $^3J_{H18'-H17'}$ = 6.8 Hz, $^3J_{H20-H19}$ = 6.8 Hz, H-18', H-20).

MS (ESI, pos. Mode, MeOH): m/z (%) = 1888.11 (1.0) $[M + Na]^+$, 1883.11 (0.7) $[M + NH_4]^+$, 1866.15 (0.9) $[M + H]^+$, 1250.35 (2.4) $[2M + NH_4 + 2H]^{2+}$, 963.48 (11) $[M + K + Na]^{2+}$, 952.49 (18) $[M + K + H]^{2+}$, 955.50 (21) $[M + 2Na]^{2+}$, 952.99 (21) $[M + Na + NH_4]^{2+}$, 944.50 (58) $[M + Na + H]^{2+}$, 942.02 (20) $[M + NH_4 + H]^{2+}$, 933.51 (98) $[M + 2H]^{2+}$.

MS/MS (m/z = 933.51): m/z (%) = 1265.82 (3.5) $[Z_{2\alpha}]^+$, 1191.79 (5.8) $[Y_{2\beta}/C_{1\alpha} + H]^+$, 1103.77 (5.6) $[Z_{3\beta}/B_{2\alpha} + H]^+$, 900.69 (14) $[Z_{2\beta}/B_{2\alpha} + H]^+$, 738.64 (15) $[Z_1]^+$, 576.58 (43) $[Z_0]^+$, 558.57 (7.6) $[Z_0 - H_2O]^+$, 454.17 (3.6) $[Y_{2\beta}/B_{1\alpha}/B_3 + 2H]$, 366.15 (99) $[B_{2\beta}]^+$, 292.10 (58) $[B_{1\alpha}]^+$, 274.10 (100) $[B_{1\alpha} - H_2O]^+$, 204.09 (61) $[B_{2\beta}/B_{1\beta} + H]^+$, 186.08 (20) $[B_{2\beta}/B_{1\beta} + H - H_2O]^+$.

CHN-Analysis:

Theoretical (wt %):	C: 54.36 H: 8.38 N: 4.42
Measured (wt %):	C: 49.00 H: 8.06 N: 4.36

5.2.10 Separation of d20:1/18:0-GT1b·3NH$_3$ and d18:1/18:0-GT1b·3NH$_3$ to obtain d20:1/18:0-GT1b·3NH$_3$ (5)

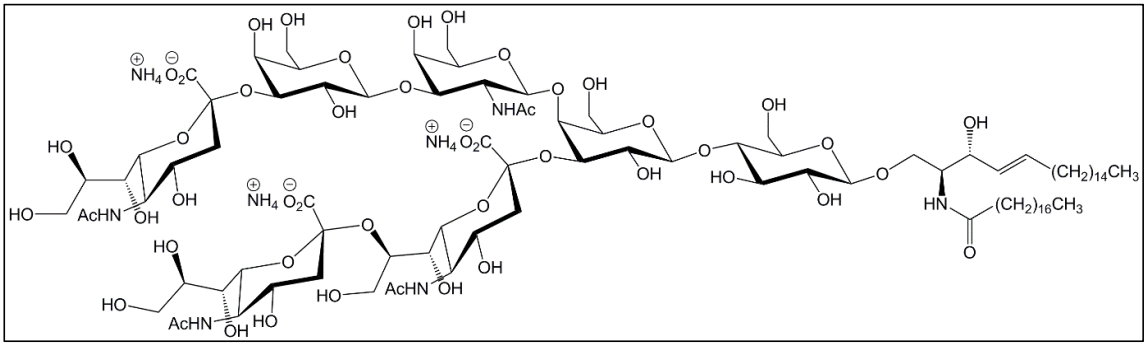

Experimental procedure:

GT1b (382 mg) was separated into its lipoforms by RP column chromatography (Merck-LiChroprep RP-18/40-63 µm, 2.7 × 4.0 cm, isocratic, eluent: MeOH/H_2O 90:40 v/v). By this, 69.6 mg of crude d18:1/18:0-GT1b and 109 mg of crude d20:1/18:0-GT1b were obtained. In order to remove column material, 45 mg of the crude d20:1/18:0-GT1b were purified by NP column chromatography on silica gel (Merck-silica gel 60/40-63 µm, 1.5 × 2.8 cm, step gradient, application: $CHCl_3$/MeOH/2.5 M NH_3 60:35:7 v/v/v, elution: $CHCl_3$/MeOH/2.5 M NH_3 60:50:15 v/v/v). After lyophilization, d20:1/18:0-GT1b·3NH_3 (**5**) was obtained as a colorless powder (40.4 mg).

Analytics:

Molecular formula: $C_{97}H_{178}N_8O_{47}$

Molecular weight: 2208.50 g/mol

R_f = 0.24 ($CHCl_3$/MeOH/2.5 M NH_3 60:50:15 v/v/v)

^{1}H-NMR (400 MHz, DMSO-d_6, RT): δ [ppm] = 7.97 (m, 3H, NH), 7.53 – 7.42 (d, 1H, $^3J_{NH\text{-}H5}$ = 8.8 Hz, NeuAc, NH), 5.52 (dt, 1H, $^3J_{H5\text{-}H4,\ trans}$ = 15.6 Hz, $^3J_{H5\text{-}H6}$ = 6.7 Hz, Cer, H-5), 5.33 (dd, 1H, $^3J_{H4\text{-}H5,\ trans}$ = 15.2 Hz, $^3J_{H4\text{-}H3}$ = 7.0 Hz, Cer, H-4), 4.91 (m, GalNAc, H-1), 4.29 (d, 1H, $^3J_{H1\text{-}H2}$ = 7.9 Hz, Gal, H-1), 4.13 (d, $^3J_{H1\text{-}H2}$ = 7.6 Hz, Glc, H-1), 4.02 – 2.89 (m, 49H), 2.08 (s, OH), 2.01 (t, 2H, $^3J_{H2'\text{-}H3'}$ = 7.3 Hz, Cer, H-2'),

1.95 – 1.88 (m, 2H, Cer, H-6), 1.86 (s, 3H, NeuAc, C$\underline{H}_3CO_2R$), 1.85 (s, 3H, NeuAc, C$\underline{H}_3CO_2R$), 1.81 (s, 3H, NeuAc, C$\underline{H}_3CO_2R$), 1.77 (s, 3H, GalNAc, C$\underline{H}_3CO_2R$), 1.41 (m, 2H, Cer, H-3'), 1.22 (m, 54H), 0.88 – 0.80 (t, 6H, $^3J_{H18'-H17'}$ = 6.8 Hz, $^3J_{H20-H19}$ = 6.8 Hz, H18', H-20).

MS (ESI, pos. Mode, MeOH, M_3 = 2185.13): m/z (%) = 1109.54 (8.0) $[M + K + Na]^{2+}$, 1107.07 (3.4) $[M + K + NH_4]^{2+}$, 1101.55 (16) $[M + 2 Na]^{2+}$, 1098.55 (14) $[M + K + H]^{2+}$, 1090.55 (24) $[M + Na + H]^{2+}$, 1088.07 (12) $[M + NH_4 + H]^{2+}$, 1079.56 (100) $[M + 2H]^{2+}$, 1131,51 (4,0) $[M_3 + 2K]^{2+}$, 1123,53 (4,4) $[M_3 + K + Na]^{2+}$, 1112,54 (8,6) $[M_3 + K + H]^{2+}$, 1109,54 (8,0) $[M_3 + 2NH_4]^{2+}$, 1093,58 (6,4) $[M_3 + 2H]^{2+}$.

MS/MS (m/z = 1242.16): m/z (%) = 1191.78 (3.8) $[Y_{3\beta}/C_{3\alpha} + H]^+$, 1079.56 (14) $[M + 2H]^{2+}$, 900.69 (7.1) $[Y_{2\alpha}/C_{2\beta} + H]^+$, 738.64 (7.9) $[Z_1]^+$, 657.25 (53) $[B_{3\alpha}]^+$, 576.58 (29) $[Z_0]^+$, 558.57 (4.6) $[Z_0 – H_2O]^+$, 454.16 (16) $[B_{2\alpha}]^+$, 366.15 (19) $[B_{3\alpha}/B_{1\alpha} + H]^+$, 292.11 (100) $[B_{1\alpha}$ o. $B_{1\beta}]^+$, 274.11 (95) $[B_{1\alpha} – H_2O]^+$, 204.11 (32) $[B_{3\alpha}/B_{2\alpha} + H]^+$, 186.11 (6.4) $[B_{3\alpha}/B_{2\alpha} + H – H_2O]^+$.

CHN-Analysis:

Theoretical (wt %):	C: 52.75	H: 8.12	N: 5.07
Measured (wt %):	C: 45.85	H: 8.09	N: 5.44

5.2.11 Separation of d20:1/18:0-GQ1b·4NH$_3$ and d18:1/18:0-GQ1b·4NH$_3$ to obtain d20:1/18:0-GQ1b·4NH$_3$ (6)

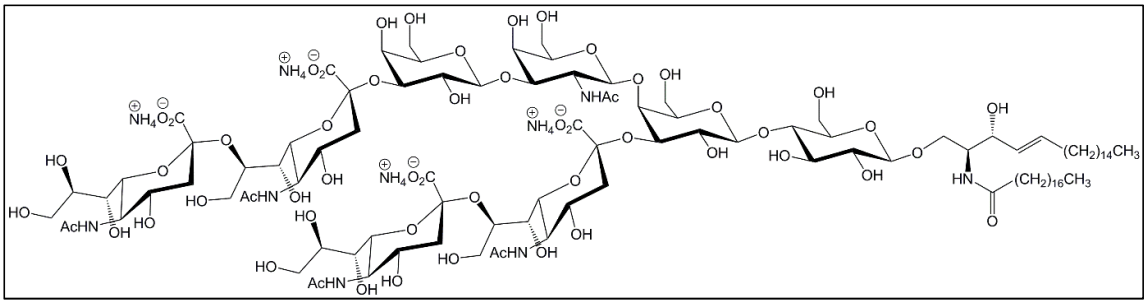

Experimental procedure:

GQ1b (130 mg) was separated into its lipoforms by RP chromatography (Merck-LiChroprep RP-18/40-63 µm, 2.0 × 3.7 cm, isocratic, eluent: MeOH/H_2O 90:50 v/v). By this, 37.9 mg of crude d18:1/18:0-GQ1b and 89.2 mg of crude d20:1/18:0-GQ1b were obtained. In order to remove column material, 59.2 mg of crude d20:1/18:0-GQ1b were purified by NP column chromatography on silica gel (Merck-silica gel 60/40-63 µm, 1.5 × 2.8 cm, step gradient, application: $CHCl_3$/MeOH/2.5 M NH_3 60:35:8 v/v/v, elution: $CHCl_3$/MeOH/2.5 M NH_3 50:50:16 v/v/v). After lyophilization, d20:1/18:0-GQ1b·4NH_3 (**6**) was obtained as a colorless powder (55.3 mg).

Analytics:

Molecular formula: $C_{108}H_{198}N_{10}O_{55}$

Molecular weight: 2516.79 g/mol

R_f = 0.25 ($CHCl_3$/MeOH/2.5 M NH_3 50:50:16 v/v/v)

^{1}H-NMR (400 MHz, DMSO-d_6, RT): δ [ppm] = 8.06 (d, 4H, $^3J_{NH\text{-}H5}$ = 7.2 Hz, NH), 7.50 (d, 1H, $^3J_{NH\text{-}H5}$ = 9.0 Hz, NeuAc, NH), 5.52 (dt, 1H, $^3J_{H5\text{-}H4,\ trans}$ = 15.5 Hz, $^3J_{H5\text{-}H6}$ = 6.7 Hz, Cer, H-5), 5.33 (dd, 1H, $^3J_{H4\text{-}H5,\ trans}$ = 15.3 Hz, $^3J_{H4\text{-}H3}$ = 7.0 Hz, Cer, H-4), 4.64 (bs, OH), 4.26 (d, 2H, $^3J_{H1\text{-}H2}$ = 7.8 Hz, Gal, H-1), 4.14 (d, 1H, $^3J_{H1\text{-}H2}$ = 7.6 Hz, Glc, H-1), 4.03 – 2.96 (m, 56H), 2.85 (m, 2H, NeuAc, H-3e), 2.75 (m, 2H, NeuAc, H-3e), 2.08 (s, OH), 2.01 (t, 2H, $^3J_{H2'\text{-}H3'}$ = 7.3 Hz, Cer, H-2'), 1.92 (m, 2H, Cer, H-6), 1.88 – 1.85 (2s, 12H, NeuAc, C<u>H</u>$_3$CO$_2$R), 1.73 (s, 3H, GalNAc, C<u>H</u>$_3$CO$_2$R), 1.41 (m, 2H, Cer, H-3'), 1.22 (m, 54H), 0.90 – 0.77 (t, 6H, $^3J_{H18'\text{-}H17'}$ = 7.0 Hz, $^3J_{H20\text{-}H19}$ = 7.0 Hz, H-18', H-20).

MS (ESI, pos. Mode, MeOH): m/z (%) = 1263.10 (48) $[M + 2K]^{2+}$, 1255.10 (60) $[M + K + Na]^{2+}$, 1252.62 (82) $[M + K + NH_4]^{2+}$, 1244.13 (88) $[M + K + H]^{2+}$, 1244.63 (83) $[M + Na + NH_4]^{2+}$, 1242.16 (100) $[M + 2NH_4]^{2+}$, 1233.65 (93) $[M + NH_4 + H]^{2+}$, 1225.14 (64) $[M + 2H]^{2+}$, 842.72 (21) $[M + 2K + H]^{3+}$, 829.74 (33) $[M + K + 2H]^{3+}$.

MS/MS (m/z = 1242.16): m/z (%) = 1500.86 (6.9) $[Y_{2\alpha} + 2H]^+$, 1482.85 (6.5) $[Z_{2\alpha}]^+$, 1225.13 (40) $[M + 2H]^{2+}$, 1191.81 (5.4) $[Y_{3\beta}/C_{4\alpha} + H]^+$, 1079.58 (8.5) $[Y_{5\alpha} + 3H]^{2+}$,

948.36 (55) $[B_{4\alpha}]^+$, 918.71 (8.2) $[Y_{2\beta}/B_{4\alpha} + 3H]^+$, 900.70 (5.6) $[Y_{2\beta}/B_{4\alpha} + 3H - H_2O]^+$, 756.66 (8.8) $[Y_1 + 2H]^+$, 745.28 (14) $[B_{3\alpha}]^+$, 738.65 (6.7) $[Z_1]^+$, 657.26 (21) $[B_{4\alpha}/B_{1\alpha} + H]^+$, 594.61 (13) $[Y_0 + 2H]^+$, 583.23 (31) $[B_{2\alpha}$ o. $B_{2\beta}]^+$, 576.60 (25) $[Z_0]^+$, 454.18 (31) $[B_{3\alpha}/B_{1\alpha} + H]^+$, 366.16 (11) $[B_{4\alpha}/B_{2\alpha} + H]^+$, 292.11 (100) $[B_{1\alpha}$ o. $B_{1\beta}]^+$, 274.09 (33) $[B_{1\beta} - H_2O]^+$, 204.07 (6.1) $[B_{4\alpha}/B_{3\alpha} + H]^+$.

CHN-Analysis:

Theoretical (wt %):	C: 51.54	H: 7.93	N: 5.57
Measured (wt %):	C: 44.16	H: 7.77	N: 5.67

5.2.12 Photometric sialic acid determination of d18:1/18:0-GM1·NH_3 and d18:1/18:0-GD1a·$2NH_3$

1. *N*-Acetylneuraminic acid as reference for calibration

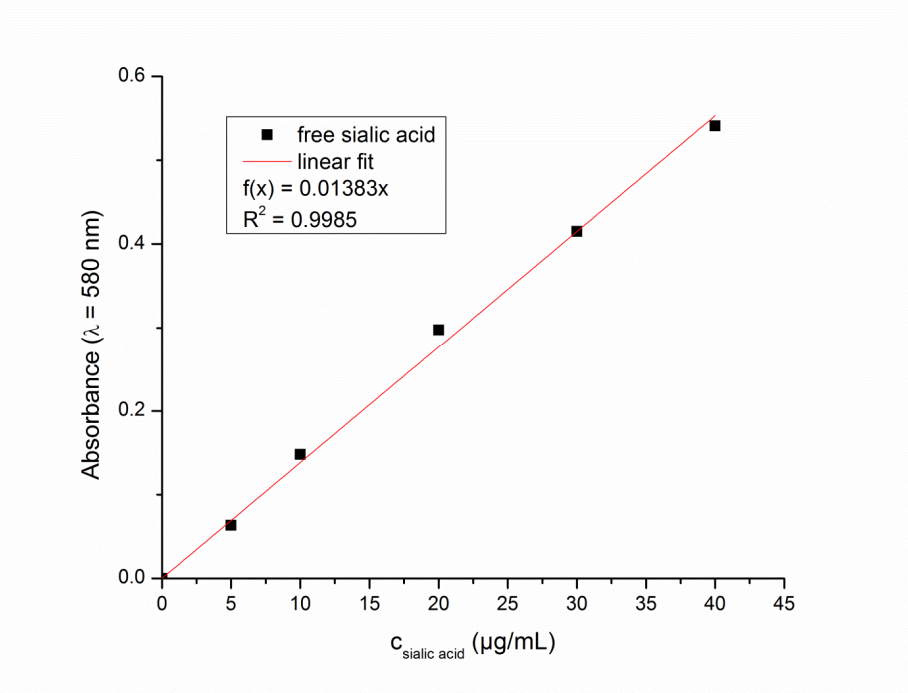

Ganglioside	M (g/mol)	c (µg/mL)	calc. c_{NANA} (µg/mL)
d18:1/18:0-GM1·NH_3 (**1**)	1563.85	25.0	4.94
d18:1/18:0-GD1a·$2NH_3$ (**3**)	1872.14	25.0	8.26

Abs. 1	Abs. 2	Mean	measured C_{NANA} (µg/mL)	Dev. (µg/mL)	Dev. (%)
0.052	0.049	0.0505	3.65	-1.29	-26.1
0.102	0.084	0.0930	6.72	-1.54	-18.6

Fig. 5.2.2: Sialic acid determination of d18:1/18:0-GM1·NH_3 (**1**) and d18:1/18:0-GD1a·$2NH_3$ (**3**) by using pure sialic acid as external standard. The calculated c_{NANA} was determined by weighing.

2. α_1-Acid glycoprotein as reference for calibration

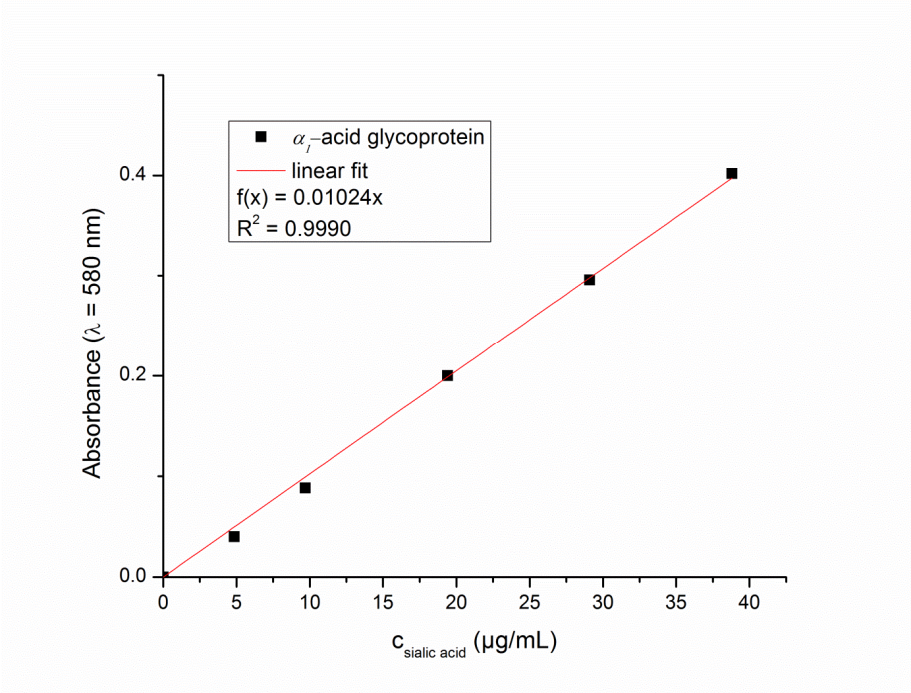

Ganglioside	M (g/mol)	c (µg/mL)	calc. c_{NANA} (µg/mL)
d18:1/C18:0-GM1·NH_3	1563.85	25.0	4.94
d18:1/C18:0-GD1a·$2NH_3$	1872.14	25.0	8.26

Abs. 1	Abs. 2	Mean	measured C_{NANA} (µg/mL)	Dev. (µg/mL)	Dev. (%)
0.052	0.049	0.0505	4.93	-0.01	-0.3
0.102	0.084	0.0930	9.08	0.82	10.0

Fig. 5.2.3: Sialic acid determination of d18:1/18:0-GM1·NH_3 (**1**) and d18:1/18:0-GD1a·$2NH_3$ (**3**) by using α_1-acid glycoprotein as external standard.

5.3 Preparation of lysogangliosides

5.3.1 Chemical preparation of d18:1-lyso-GM1·NH_3 (7)

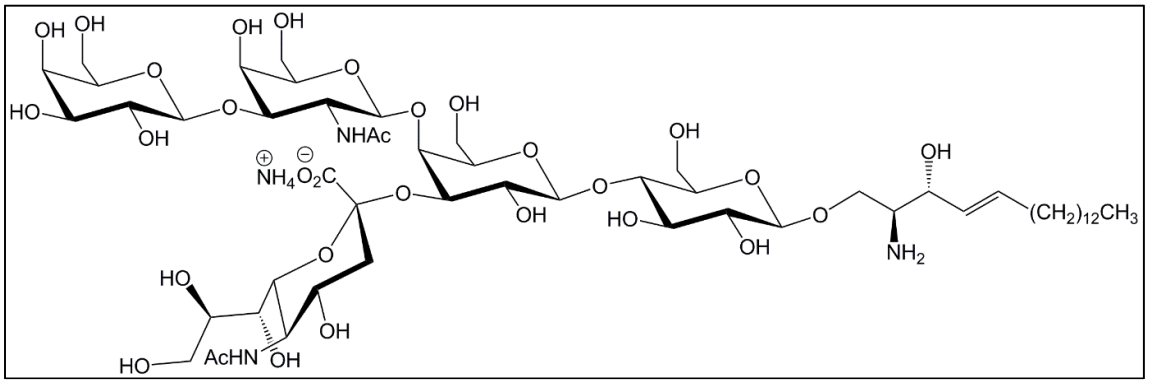

Experimental procedure:

All steps were performed under an argon atmosphere. Anhydrous 1-propanol was degassed by adding a stream of argon for 1 h. Then, 20.0 mg (12.8 µmol) of d18:1/18:0-GM1·NH_3 (**1**) were dissolved in 9.2 mL of this solvent. 2.3 mL of a 1 M KOH solution in 1-propanol were added and the reaction mixture was heated to 90 °C for 20 h. After cooling to RT, the reaction mixture was brought to pH 9 by adding an aq. ammonium chloride buffer. The solvent was removed in a stream of nitrogen, the crude product was dried in vacuum and subsequently purified by RP column chromatography (Merck LiChroprep RP-18/40-63 µm, 1.5 × 3.6 cm, isocratic, eluent: MeOH/H_2O 90:40 v/v). A second purification step was performed by NP column chromatography (Merck-silica gel 60/25-40 µm, 2.0 × 21.5 cm, isocratic, eluent:$CHCl_3$/MeOH/2.5 M NH_3 60:40:9 v/v/v). In order to remove column material, the product was purified by NP column chromatography on silica gel (Merck-silica gel/40-63 µm, 0.9 × 2.5 cm, step gradient, application: $CHCl_3$/MeOH/2.5 M NH_3 60:35:6 v/v/v, elution: $CHCl_3$/MeOH/2.5 M NH_3 60:44:12 v/v/v) again. After lyophilization, d18:1-lyso-GM1·NH_3 was obtained as a colorless powder (8.69 mg, 52 %).

Analytics:

Molecular formula: $C_{55}H_{100}N_4O_{30}$

Molecular weight: 1297.40 g/mol

R_f = 0.12 ($CHCl_3$/MeOH/2.5 M NH_3 60:40:10 v/v/v)

MS (ESI, pos. Mode, MeOH): m/z (%) = 1292.12 (3.1) $[3M + 2NH_4 + H]^{3+}$, 1280.62 (100) $[M + H]^+$, 989.53 (29) $[Y_{2\beta} + 2H]^+$, 981.35 (22) $[B_4]^+$, 915.49 (78) $[Y_{2\alpha} + 2H]^+$, 659.79 (5.3) $[M + K + H]^{2+}$, 651.80 (26) $[M + Na + H]^{2+}$, 649.33 (6.3) $[M + NH_4 + H]^{2+}$, 640.81 (64) $[M + 2H]^{2+}$.

MS/MS (m/z = 1280.62): m/z (%) = 1280.63 (17) $[M + H]^+$, 989.54 (50) $[Y_{2\beta} + 2H]^+$, 971.53 (5.3) $[Z_{2\beta}]^+$, 915.50 (8.0) $[Y_{2\alpha} + 2H]^+$, 624.41 (17) $[Y_{2\alpha}/B_{1\beta} + 3H]^+$, 606.40 (7.1) $[Y_{2\alpha}/C_{1\beta} + H]^+$, 462.35 (9.7) $[Y_1 + 2H]^+$, 444.34 (8.8) $[Z_1]^+$, 366.15 (100) $[B_{2\alpha}]^+$, 300.30 (6.9) $[Y_0 + 2H]^+$, 292.11 (7.3) $[B_{1\beta}]^+$, 282.29 (20) $[Z_0]^+$, 264.28 (85) $[Z_0 - H_2O]^+$, 204.09 (64) $[B_{2\alpha}/B_{1\alpha} + H]^+$, 186.08 (15) $[B_{2\alpha}/B_{1\alpha} + H - H_2O]^+$.

Photometric sialic acid determination:

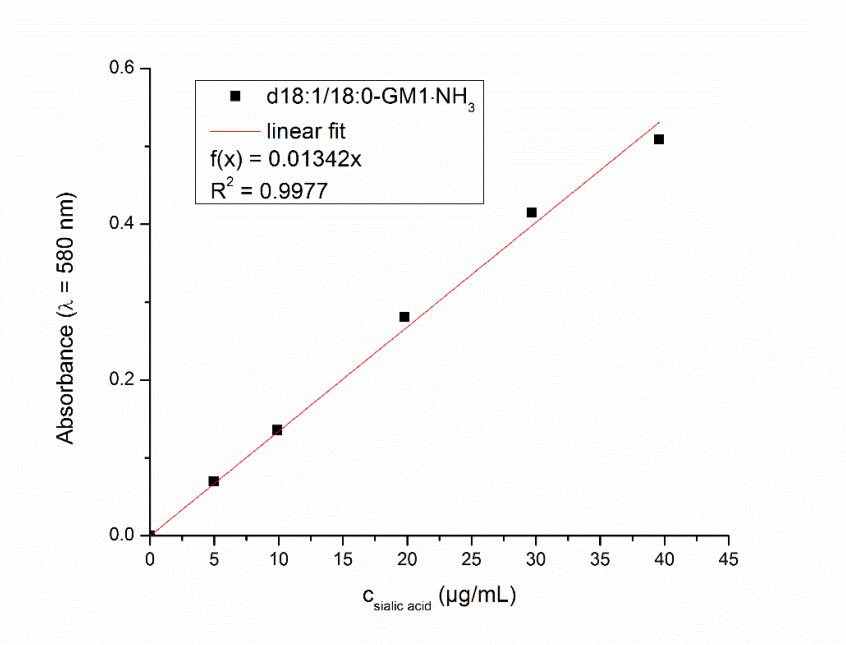

Ganglioside	M (g/mol)	c (µg/mL)	calc. c_{NANA} (µg/mL)
d18:1-lyso-GM1·NH_3 (**7**)	1297.40	124	29.6
d18:1/14:0-GM2·NH_3 (**21**)	1345.62	85.9	19.7

Abs. 1	Abs. 2	Mean	measured C_{NANA} (µg/mL)	Dev. (µg/mL)	Dev. (%)
0.369	0.406	0.3875	28.9	-0.73	-2.5
0.255	0.259	0.2570	19.2	-0.59	-3.0

Fig. 5.3.1: Sialic acid determination of d18:1-lyso-GM1·NH_3 (**7**) and d18:1/14:0-GM2·NH_3 (**21**) by using d18:1/18:0-GM1·NH_3 (**1**) as reference standard

5.3.2 Chemical preparation of d18:1-lyso-GD1a·2NH_3 (8)

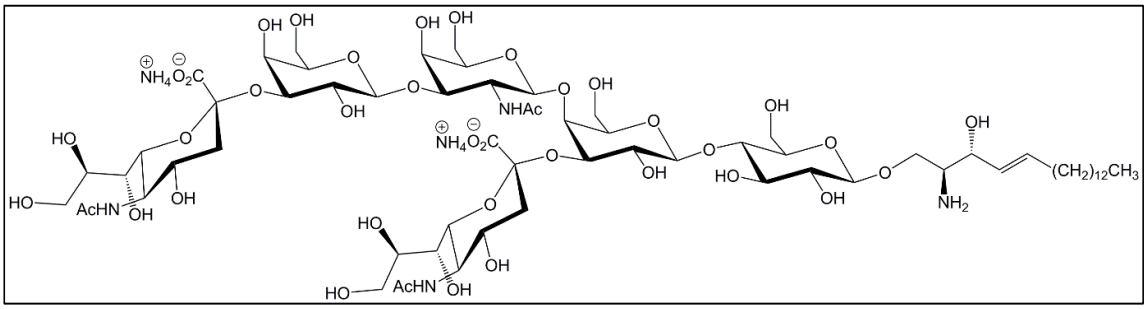

Experimental procedure:

All steps were performed under an argon atmosphere. Dry MeOH was degassed by adding a stream of argon gas for 1 h. 30.0 mg (16.0 µmol) of d18:1/18:0-GD1a·2NH_3 (**3**) were dissolved in 11.7 mL of this solvent. Afterwards, 2.9 mL of a 1 M KOH solution in MeOH were added and the reaction mixture was heated to 90 °C for 23 h. After cooling to RT, the reaction mixture was brought to pH 9 by adding an aq. ammonium chloride buffer. The solvent was removed in a stream of nitrogen, the crude product was dried in vacuum and subsequently purified by RP column chromatography (Merck LiChroprep RP-18/40-63 µm, 1.5 × 3.5 cm, isocratic, eluent: MeOH/H_2O 90:60 v/v). A second purification step was performed by NP column chromatography (Merck-silica gel 60/25-40 µm, 2.2 × 25.5 cm, isocratic, eluent: $CHCl_3$/MeOH/2.5 M NH_3 60:40:10 v/v/v). Product containing fractions that were not pure enough were purified by preparative HPTLC (developing solvent: $CHCl_3$/MeOH/2.5 M NH_3 60:44:12 v/v/v). All product containing fractions were pooled, the solvent was removed under reduced pressure and the product was dried in vacuum. In order to remove column material the product was purified by NP column chromatography on silica gel (Merck-silica gel 60/40-63 µm, 0.9 × 2.5 cm, step gradient, application: $CHCl_3$/MeOH/2.5 M NH_3 60:35:6 v/v/v, elution: $CHCl_3$/MeOH/2.5 M NH_3 60:50:15 v/v/v) again. After lyophilization, d18:1-lyso-GD1a·2NH_3 was obtained as a colorless powder (1.23 mg, 4.8 %).

Analytics:

Molecular Formula: $C_{66}H_{120}N_6O_{38}$

Molecular Weight: 1605.69 g/mol

R_f = 0.24 ($CHCl_3$/MeOH/2.5 M NH_3 60:44:12 v/v/v)

MS (ESI, pos. Mode, MeOH): m/z (%) = 1571.75 (3.3) $[M + H]^+$, 1272.45 (11) $[B_5]^+$, 1048.14 (5.2) $[2M + 3H]^{3+}$, 915.50 (100) $[Y_{2\alpha} + 2H]^+$, 808.35 (5.9) $[M + 2Na]^{2+}$, 805.35 (3.0) $[M + K + H]^{2+}$, 808.35 (5.9) $[M + 2Na]^{2+}$, 797.36 (38) $[M + Na + H]^{2+}$, 794.88 (14) $[M + NH_4 + H]^{2+}$, 786.37 (13) $[M + 2H]^{2+}$.

MS/MS (m/z = 786.37): m/z (%) = 1280.63 (6.0) $[Y_{4\alpha} + 2H]^+$, 1272.46 (4.9) $[B_5]^+$, 1118.59 (3.9) $[Y_{3\alpha} + 2H]^+$, 915.50 (89) $[Y_{2\alpha} + 2H]^+$, 786.36 (8.5) $[M + 2H]^{2+}$, 657.24 (100) $[B_{3\alpha}]^+$, 624.40 (15) $[Y_{2\alpha}/B_{1\beta} + 3H]^+$, 606.39 (4.5) $[Y_{2\alpha}/C_{1\beta} + H]^+$, 462.35 (8.3) $[Y_1 + 2H]^+$, 454.16 (14) $[B_{2\alpha}]^+$, 444.34 (3.1) $[Z_1]^+$, 366.15 (14) $[B_{3\alpha}/B_{1\alpha} + H]^+$, 300.30 (36) $[Y_0 + 2H]^+$, 292.11 (80) $[B_{1\alpha}$ o. $B_{1\beta}]^+$, 282.29 (34) $[Z_0]^+$, 274.10 (68) $[B_{1\alpha} – H_2O$ o. $B_{1\beta} – H_2O]^+$, 204.09 (35) $[B_{3\alpha}/B_{2\alpha} + H]^+$, 186.08 (5.6) $[B_{3\alpha}/B_{2\alpha} – H_2O]^+$.

Photometric sialic acid determination:

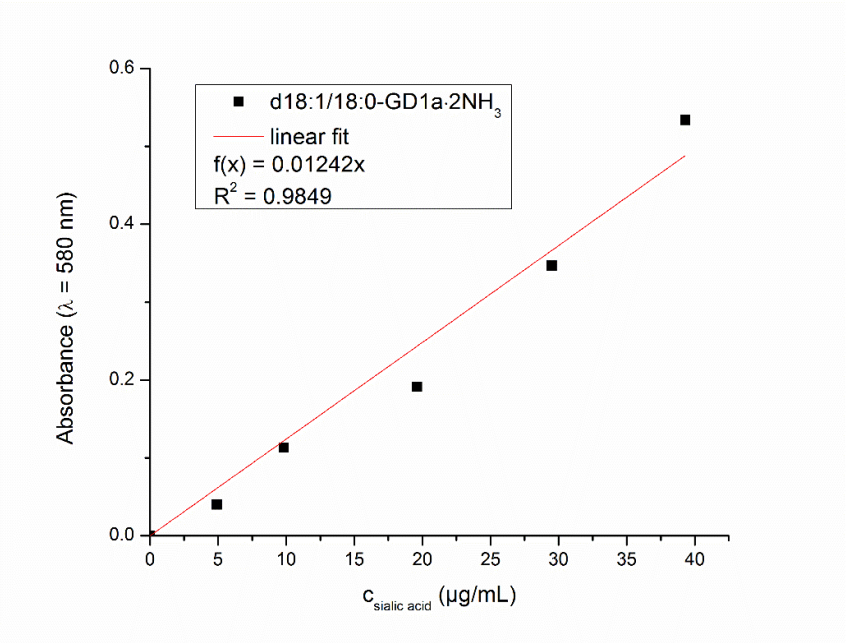

Ganglioside	M (g/mol)	c (µg/mL)	calc. c_{NANA} (µg/mL)
d18:1-lyso-GD1a·2NH$_3$	1605.68	76.2	29.4
d18:1/17:0-GD1a·2NH$_3$	1858.11	73.7	24.5

Abs. 1	Abs. 2	Mean	measured c_{NANA} (µg/mL)	Dev. (µg/mL)	Dev. (%)
0.291	0.294	0.2925	23.6	-5.80	-19.8
0.299	0.278	0.2885	23.2	-1.31	-5.35

Fig. 5.3.2: Sialic acid determination of d18:1-lyso-GD1a·2NH$_3$ (**8**) and d18:1/17:0-GD1a·2NH$_3$ (**16**) by using d18:1/18:0-GD1a·2NH$_3$ (**3**) as reference standard

5.3.3 Control experiment for the chemical deacylation of d18:1/18:0-GD1a·2NH$_3$

Experimental procedure:

All steps were performed under an argon atmosphere. 15.0 mg (8.01 µmol) of d18:1/18:0-GD1a·2NH$_3$ were dissolved in 5.8 mL of dry degassed 1-propanol.

Afterwards, 1.5 mL of a 1 M potassium *tert*-butoxide solution in the same solvent were added and the reaction mixture was heated to 90 °C for 12 h.
A second experiment was performed under the same reaction conditions except that the reaction temperature was changed to 80 °C. The formed d18:1-lyso-GD1a was quantified at different reaction times. 4 µL of the reaction mixture were taken each time and quantified by HPTLC followed by densitometry.

5.3.4 Enzymatic preparation of d18:1-lyso-GD1a·2NH_3 (8)

Experimental procedure:

0.919 mg (491 nmol) of d18:1/18:0-GD1a·2NH_3 (**3**) were dissolved in 500 µL of 50 mM sodium acetate buffer (pH 6.0), which contained 0.8 % of Triton™ X-100. The mixture was exposed to an ultrasonic bath for 15 s. Then, 3.6 µL (18 mU) of a SCDase solution (in 50 mM sodium acetate buffer, pH 6.0) were added, the aqueous phase was covered with 5 mL of *n*-decane to remove the fatty acid from the equilibrium, and the mixture was incubated at 37 °C. Every 2 h the *n*-decane phase was replaced. To obtain a complete conversion of the educt further 36 mU of enzyme were added over a period of 2 d. The reaction was stopped by the addition of a few drops of 2.5 M ammonia. The solvent was removed in a stream of nitrogen, the crude product was dried in vacuum and subsequently purified by NP column chromatography (2.0 × 23 cm, $CHCl_3$/MeOH/2.5 M NH_3 60:40:10 v/v/v). In order to remove column material, the crude product was purified by NP column chromatography again (Merck-silica gel 60/40-63 µm, 0.6 × 2.0 cm, step gradient, application: $CHCl_3$/MeOH/2.5 M NH_3 60:35:7 v/v/v, elution: $CHCl_3$/MeOH/2.5 M NH_3 60:44:12 v/v/v). After lyophilization, d18:1-lyso-GD1a·2NH_3 (**8**), was obtained as a colorless powder (0.74 mg, 47 % from two preparations),

Analytics:

Molecular Formula: $C_{66}H_{120}N_6O_{38}$
Molecular Weight: 1605.69 g/mol
R_f = 0.25 ($CHCl_3$/MeOH/2.5 M NH_3 60:44:12 v/v/v)

MS (ESI, pos. Mode, MeOH): m/z (%) = 1571.67 (5.2) $[M + H]^+$, 1272.39 (14) $[B_5]^+$, 915.46 (100) $[Y_{2\alpha} + 2H]^+$, 816.30 (1.6) $[M + K + Na]^{2+}$, 808.31 (4.4) $[M + 2Na]^{2+}$, 805.30 (5.2) $[M + K + H]^{2+}$, 797.32 (31) $[M + Na + H]^{2+}$, 794.84 (15) $[M + NH_4 + H]^{2+}$, 786.33 (15) $[M + 2H]^{2+}$.

MS/MS (m/z = 786.33): m/z (%) = 1280.55 (4.2) $[Y_{4\alpha} + 2H]^+$, 1272.35 (5.9) $[B_5]^+$, 915.44 (76) $[Y_{2\alpha} + 2H]^+$, 786.32 (4.0) $[M + 2H]^{2+}$, 657.20 (100) $[B_{3\alpha}]^+$, 624.37 (8.3) $[Y_{2\alpha}/B_{1\beta} + 3H]^+$, 606.36 (3.6) $[Y_{2\alpha}/C_{1\beta} + H]^+$, 462.32 (7.2) $[Y_1 + 2H]^+$, 454.13 (8.5) $[B_{2\alpha}]^+$, 444.32 (4,2) $[Z_1]^+$, 366.12 (11) $[B_{3\alpha}/B_{1\alpha} + H]^+$, 300.28 (25) $[Y_0 + 2H]^+$, 292.09 (46) $[B_{1\alpha}$ o. $B_{1\beta}]^+$, 282.26 (37) $[Z_0]^+$, 274.08 (59) $[B_{1\alpha}$ o. $B_{1\beta} - H_2O]^+$, 204.07 (29) $[B_{3\alpha}/B_{2\alpha} + H]^+$, 186.08 (7.1) $[B_{3\alpha}/B_{2\alpha} + H - H_2O]^+$.

Fluorimetric sialic acid determination:

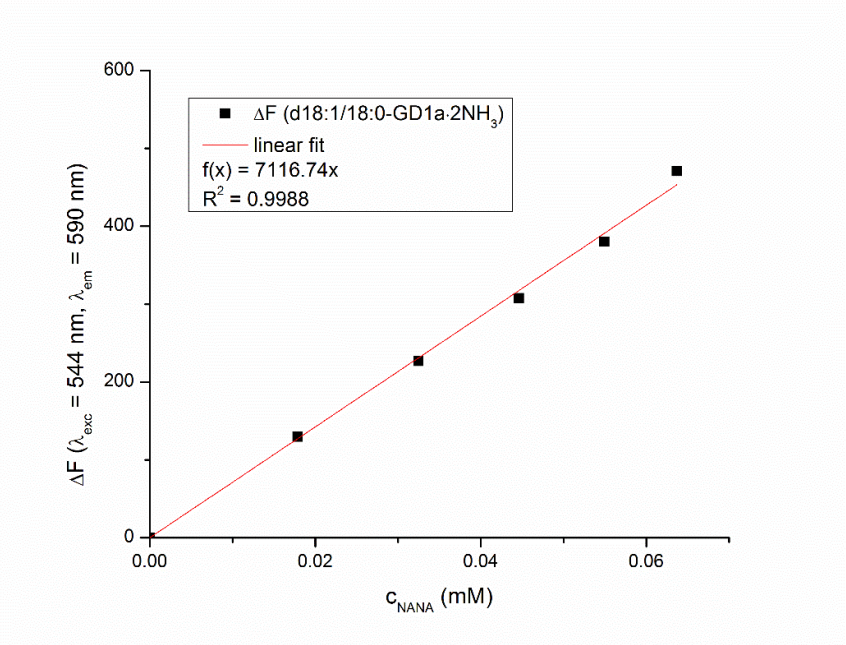

Ganglioside	**M (g/mol)**	**c (mM)**	**calc. c_{NANA} (mM)**
d18:1-lyso-GD1a·2NH_3	1605.69	0.152	0.0507

measured ΔF	**measured c_{NANA} (mM)**	**Dev. (mM)**	**Dev. (%)**
237.85	0.0334	-0.0172	-34.0

Fig. 5.3.3: Sialic acid determination of d18:1-lyso-GD1a·2NH_3 (**8**) by using d18:1/18:0-GD1a·2NH_3 (**3**) as reference standard

5.3.5 Enzymatic preparation of d20:1-lyso-GD1b·2NH_3 (9)

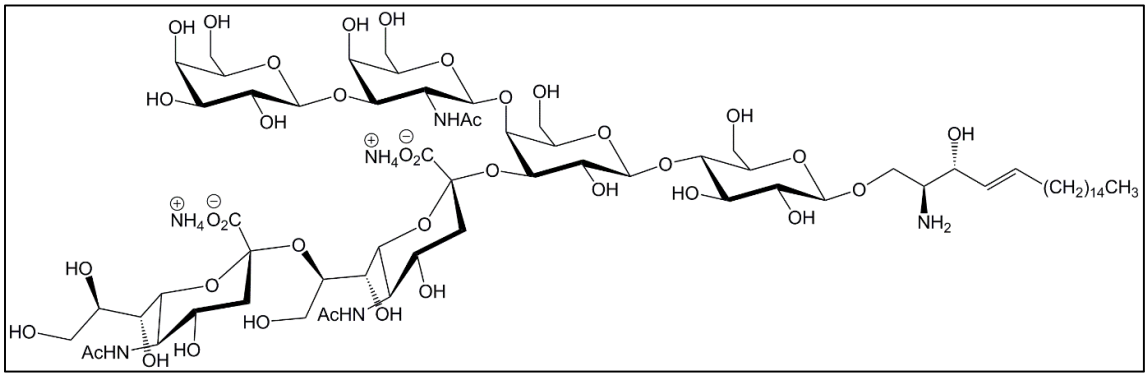

Experimental procedure:

d20:1-Lyso-GD1b·2NH_3 was prepared by the method described in section 5.3.4. 3.74 mg (1.97 mmol) of d20:1/18:0-GD1b·2NH_3 (**4**) and 216 mU of SCDase were applied over a period of 3 d. The crude product was purified by NP column chromatography on silica gel (Merck-silica gel 60/25-40 µm, column: Ø = 2.5 × 19.9 cm, isocratic, eluent: $CHCl_3$/MeOH/2.5 M NH_3 60:44:12 v/v/v). In order to remove column material, it was purified by NP column chromatography (Merck-silica gel 60/40-63 µm, 0.6 × 2.0 cm, step gradient, application: $CHCl_3$/MeOH/2.5 M NH_3 60:35:7 v/v/v, elution: $CHCl_3$/MeOH/2.5 M NH_3 60:44:12 v/v/v) again. After lyophilization, d20:1-lyso-GD1b·2NH_3 was obtained as a colorless powder (1.72 mg, 53 %).

Analytics:

Molecular Formula: $C_{68}H_{124}N_6O_{38}$

Molecular Weight: 1633.74 g/mol

R_f = 0.18 ($CHCl_3$/MeOH/2.5 M NH_3 60:44:12 v/v/v)

MS (ESI, pos. Mode, MeOH): m/z (%) = 1621.64 (0.41) $[M + Na]^+$, 1599.67 (8.8) $[M + H]^+$, 1571.66 (0.28) $[M – 2CH_2 + H]^+$, 1308.59 (6.8) $[Y_{3\alpha} + 2H]^+$, 819.32 (5,4) $[M + K + H]^{2+}$, 822.32 (5.3) $[M + 2Na]^{2+}$, 811.32 (29) $[M + Na + H]^{2+}$, 808.85 (16) $[M + NH_4 + H]^{2+}$, 800.33 (100) $[M + 2H]^{2+}$, 786.32 (3.2) $[M – 2CH_2 + 2H]^{2+}$.

MS/MS (m/z = 800.28): m/z (%) = 1308.58 (37) $[Y_{3\alpha} + 2H]^+$, 1234.55 (9.7) $[Y_{2\beta} + 2H]^+$, 1146.54 (5.7) $[Y_{3\beta}/B_{1\alpha} + 3H]^+$, 1017.51 (21) $[Y_{2\alpha} + 2H]^+$, 943.48 (6.0) $[Y_{2\beta}/B_{1\alpha} + 3H]^+$, 855.47 (4.4) $[Y_{3\alpha}/B_{2\alpha} + 3H]^+$, 800.33 (7.3) $[M + 2H]^{2+}$, 652.40 (5.4) $[Y_{2\beta}/B_{2\alpha} + 3H]^+$, 490.36 (4.2) $[Y_1 + 2H]^+$, 366.13 (45) $[B_{2\beta}]^+$, 328.31 (7.6) $[Y_1 + 2H]^+$, 310.30 (7.6) $[Z_1]^+$, 292.09 (78) $[B_{1\alpha}]^+$, 274.08 (100) $[B_{1\alpha} - H_2O]^+$, 204.07 (20) $[B_{2\beta}/B_{1\beta} + H]^+$.

Fluorimetric sialic acid determination:

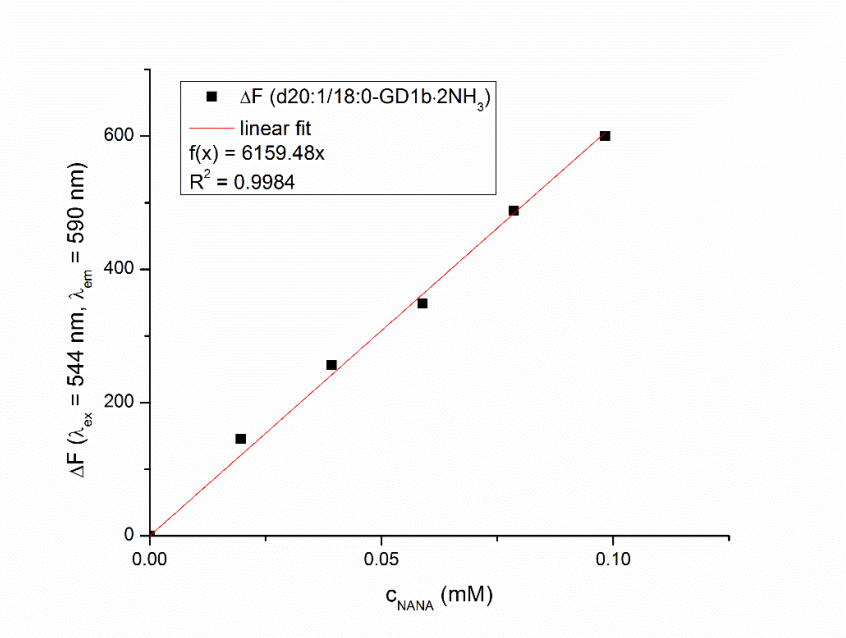

Ganglioside	**M (g/mol)**	**c (mM)**	**calc. c_{NANA} (mM)**
d20:1-lyso-GD1b·2NH_3	1633.74	0.152	0.0506

measured ΔF	**measured c_{NANA} (mM)**	**Dev. (mM)**	**Dev. (%)**
307.15	0.0499	-0.0007	-1.38

Fig. 5.3.4: Sialic acid determination of d20:1-lyso-GD1b·2NH_3 (**9**) by using d20:1/18:0-GD1b·2NH_3 (**4**) as reference standard

5.3.6 Enzymatic preparation of d20:1-lyso-GT1b·3NH$_3$ (10)

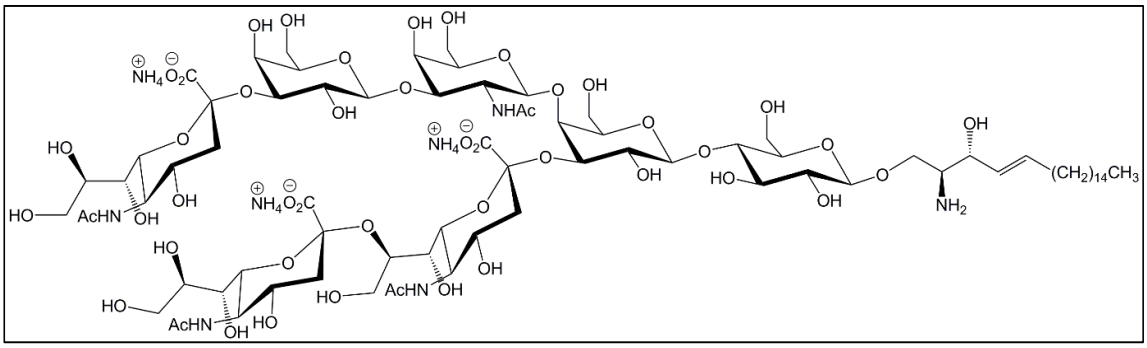

Experimental procedure:

d20:1-Lyso-GT1b·3NH$_3$ was prepared by the method described in section 5.3.4. 2.16 mg (978 nmol) of d20:1/18:0-GT1b·3NH$_3$ (**5**) and 72 mU of SCDase were applied over a period of 2 d. The crude product was purified by NP column chromatography on silica gel (Merck-silica gel 60/25-40 µm, 2.0 × 19.5 cm, isocratic, eluent: CHCl$_3$/MeOH/2.5 M NH$_3$ 60:44:12 v/v/v). In order to remove column material, it was purified by NP column chromatography (Merck-silica gel 60/40-63 µm, 0.6 × 2.0 cm, step gradient, application: CHCl$_3$/MeOH/2.5 M NH$_3$ 60:40:8 v/v/v, elution: CHCl$_3$/MeOH/2.5 M NH$_3$ 50:50:16 v/v/v) again. After lyophilization, d20:1-lyso-GT1b·3NH$_3$ was obtained as a colorless powder (1.16 mg, 61 %).

Analytics:

Molecular Formula: $C_{79}H_{144}N_8O_{46}$

Molecular Weight: 1942.03 g/mol

R_f = 0.26 (CHCl$_3$/MeOH/2.5 M NH$_3$ 50:50:16 v/v/v)

MS (ESI, pos. Mode, MeOH): m/z (%) = 1890.74 (0.53) $[M + H]^+$, 1260.87 (0.89) $[2M + 3H]^{3+}$, 1234.59 (3.1) $[Y_{2\alpha} + 2H]^+$, 964.87 (4.5) $[M + K + H]^{2+}$, 967.89 (3.7) $[M + 2Na]^{2+}$, 956.89 (17) $[M + Na + H]^{2+}$, 954.40 (8.3) $[M + NH_4 + H]^{2+}$, 945.90 (100) $[M + 2H]^{2+}$, 931.88 (4.9) $[M – 2CH_2 + 2H]^{2+}$.

MS/MS (m/z = 945.90): m/z (%) = 1599.64 (14) $[Y_{4\alpha} + 2H]^+$, 1563.42 (4.0) $[B_5]^+$, 1437.59 (4.1) $[Y_{3\alpha} + 2H]^+$, 1308.56 (11) $[Y_{2\beta} + 2H]^+$, 1234.54 (25) $[Y_{2\alpha} + 2H]^+$, 1017.50 (4.0) $[Y_{4\alpha}/B_{2\beta} + 3H]^+$, 943.47 (20) $[Y_{2\alpha}/B_{1\beta} + 3H]^+$, 855.46 (4.5) $[Y_{3\alpha}/B_{2\beta} + 3H]^+$, 657.20 (88) $[B_{3\alpha}]^+$, 652.39 (6.7) $[Y_{2\alpha}/B_{2\beta} + 3H]^+$, 583.17 (6.9) $[B_{2\beta}]^+$, 490.35 (6.6) $[Y_1 + 2H]^+$, 454.13 (15) $[B_{2\alpha}]^+$, 366.12 (9.4) $[B_{3\alpha}/B_{1\alpha} + H]^+$, 328.30 (37) $[Y_0 + 2H]^+$, 310.30 (15) $[Z_0]^+$, 292.09 (100) $[B_{1\alpha}$ o. $B_{1\beta}]^+$, 274.08 (85) $[B_{1\alpha}$ o. $B_{1\beta} - H_2O]^+$, 204.07 (14) $[B_{3\alpha}/B_{2\alpha} + H]^+$.

Fluorimetric sialic acid determination:

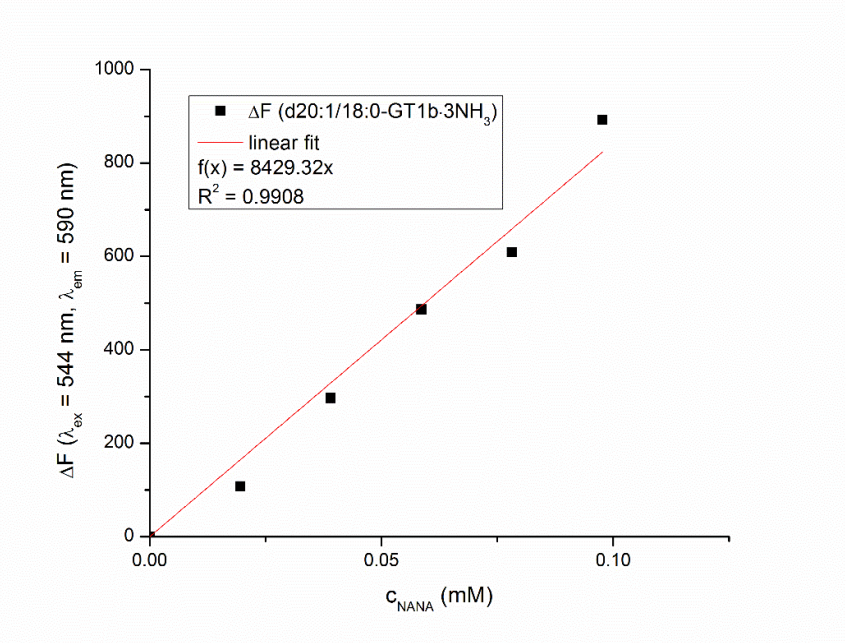

Ganglioside	**M (g/mol)**	**c (mM)**	**calc. c_{NANA} (mM)**
d20:1-lyso-GT1b·3NH$_3$	1942.01	0.170	0.0848

measured ΔF	**measured c_{NANA} (mM)**	**Dev. (mM)**	**Dev. (%)**
706.20	0.0838	-0.001	-1.18

Fig. 5.3.5: Sialic acid determination of d20:1-lyso-GT1b·3NH$_3$ (**10**) by using d20:1/18:0-GT1b·3NH$_3$ (**5**) as reference standard

5.3.7 Enzymatic preparation of d20:1-lyso-GQ1b·4NH$_3$ (11)

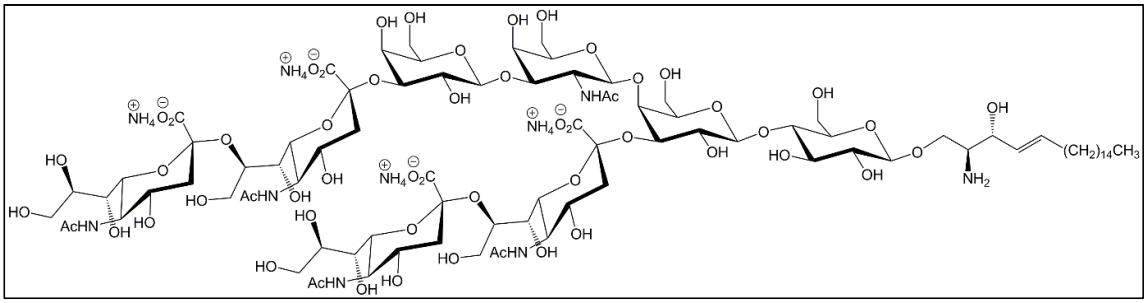

Experimental procedure:

d20:1-Lyso-GQ1b·4NH$_3$ was prepared by the method described in section 5.3.4. 2.44 mg (969 nmol) of d20:1/18:0-GQ1b·4NH$_3$ (**6**) and 72 mU of SCDase were applied over a period of 2 d. The crude product was purified by NP column chromatography on silica gel (Merck-silica gel 60/25-40 µm, 2.0 × 21.1 cm, isocratic, eluent: CHCl$_3$/MeOH/2.5 M NH$_3$ 60:50:13 v/v/v). In order to remove column material, it was purified by NP column chromatography (Merck-silica gel 60/40-63 µm, 0.6 × 2.0 cm, step gradient, application: CHCl$_3$/MeOH/2.5 M NH$_3$ 60:40:10 v/v/v, elution: CHCl$_3$/MeOH/2.5 M NH$_3$ 50:50:16 v/v/v) again. After lyophilization, d20:1-lyso-GQ1b·4NH$_3$ was obtained as a colorless powder (0.97 mg, 44 %).

Analytics:

Molecular Formula: $C_{90}H_{164}N_{10}O_{54}$

Molecular Weight: 2250.32 g/mol

R_f = 0.26 (CHCl$_3$/MeOH/2.5 M NH$_3$ 50:50:16 v/v/v)

MS (ESI, pos. Mode, MeOH): m/z (%) = 1462.91 (5.0) $[2M + Na + 2H]^{3+}$, 1455.59 (2.8) $[2M + 3H]^{3+}$, 1121.90 (7.2) $[M + K + Na]^{2+}$, 1110.92 (10) $[M + K + H]^{2+}$, 1113.92 (15) $[M + 2Na]^{2+}$, 1102.93 (71) $[M + Na + H]^{2+}$, 1099.95 (18) $[M + NH_4 + H]^{2+}$, 1091.93 (100) $[M + 2H]^{2+}$.

MS/MS (m/z = 1091.46): m/z (%) = 1890.78 (3.3) $[Y_{5\alpha} + 2H]^{+}$, 1599.70 (10) $[Y_{4\alpha} + 2H]^{+}$, 1437.65 (3.2) $[Y_{3\alpha} + 2H]^{+}$, 1308.62 (4.4) $[Y_{2\beta}/B_{1\alpha} + 2H]^{+}$, 1234.58 (27) $[Y_{2\alpha} +$

2H]$^{+}$, 1091.94 (18) [M + 2H]$^{2+}$, 948.31 (36) [$B_{4\alpha}$]$^{+}$, 943.50 (24) [$Y_{2\alpha}/B_{1\beta}$ + 3H]$^{+}$, 745.24 (7.3) [$Y_{2\alpha}/Y_1$ + H]$^{+}$, 657.22 (14) [$B_{4\alpha}/B_{1\alpha}$ + H]$^{+}$, 583.19 (21) [$B_{2\alpha}$ o. $B_{2\beta}$]$^{+}$, 490.37 (5.1) [Y_1 + 2H]$^{+}$, 454.15 (22) [$B_{3\alpha}/B_{1\alpha}$ + H]$^{+}$, 366.13 (6.5) [$B_{4\alpha}/B_{2\alpha}$ + H]$^{+}$, 328.32 (34) [Y_0 + 2H]$^{+}$, 310.30 (9.6) [Z_0]$^{+}$, 292.09 (100) [$B_{1\alpha}$ o. $B_{1\beta}$]$^{+}$, 274.08 (53) [$B_{1\alpha}$ o. $B_{1\beta}$ – H_2O]$^{+}$, 204.07 (4.6) [$B_{4\alpha}/B_{3\alpha}$ + H]$^{+}$.

Fluorimetricsialic acid determination:

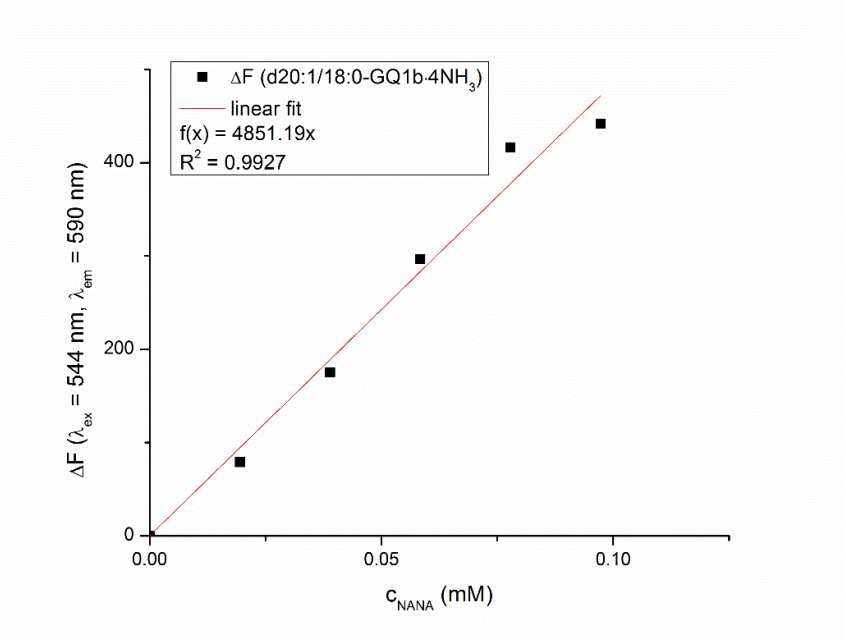

Ganglioside	**M (g/mol)**	**c (mM)**	**calc. c_{NANA} (mM)**
d20:1-lyso-GQ1b·4NH_3	2250.30	0.110	0.0734

measured ΔF	**measured c_{NANA} (mM)**	**Dev. (mM)**	**Dev. (%)**
229.7	0.0473	-0.0261	-35.5

Fig. 5.3.6: Sialic acid determination of d20:1-lyso-GQ1b·4NH_3 (**11**) by using d20:1/18:0-GQ1b·4NH_3 (**6**) as reference standard

5.4 Reacylation of lysogangliosides

5.4.1 Synthesis of 2,5-dioxopyrrolidin-1-yl tetradecanoate (12)

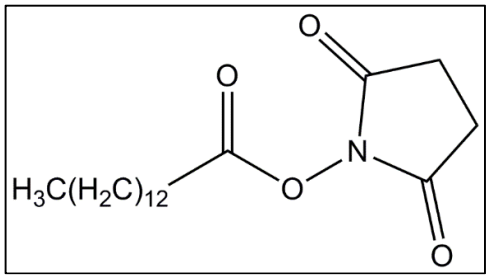

Experimental procedure:

All steps were performed under an argon atmosphere. 3.00 g (13.1 mmol) of tetradecanoic acid and 3.24 g (15.7 mmol) of DCC were dissolved in 26.2 mL of dry THF and stirred at RT for 10 min. Then, 1.81 g (15.7 mmol) of *N*-hydroxysuccinimide in 14.1 mL of dry THF were added and the reaction mixture was stirred at RT for 22.5 h. TLC-analysis ($CHCl_3$/MeOH 50:1 v/v) revealed a complete conversion of the educt. After this, the reaction mixture was filtrated by suction. The solvent was removed under reduced pressure and the residue was recrystallized from EtOH containing a trace of water. The product was obtained as a colorless solid (3.08 g, 72 %).

Analytics:

Molecular Formula: $C_{18}H_{31}NO_4$
Molecular Weight: 325.45 g/mol
R_f = 0.09 ($CHCl_3$)

^{1}H-NMR (300 MHz, $CDCl_3$, RT): δ [ppm] = 2.83 (s, 4H, H-3, 4), 2.60 (t, 2H, $^3J_{H2'\text{-}H3'}$ = 7.5 Hz, H-2'), 1.74 (tt, 2H, $^3J_{H3'\text{-}H4'}$ = 7.5 Hz, $^3J_{H3'\text{-}H2'}$ = 7.5 Hz, H-3'), 1.46 – 1.18 (m, 20H), 0.88 (t, 3H, $^3J_{H14'\text{-}H13'}$ = 6.7 Hz, H-14').

^{13}C-NMR (75 MHz, $CDCl_3$, RT): δ [ppm] = 169.15 (R<u>C</u>ON, C-2, 5), 168.68 (R<u>C</u>O_2R', C-1'), 31.90 (CH_2, C-2'), 30.93 (CH_2, C-12'), 29.63-28.77 (8 CH_2), 25.57 (CH_2, C-3, 4), 24.56 (CH_2, C-3'), 22.67 (CH_2, C-13'), 14.09 (CH_3, C-14').

DEPT 135 (75 MHz, $CDCl_3$, RT): δ [ppm] = 31.90 (CH_2, C-2'), 30.93 (CH_2, C-12'), 29.63-28.77 (8 CH_2), 25.57 (CH_2, C-3, 4), 24.56 (CH_2, C-3'), 22.67 (CH_2, C-13'), 14.09 (CH_3, C-14').

MS: (EI, 70eV, 100 °C) m/z (%) = 211.3 (100) [$M^{+\cdot}$ - $C_4H_4NO_3^{\cdot}$], 129.1 (15) [$C_8H_{17}O^+$], 112.2 (17) [$C_8H_{16}^+$], 98.2 (42) [$C_7H_{14}^{+\cdot}$], 84.1 (18) [$C_6H_{12}^{+\cdot}$], 71.2 (16) [$C_5H_{11}^+$], 57.2 (25) [$C_4H_9^+$].

CHN-Analysis:

Theoretical (wt %):	C: 66.43	H: 9.60	N: 4.30
Measured (wt %):	C: 66.03	H: 9.63	N: 4.29

5.4.2 Synthesis of 2,5-dioxopyrrolidin-1-yl heptadecanoate (13)

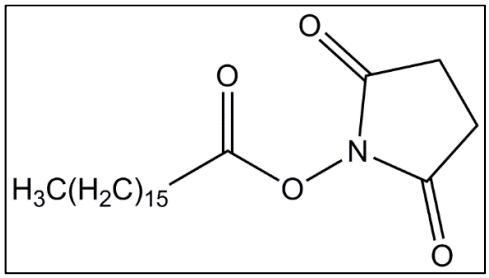

Experimental procedure:

2,5-Dioxopyrrolidin-1-yl heptadecanoate was synthesized by the method described in section 5.4.1. 1.00 g (3.70 mmol) of heptadecanoic acid were applied. The product was obtained as a colorless solid (0.897 g, 66 %).

Analytics:

Molecular Formula: $C_{21}H_{37}NO_4$
Molecular Weight: 367.53 g/mol
R_f = 0.09 ($CHCl_3$)

^{1}H NMR (400 MHz, $CDCl_3$, RT): δ [ppm] = 2.83 (s, 4H, H-3, 4), 2.59 (t, 1H, $^3J_{H2'-H3'}$ = 7.5 Hz, H-2'), 1.74 (tt, 2H, $^3J_{H3'-H4'}$ = 7.5 Hz, $^3J_{H3'-H2'}$ = 7,5 Hz, H-3'), 1.45 – 1.19 (m, 26H), 0.88 (t, 3H, $^3J_{H17'-H16'}$ = 6.9 Hz, H-17').

^{13}C-NMR (75 MHz, $CDCl_3$, RT): δ [ppm] = 169.15 (R<u>C</u>ON, C-2, 5), 168.68 (R<u>C</u>O_2R', C-1'), 31.90 (CH_2, C-2'), 30.93 (CH_2, C-15'), 29.66-28.78 (11 CH_2), 25.57 (CH_2, C-3,4), 24.56 (C-3'), 22.67 (CH_2, C-16'), 14.10 (CH_3, C-17').

DEPT 135 (75 MHz, $CDCl_3$, RT): δ [ppm] = 31.90 (CH_2, C-2'), 30.93 (CH_2, C-15'), 29.66-28.78 (11 CH_2), 25.57 (CH_2, C-3,4), 24.56 (C-3'), 22.67 (CH_2, C-16'), 14.10 (CH_3, C-17').

MS (EI, 70 eV): m/z (%) = 367.3 (16) [$M^{+\cdot}$], 349.3 (16) [$M^{+\cdot}$– H_2O], 335.3 (11) [$M^{+\cdot}$– O_2], 253.3 (100) [$M^{+\cdot}$– $C_4H_4NO_3^{\cdot}$], 154.2 (4,9) [$C_{11}H_{22}^{+\cdot}$], 112.2 (17) [$C_8H_{16}^{+\cdot}$], 98.1 (47) [$C_7H_{14}^{+\cdot}$], 84.1 (16) [$C_6H_{12}^{+\cdot}$], 71.2 (18) [$C_5H_{11}^{+}$], 57.1 (22) [$C_4H_9^{+}$].

CHN-Analysis:

Theoretical (wt %):	C: 68.63	H: 10.15	N: 3.81
Measured (wt %):	C: 68.63	H: 10.14	N: 3.75

5.4.3 Synthesis of d18:1/14:0-GM1·NH_3 (14)

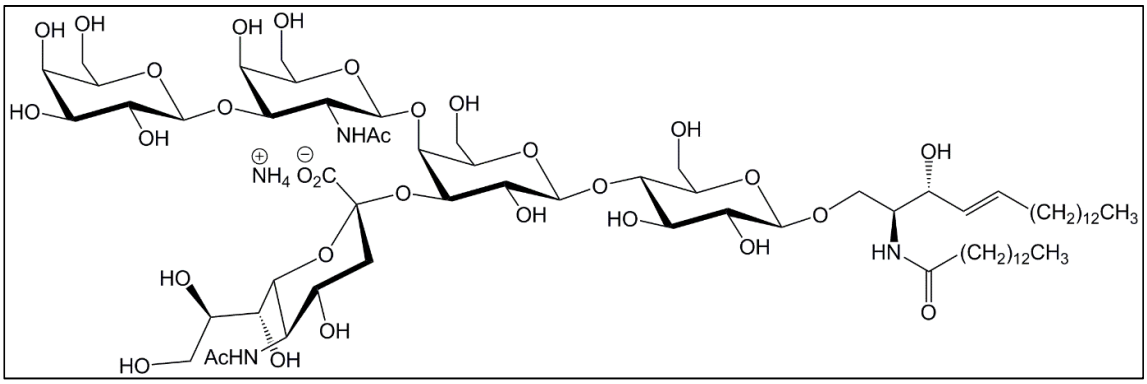

Experimental procedure:

All steps were performed under an argon atmosphere. 19.4 mg (15.0 µmol) of d18:1-lyso-GM1·NH_3 were mixed with 75 µL (0.44 mmol) of Hünig's base and dissolved in 1.5 mL abs. DMF. Then, 12.0 mg (36.9 µmol) of 2,5-dioxopyrrolidin-1-yl tetradecanoate in 0.38 mL of abs. DMF were added and the reaction mixture was stirred at 30 °C for 3 d and 18 h. The reaction was stopped by the addition of a few drops of 2.5 M ammonia. The solvent was removed in a nitrogen stream, the crude product was dried in vacuum and subsequently purified by NP column chromatography (Merck-silica gel 60/40-63 µm, 2.5 × 20.0 cm, isocratic, eluent: $CHCl_3$/MeOH/2.5 M aq. NH_3 60:40:9 v/v/v). After lyophilization, d18:1/14:0-GM1·NH_3 was obtained as a colorless powder (6.32 mg, 28 %).

Analytics:

Molecular Formula: $C_{69}H_{126}N_4O_{31}$

Molecular Weight: 1507.76 g/mol

R_f = 0.20 ($CHCl_3$/MeOH/2.5 M NH_3 60:40:9 v/v/v)

MS (ESI, pos. Mode, MeOH): m/z (%) = 1528.66 (0.5) $[M + K]^+$, 1512.71 (0.32) $[M + Na]^+$, 1507.73 (2.5) $[M + NH_4]^+$, 1499.23 (0.30) $[2M + NH_4 + H]^{2+}$, 1490.72 (0.71) $[M + H]^+$, 783.81 (3.8) $[M + 2K]^{2+}$, 775.83 (2.8) $[M + K + Na]^{2+}$, 773.35 (3.1) $[M + K + NH_4]^{2+}$, 764.83 (17) $[M + K + H]^{2+}$, 756.85 (6.5) $[M + Na + H]^{2+}$, 762.88 (5.3) $[M + 2NH_4]^{2+}$, 754.37 (39) $[M + NH_4 + H]^{2+}$, 745.86 (100) $[M + 2H]^{2+}$.

MS/MS (m/z = 745.86): m/z (%) = 1181.63 (3.1) $[Z_{2\beta}]^+$, 1107.60 (15) $[Z_{2\alpha}]^+$, 1019.59 (9.7) $[Y_{3\alpha}/C_{1\beta} + H]^+$, 816.52 (25) $[Y_{2\alpha}/C_{1\beta} + H]^+$, 672.50 (4.3) $[Y_1 + 2H]^+$, 654.49 (28) $[Z_1]^+$, 510.45 (6.9) $[Y_0 + 2H]^+$, 492.45 (55) $[Z_0]^+$, 474.44 (11) $[Z_0 - H_2O]^+$, 366.12 (100) $[B_{2\alpha}]^+$, 292.09 (27) $[B_{1\beta}]^+$, 274.09 (53) $[B_{1\beta} - H_2O]^+$, 264.27 (18) [Z_0 – myristic acid]$^+$, 204.11 (90) $[B_{2\alpha}/B_{1\alpha} + H]^+$, 186.12 (28) $[B_{2\alpha}/B_{1\alpha} + H - H_2O]^+$.

Densitometry:

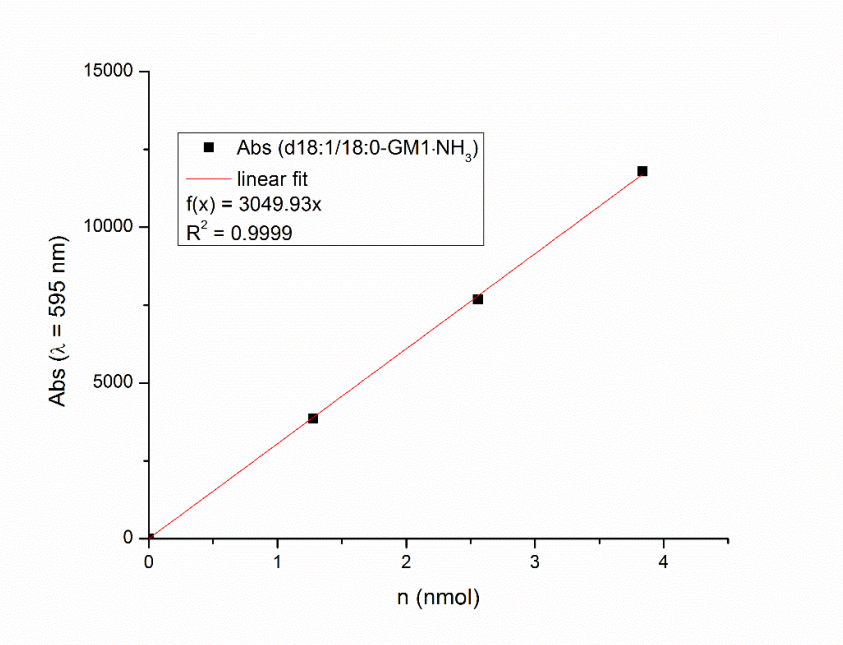

Ganglioside	M (g/mol)	calc. n (nmol)	measured Abs
d18:1/14:0-GM1·NH_3	1507,76	3,32	8150,8

measured n (nmol)	Dev. (nmol)	Dev. (%)
2,67	-0,650	-19,6

Fig. 5.4.1: Densitometric analysis of d18:1/14:0-GM1·NH_3 (**14**) by using d18:1/18:0-GM1·NH_3 (**1**) as reference standard

Photometric sialic acid determination:

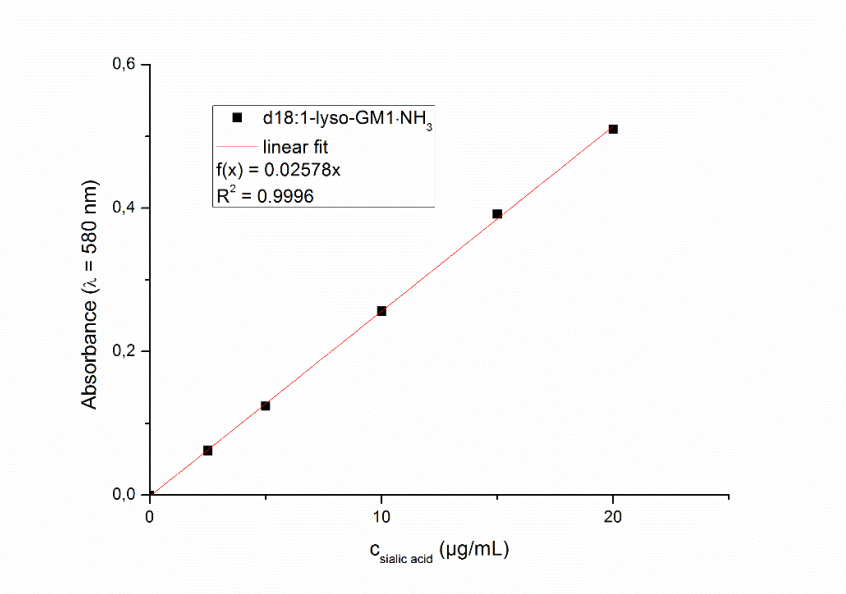

Ganglioside	M (g/mol)	c (mg/mL)	calc. c_{NANA} (µg/mL)
d18:1/14:0-GM1·NH_3	1507.76	1.00	10.0
d18:1/18:0-GM2·NH_3	1401.73	0.200	10.0

Abs. 1	Abs. 2	Mean	$Mean_{corr.}$	meas. c_{NANA} (µg/mL)	Dev. (µg/mL)	Dev. (%)
0.893	0.883	0.888	0.230	8.92	-1.08	-10.8
0.732	0.734	0.733	0.0745	2.89	-7,11	-71.1

Fig. 5.4.2: Sialic acid determination of d18:1/14:0-GM1·NH_3 (**14**) and d18:1/18:0-GM2·NH_3 (**20**) by using d18:1-lyso-GM1·NH_3 (**7**) as reference standard

5.4.4 Synthesis of d18:1/14:0-GD1a·2NH$_3$ (15)

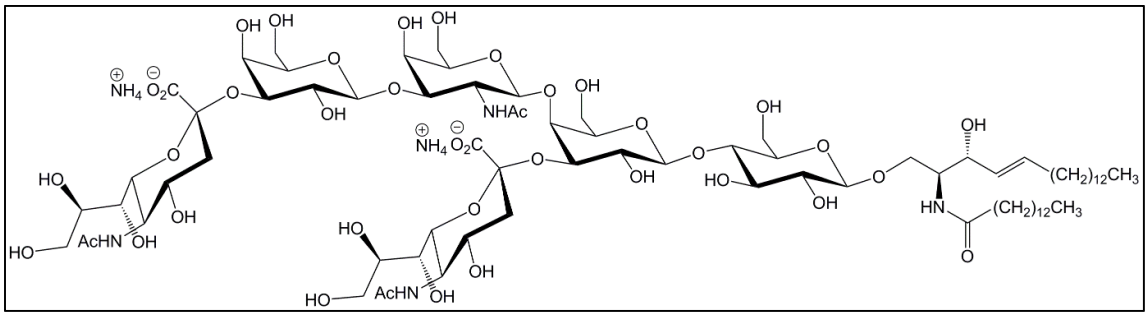

Experimental procedure:

d18:1/14:0-GD1a·2NH$_3$ was synthesized by the method described in section 5.4.3. 1.87 mg (1.16 µmol) of d18:1-lyso-GD1a·2NH$_3$ were applied. 11.0 mg (33.8 µmol) of 2,5-dioxopyrrolidin-1-yl tetradecanoate and 67.8 µL (0.399 µmol) of Hünig's base were added over a period of 4.5 d. The crude product was purified by RP column chromatography (Merck LiChroprep RP-18/40-63 µm, 2.7 × 3.9 cm, eluent: MeOH/H$_2$O 90:50 v/v). After lyophilization, d18:1/C14:0-GD1a·2NH$_3$ was obtained as a colorless powder (0.88 mg, 42 %).

Analytics:

Molecular Formula: $C_{80}H_{146}N_6O_{39}$

Molecular Weight: 1816.05 g/mol

R_f = 0.25 ($CHCl_3$/MeOH/2.5 M NH_3 60:44:12 v/v/v)

MS (ESI, pos. Mode, MeOH): m/z (%) = 929.32 (20) $[M + 2K]^{2+}$, 921.34 (27) $[M + K + Na]^{2+}$, 918.86 (35) $[M + K + NH_4]^{2+}$, 913.35 (9.8) $[M + 2Na]^{2+}$, 910.86 (38) $[M + Na + NH_4]^{2+}$, 902.36 (13) $[M + Na + H]^{2+}$, 908.39 (100) $[M + 2NH_4]^{2+}$, 899.88 (59) $[M + NH_4 + H]^{2+}$, 891.37 (77) $[M + 2H]^{2+}$.

MS/MS (m/z = 891.37): m/z (%) = 1310.62 (5.8) $[Z_{3\alpha}]^+$, 1107.56 (10) $[Z_{2\alpha}]^+$, 1019.55 (5.5) $[Z_{3\alpha}/B_{1\beta} + H]^+$, 816.50 (14) $[Z_{2\alpha}/B_{1\beta} + H]^+$, 672.47 (5.6) $[Y_1 + 2H]^+$, 657.17 (33) $[B_{3\alpha}]^+$, 654.47 (22) $[Z_1]^+$, 510.44 (5.9) $[Y_0 + 2H]^+$, 492.43 (49) $[Z_0]^+$, 454.11 (12) $[B_{2\alpha}]^+$,

366.11 (26) $[B_{3\alpha}/B_{1\alpha}+ H]^+$, 292.08 (88) $[B_{1\alpha}]^+$, 274.08 (100) $[B_{1\alpha} – H_2O]^+$, 204.11 (51) $[B_{3\alpha}/B_{2\alpha}+ H]^+$, 186.11 (7,9) $[B_{3\alpha}/B_{2\alpha}+ H – H_2O]^+$.

Photometric sialic acid determination:

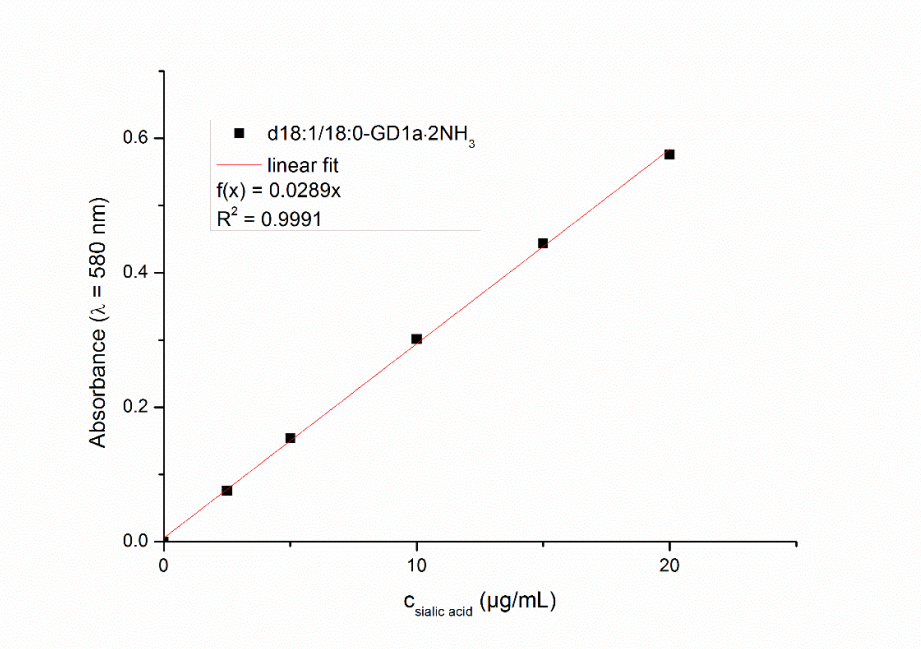

Ganglioside	M (g/mol)	c (mg/mL)	calc. c_{NANA} (µg/mL)
d18:1-lyso-GD1a·NH_3	1605.69	0.200	10.0
d18:1/14:0-GD1a·$2NH_3$	1816.05	0.200	10.0

Abs. 1	Abs. 2	Mean	$Mean_{corr.}$	meas. c_{NANA} (µg/mL)	Dev. (µg/mL)	Dev. (%)
0.821	0.822	0.822	0.190	6.57	-3.43	-34,3
0.722	0.722	0.722	0.0905	3.13	-6.87	-68,7

Fig. 5.4.3: Sialic acid determination of d18:1/14:0-GD1a·$2NH_3$ (**15**) and d18:1-lyso-GD1a·$2NH_3$ (**8**) by using d18:1/18:0-GD1a·$2NH_3$ (**3**) as reference standard. **8** was already quantified by fluorimetric sialic acid determination (section 5.3.4). The deviance between both methods was 0.87 %.

5.4.5 Synthesis of d18:1/17:0-GD1a·2NH$_3$ (16)

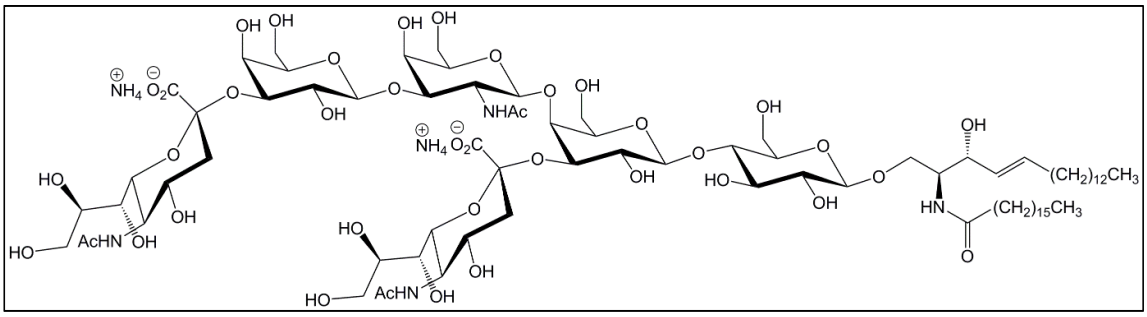

Experimental procedure:

d18:1/17:0-GD1a·2NH$_3$ was synthesized by the method described in section 5.4.3. 0.98 mg (0,610 µmol) of d18:1-lyso-GD1a·2NH$_3$ were applied. 1.43 mg (3.89 µmol) of 2,5-dioxopyrrolidin-1-yl heptadecanoate and 7.75 µL (45.6 µmol) of Hünig's base were added over a period of 30 h. The crude product was purified by NP column chromatography (Merck-silica gel 60/15-40 µm, 2.0 × 20.0 cm, isocratic, eluent: $CHCl_3$/MeOH/2.5 M NH_3 60:40:10 v/v/v). In order to remove column material it was purified by NP column chromatography (Merck-silica gel 60/40-63 µm, 0.6 × 1.0 cm, step gradient, application: $CHCl_3$/MeOH/2.5 M NH_3 60:35:5 v/v/v, elution: $CHCl_3$/MeOH/2.5 M NH_3 60:44:12 v/v/v) again. After lyophilization, d18:1/17:0-GD1a·2NH$_3$ was obtained as a colorless powder (0.98 mg, 86 %).

Analytics:

Molecular Formula: $C_{83}H_{152}N_6O_{39}$

Molecular Weight: 1858.13 g/mol

R_f = 0.18 ($CHCl_3$/MeOH/2.5 M NH_3 60:40:10 v/v/v)

MS (ESI, pos. Mode, MeOH): m/z (%) = 1216.97 (3.2) $[2M + 3H]^{3+}$, 1167.74 (24) $[Y_{2\alpha} + 2H]^+$, 931.98 (3.7) $[M + Na + NH_4]^{2+}$, 929.51 (16) $[M + 2NH_4]^{2+}$, 923.48 (6.1) $[M + Na + H]^{2+}$, 921.00 (22) $[M + NH_4 + H]^{2+}$, 912.48 (100) $[M + 2H]^{2+}$.

MS/MS (m/z = 912.48): m/z (%) = 1352.80 (6.4) $[Z_{3\alpha}]^+$, 1167.74 (13) $[Y_{2\alpha} + 2H]^+$, 1149.73 (15) $[Z_{2\alpha}]^+$, 1061.71 (4.8) $[Z_{3\alpha}/B_{1\beta} + H]^+$, 912.48 (13) $[M + 2H]^{2+}$, 858.64 (11) $[Z_{2\alpha}/B_{1\beta} + H]^+$, 819.30 (3.6) $[B_4/B_{1\beta} + H]^+$, 714.59 (15) $[Y_1 + 2H]^+$, 696.58 (21) $[Z_1]^+$,

657.24 (94) $[B_{3\alpha}]^+$, 552.54 (10) $[Y_0 + 2H]^+$, 534.53 (44) $[Z_0]^+$, 516.52 (6.8) $[Z_0 – H_2O]^+$, 454.16 (22) $[B_{2\alpha}]^+$, 366.15 (26) $[B_{3\alpha}/B_{1\alpha} + H]^+$, 292.11 (100) $[B_{1\alpha}$ o. $B_{1\beta}]^+$, 274.10 (93) $[B_{1\alpha} – H_2O$ o. $B_{1\beta} – H_2O]^+$, 204.09 (49) $[B_{3\alpha}/B_{2\alpha} + H]^+$, 186,08 (7.5) $[B_{3\alpha}/B_{2\alpha} + H – H_2O]^+$.

Photometric sialic acid determination:

The results of the photometric sialic acid determination are given in Fig. 5.3.2. The content of d18:1/17:0-GD1a·2NH_3 (**16**) was 94.7 % compared to d18:1/18:0-GD1a·2NH_3 (**3**) as reference standard.

5.4.6 Synthesis of d20:1/14:0-GD1b·2NH_3 (17)

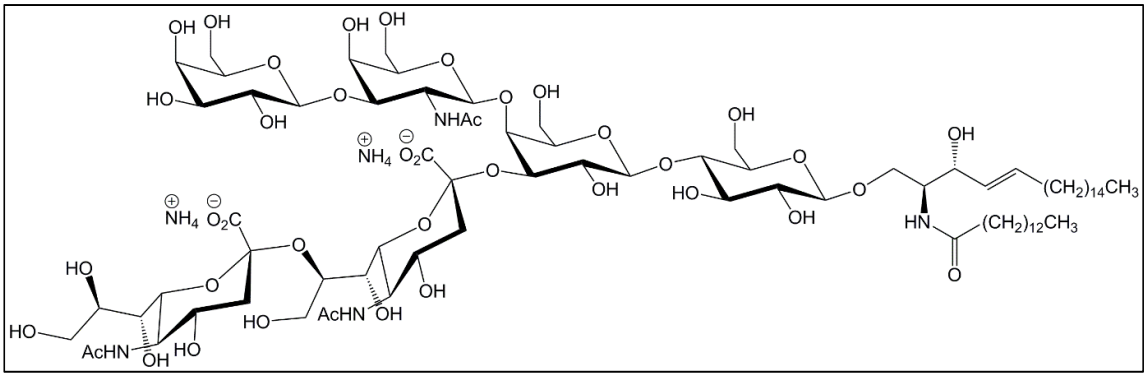

Experimental procedure:

d20:1/14:0-GD1b·2NH_3 was synthesized by the method described in section 5.4.3. 1.63 mg (0,998 µmol) of d20:1-lyso-GD1b·2NH_3 were applied. 1.34 mg (4.12 µmol) of 2,5-dioxopyrrolidin-1-yl tetradecanoate and 8.2 µL (48.2 µmol) of Hünig's base were added over a period of 23 h. The crude product was purified by NP column chromatography (Merck-silica gel 60/15-40 µm, 2.0 × 22.0 cm, isocratic, eluent: $CHCl_3$/MeOH/2.5 M NH_3 60:40:10 v/v/v). In order to remove column material, it was purified by NP column chromatography (Merck-silica gel 60/40-63 µm, 0.6 × 2.0 cm, step gradient, application: $CHCl_3$/MeOH/2.5 M NH_3 60:35:6 v/v/v, elution: $CHCl_3$/MeOH/2.5 M NH_3 60:44:12 v/v/v) again. After lyophilization, d20:1/14:0-GD1b·2NH_3 was obtained as a colorless powder (1.28 mg, 70 %).

The experiment was repeated one time. 0.97 mg (0.594 µmol) of d20:1-lyso-GD1b·2NH_3 were applied. The crude product was purified by RP column chromatography (Merck LiChroprep RP-18/40-63 µm, 1.5 cm × 3.2 cm, eluent: MeOH/H_2O 90:40 v/v). Then, it was purified by preparative HPTLC (Merck TLC silica gel 60, 20 x 20 cm glass plate, eluent: $CHCl_3$/MeOH/2.5 M NH_3 60:44:12 v/v/v). In order to remove TLC material it was purified by NP column chromatography (Merck-silica gel/40-63 µm, column: Ø = 0.6 × 2.0 cm, step gradient, application: $CHCl_3$/MeOH/2.5 M NH_3 60:35:6 v/v/v, elution: $CHCl_3$/MeOH/2.5 M NH_3 60:44:12 v/v/v) again. After lyophilization, d20:1/14:0-GD1b·2NH_3 was obtained as a colorless powder (0.62 mg, 57 %).

Analytics (experiment 1):

Molecular Formula: $C_{82}H_{150}N_6O_{39}$
Molecular Weight: 1844.10 g/mol
R_f = 0.21 ($CHCl_3$/MeOH/2.5 M NH_3 60:44:12 v/v/v)

MS (ESI, pos. Mode, MeOH): m/z (%) = 1831.89 (0.29) $[M + Na]^+$, 1826.92 (0.68) $[M + NH_4]^+$, 1818.44 (0.13) $[2M + NH_4 + H]^{2+}$, 1809.92 (1.3) $[M + H]^+$, 927.44 (6.4) $[M + 2Na]^{2+}$, 924.94 (3.9) $[M + Na + NH_4]^{2+}$, 916.44 (22) $[M + Na + H]^{2+}$, 913.96 (8.6) $[M + NH_4 + H]^{2+}$, 905.45 (100) $[M + 2H]^{2+}$, 891.44 (3.5) $[M + 2H - 2CH_2]^{2+}$.

MS/MS (m/z = 905.45): m/z (%) = 1518.73 (2.5) $[Y_{3\alpha} + 2H]^{2+}$, 1500.75 (2.0) $[Z_{3\alpha}]^+$, 1426.70 (3.1) $[Z_{2\beta}]^+$, 1209.66 (3.5) $[Z_{2\alpha}]^+$, 1135.64 (4.7) $[Y_{2\beta}/C_{1\alpha} + H]^+$, 1047.62 (4.9) $[Y_{3\beta}/C_{2\alpha} + H]^+$, 905.41 (22) $[M + 2H]^{2+}$, 844.56 (11) $[Y_{2\beta}/C_{2\alpha} + H]^+$, 700.53 (3.3) $[Y_1 + 2H]^{2+}$, 682.52 (13) $[Z_1]^+$, 583.17 (5.8) $[B_{2\alpha}]^+$, 538.49 (5.2) $[Y_0 + 2H]^{2+}$, 520.48 (39) $[Z_0]^+$, 502.47 (9.3) $[Z_0 - H_2O]^+$, 454.13 (3.3) $[Y_{2\beta}/B_{1\alpha}/Y_1 + 2H]^+$, 366.12 (99) $[B_{2\beta}]^+$, 292.09 (69) $[B_{1\alpha}]^+$, 274.08 (100) $[B_{1\alpha} - H_2O]^+$, 204.08 (68) $[B_{2\beta}/B_{1\beta} + H]^+$, 186.08 (28) $[B_{2\beta}/B_{1\beta} + H - H_2O]^+$.

Photometric sialic acid determination:

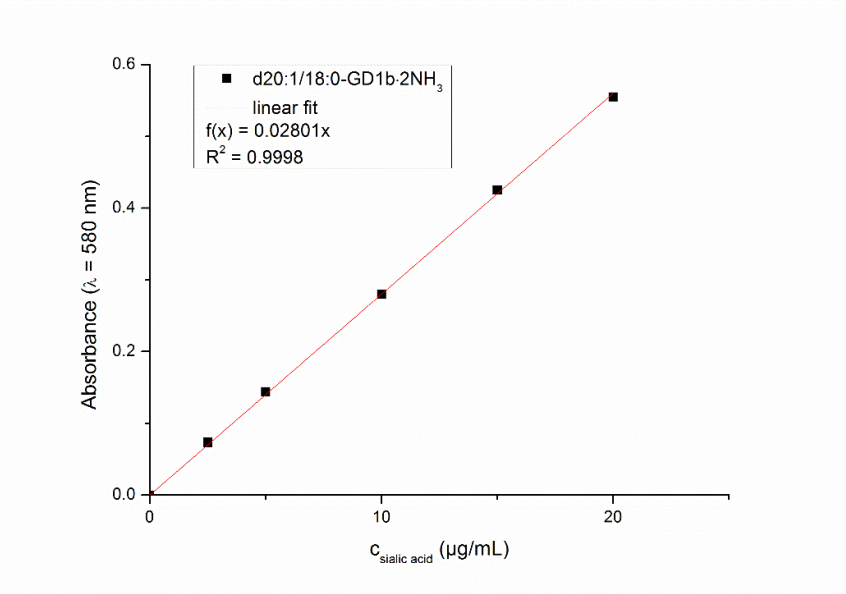

Ganglioside	M (g/mol)	c (mg/mL)	calc. c_{NANA} (µg/mL)
d20:1/14:0-GD1b·2NH_3	1844.10	0.200	10.0
d18:1/18:0-GD2·2NH_3	1738.07	0.200	10.0
d18:1/14:0-GD2·2NH_3	1681.96	0.200	10.0

Abs. 1	Abs. 2	Mean	$Mean_{corr.}$	meas. c_{NANA} (µg/mL)	Dev. (µg/mL)	Dev. (%)
0.844	0.847	0.846	0.211	7.53	-2.47	-24.7
0.711	0.711	0.711	0.0765	2.73	-7.27	-72.7
0.838	0.835	0.837	0.202	7.21	-2.79	-27.9

Fig. 5.4.4: Sialic acid determination of d20:1/14:0-GD1b·2NH_3 (**17**), d20:1/18:0-GD2·2NH_3 (**22**), and d20:1/14:0-GD2·2NH_3 (**23**) by using d20:1/18:0-GD1b·2NH_3 (**4**) as reference standard

Analytics (experiment 2):

MS (ESI, pos. Mode, MeOH): m/z (%) = 1826.86 (0.68) $[M + NH_4]^+$, 1809.87 (0.34) $[M + H]^+$, 935.45 (2.7) $[M + K + Na]^{2+}$, 927.45 (11) $[M + 2Na]^{2+}$, 924.97 (16) $[M + Na + NH_4]^{2+}$, 916.47 (21) $[M + Na + H]^{2+}$, 922,49 (13) $[M + 2NH_4]^{2+}$, 913.99 (33) $[M + NH_4 + H]^{2+}$, 905.48 (100) $[M + 2H]^{2+}$.

MS/MS (m/z = 905.48): m/z (%) = 1518.84 (4.5) $[Y_{3\alpha} + 2H]^{2+}$, 1426.80 (5.4) $[Z_{2\beta}]^{+}$, 1209.75 (4.7) $[Z_{2\alpha}]^{+}$, 1135.71 (4.5) $[Y_{2\beta}/C_{1\alpha} + H]^{+}$, 1047.69 (3.9) $[Y_{3\beta}/C_{2\alpha} + H]^{+}$, 905.47 (80) $[M + 2H]^{2+}$, 896.46 (14) $[Y_{2\beta}/B_{2\alpha} + 2NH_4 + H]^{+}$, 862.63 (7.1) $[Y_{2\beta}/B_{2\alpha} + 3H]^{+}$, 844.62 (5.1) $[Y_{2\beta}/C_{2\alpha} + H]^{+}$, 700.58 (5.8) $[Y_1 + 2H]^{2+}$, 682.56 (6.1) $[Z_1]^{+}$, 583.20 (9.7) $[B_{2\alpha}]^{+}$, 538.53 (7.0) $[Y_0 + 2H]^{2+}$, 520.51 (14) $[Z_0]^{+}$, 454.16 (4.5) $[Y_{2\beta}/B_{1\alpha}/Y_1 + 2\ H]^{+}$, 366.14 (100) $[B_{2\beta}]^{+}$, 292.10 (76) $[B_{1\alpha}]^{+}$, 274.09 (43) $[B_{1\alpha} - H_2O]^{+}$, 204.09 (20) $[B_{2\beta}/B_{1\beta} + H]^{+}$, 186.08 (2.4) $[B_{2\beta}/B_{1\beta} + H - H_2O]^{+}$.

5.4.7 Synthesis of d20:1/14:0-GT1b·3NH$_3$ (18)

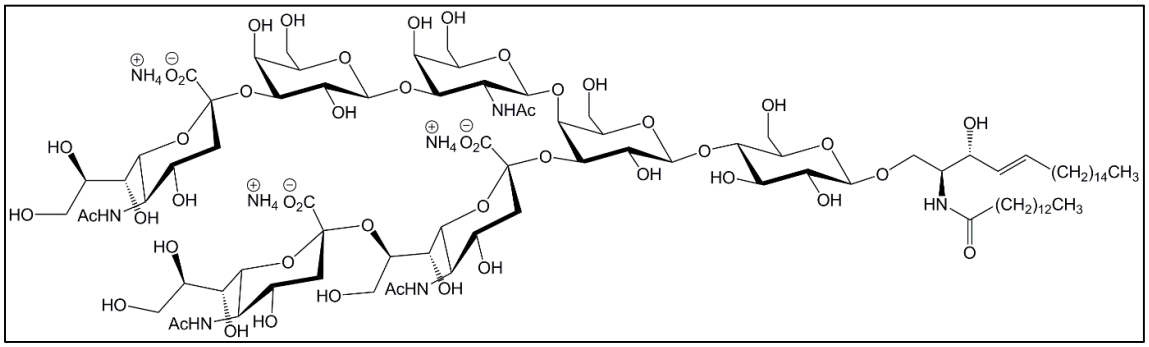

Experimental procedure:

d20:1/14:0-GT1b·3NH$_3$ was synthesized by the method described in section 5.4.3. 1.06 mg (0.546 µmol) of d20:1-lyso-GT1b·3NH$_3$ were applied. 2.21 mg (6.79 µmol) of 2,5-dioxopyrrolidin-1-yl tetradecanoate and 13.6 µL (80.0 µmol) of Hünig's base were added over a period of 6 d. The crude product was purified by NP column chromatography on silica gel (Merck-silica gel 60/15-40 µm, 2.0 × 25.0 cm, isocratic, eluent: $CHCl_3$/MeOH/2.5 M NH_3 60:44:12 v/v/v). In order to remove column material, it was purified by NP column chromatography (Merck-silica gel 60/40-63 µm, 0.6 × 2.0 cm, step gradient, application: $CHCl_3$/MeOH/2.5 M NH_3 60:40:8 v/v/v, elution: $CHCl_3$/MeOH/2.5 M NH_3 60:50:15 v/v/v) again. After lyophilization, d20:1/14:0-GT1b·3NH$_3$ was obtained as a colorless powder (0.40 mg, 34 %).

Analytics:

Molecular Formula: $C_{93}H_{170}N_8O_{47}$

Molecular Weight: 2152.39 g/mol

R_f = 0.24 ($CHCl_3$/MeOH/2.5 M NH_3 60:50:15 v/v/v)

MS (ESI, pos. Mode, MeOH): m/z (%) = 1081.47 (6.6) $[M + K + Na]^{2+}$, 1070.48 (13) $[M + K + H]^{2+}$, 1073.48 (8.1) $[M + 2Na]^{2+}$, 1070.99 (11) $[M + Na + NH_4]^{2+}$, 1062.49 (20) $[M + Na + H]^{2+}$, 1060.02 (7.2) $[M + NH_4 + H]^{2+}$, 1051.50 (100) $[M + 2H]^{2+}$, 1037.49 (5.0) $[M + 2H - 2CH_2]^{2+}$.

MS/MS (m/z = 1051.50): m/z (%) = 1135.69 (3.3) $[Y_{3\beta}/C_{3\alpha} + H]^+$, 1051.50 (17) $[M + 2H]^{2+}$, 844.60 (4.8) $[Y_{2\beta}/C_{3\alpha} + H]^+$, 682.55 (7.1) $[Z_1]^+$, 657.23 (38) $[B_{3\alpha}]^+$, 583.19 (4.9) $[B_{2\beta}]^+$, 538.51 (2.7) $[Y_0 + 2H]^+$, 520.50 (26) $[Z_0]^+$, 502.48 (4.8) $[Z_0 - H_2O]^+$, 454.15 (11) $[Y_{2\alpha}/B_{1\beta}/Y_1 + 2H]^+$, 366.14 (14) $[B_{3\alpha}/B_{1\alpha} + H]^+$, 292.10 (81) $[B_{1\alpha}$ o. $B_{1\beta}]^+$, 274.09 (100) $[B_{1\alpha}$ o. $B_{1\beta} - H_2O]^+$, 204.09 (33) $[B_{3\alpha}/B_{2\alpha} + H]^+$, 186.08 (9.9) $[B_{3\alpha}/B_{2\alpha} + H - H_2O]^+$.

Photometric sialic acid determination:

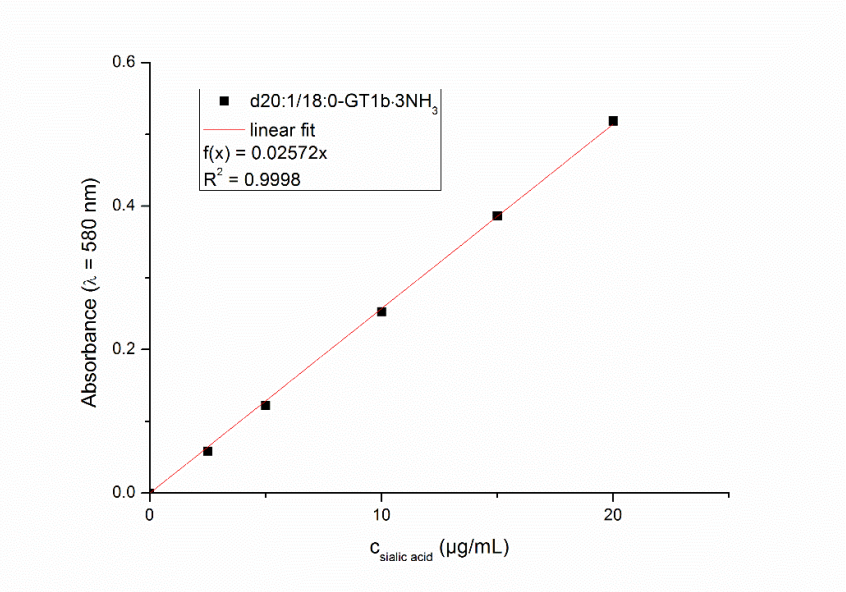

Ganglioside	**M (g/mol)**	**c (mg/mL)**	**calc. c_{NANA} (µg/mL)**
d20:1/14:0-GT1b·3NH_3	2152.39	0.200	10.0

Abs. 1	**Abs. 2**	**Mean**	**$Mean_{corr.}$**	**meas. c_{NANA} (µg/mL)**	**Dev. (µg/mL)**	**Dev. (%)**
0.783	0.784	0.784	0.125	4,86	-5,14	-51,4

Fig. 5.4.5: Sialic acid determination of d20:1/14:0-GT1b·3NH_3 (**18**), by using d20:1/18:0-GT1b·3NH_3 (**5**) as reference standard

5.4.8 Synthesis of d20:1/14:0-GQ1b·4NH_3 (19)

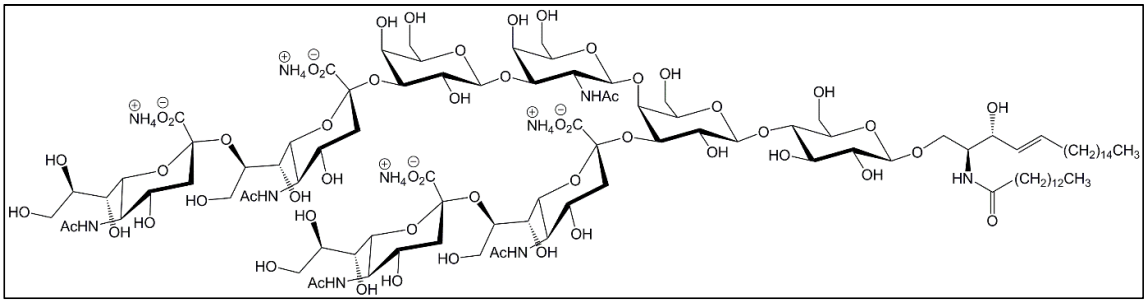

Experimental procedure:

d20:1/14:0-GQ1b·4NH_3 was synthesized by the method described in section 5.4.3. 0.92 mg (0,409 µmol) of d20:1-lyso-GQ1b·4NH_3 were applied. 2.54 mg (7.80 µmol) of 2,5-dioxopyrrolidin-1-yl tetradecanoate and 15.6 µL (91.7 µmol) of Hünig's base were added over a period of 6 d. The crude product was purified by NP column chromatography (Merck-silica gel 60/15-40 µm, 2.0 × 25.4 cm, isocratic, eluent: $CHCl_3$/MeOH/2.5 M NH_3 60:50:13 v/v/v). In order to remove column material, it was purified by NP column chromatography (Merck-silica gel 60/40-63 µm, 0.6 × 2.0 cm, step gradient, application: $CHCl_3$/MeOH/2.5 M NH_3 60:40:8 v/v/v, elution: $CHCl_3$/MeOH/2.5 M NH_3 50:50:16 v/v/v) again. After lyophilization, d20:1/14:0-GQ1b·4NH_3 was obtained as a colorless powder (0.19 mg, 19 %).

Analytics:

Molecular Formula: $C_{104}H_{190}N_{10}O_{55}$

Molecular Weight: 2460.68 g/mol

R_f = 0.27 ($CHCl_3$/MeOH/2.5 M NH_3 50:50:16 v/v/v)

MS (ESI, pos. Mode, MeOH): m/z (%) = 1235.01 (3.9) $[M + 2K]^{2+}$, 1227.01 (17) $[M + K + Na]^{2+}$, 1224.55 (9.1) $[M + K + NH_4]^{2+}$, 1216.02 (100) $[M + K + H]^{2+}$, 1208.03 (22) $[M + Na + H]^{2+}$, 1205.55 (12) $[M + NH_4 + H]^{2+}$, 1197.04 (95) $[M + 2H]^{2+}$.

MS/MS (m/z = 1196.54): m/z (%) = 1197.05 (8.0) $[M + 2H]^{2+}$, 1135.67 (3.3) $[Y_{3\beta}/C_{4\alpha} + H]^{+}$, 948.31 (16) $[B_{4\alpha}]^{+}$, 844.61 (7.4) $[Y_{2\beta}/C_{4\alpha} + H]^{+}$, 745.24 (4.5) $[B_{3\alpha}]^{+}$, 682.55 (8.7)

$[Z_1]^+$, 657.23 (13) $[B_{4\alpha}/B_{1\alpha} + H]^+$, 583.19 (9.7) $[B_{2\alpha}$ o. $B_{2\beta}]^+$, 520.51 (29) $[Z_0]^+$, 454.15 (18) $[Y_{2\alpha}/B_{1\beta}/Y_1 + 2H]^+$, 366.14 (17) $[B_{4\alpha}/B_{2\alpha} + H]^+$, 292.10 (100) $[B_{1\alpha}$ o. $B_{1\beta}]^+$, 274.09 (67) $[B_{1\alpha}$ o. $B_{1\beta} - H_2O]^+$, 204.09 (15) $[B_{4\alpha}/B_{3\alpha} + H]^+$.

Photometric sialic acid determination:

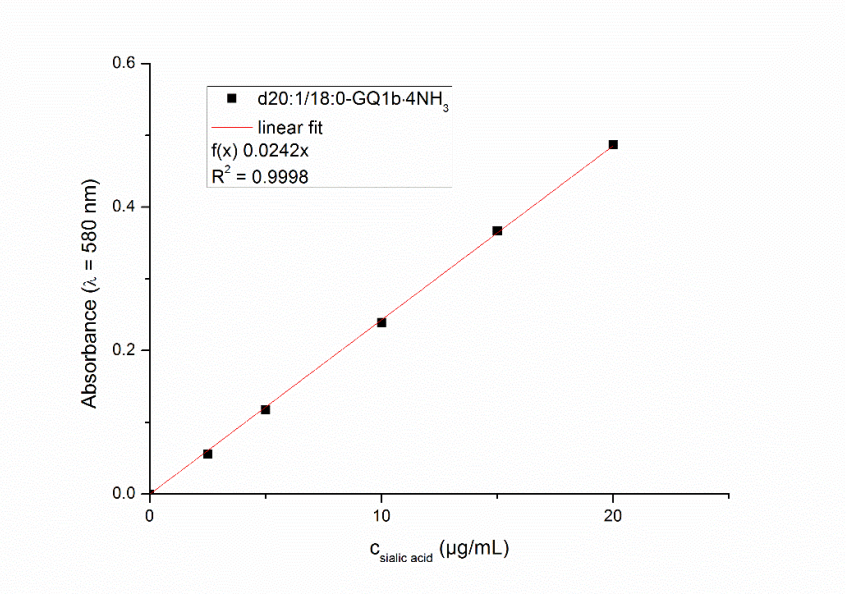

Ganglioside	M (g/mol)	c (mg/mL)	calc. c_{NANA} (µg/mL)
d20:1/14:0-GQ1b·4NH$_3$	2460.68	0.200	10.0

Abs. 1	Abs. 2	Mean	$Mean_{corr.}$	meas. c_{NANA} (µg/mL)	Dev. (µg/mL)	Dev. (%)
0.704	0.708	0.706	0.0470	1.94	-8.06	-80.6

Fig. 5.4.6: Sialic acid determination of d20:1/14:0-GQ1b·4NH$_3$ (**19**), by using d20:1/18:0-GQ1b·4NH$_3$ (**6**) as reference standard

5.5 Preparation of ganglioside standards by enzymatic degalactosylation

5.5.1 Preparation of d18:1/18:0-GM2·NH_3 (20)

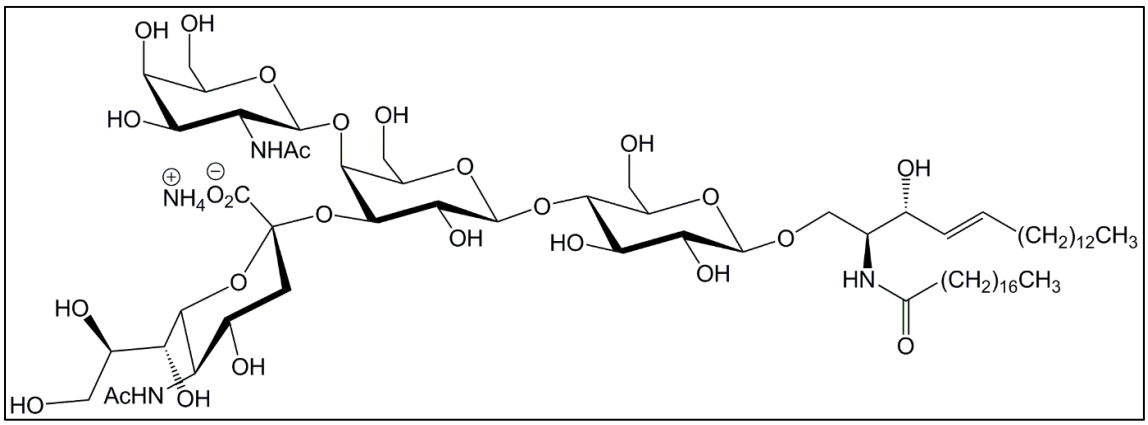

Experimental procedure:

1.00 mg (0.639 µmol) of d18:1/18:0-GM1·NH_3 (**1)** were dissolved in 87.8 µL of 100 mM McIlvaine buffer (citric acid/disodium hydrogen phosphate, pH 4.3), which contained 3.9 mM sodium taurodeoxycholate. The mixture was exposed to an ultrasonic bath for 15 s. Then, 83.2 µL (85.7 mU) of a beta-galactosidase solution (in aq. 3.2 M $(NH_4)_2SO_4$) were added and the mixture was incubated at 37 °C. After 4 d, TLC-analysis ($CHCl_3$/MeOH/2.5 M NH_3 60:40:9 v/v/v) revealed only a slight conversion of the educt. The reaction volume was duplicated to reduce micelle formation of the gangliosides. After a further day no increase of the conversion was observed. Next, 171 µL of a 2.4 mM Triton X-100 solution that contained 2 mM sodium taurodeoxycholate were added. After two further days a slightly better conversion was observed. Then, 83.2 µL (85.7 mU) of beta-galactosidase solution were added. After 3 further days almost 90 % of the educt was converted. Hence, 23.6 µL (24.3 mU) of beta-galactosidase solution were added. After at all 12 d the reaction was stopped by the addition of a few drops 2.5 M aq. NH_3. The solvent was removed in a nitrogen stream and the residue was redissolved in 0.5 mL of methanol. The enzyme was separated by centrifugation (12100 × g), which was repeated five times. The supernatant was separated and the solvent was evaporated in a nitrogen stream. The crude product was purified by preparative HPTLC (Merck TLC silica gel 60, 20 x 20 cm glass plate, eluent: $CHCl_3$/MeOH/2.5 M aq. NH_3 60:40:9 v/v/v). In

order to remove TLC material, it was purified by NP column chromatography (Merck-silica gel 60/40-63 µm, 0.5 × 3.0 cm, step gradient, application: $CHCl_3$/MeOH 2:1 v/v, elution: $CHCl_3$/MeOH/2.5 M NH_3 60:40:9 v/v/v) again. After lyophilization, d18:1/18:0-GM2·NH_3 was obtained as a colorless powder (0.32 mg, 36 %).

Analytics:

Molecular Formula: $C_{67}H_{124}N_4O_{26}$
Molecular Weight: 1401.73 g/mol
R_f = 0.25 ($CHCl_3$/MeOH/2.5 M NH_3 60:40:9 v/v/v)

MS (ESI, pos. Mode, MeOH): m/z (%) = 1422.78 (4.0) $[M + K]^+$, 1406.80 (6.5) $[M + Na]^+$, 1401.85 (12) $[M + NH_4]^+$, 1384.83 (2.0) $[M + H]^+$, 730.87 (4.4) $[M + 2K]^{2+}$, 722.88 (8.2) $[M + K + Na]^{2+}$, 711.89 (19) $[M + K + H]^{2+}$, 712.40 (16) $[M + Na + NH_4]^{2+}$, 703.90 (16) $[M + Na + H]^{2+}$, 701.42 (15) $[M + NH_4 + H]^{2+}$, 692.91 (100) $[M + 2H]^{2+}$.

MS/MS (m/z = 692.91): m/z (%) = 1163.66 (7.3) $[Z_{2\beta}]^+$, 1075.65 (12) $[Z_{2\alpha}]^+$, 872.59 (26) $[Y_{2\beta}/C_{1\alpha} + H]^+$, 710.55 (27) $[Z_1]^+$, 548.51 (59) $[Z_0]^+$, 530.50 (27) $[Z_0 - H_2O]^+$, 366.12 (9.4) $[B_2/B_{1\alpha} + H]^+$, 292.09 (21) $[B_{1\alpha}]^+$, 274.09 (61) $[B_{1\alpha} - H_2O]^+$, 264.27 (28) $[Z_0$ – stearic acid$]^+$, 204.09 (100) $[B_{1\beta}]^+$, 186.09 (35) $[B_{1\beta} - H_2O]^+$, 126.09 (11) $[B_{1\beta} - H_2O - 2CO]^+$.

Photometric sialic acid determination:

The results of the photometric sialic acid determination are given in Fig. 5.4.2. The content of d18:1/C18:0-GM2·NH_3 (**20**) was 28.9 % compared to d18:1-lyso-GM1·NH_3 (**7**) as reference standard.

5.5.2 Preparation of d18:1/14:0-GM2·NH_3 (21)

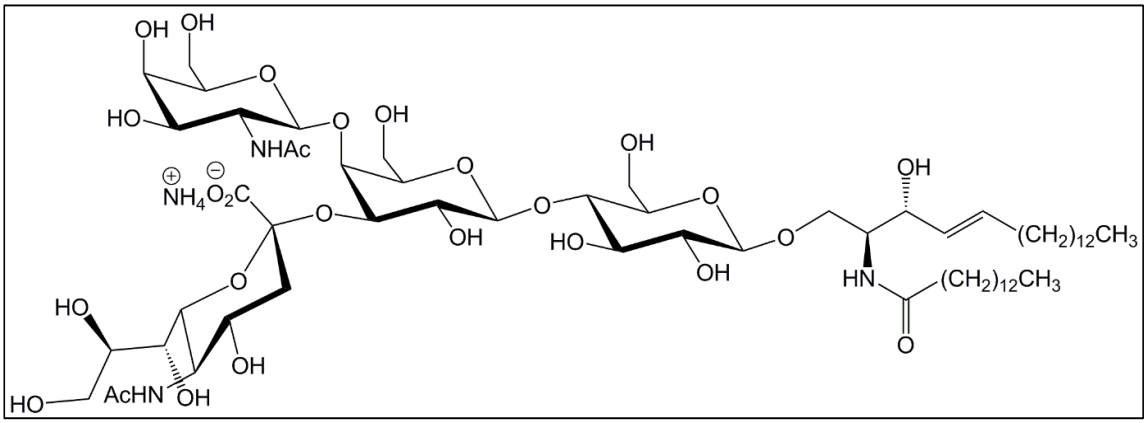

Experimental procedure:

1.34 mg (0.889 µmol) of d18:1/C14:0-GM1·NH_3 (**14**) were dissolved in 410 µL of 100 mM McIlvaine buffer (pH = 4.3), which contained 3.9 mM sodium taurodeoxycholate. Then, 200 µL of buffer containing 3.2 mM Triton X-100 and 40.5 µL of pure buffer were added. The mixture was exposed to an ultrasonic bath for 15 s. Then, 149.5 µL (133.5 mU) of a beta-galactosidase solution were added and the mixture was incubated at 37 °C. After 1 d, TLC-analysis ($CHCl_3$/MeOH/2.5 M aq. NH_3 60:40:9 v/v/v) revealed a conversion of approx. 50 %. Hence, 149.5 µL of the enzyme solution were added. After at all 2 d the conversion was complete and the reaction was stopped by addition of a few drops 2.5 M aq. NH_3. The solvent was removed in a nitrogen stream and the residue was redissolved in 1 mL of MeOH. The enzyme was separated by centrifugation (12100 × g), which was repeated 5 times. The supernatant was separated and evaporated in a nitrogen stream. The crude product was purified by preparative HPTLC (Merck TLC silica gel 60, 20 x 20 cm glass plate, eluent: $CHCl_3$/MeOH/2.5 M NH_3 60:40:9 v/v/v). In order to remove TLC material, it was purified by NP column chromatography (Merck-silica gel 60/40-63 µm, 0.6 × 2.0 cm, step gradient, application: $CHCl_3$/MeOH/2.5 M NH_3 60:35:2 v/v/v, elution: $CHCl_3$/MeOH/2.5 M NH_3 60:40:9 v/v/v) again. After lyophilization, d18:1/C14:0-GM2·NH_3 was obtained as a colorless powder (1.84 mg, 77 % from two preparations).

Analytics:

Molecular Formula: $C_{63}H_{116}N_4O_{26}$
Molecular Weight: 1345.62 g/mol
R_f = 0.27 ($CHCl_3$/MeOH/2.5 M NH_3 60:40:9 v/v/v)

MS (ESI, pos. Mode, MeOH): m/z (%) = 1350.76 (2.2) $[M + Na]^+$, 1345.81 (22) $[M + NH_4]^+$, 1337.79 (1.1) $[2M + NH_4 + H]^{2+}$, 1328.78 (5.0) $[M + H]^+$, 675.88 (10) $[M + Na + H]^{2+}$, 681.49 (16) $[M + 2NH_4]^{2+}$, 673.41 (9.3) $[M + NH_4 + H]^{2+}$, 664.89 (100) $[M + 2H]^{2+}$.

MS/MS (m/z = 664.89): m/z (%) = 1107.67 (13) $[Z_{2\beta}]^+$, 1019.66 (17) $[Z_{2\alpha}]^+$, 834.60 (6.0) $[Y_{2\beta}/B_{1\alpha} + 3H]^+$, 816.59 (21) $[Y_{2\beta}/C_{1\alpha} + H]^+$, 672.55 (7.0) $[Y_1 + 2H]^+$, 664.47 (9.3) $[M + H]^{2+}$, 654.53 (22) $[Z_1]^+$, 552.34 (3.5) $[^{2,6}X_1 + H]^+$, 510.49 (5.3) $[Y_0 + 2H]^+$, 492.48 (42) $[Z_0]^+$, 474.47 (12) $[Z_0 - H_2O]^+$, 366.14 (11) $[B_2/B_{1\alpha} + H]^+$, 292.10 (35) $[B_{1\alpha}]^+$, 274.09 (56) $[B_{1\alpha} - H_2O]^+$, 264.27 (36) [Z_0 – myristic acid]$^+$, 204.09 (100) $[B_{1\beta}]^+$, 186.09 (28) $[B_{1\beta} - H_2O]^+$, 126.10 (9.5) $[B_{1\beta} - H_2O - 2CO]^+$.

Photometric sialic acid determination:

The results of the photometric sialic acid determination are given in Fig. 5.3.1. The content of d18:1/14:0-GM2·NH_3 (**21**) was 97.0 % compared to d18:1/18:0-GM1·NH_3 (**1**) as reference standard.

5.5.3 Preparation of d20:1/18:0-GD2·2NH$_3$ (22)

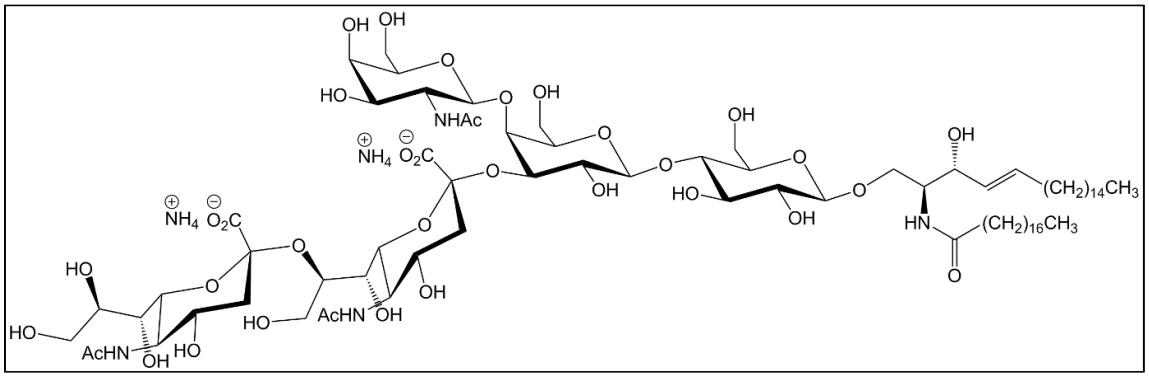

Experimental procedure:

d20:1/18:0-GD2·2NH$_3$ was prepared by the method described in section 5.5.2. The concentrations of enzyme and detergents were doubled. 0.500 mg (0.263 µmol) of d20:1/18:0-GD1b·2NH$_3$ and 160 µL (142 mU) of beta-galactosidase solution were applied. The crude product was purified by NP-chromatography (Merck-silica gel 60/40-63 µm, 0.6 × 2.0 cm, step gradient, application: $CHCl_3$/MeOH/2.5 M NH_3 60:35:4 v/v/v, elution 1: $CHCl_3$/MeOH/2.5 M NH_3 60:35:6 v/v/v, elution 2: $CHCl_3$/MeOH/2.5 M NH_3 60:40:10 v/v/v). This purification step was repeated one time. After lyophilization, d20:1/18:0-GD2·2NH$_3$ was obtained as a colorless powder (0.28 mg, 61 %).

Analytics:

Molecular Formula: $C_{80}H_{148}N_6O_{34}$

Molecular Weight: 1738.07 g/mol

R_f = 0.30 ($CHCl_3$/MeOH/2.5 M NH_3 60:44:12 v/v/v)

MS (ESI, pos. Mode, MeOH): m/z (%) = 1725.90 (0.95) $[M + Na]^+$, 1720.93 (1.6) $[M + NH_4]^+$, 1712.38 (0.43) $[2M + NH_4 + H]^{2+}$, 1703.91 (2.9) $[M + H]^+$, 1412.82 (3.2) $[Y_{3\alpha} + 2H]^+$, 874.43 (8.2) $[M + 2Na]^{2+}$, 871.93 (3.8) $[M + Na + NH_4]^{2+}$, 863.44 (23) $[M + Na + H]^{2+}$, 860.96 (6.4) $[M + NH_4 + H]^{2+}$, 852.45 (100) $[M + 2H]^{2+}$.

MS/MS (m/z = 852.48): m/z (%) = 1394.81 (6.8) $[C_{1\alpha}]^+$, 1191.74 (4.8) $[C_{1\alpha}/B_{1\beta} + H]^+$, 1103.73 (16) $[C_{2\alpha}]^+$, 918.66 (3.9) $[Y_{2\alpha}/B_{1\beta} + 3H]^+$, 900.66 (11) $[C_{2\alpha}/B_{1\beta} + H]^+$, 738.61 (12) $[Z_1]^+$, 583.19 (6.6) $[B_{1\alpha}]^+$, 576.56 (36) $[Z_0]^+$, 558.55 (7.6) $[Z_0 – H_2O]^+$, 454.15 (3.6) $[C_3/C_{1\beta}/B_{1\alpha}+ 2H]^+$, 366.13 (11) $[C_3/C_{2\alpha} + H]^+$, 292.10 (76) $[B_{1\alpha}]^+$, 274.09 (100) $[B_{1\alpha} – H_2O]^+$, 204.09 (72) $[B_{1\beta}]^+$, 186.08 (17) $[B_{1\beta} – H_2O]^+$.

Photometric sialic acid determination:

The results of the photometric sialic acid determination are given in Fig. 5.4.4. The content of d20:1/18:0-GD2·2NH_3 (**22***)* was 27.3 % compared to d20:1/18:0-GD1b·2NH_3 (**4**) as reference standard.

5.5.4 Preparation of d20:1/14:0-GD2·2NH_3 (23)

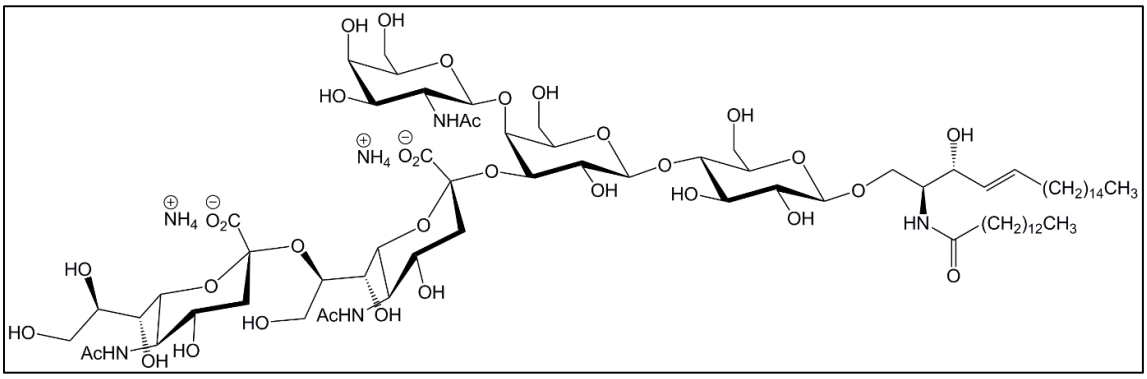

Experimental procedure:

d20:1/14:0-GD2·2NH_3 was synthesized by the method described in section 5.5.3. 0.452 mg (0.245 µmol) of d20:1/14:0-GD1b·2NH_3 and 98.4 µL (87.9 mU) of beta-galactosidase solution were applied. The crude product was purified by NP column chromatography (Merck-silica gel 60/15-40 µm, 1.1 × 23.1 cm, isocratic, eluent: $CHCl_3$/MeOH/2.5 M NH_3 60:40:10 v/v/v). In order to remove column material, it was purified by NP column chromatography again (Merck-silica gel 60/40-63 µm, 0.6 × 1.0 cm, step gradient, application: $CHCl_3$/MeOH/2.5 M NH_3 60:35:4 v/v/v, elution: $CHCl_3$/MeOH/2.5 M NH_3 60:44:12 v/v/v). After lyophilization, d20:1/14:0-GD2·2NH_3 was obtained as a colorless powder (0.25 mg, 61 %).

Analytics:

Molecular Formula: $C_{76}H_{140}N_6O_{34}$
Molecular Weight: 1681.96 g/mol
R_f = 0.30 ($CHCl_3$/MeOH/2.5 M NH_3 60:44:12 v/v/v)

MS (ESI, pos. Mode, MeOH): m/z (%) = 1669.89 (1.0) $[M + Na]^+$, 1664.93 (1.7) $[M + NH_4]^+$, 1647.92 (0.6) $[M + H]^+$, 854.42 (3.4) $[M + K + Na]^{2+}$, 846.43 (18) $[M + 2Na]^{2+}$, 843.94 (8.4) $[M + Na + NH_4]^{2+}$, 835.44 (36) $[M + Na + H]^{2+}$, 841.47 (28) $[M + 2NH_4]^{2+}$, 832.96 (53) $[M + NH_4 + H]^{2+}$, 824.45 (100) $[M + 2H]^{2+}$, 810.44 (3.3) $[M + 2H - 2CH_2]^{2+}$.

MS/MS (m/z = 824.45): m/z (%) = 1338.73 (2.7) $[C_{1\alpha}]^+$, 1135.66 (2.5) $[C_{1\alpha}/B_{1\beta} + H]^+$, 1047.65 (8.5) $[C_{2\alpha}]^+$, 844.58 (7.9) $[C_{2\alpha}/B_{1\beta} + H]^+$, 682.54 (9.4) $[Z_1]^+$, 520.50 (33) $[Z_0]^+$, 502.49 (8.4) $[Z_0 - H_2O]^+$, 366.13 (7.3) $[C_3/C_{2\alpha} + H]^+$, 310.30 (8.7) $[Y_0 + 2H$ – myristic acid$]^+$, 292.29 (78) $[B_{1\alpha}]^+$, 274.08 (100) $[B_{1\alpha} - H_2O]^+$, 204.08 (65) $[B_{1\beta}]^+$, 186.06 (29) $[B_{1\beta} - H_2O]^+$.

Photometric sialic acid determination:

The results of the photometric sialic acid determination are given in Fig. 5.4.4. The content of d20:1/14:0-GD2·2NH_3 (**23**) was 72.1 % compared to d20:1/18:0-GD1b·2NH_3 (**4**) as reference standard.

5.5.5 Preparation of d18:1-lyso-GM2·NH_3 (24)

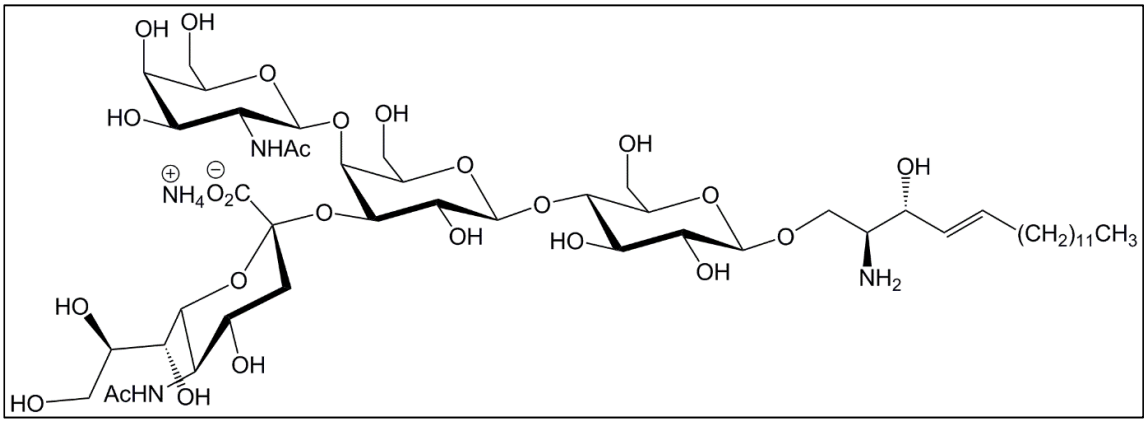

Experimental procedure:

d18:1-lyso-GM2·NH_3 was prepared by the method described in section 5.5.2. 0.585 mg (0.451 µmol) of d18:1-lyso-GM1·NH_3 (**7**) and 140 µL (125 mU) of beta-galactosidase solution were applied. The crude product was purified by NP column chromatography (Merck-silica gel 60/15-40 µm, 1.1 × 20.2 cm, isocratic, eluent: $CHCl_3$/MeOH/2.5 M NH_3 60:40:10 v/v/v). In order to remove column material, it was purified by NP column chromatography again (Merck-silica gel 60/40-63 µm, 0.6 × 1.0 cm, step gradient, application: $CHCl_3$/MeOH/2.5 M NH_3 60:35:2 v/v/v, elution: $CHCl_3$/MeOH/2.5 M NH_3 60:40:10 v/v/v). After lyophilization, d18:1-lyso-GM2·NH_3 was obtained as a colorless powder (0.40 mg, 78 %).

Analytics:

Molecular Formula: $C_{49}H_{90}N_4O_{25}$

Molecular Weight: 1135.26 g/mol

R_f = 0.16 ($CHCl_3$/MeOH/2.5 M NH_3 60:40:9 v/v/v)

MS (ESI, pos. Mode, MeOH): m/z (%) = 1140.57 (3.7) $[M + Na]^+$, 1129,57 (1.6) $[2M + Na + H]^{2+}$, 1118.57 (100) $[M + H]^+$, 827.49 (3.7) $[Y_{2\alpha} + 2H]^+$, 581.77 (2.5) $[M + 2Na]^{2+}$, 578.77 (0.74) $[M + K + H]^{2+}$, 570.78 (7.5) $[M + Na + H]^{2+}$, 568.31 (3.5) $[M + NH_4 + H]^{2+}$, 559.79 (13) $[M + 2H]^{2+}$.

MS/MS (m/z = 1118.57): m/z (%) = 1118.58 (28) $[M + H]^+$, 1100.56 (2.5) $[M + H - H_2O]^+$, 827.49 (51) $[Y_{2\alpha} + 2H]^+$, 809.48 (8.9) $[Z_{2\alpha}]^+$, 624.41 (5.1) $[Y_{2\beta}/B_{1\alpha} + 3H]^+$, 606.40 (3.8) $[Y_{2\alpha}/C_{1\beta} + H]^+$, 462.35 (8.2) $[Y_1 + 2H]^+$, 444.34 (9.6) $[Z_1]^+$, 426.33 (3.9) $[Z_1 - H_2O]^+$, 366.15 (20) $[B_2/B_{1\alpha} + H]^+$, 300.30 (6.7) $[Y_0 + 2H]^+$, 292.12 (10) $[B_{1\alpha}]^+$, 282.30 (24) $[Z_0]^+$, 274.11 (10) $[B_{1\alpha} - H_2O]^+$, 264.29 (7.1) $[Z_0 - H_2O]^+$, 222.12 (4.7) $[C_{1\beta} + 2H]^+$, 204.11 (100) $[B_{1\beta}]^+$, 186.11 (16) $[B_{1\beta} - H_2O]^+$.

Photometric sialic acid determination:

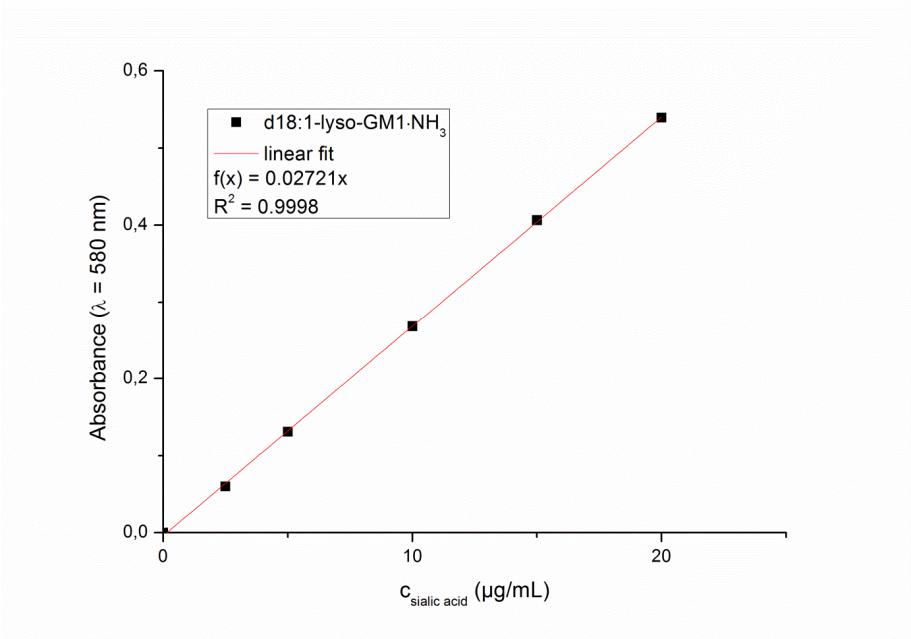

Ganglioside	M (g/mol)	c (mg/mL)	calc. c_{NANA} (µg/mL)
d17:1-lyso-GM1·NH_3	1283.38	0.200	10.0
d18:1-lyso-GM2·NH_3	1135.36	0.200	10.0
d17:1-lyso-GM2·NH_3	1121.24	0.200	10.0

Abs. 1	Abs. 2	Mean	$Mean_{corr.}$	meas. c_{NANA} (µg/mL)	Dev. (µg/mL)	Dev. (%)
0.860	0.860	0.860	0.205	7.53	-2.47	-24,8
0.849	0.850	0.850	0.194	7.13	-2.87	-28,7
0.900	0.902	0.901	0.246	9.04	-0.960	-9,60

Fig. 5.5.1: Sialic acid determination of d17:1-lyso-GM1·NH_3 (**31**), d18:1-lyso-GM2 (**24**), and d17:1-lyso-GM2·NH_3 (**32**) by using d18:1-lyso-GM1·NH_3 (**7**) as reference standard

5.6 Development of a new synthetic method to modify the sphingosine chain of gangliosides

5.6.1 Synthesis of methyl (*E*)-10-phenyldec-9-enoate (25)

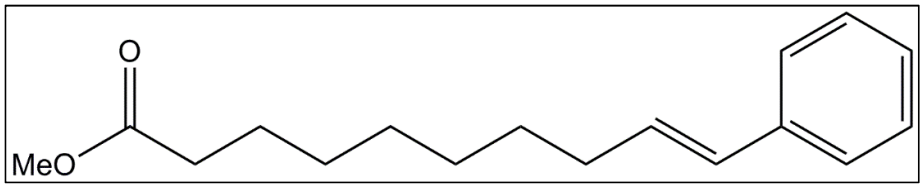

Experimental procedure:

All steps were performed under an argon atmosphere. 25.0 mg (84.3 µmol) of methyl oleate and 152 mg (843 µmol) of (*E*)-stilbene were dissolved in 2.5 mL of dry CH_2Cl_2. Then, 2.64 mg (4.22 µmol, 0.46 mol%) of Hoveyda-Grubbs catalyst 2nd gen (Fig. 2.3.1). were added and the reaction mixture was stirred at RT for 2 h. TLC monitoring (hexane/EtOAc 40:1 v/v) revealed a conversion of approx. 80 %. The solvent was removed in a nitrogen stream, the crude product was dried in vacuum and subsequently purified by NP column chromatography (Merck-silica gel 60/40-63 µm, 1.5 × 3.0 cm, step gradient, application: Hexane/EtOAc 80:1 v/v, elution: Hexane//EtOAc 40:1 v/v). This purification step was repeated one time in order to remove residuals of (*E*)-stilbene. After drying in vacuum, the product was obtained as colorless oil (18.5 mg, 84 %).

Analytics:

Molecular Formula: $C_{17}H_{24}O_2$

Molecular Weight: 260.38 g/mol

R_f = 0.18 (Hexane/EtOAc 40:1 v/v)

^{1}H NMR (300 MHz, $CDCl_3$, RT): δ [ppm] = 7.34 (dd, 2H, $^3J_{H2'\text{-}H3'}$ = 8.4 Hz, $^4J_{H2'\text{-}H4'}$ = 1.5 Hz, H-2', 6'), 7.28 (m, 2H, H-3', 5'), 7.22 – 7.15 (m, 1H, H-4'), 6.37 (d, 1H, $^3J_{H10\text{-}H9,\ trans}$ = 15.8 Hz, H-10), 6.21 (dt, 1H, $^3J_{H9\text{-}H10,\ trans}$ = 15.8 Hz, $^3J_{H9\text{-}H8}$ = 6.7 Hz, H-9), 3.67

(s, 3H, H-1''), 2.31 (t, 2H, $^{3}J_{H2\text{-}H3}$ = 7.5 Hz, H-2), 2.25 – 2.15 (m, 2H, H-8), 1.72 – 1.57 (m, 2H, H-3), 1.52 – 1.25 (m, 8H).

^{13}C NMR (75 MHz, $CDCl_3$, RT): δ [ppm] = 174.28 (R$\underline{C}O_2$R', C-1), 137.89 (sp^2-C, C-1'), 131.07 (sp^2-CH, C-10), 129.75 (sp^2-CH, C-4'), 128.44 (sp^2-CH, C-3', 5'), 126.73 (sp^2-CH, C-9), 125.88 (sp^2-CH, C-2', 6'), 51.42 (CH_3, C-1''), 34.08 (CH_2, C-2), 32.97 (CH_2, C-8), 29.26-28.98 (4 CH_2), 24.92 (CH_2, C-3).

DEPT 135 (75 MHz, $CDCl_3$, RT): δ [ppm] = 131.07 (sp^2-CH, C-10), 129.75 (sp^2-CH, C-4'), 128.44 (sp^2-CH, C-3', 5'), 126.73 (sp^2-CH, C-9), 125.88 (sp^2-CH, C-2', 6'), 51.42 (CH_3, C-1''), 34.08 (CH_2, C-2), 32.97 (CH_2, C-8), 29.26-28.98 (4 CH_2), 24.92 (CH_2, C-3).

MS (EI, 70 eV): m/z (%) = 260.20 (18) [$M^{+\cdot}$], 228.15 (7.4) [$M^{+\cdot}$– MeOH], 137.1 (11) [$M^{+\cdot}$– MeOH – Toluene$^{\cdot}$], 131.10 (17) [Butenylbenzene^{+}], 117.10 (83) [Propenylbenzene^{+}], 104.10 (100) [Ethylbenzene$^{+\cdot}$], 91.10 (26) [Toluene^{+}].

GC-MS:

Peak	**t_R (min)**	**Peak area (%)**	**Compound**
1	11.463	0.75	Methyl (*Z*)-10-phenyldec-9-enoate
2	11.848	99.25	Methyl (*E*)-10-phenyldec-9-enoate

Tab. 5.6.1: GC-MS analysis of the synthesized methyl (*E*)-10-phenyldec-9-enoate (**25**).

5.6.2 Synthesis of methyl (*E*)-tetradec-9-enoate (26)

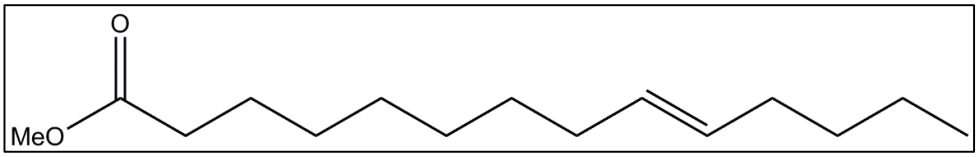

Experimental procedure:

All steps were performed under an argon atmosphere. 16.4 mg (63.0 µmol) of methyl (*E*)-10-phenyldec-9-enoate (**25**) and 88.4 mg (630 µmol) of (*E*)-dec-5-ene were dissolved in 1.70 mL of dry CH_2Cl_2. Then, 1.97 mg (3.14 µmol, 0.45 mol%) of Hoveyda-Grubbs catalyst 2nd gen. were added and the reaction mixture was stirred at RT for 2 h. TLC monitoring (hexane/EtOAc 40:1 v/v) revealed a conversion of approx. 70 %. The solvent was removed in a nitrogen stream and the crude product was purified by NP column chromatography (Merck-silica gel 60/40-63 µm, 1.5 × 3.0 cm, step gradient, application: hexane/EtOAc 80:1 v/v, elution: hexane/EtOAc 40:1 v/v). After drying in vacuum (50 mbar), the product was obtained as colorless oil (9.72 mg, 64 %).

Analytics:

Molecular Formula: $C_{15}H_{28}O_2$
Molecular Weight: 240.39 g/mol
R_f = 0.26 (Hexane/EtOAc 40:1 v/v)

^{1}H NMR (400 MHz, $CDCl_3$, RT) δ [ppm] = 5.38 (pt, 2H, $^3J_{H9\text{-}H8}$ = 3.68 Hz, H-9, 10), 5.36 – 5.32 (t, 2H, $^3J_{H9\text{-}H8}$ = 3.30 Hz, H-9*isomer*, 10*isomer*), 3.66 (s, 3H, H-1'), 2.30 (t, 2H, $^3J_{H2\text{-}H3}$ = 7.6 Hz, H-2), 2.17 (s, EtOAc), 2.04 – 1.91 (m, 4H, H-8, 11), 1.61 (tt, 2H, $^3J_{H3\text{-}H2}$ = 7.4 Hz, $^3J_{H3\text{-}H4}$ = 7.4 Hz, H-3), 1.38 – 1.21 (m, 12H), 0.88 (t, 2H, $^3J_{H14\text{-}H13}$ = 7.1 Hz, H-14).

^{13}C NMR (75 MHz, $CDCl_3$, RT): δ [ppm] = 174.32 (R$\underline{C}O_2$R', C-1), 130.40 (CH, C-9), 130.22 (CH, C-10), 129.93 (CH, C-9*isomer*), 129.75 (CH, C-10*isomer*), 51.41 (CH_3, C-1'),

34.10 (CH_2, C-2), 32.53-26.90 (7 CH_2), 24.93 (CH_2, C-3), 22.33 (CH_2, C-13*isomer*), 22.17 (CH_2, C-13), 13.94 (CH_3, C-14).

DEPT 135 (75 MHz, $CDCl_3$, RT): δ [ppm] = 130.40 (CH, C-9), 130.22 (CH, C-10), 129.93 (CH, C-9*isomer*), 129.75 (CH, C-10*isomer*), 51.41 (CH_3, C-1'), 34.10 (CH_2, C-2), 32.53-26.90 (7 CH_2), 24.93 (CH_2, C-3), 22.33 (CH_2, C-13*isomer*), 22.17 (CH_2, C-13), 13.94 (CH_3, C-14).

MS (EI, 70 eV): m/z (%) = 240.20 (5,9) [$M^{+\cdot}$], 208.20 (20) [$M^{+\cdot}$– MeOH], 166.20 (27) [Dodecene$^{+\cdot}$], 137.15 (15) [$M^{+\cdot}$ – MeOH – Pentane$^{\cdot}$], 124.15 (31) [Nonene$^{+\cdot}$], 110.11 (31) [Octene$^{+\cdot}$], 98.10 (44) [$C_6H_{10}O^{+\cdot}$], 96.10 (50) [Heptene$^{+\cdot}$], 86.10 (48) [Methyl propanoate$^{+\cdot}$] 84.10 (46) [$C_5H_8O^{+\cdot}$], 74.10 (63) [Methyl acetate$^{+\cdot}$], 69.10 (59) [$C_5H_9^+$], 55.05 (100) [$C_4H_7^+$].

GC-MS:

Peak	t_R (min)	Peak area (%)	Compound
1	9.270	2.91	Methyl (*E*)-tridec-8-enoate
2	9.839	91.54	Methyl (*E*)-tetradec-9-enoate
3	10.378	5.55	Methyl (*E*)-pentadec-10-enoate

Tab. 5.6.2: GC-MS analysis of the synthesized methyl (*E*)-tetradec-9-enoate (**26**)

5.6.3 Synthesis of (*E*)-hexacos-13-ene (27)

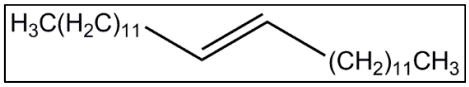

Experimental procedure:

All steps were performed under an argon atmosphere. 380 mg (1.94 mmol) of 1-tetradecene and 44.1 mg (0.408 mmol, 21 mol%) *p*-benzoquinone were dissolved in 5.50 mL of dry CH_2Cl_2. Then, 12.0 mg (19.2 µmol, 0.99 mol%) of Hoveyda-Grubbs catalyst 2nd gen. were added and the reaction mixture was stirred at RT for 3 h. RP-TLC monitoring ($CHCl_3$/MeOH 2:5 v/v) revealed a conversion of approx. 60 %. The solvent was removed in a nitrogen stream and the catalyst was removed by NP

column chromatography (Merck-silica gel 60/40-63 µm, 1.5 × 3.0 cm, step gradient). The crude product was applied to the column in hexane/EtOAc 80:1 v/v. The column was washed by four column volumes of the same solvent. Fractions containing the product were pooled, the solvent was removed in a nitrogen stream and subsequently dried in vacuum. Then, it was recrystallized from 4 °C cold ethanol. The product was obtained as a colorless solid (0.106 g, 30 %).

The experiment was repeated one time using dry toluene instead of dry CH_2Cl_2 and tetrafluoro-1,4-benzoquinone instead of *p*-benzoquinone. Ethylene was removed during the reaction by an argon stream which was introduced via two needles through the vial septum. The yield was 32 %.

Analytics (Experiment 1):

Molecular Formula: $C_{26}H_{52}$
Molecular Weight: 364.70 g/mol
R_f = 0.18 (RP TLC, $CHCl_3$/MeOH 2:5 v/v)

^{1}H NMR (400 MHz, $CDCl_3$, RT): δ [ppm] = 5.38 (tt, 2H, $^3J_{H13\text{-}H12}$ = 3.6 Hz, $^4J_{H13\text{-}H11}$ = 1.4 Hz, H-13, 14), 1.97 (m, 4H, H12, 15), 1.26 (m, 40H), 0.88 (t, 6H, $^3J_{H1\text{-}H2}$ = 6.8 Hz, H-1, 26).

^{13}C NMR (100 MHz, $CDCl_3$, RT): δ [ppm] = 130.36 (sp^2-CH, C-13, 14), 32.62 (CH_2, C-3, 24), 31.94 (CH_2, C-12, 15), 29.71-29.18 (16 CH_2), 22.70 (CH_2, C-2, 25), 14.12 (CH_3, C-1, 26).

DEPT 135 (100 MHz, $CDCl_3$, RT): δ [ppm] = 130.36 (sp^2-CH, C-13, 14), 32.62 (CH_2, C-3, 24), 31.94 (CH_2, C-12, 15), 29.71-29.18 (16 CH_2), 22.70 (CH_2, C-2, 25), 14.12 (CH_3, C-1, 26).

MS (EI, 70 eV): m/z (%) = 364.45 (13) [$M^{+\cdot}$], 153.20 (11) [$C_{11}H_{21}^+$], 139.20 (22) [$C_{10}H_{19}^+$], 125.20 (39) [$C_9H_{17}^+$], 111.20 (65) [$C_8H_{15}^+$], 97.15 (100) [$C_7H_{13}^+$], 83.10 (79) [$C_6H_{11}^+$], 69.07 (56) [$C_5H_9^+$], 57.10 (65) [$C_4H_9^+$], 55.05 (47) [$C_4H_7^+$].

GC-MS:

Peak	t_R (min)	Peak area (%)	Compound
1	13.030	0.45	(*E*)-Tetracos-13-ene
2	13.538	0.49	(*E*)-Pentacos-13-ene
3	14.126	98.21	(*E*)-Hexacos-13-ene
4	15.609	0.84	(*E*)-Octacos-13-ene

Tab. 5.6.3: GC-MS analysis of the synthesized (*E*)-hexacos-13-ene (**27**)

CHN-Analysis:

Theoretical (wt %): C: 85.63 H: 14.37

Measured (wt %): C: 85.44 H: 14.19

Analytics (Experiment 2):

MS (EI, 70 eV): m/z (%) = 364.45 (13) [$M^{+\cdot}$], 153.20 (11) [$C_{11}H_{21}^+$], 139.20 (20) [$C_{10}H_{19}^+$], 125.20 (39) [$C_9H_{17}^+$], 111.15 (63) [$C_8H_{15}^+$], 97.10 (100) [$C_7H_{13}^+$], 83.10 (80) [$C_6H_{11}^+$], 69.00 (55) [$C_5H_9^+$], 57.10 (74) [$C_4H_9^+$], 55.05 (52) [$C_4H_7^+$].

GC-MS:

Peak	t_R (min)	Peak area (%)	Compound
1	14.143	100	(*E*)-Hexacos-13-ene

Tab. 5.6.4: GC-MS analysis of the synthesized (*E*)-hexacos-13-ene (**27**)

CHN-Analysis:

Theoretical (wt %): C: 85.63 H: 14.37

Measured (wt %): C: 85.21 H: 14.11

5.6.4 Synthesis of pentadeca-*O*-acetyl-GM1 (d20:1/18:0) sialoyl-II^2-lactone (28)

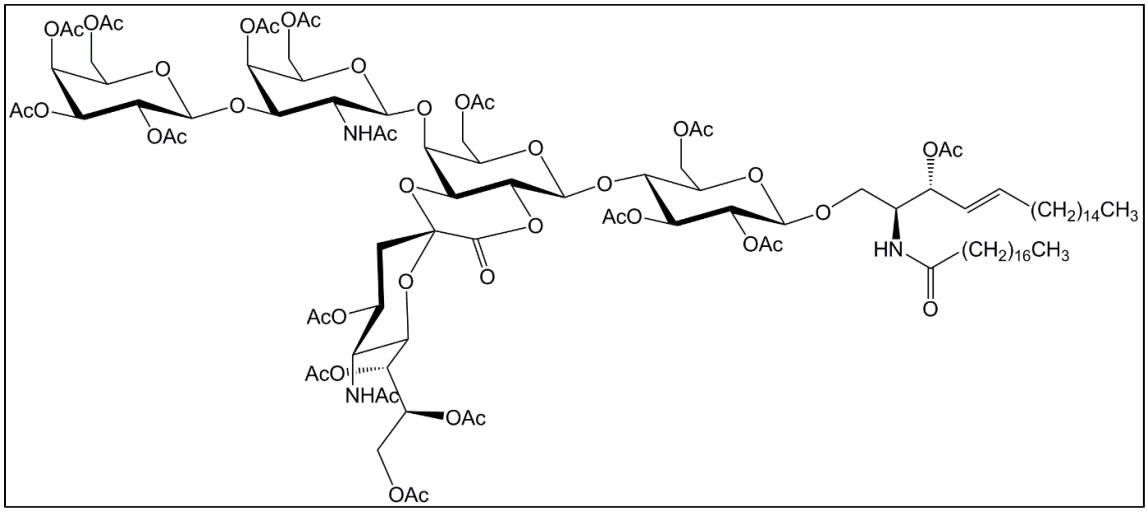

Experimental procedure:

All steps were performed under an argon atmosphere. 30.9 mg (19.4 µmol) of d20:1/18:0-GM1·NH_3 (**2**) and 0.5 mg (4.09 µmol) of DMAP were suspended in 832 µL of anhydrous pyridine and 413 µL of Ac_2O. The reaction mixture was stirred at RT for 15 h (after a few hours the reactants dissolved completely). The solvent was removed in a nitrogen stream and the crude product was purified by NP column chromatography (Merck-silica gel 60/15-40 µm, 2.0 × 21 cm, isocratic, eluent: toluene/acetone 5:4 v/v). After drying in vacuum, the product was obtained as colorless solid (26.3 mg, 62 %).

Analytics:

Molecular Formula: $C_{105}H_{163}N_3O_{45}$

Molecular Weight: 2187.43 g/mol

R_f = 0.23 (toluene/acetone 5:4 v/v)

^{1}H NMR (400 MHz, $CDCl_3$, RT): δ [ppm] = 6.44 (d, 3H, $^3J_{NH\text{-}H2}$ = 7.9 Hz, N<u>H</u>), 5.76 (dt, 1H, $^3J_{H5\text{-}H4,\ trans}$ = 15.1 Hz, $^3J_{H5\text{-}H6}$ = 6.8 Hz, Cer, H-5), 5.63 (d, 1H, $^3J_{H1\text{-}H3}$ = 9.1 Hz, GalNAc, H-1), 5.49 (dt, 1H, $^3J_{H4\text{-}H5}$ = 10.8 Hz, $^3J_{H4\text{-}H3}$ = 5.5 Hz, NeuAc, H-4), 5.44

– 5.20 (m, 8H), 5.08 – 5.05 (m, 1H, NeuAc, H-9a), 5.04 (d, 1H, $^{3}J_{H1\text{-}H2}$ = 7.7 Hz, Gal, H-1), 4.94 (dd, 1H, $^{3}J_{H5\text{-}H4}$ = 10.5 Hz, $^{4}J_{H5\text{-}H6}$ = 3.4 Hz, NeuAc, H-5), 4.88 (dd, 1H, $^{3}J_{H3\text{-}H2}$ = 9.6 Hz, $^{3}J_{H3\text{-}H4}$ = 7.8 Hz, GalNAc, H-3), 4.76 (d, 1H, $^{3}J_{H1\text{-}H2}$ = 7.8 Hz, Glc, H-1), 4.62 – 3.50 (m, 28H), 2.48 (dd, $^{2}J_{H3e\text{-}H3a}$ = 13.5 Hz, $^{3}J_{H3e\text{-}H4}$ = 5.5 Hz, NeuAc, H-3e), 2.26 – 1.77 (13s, 51 H, C<u>H</u>$_3$CO$_2$R), 2.26-1.77 (m, 2H, Cer, H-2'), 1.57 (m, 2H, Cer, H-3'), 1.24 (m, 54H), 0.90 – 0.84 (t, 6H, $^{3}J_{H18'\text{-}H17'}$ = 6.9 Hz, $^{3}J_{H20\text{-}H19}$ = 6.9 Hz, Cer, H-18, 18').

MS (ESI, pos. Mode, MeOH, M = 2187.06): m/z (%) = 2237.11 (3.4) [M + MeOH + NH_4]$^+$, 2220.10 (0.26) [M + MeOH + H]$^+$, 2205.09 (1.7) [M + NH_4]$^+$, 2188.07 (0.11) [M + H]$^+$, 1127.56 (100) [M + MeOH + 2NH_4]$^{2+}$, 1119.05 (62) [M + MeOH + NH_4 + H]$^{2+}$, 1110.54 (10) [M + MeOH + 2H]$^{2+}$, 1111.55 (85) [M + 2NH_4]$^{2+}$, 1103.04 (61) [M + NH_4 + H]$^{2+}$, 1094.53 (4.7) [M + 2H]$^{2+}$.

MS/MS (m/z = 1102.54): m/z (%) = 1797.95 (22) [$Y_{3\alpha}$ + 2H – H_3CCO_2H]$^+$, 1509.85 (3.5) [$Y_{2\alpha}$ + 2H – H_3CCO_2H]$^+$, 1064.52 (15) [M + 2H – H_3CCO_2H]$^{2+}$, 772.24 (5.5) [$Y_{2\alpha}$/Z_0 + 3H – 3H_3CCO_2H]$^+$, 618.21 (12) [$B_{2\alpha}$]$^+$, 586.18 (6.9) [$Y_{2\alpha}$/Y_1 + H – H_3CCO_2H]$^+$, 558.57 (3.7) [Z_0 – H_3CCO_2H]$^+$, 331.11 (100) [$B_{1\alpha}$]$^+$, 292.30 (16) [Y_0 + 2H – stearic acid – H_3CCO_2H]$^+$, 288.11 (16) [$B_{2\alpha}$/$B_{1\alpha}$ + H]$^+$, 211.06 (14) [$B_{1\alpha}$ – 2H_3CCO_2H]$^+$, 169.04 (85) [$C_{1\alpha}$ + 2H – 3H_3CCO_2H]$^+$, 150.05 (11) [$B_{2\alpha}$/$B_{1\alpha}$ + H – 2H_3CCO_2H – H_2O]$^+$, 127.03 (11) [$C_{1\alpha}$ + 2H + H_2O – 4 H_3CCO_2H]$^+$, 109.02 (19) [$C_{1\alpha}$ + 2H – 4H_3CCO_2H]$^+$.

5.6.5 Synthesis of *O*-(tetradeca-*O*-acetylmonosialogangliotetraosyl)-(1→1)-(2*R*,3*S*,4*E*)-3-*O*-acetyl-2-octadecanoylamino-5-phenyl-pent-4-ene-1-ol sialoyl-II^2-lactone (29)

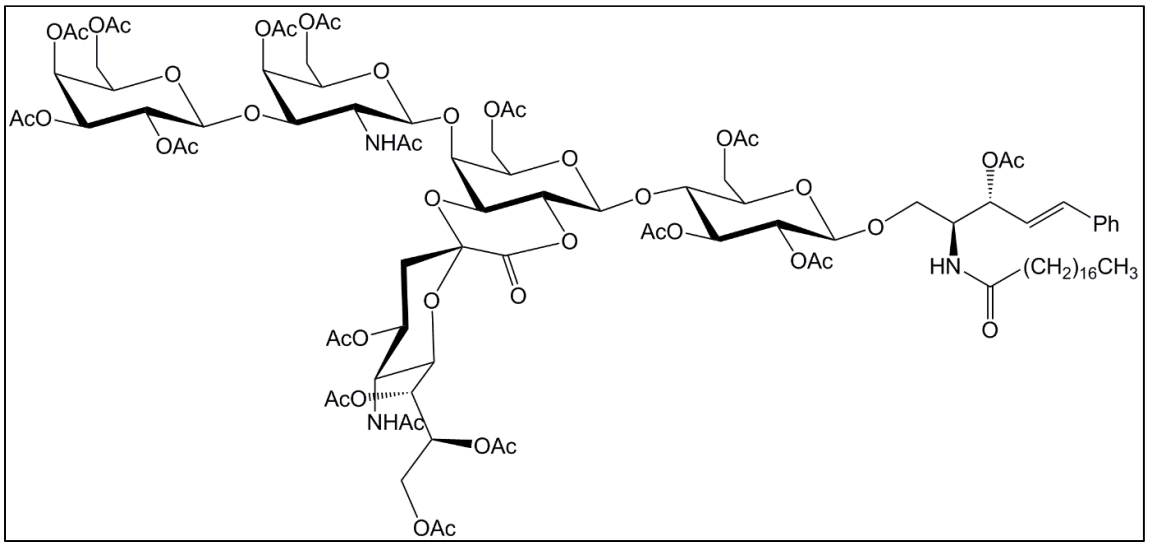

Experimental procedure:

All steps were performed under an argon atmosphere. 39.7 mg (18.3 µmol) of a 1:1 mixture of pentadeca-*O*-acetyl-GM1 (d20:1/18:0) sialoyl-II^2-lactone (**28**) and pentadeca-*O*-acetyl-GM1 (d20:1/18:0) sialoyl-II^2-lactone ($\overline{M}$ = 2173.41 gmol^{-1}) were dissolved in 477 µL of dry CH_2Cl_2 in a 1 mL glass vial. 33.0 mg (183 µmol) of (*E*)-stilbene and 23.9 mg (28.2 µmol, 14 mol%) of Grubbs catalyst 2nd gen. were added and the reaction mixture was stirred at 43 °C for 46 h. TLC monitoring (toluene/acetone 1:1 v/v) revealed a conversion larger than 90 %. The solvent was removed in a nitrogen stream, the crude product was dried in vacuum and subsequently purified by NP column chromatography (Merck-silica gel 60/15-40 µm, 2.0 × 22.2 cm, isocratic, toluene/acetone 10:9 v/v). To remove traces of catalyst it was purified by NP column chromatography again (Merck-silica gel 60/40-63 µm, 1.5 × 2.5 cm, step gradient, application: toluene/acetone 2:1 v/v, elution: toluene/acetone 4:5 v/v). After drying in vacuum, the product was obtained as colorless solid (25.7 mg, 68 %).

Analytics:

Molecular Formula: $C_{96}H_{137}N_3O_{45}$

Molecular Weight: 2053.13 g/mol

R_f = 0.15 (Toluene/Acetone 5:4 v/v)

^{1}H NMR (400 MHz, $CDCl_3$, RT): δ [ppm] = 7.36 (dd, 2H, $^3J_{H2''-H3''}$ = 7.1 Hz, $^4J_{H2''-H3''}$ = 1.6 Hz, H-2'', 6''), 7.30 (pt, 2H, $^3J_{H3''-H2'''}$ = 7.3 Hz, H-3'', 5''), 7.21 – 7.12 (m, 1H, H-4''), 6.65 (d, 1H, $^3J_{H5-H4,\ trans}$ = 15.9 Hz, Cer, H-5), 6.52 (s, 3H, N<u>H</u>), 6.09 (dd, 1H, $^3J_{H4'-H5',\ trans}$ = 15.9 Hz, $^3J_{H4-H3}$ = 7.7 Hz, Cer, H-4), 5.74 (d, 1H, $^3J_{H1-H2}$ = 9.2 Hz, GalNAc, H-1), 5.35 (m, 8H), 5.07 (dd, $^3J_{H9a-H8}$ = 8.0 Hz, $^4J_{H9a-H7}$ = 4.3 Hz, NeuAc, H-9a), 5.04 (d, 1H, $^3J_{H1-H2}$ = 7.7 Hz, Gal, H-1), 4.94 (dd, 1H, $^3J_{H5-H4}$ = 10.5 Hz, $^3J_{H5-H6}$ = 3.3 Hz, NeuAc, H-5), 4.90 (dd, 1H, $^3J_{H3-H2}$ = 9.59 Hz, $^3J_{H3-H4}$ = 7.95 Hz, GalNAc, H-3), 4.76 (d, 1H, $^3J_{H1-H2}$ = 7.8 Hz, Glc, H-1), 4.63 – 3.45 (m, 28H), 2.49 (dd, $^2J_{H3e-H3a}$ = 13.5 Hz, $^3J_{H3e-H4}$ = 5.4 Hz, NeuAc, H-3e), 2.25 – 1.76 (13s, 51H, C<u>H</u>$_3$CO$_2$R), 1.50 (m, 2H, Cer, H-3'), 1.31 – 1.03 (m, 28H), 0.86 (t, 3H, $^3J_{H18'-H17'}$ = 6.9 Hz, Cer, H-18').

MS (ESI, pos. Mode, MeOH, M = 2052,86): m/z (%) = 2107.93 (0.58) $[M + MeOH + Na]^+$, 2102.94 (15) $[M + MeOH + NH_4]^+$, 2086.94 (2.3) $[2M + MeOH + 2NH_4]^+$, 2085.94 (1.2) $[M + MeOH + H]^+$, 2070.92 (8.3) $[M + NH_4]^+$, 2053.90 (0.92) $[M + H]^+$, 1065.46 (3.9) $[M + MeOH + 2Na]^{2+}$, 1062.46 (6.9) $[M + MeOH + K + H]^{2+}$, 1060.46 (100) $[M + MeOH + 2NH_4]^{2+}$, 1051.95 (99) $[M + MeOH + NH_4 + H]^{2+}$, 1043.44 (20) $[M + MeOH + 2H]^{2+}$, 1044.45 (93) $[M + 2NH_4]^{2+}$, 1035.94 (56) $[M + NH_4 + H]^{2+}$, 1027.43 (5.0) $[M + 2H]^{2+}$, 1021.94 (19) $[M + MeOH + NH_4 + H - H_3CCO_2H]^{2+}$, 1013.43 (14) $[M + MeOH + 2H - H_3CCO_2H]^{2+}$, 1005.93 (34) $[M + NH_4 + H - H_3CCO_2H]^{2+}$, 997.42 (4.0) $[M + 2H - H_3CCO_2H]^{2+}$.

MS/MS (m/z = 1035.44): m/z (%) = 1662.69 (20) $[Y_{3\alpha} + 2H - H_3CCO_2H]^+$, 1101.31 (3.3) $[B_4/B_{1\alpha} + H - 2H_3CCO_2H]^+$, 997.38 (17) $[M + 2H - H_3CCO_2H]^{2+}$, 772.21 (5.6) $[Y_{2\alpha}/Z_0 + 3H - 3H_3CCO_2H]^+$, 618.19 (9.5) $[B_{2\alpha}]^+$, 586.17 (6.8) $[Y_{2\alpha}/Y_1 + H - H_3CCO_2H]^+$, 424.35 (5.5) $[Z_0 - H_3CCO_2H]^+$, 331,10 (100) $[B_{1\alpha}]^+$, 288.1 (20) $[B_{2\alpha}/B_{1\alpha} + H]^+$, 211.06 (14) $[B_{1\alpha} - 2H_3CCO_2H]^+$, 169.04 (89) $[C_{1\alpha} + 2H - 3H_3CCO_2H]^+$, 150.06 (13) $[B_{2\alpha}/B_{1\alpha} + H - 2H_3CCO_2H - H_2O]^+$, 127.05 (11) $[C_{1\alpha} + 2H + H_2O - 4H_3CCO_2H]^+$, 109.04 (21) $[C_{1\alpha} + 2H - 4H_3CCO_2H]^+$.

5.6.6 Synthesis of pentadeca-*O*-acetyl-GM1 (d17:1/18:0) sialoyl-II^2-lactone (30)

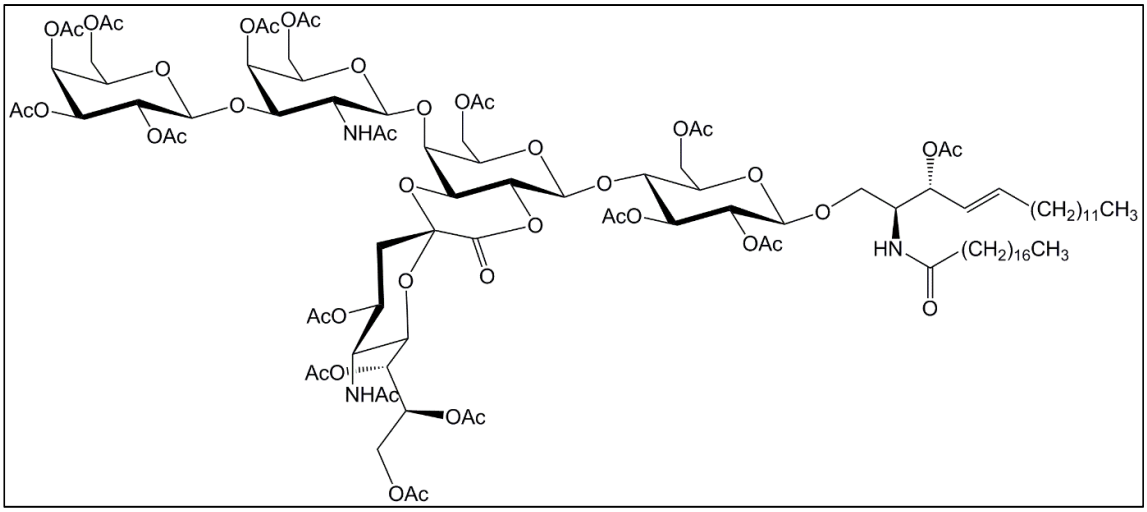

Experimental procedure:

All steps were performed under an argon atmosphere. 15.5 mg (7.55 µmol) of **29**, 55.0 mg (151 µmol) of (*E*)-hexacos-13-ene (**27**), and 3.43 mg (31.7 µmol, 20 mol%) of *p*-benzoquinone were dissolved in 271 µL of dry CH_2Cl_2 in a 1 mL glass vial. Then, 19.8 mg (31.6 µmol, 20 mol%) of Hoveyda-Grubbs catalyst 2nd gen. were added and the reaction mixture was stirred at 40 °C. After 1d TLC monitoring (toluene/acetone 1:1 v/v) revealed a conversion of approximately 70 %. Further 19.8 mg of catalyst and 3.43 mg of *p*-benzoquinone were added and the reaction was stirred at 40 °C for another day. After a total of 41 h, the solvent was removed in a nitrogen stream, the crude product was dried in vacuum and subsequently purified by NP column chromatography (Merck-silica gel 60/15-40 µm, 2.0 × 23.0 cm, isocratic, eluent: toluene/acetone 10:9 v/v). In order to remove column material it was purified by NP column chromatography again (Merck-silica gel 60/40-63 µm, 0.9 × 2.5 cm, step gradient, application: toluene/acetone 3:1 v/v, elution: toluene/acetone 1:1 v/v). After drying in vacuum, the product was obtained as colorless solid (9.91 mg, 61 %).

Analytics:

Molecular Formula: $C_{102}H_{157}N_3O_{45}$
Molecular Weight: 2145.35 g/mol
R_f = 0.20 (Toluene/Acetone 5:4 v/v)

^{1}H NMR (400 MHz, $CDCl_3$, RT): δ [ppm] = 6.47 (s, 3H, N<u>H</u>), 5.83 – 5.71 (dt, 1H, $^3J_{H5\text{-}H4,\ trans}$ = 15.2 Hz, $^3J_{H5\text{-}H6}$ = 6.7 Hz, Cer, H-5), 5.64 (d, 1H, $^3J_{H1\text{-}H2}$ = 9.2 Hz, GalNAc, H-1), 5.49 (dt, 1H, $^3J_{H4\text{-}H5}$ = 10.8 Hz, $^3J_{H4\text{-}H3}$ = 5.5 Hz, NeuAc, H-4), 5.44 – 5.17 (m, 8H), 5.07 (dd, $^3J_{H9a\text{-}H8}$ = 8.0 Hz, $^4J_{H9a\text{-}H7}$ = 1.9 Hz, NeuAc, H-9a), 5.04 (d, 1H, $^3J_{H1\text{-}H2}$ = 7.7 Hz, Gal, H-1), 4.94 (dd, 1H, $^3J_{H5\text{-}H4}$ = 10.4 Hz, $^4J_{H5\text{-}H6}$ = 3.5 Hz, NeuAc, H-5), 4.89 (dd, 1H, $^3J_{H3\text{-}H2}$ = 9.6 Hz, $^3J_{H3\text{-}H4}$ = 7.8 Hz, GalNAc, H-3), 4.76 (d, 1H, $^3J_{H1\text{-}H2}$ = 7.8 Hz, Glc, H-1), 4.64 – 3.49 (m, 28H), 2.48 (dd, $^2J_{H3e\text{-}H3a}$ = 13.5 Hz, $^3J_{H3e\text{-}H4}$ = 5.5 Hz, NeuAc, H3e), 2.21 – 1.85 (13s, 51H, C<u>H</u>$_3$CO$_2$R), 1.58 (m 2H, Cer, H-3'), 1.25 (m, 48H), 0.92 – 0.83 (t, 6H, $^3J_{H17\text{-}H16}$ = 6.9 Hz, $^3J_{H18'\text{-}H17'}$ = 6.9 Hz, Cer, H-17', 18).

MS (ESI, pos. Mode, MeOH, M = 2145.01): m/z (%) = 2200.07 (0.20) $[M + MeOH + Na]^+$, 2195.10 (1.6) $[M + MeOH + NH_4]^+$, 2179.07 (0.38) $[2M + MeOH + 2NH_4]^+$, 2178.10 (0.24) $[M + MeOH + H]^+$, 2163.07 (3.1) $[M + NH_4]^+$, 2146.05 (0.40) $[M + H]^+$, 1106.56 (35) $[M + MeOH + 2NH_4]^{2+}$, 1098.04 (41) $[M + MeOH + NH_4 + H]^{2+}$, 1092.53 (7.0) $[M + K + H]^{2+}$, 1089.53 (12) $[M + MeOH + 2H]^{2+}$, 1090.54 (76) $[M + 2NH_4]^{2+}$, 1082.02 (100) $[M + NH_4 + H]^{2+}$, 1073.52 (14) $[M + 2H]^{2+}$, 1052.02 (7.4) $[M + NH_4 + H - H_3CCO_2H]^{2+}$.

MS/MS (m/z = 1081.52): m/z (%) = 1754.90 (18) $[Y_{3\alpha} + 2H - H_3CCO_2H]^+$, 1467.83 (3.2) $[Y_{2\alpha} + 2H - H_3CCO_2H]^+$, 1082.02 (66) $[M + NH_4 + H]^{2+}$, 1073.52 (11) $[M + 2H]^{2+}$, 1043.51 (15) $[M + 2H - H_3CCO_2H]^{2+}$, 618.22 (10) $[B_{2\alpha}]^+$, 331.11 (100) $[B_{1\alpha}]^+$, 288.11 (6) $[B_{2\alpha}/B_{1\alpha} + H]^+$, 211.06 (11) $[B_{1\alpha} - 2H_3CCO_2H]^+$, 169.04 (48) $[C_{1\alpha} + 2H - 3H_3CCO_2H]^+$, 109.00 (6.9) $[C_{1\alpha} + 2H - 4H_3CCO_2H]^+$.

5.6.7 Preparation of d17:1-lyso-GM1·NH_3 (31)

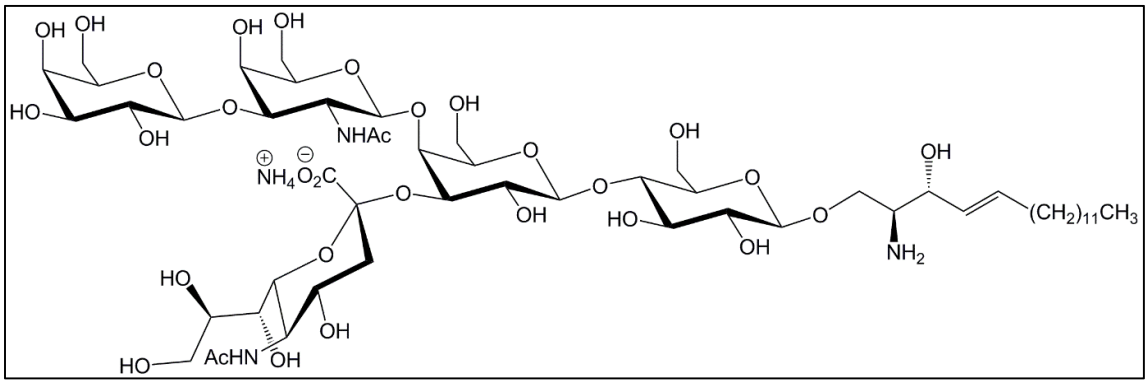

Experimental procedure:

Pentadeca-*O*-acetyl-GM1 (d17:1/18:0) sialoyl-II^2-lactone (**30**) was deacetylated and deacylated by the method described in section 5.3.1. 9.40 mg (4.38 µmol) of **30** were applied. The reaction time was 19 h. The crude product was purified by RP column chromatography (Merck LiChroprep RP-18/40-63 µm, 0.9 × 2.8 cm, eluent: MeOH/H_2O 90:40 v/v). A second purification step was done by NP column chromatography (Merck-silica gel 60/25-40 µm, 2.0 × 19.0 cm, isocratic, eluent: $CHCl_3$/MeOH/2.5 M NH_3 60:40:10 v/v/v). MS analysis revealed that the product contained 4.8 % of the d16:1-lyso-GM1 isomer, so the product was purified by isocratic RP column chromatography again (Merck LiChroprep RP-18/40-63 µm, 1.0 × 22.5 cm, eluent: MeOH/H_2O 90:31 v/v). Then, column material was removed by NP column chromatography (Merck-silica gel 60/40-63 µm, 0.9 × 2.0 cm, step gradient, application: $CHCl_3$/MeOH/2.5 M NH_3 60:35:6 v/v/v, elution: $CHCl_3$/MeOH/2.5 M NH_3 60:44:12 v/v/v) again. After lyophilization, d17:1-lyso-GM1·NH_3 was obtained as a colorless powder (1.93 mg, 34 %).

Analytics:

Molecular Formula: $C_{54}H_{98}N_4O_{30}$

Molecular Weight: 1283.38 g/mol

R_f = 0.12 ($CHCl_3$/MeOH/2.5 M NH_3 60:40:10 v/v/v)

MS (ESI, pos. Mode, MeOH): m/z (%) = 1288.60 (1.3) $[M + Na]^+$, 1266.62 (43) $[M + H]^+$, 1252.61 (1.8) $[M + H - CH_2]^+$, 981.35 (14) $[B_4]^+$, 975.52 (13) $[Y_{2\beta} + 2H]^+$, 901.48 (33) $[Y_{2\alpha} + 2H]^+$, 663.78 (1.2) $[M + K + Na]^{2+}$, 655.79 (4.6) $[M + 2Na]^{2+}$, 652.78 (5.0) $[M + K + H]^{2+}$, 644.80 (23) $[M + Na + H]^{2+}$, 642.32 (24) $[M + NH_4 + H]^{2+}$, 633.81 (100) $[M + 2H]^{2+}$, 626.80 (5.0) $[M + 2H - CH_2]^{2+}$.

MS/MS (m/z = 1266.62): m/z (%) = 1266.61 (26) $[M + H]^+$, 975.52 (56) $[Y_{2\beta} + 2H]^+$, 957.51 (5.8) $[Z_{2\beta}]^+$, 901.48 (8.7) $[Y_{2\alpha} + 2H]^+$, 610.39 (18) $[Y_{2\alpha}/B_{1\beta} + 3H]^+$, 592.38 (8.2) $[Y_{2\alpha}/C_{1\beta} + H]^+$, 448.34 (11) $[Y_1 + 2H]^+$, 430.33 (9.8) $[Z_1]^+$, 366.15 (100) $[B_{2\alpha}]^+$, 292.11 (7.2) $[B_{1\beta}]^+$, 286.28 (7.0) $[Y_0 + 2H]^+$, 274.11 (6.8) $[B_{1\beta} - H_2O]^+$, 268.28 (22) $[Z_0]^+$, 250.27 (8.2) $[Z_0 - H_2O]^+$, 204.11 (69) $[B_{2\alpha}/B_{1\alpha} + H]^+$, 186.10 (17) $[B_{2\alpha}/B_{1\alpha} + H - H_2O]^+$.

After RP-chromatography:

MS (ESI, pos. Mode, MeOH): m/z (%) = 1304.58 (3.0) $[M + K]^+$, 1288.59 (11) $[M + Na]^+$, 1283.6 (7.1) $[M + NH_4]^+$, 1266.60 (100) $[M + H]^+$, 1104.55 (37) $[Y_{3\alpha} + 2H]^+$, 981.34 (11) $[B_4]^+$, 975.51 (23) $[Y_{2\beta} + 2H]^+$, 901.47 (92) $[Y_{2\alpha} + 2H]^+$, 813,46 (25) $[Y_{3\alpha}/B_{1\beta} + 3H]^+$, 671.77 (4.4) $[M + 2K]^{2+}$, 663.77 (13) $[M + K + Na]^{2+}$, 661,28 (7.3) $[M + K + NH_4]^{2+}$, 655.78 (22) $[M + 2Na]^{2+}$, 652.78 (38) $[M + K + H]^{2+}$, 644.79 (91) $[M + Na + H]^{2+}$, 642.31 (41) $[M + NH_4 + H]^{2+}$, 633.88 (84) $[M + 2H]^{2+}$.

Photometric sialic acid determination:

The results of the photometric sialic acid determination are given in Fig. 5.5.1. The content of d17:1-lyso-GM1·NH_3 (**31**) was 74.2 % compared to d18:1-lyso-GM1·NH_3 (**7**) as reference standard.

5.6.8 Preparation of d17:1-lyso-GM2·NH_3 (32)

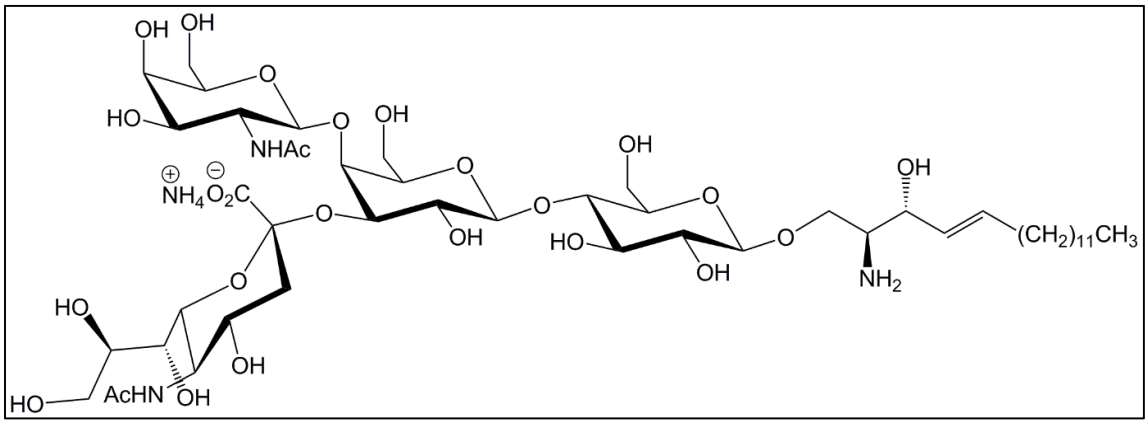

Experimental procedure:

d17:1-Lyso-GM2·NH_3 was prepared by the method described in section 5.5.2. 1.09 mg (0.849 µmol) of d17:1-lyso-GM1·NH_3 and 352 µL (314 mU) of beta-galactosidase solution were applied. The reaction time was 15.5 h. The crude product was purified by NP column chromatography (Merck-silica gel 60/15-40 µm, 2.0 × 19.2 cm, isocratic, eluent: $CHCl_3$/MeOH/2.5 M NH_3 60:40:10 v/v/v). In order to remove column material, it was purified by NP column chromatography again (Merck-silica gel 60/40-63 µm, 0.6 × 2.0 cm, step gradient, application: $CHCl_3$/MeOH/2.5 M NH_3 60:35:2 v/v/v, elution: $CHCl_3$/MeOH/2.5 M NH_3 60:40:10 v/v/v). After lyophilization, d17:1-lyso-GM2·NH_3 was obtained as a colorless powder (0.66 mg, 69 %).

Analytics:

Molecular Formula: $C_{48}H_{88}N_4O_{25}$

Molecular Weight: 1121.24 g/mol

R_f = 0.14 ($CHCl_3$/MeOH/2.5 M NH_3 60:40:9 v/v/v)

MS (ESI, pos. Mode, MeOH): m/z (%) = 1126.53 (18) $[M + Na]^+$, 1124,03 (4.7) $[2M + Na + NH_4]^{2+}$, 1115,54 (14) $[2M + Na + H]^{2+}$, 1104.54 (100) $[M + H]^+$, 901.47 (4.1) $[Y_{2\beta} + 2H]^+$, 813.46 (12) $[Y_{2\alpha} + 2H]^+$, 582.74 (7.9) $[M + K + Na]^{2+}$, 574.76 (17) $[M + 2Na]^{2+}$,

571.75 (15) $[M + K + H]^{2+}$, 563.76 (50) $[M + Na + H]^{2+}$, 561.28 (42) $[M + NH_4 + H]^{2+}$, 552.77 (59) $[M + 2H]^{2+}$.

MS/MS (m/z = 1104.54): m/z (%) = 1104.55 (11) $[M + H]^+$, 901.48 (1.9) $[Y_{2\beta} + 2H]^+$, 813.46 (38) $[Y_{2\alpha} + 2H]^+$, 795.45 (7.7) $[Z_{2\alpha}]^+$, 610.38 (5.2) $[Y_{2\beta}/B_{1\alpha} + 3H]^+$, 592.37 (4.0) $[Y_{2\alpha}/C_{1\beta} + H]^+$, 448.33 (8.5) $[Y_1 + 2H]^+$, 430.32 (10) $[Z_1]^+$, 412.31 (3.9) $[Z_1 - H_2O]^+$, 366.14 (19) $[B_2/B_{1\alpha} + H]^+$, 292.11 (11) $[B_{1\alpha}]^+$, 286.26 (7.6) $[Y_0 + 2H]^+$, 274.09 (11) $[B_{1\alpha} - H_2O]^+$, 268.27 (25) $[Z_0]^+$, 250.25 (7.4) $[Z_0 - H_2O]^+$, 222.09 (5.3) $[C_{1\beta} + 2H]^+$, 204.08 (100) $[B_{1\beta}]^+$, 186.07 (16) $[B_{1\beta} - H_2O]^+$.

Photometric sialic acid determination:

The results of the photometric sialic acid determination are given in Fig. 5.5.1. The content of d17:1-lyso-GM2·NH_3 (**32**) was 90.2 % compared to d18:1-lyso-GM1·NH_3 (**7**) as reference standard.

5.6.9 Validation of 31 and 32 as calibrators

Six different concentrations of d18:1-lyso-GM1·NH_3 and of d18:1-lyso-GM2·NH_3 (0 µM, 5 µM, 10 µM, 15 µM, 20 µM, 25 µM, and 35 µM) in methanol were prepared. The d18:1-lyso-GM1·NH_3 solutions were spiked each by d17:1-lyso-GM1·NH_3 (**31**) to a final concentration of 13.4 µM of the internal standard, and the d18:1-lyso-GM2·NH_3 solutions were spiked by d17:1-lyso-GM2·NH_3 (**32**) to a final concentration of 14.0 µM of the internal standard. The solutions were measured in the full scan mode and the ratio of the peak height of the most intensive peak ($[M + K + H]^{2+}$) was plotted against the concentration of the analyte (Fig. 3.5.5). All measurement were performed in duplicate.

6 References

1. Kracun, I., H. Rosner, C. Cosovic, and A. Stavljenic. 1984. Topographical atlas of the gangliosides of the adult human brain. *J. Neurochem.* **43**: 979-989.
2. Muthing, J. 1996. High-resolution thin-layer chromatography of gangliosides. *J. Chromatogr. A* **720**: 3-25.
3. Matreya LLC. January 20, 2014. Matreya LLC Lipids and Biochemicals. *In*. http://www.matreya.com/category.aspx?categoryid=106&startpage=0.
4. Hanai, N., K. Nakamura, and K. Shitara. 2000. Recombinant antibodies against ganglioside expressed on tumor cells. *Cancer chemotherapy and pharmacology* **46 Suppl**: S13-17.
5. Ruf, P., B. Schafer, N. Eissler, R. Mocikat, J. Hess, M. Ploscher, S. Wosch, I. Suckstorff, C. Zehetmeier, and H. Lindhofer. 2012. Ganglioside GD2-specific trifunctional surrogate antibody Surek demonstrates therapeutic activity in a mouse melanoma model. *J. Transl. Med.* **10**: 219.
6. Schnaar, R. L., R. Gerardy-Schahn, and H. Hildebrandt. 2014. Sialic acids in the brain: gangliosides and polysialic acid in nervous system development, stability, disease, and regeneration. *Physiol. Rev.* **94**: 461-518.
7. Sonnino, S., and V. Chigorno. 2000. Ganglioside molecular species containing C18- and C20-sphingosine in mammalian nervous tissues and neuronal cell cultures. *Biochim. Biophys. Acta* **1469**: 63-77.
8. Sugiura, Y., S. Shimma, Y. Konishi, M. K. Yamada, and M. Setou. 2008. Imaging mass spectrometry technology and application on ganglioside study; visualization of age-dependent accumulation of C20-ganglioside molecular species in the mouse hippocampus. *PloS one* **3**: e3232.
9. Dawson, G., R. Matalon, and A. Dorfman. 1972. Glycosphingolipids in cultured human skin fibroblasts. I. Characterization and metabolism in normal fibroblasts. *J. Biol. Chem.* **247**: 5944-5950.
10. Gomez-Isla, T., J. L. Price, D. W. McKeel, Jr., J. C. Morris, J. H. Growdon, and B. T. Hyman. 1996. Profound loss of layer II entorhinal cortex neurons occurs in very mild Alzheimer's disease. *J. Neurosci.* **16**: 4491-4500.
11. Rouser, G., and A. Yamamoto. 1972. The fatty acid composition of total gangliosides in normal human whole brain at different ages. *J. Neurochem.* **19**: 2697-2698.
12. Varki, A. 2001. Loss of N-glycolylneuraminic acid in humans: Mechanisms, consequences, and implications for hominid evolution. *Am. J. Phys. Anthropol.* **Suppl 33**: 54-69.
13. Kohla, G., and R. Schauer. 2005. Sialic acids in gangliosides: origin and function. *In* Neuroglycobiology. Oxford University Press, Oxford.
14. Kolter, T. 2012. Ganglioside Biochemistry. *ISRN Biochemistry* **2012**: 36.
15. Yu, R. K., and R. W. Ledeen. 1970. Gas--liquid chromatographic assay of lipid-bound sialic acids: measurement of gangliosides in brain of several species. *J. Lipid Res.* **11**: 506-516.
16. Mikami, T., M. Kashiwagi, K. Tsuchihashi, T. Daino, T. Akino, and S. Gasa. 1998. Further characterization of equine brain gangliosides: the presence of GM3 having N-glycolyl neuraminic acid in the central nervous system. *J. Biochem.* **123**: 487-491.

17. Schauer, R., G. V. Srinivasan, B. Coddeville, J. P. Zanetta, and Y. Guerardel. 2009. Low incidence of N-glycolylneuraminic acid in birds and reptiles and its absence in the platypus. *Carbohydr. Res.* **344**: 1494-1500.
18. Svennerholm, L. 1963. CHROMATOGRAPHIC SEPARATION OF HUMAN BRAIN GANGLIOSIDES*. *J. Neurochem.* **10**: 613-623.
19. Yu, R. K., Y. T. Tsai, T. Ariga, and M. Yanagisawa. 2011. Structures, biosynthesis, and functions of gangliosides--an overview. *J. Oleo Sci.* **60**: 537-544.
20. Jcbn. 1998. Nomenclature of glycolipids. *Carbohydr. Res.* **312**: 167-175.
21. Liebisch, G., J. A. Vizcaino, H. Kofeler, M. Trotzmuller, W. J. Griffiths, G. Schmitz, F. Spener, and M. J. Wakelam. 2013. Shorthand notation for lipid structures derived from mass spectrometry. *J. Lipid Res.* **54**: 1523-1530.
22. Wang, B., and J. Brand-Miller. 2003. The role and potential of sialic acid in human nutrition. *Eur. J. Clin. Nutr.* **57**: 1351-1369.
23. Garofalo, T., A. Tinari, P. Matarrese, A. M. Giammarioli, V. Manganelli, L. Ciarlo, R. Misasi, M. Sorice, and W. Malorni. 2007. Do mitochondria act as "cargo boats" in the journey of GD3 to the nucleus during apoptosis? *FEBS Lett.* **581**: 3899-3903.
24. Ledeen, R., and G. Wu. 2011. New findings on nuclear gangliosides: overview on metabolism and function. *J. Neurochem.* **116**: 714-720.
25. Riboni, L., S. Sonnino, D. Acquotti, A. Malesci, R. Ghidoni, H. Egge, S. Mingrino, and G. Tettamanti. 1986. Natural occurrence of ganglioside lactones. Isolation and characterization of GD1b inner ester from adult human brain. *J. Biol. Chem.* **261**: 8514-8519.
26. Nores, G. A., T. Dohi, M. Taniguchi, and S. Hakomori. 1987. Density-dependent recognition of cell surface GM3 by a certain anti-melanoma antibody, and GM3 lactone as a possible immunogen: requirements for tumor-associated antigen and immunogen. *J. Immunol.* **139**: 3171-3176.
27. Ando, S., R. K. Yu, J. N. Scarsdale, S. Kusunoki, and J. H. Prestegard. 1989. High resolution proton NMR studies of gangliosides. Structure of two types of GD3 lactones and their reactivity with monoclonal antibody R24. *J. Biol. Chem.* **264**: 3478-3483.
28. Levy, M., and A. H. Futerman. 2010. Mammalian ceramide synthases. *IUBMB life* **62**: 347-356.
29. Brodesser, S., and T. Kolter. 2011. Dihydroceramide desaturase inhibition by a cyclopropanated dihydroceramide analog in cultured keratinocytes. *J. Lipids* **2011**: 724015.
30. Hannun, Y. A., and R. M. Bell. 1987. Lysosphingolipids inhibit protein kinase C: implications for the sphingolipidoses. *Science* **235**: 670-674.
31. Pohlentz, G., D. Klein, G. Schwarzmann, D. Schmitz, and K. Sandhoff. 1988. Both GA2, GM2, and GD2 synthases and GM1b, GD1a, and GT1b synthases are single enzymes in Golgi vesicles from rat liver. *Proc. Natl. Acad. Sci. U. S. A.* **85**: 7044-7048.
32. Takamiya, K., A. Yamamoto, K. Furukawa, S. Yamashiro, M. Shin, M. Okada, S. Fukumoto, M. Haraguchi, N. Takeda, K. Fujimura, M. Sakae, M. Kishikawa, H. Shiku, K. Furukawa, and S. Aizawa. 1996. Mice with disrupted GM2/GD2 synthase gene lack complex gangliosides but exhibit only subtle defects in their nervous system. *Proc. Natl. Acad. Sci. U. S. A.* **93**: 10662-10667.
33. Sheikh, K. A., J. Sun, Y. Liu, H. Kawai, T. O. Crawford, R. L. Proia, J. W. Griffin, and R. L. Schnaar. 1999. Mice lacking complex gangliosides develop

Wallerian degeneration and myelination defects. *Proc. Natl. Acad. Sci. U. S. A.* **96**: 7532-7537.
34. Chiavegatto, S., J. Sun, R. J. Nelson, and R. L. Schnaar. 2000. A functional role for complex gangliosides: motor deficits in GM2/GD2 synthase knockout mice. *Exp. Neurol.* **166**: 227-234.
35. Liu, Y., R. Wada, H. Kawai, K. Sango, C. Deng, T. Tai, M. P. McDonald, K. Araujo, J. N. Crawley, U. Bierfreund, K. Sandhoff, K. Suzuki, and R. L. Proia. 1999. A genetic model of substrate deprivation therapy for a glycosphingolipid storage disorder. *J. Clin. Invest.* **103**: 497-505.
36. Kawai, H., M. L. Allende, R. Wada, M. Kono, K. Sango, C. Deng, T. Miyakawa, J. N. Crawley, N. Werth, U. Bierfreund, K. Sandhoff, and R. L. Proia. 2001. Mice expressing only monosialoganglioside GM3 exhibit lethal audiogenic seizures. *J. Biol. Chem.* **276**: 6885-6888.
37. Yamashita, T., A. Hashiramoto, M. Haluzik, H. Mizukami, S. Beck, A. Norton, M. Kono, S. Tsuji, J. L. Daniotti, N. Werth, R. Sandhoff, K. Sandhoff, and R. L. Proia. 2003. Enhanced insulin sensitivity in mice lacking ganglioside GM3. *Proc. Natl. Acad. Sci. U. S. A.* **100**: 3445-3449.
38. Yoshikawa, M., S. Go, K. Takasaki, Y. Kakazu, M. Ohashi, M. Nagafuku, K. Kabayama, J. Sekimoto, S. Suzuki, K. Takaiwa, T. Kimitsuki, N. Matsumoto, S. Komune, D. Kamei, M. Saito, M. Fujiwara, K. Iwasaki, and J. Inokuchi. 2009. Mice lacking ganglioside GM3 synthase exhibit complete hearing loss due to selective degeneration of the organ of Corti. *Proc. Natl. Acad. Sci. U. S. A.* **106**: 9483-9488.
39. Yamashita, T., Y. P. Wu, R. Sandhoff, N. Werth, H. Mizukami, J. M. Ellis, J. L. Dupree, R. Geyer, K. Sandhoff, and R. L. Proia. 2005. Interruption of ganglioside synthesis produces central nervous system degeneration and altered axon-glial interactions. *Proc. Natl. Acad. Sci. U. S. A.* **102**: 2725-2730.
40. Simpson, M. A., H. Cross, C. Proukakis, D. A. Priestman, D. C. Neville, G. Reinkensmeier, H. Wang, M. Wiznitzer, K. Gurtz, A. Verganelaki, A. Pryde, M. A. Patton, R. A. Dwek, T. D. Butters, F. M. Platt, and A. H. Crosby. 2004. Infantile-onset symptomatic epilepsy syndrome caused by a homozygous loss-of-function mutation of GM3 synthase. *Nat. Genet.* **36**: 1225-1229.
41. Fragaki, K., S. Ait-El-Mkadem, A. Chaussenot, C. Gire, R. Mengual, L. Bonesso, M. Beneteau, J. E. Ricci, V. Desquiret-Dumas, V. Procaccio, A. Rotig, and V. Paquis-Flucklinger. 2013. Refractory epilepsy and mitochondrial dysfunction due to GM3 synthase deficiency. *Eur. J. Hum. Genet.* **21**: 528-534.
42. Boukhris, A., R. Schule, J. L. Loureiro, C. M. Lourenco, E. Mundwiller, M. A. Gonzalez, P. Charles, J. Gauthier, I. Rekik, R. F. Acosta Lebrigio, M. Gaussen, F. Speziani, A. Ferbert, I. Feki, A. Caballero-Oteyza, A. Dionne-Laporte, M. Amri, A. Noreau, S. Forlani, V. T. Cruz, F. Mochel, P. Coutinho, P. Dion, C. Mhiri, L. Schols, J. Pouget, F. Darios, G. A. Rouleau, W. Marques, Jr., A. Brice, A. Durr, S. Zuchner, and G. Stevanin. 2013. Alteration of ganglioside biosynthesis responsible for complex hereditary spastic paraplegia. *Am. J. Hum. Genet.* **93**: 118-123.
43. Penno, A., M. M. Reilly, H. Houlden, M. Laura, K. Rentsch, V. Niederkofler, E. T. Stoeckli, G. Nicholson, F. Eichler, R. H. Brown, Jr., A. von Eckardstein, and T. Hornemann. 2010. Hereditary sensory neuropathy type 1 is caused by the accumulation of two neurotoxic sphingolipids. *J. Biol. Chem.* **285**: 11178-11187.
44. Kolter, T. 2004. Glycosphingolipids. *In* Bioactive Lipids. A. Nicolaou and K. B., editors. The Oily Press, Bridgwater. 169-196.

45. Lopez, P. H., and R. L. Schnaar. 2009. Gangliosides in cell recognition and membrane protein regulation. *Curr. Opin. Struct. Biol.* **19**: 549-557.
46. Hakomori, S.-i. 2002. The glycosynapse. *Proc. Natl. Acad. Sci. U. S. A.* **99**: 225-232.
47. Simons, K., and M. J. Gerl. 2010. Revitalizing membrane rafts: new tools and insights. *Nat. Rev. Mol. Cell Biol.* **11**: 688-699.
48. Eggeling, C., C. Ringemann, R. Medda, G. Schwarzmann, K. Sandhoff, S. Polyakova, V. N. Belov, B. Hein, C. von Middendorff, A. Schonle, and S. W. Hell. 2009. Direct observation of the nanoscale dynamics of membrane lipids in a living cell. *Nature* **457**: 1159-1162.
49. Kabayama, K., T. Sato, K. Saito, N. Loberto, A. Prinetti, S. Sonnino, M. Kinjo, Y. Igarashi, and J. Inokuchi. 2007. Dissociation of the insulin receptor and caveolin-1 complex by ganglioside GM3 in the state of insulin resistance. *Proc. Natl. Acad. Sci. U. S. A.* **104**: 13678-13683.
50. Coskun, U., M. Grzybek, D. Drechsel, and K. Simons. 2011. Regulation of human EGF receptor by lipids. *Proc. Natl. Acad. Sci. U. S. A.* **108**: 9044-9048.
51. Mukherjee, P., A. C. Faber, L. M. Shelton, R. C. Baek, T. C. Chiles, and T. N. Seyfried. 2008. Thematic review series: sphingolipids. Ganglioside GM3 suppresses the proangiogenic effects of vascular endothelial growth factor and ganglioside GD1a. *J. Lipid Res.* **49**: 929-938.
52. Kolter, T., and K. Sandhoff. 2010. Lysosomal degradation of membrane lipids. *FEBS Lett.* **584**: 1700-1712.
53. Kobayashi, T., M. H. Beuchat, J. Chevallier, A. Makino, N. Mayran, J. M. Escola, C. Lebrand, P. Cosson, T. Kobayashi, and J. Gruenberg. 2002. Separation and characterization of late endosomal membrane domains. *J. Biol. Chem.* **277**: 32157-32164.
54. d'Azzo, A., and E. Bonten. 2010. Molecular mechanisms of pathogenesis in a glycosphingolipid and a glycoprotein storage disease. *Biochem. Soc. Trans.* **38**: 1453-1457.
55. Kolter, T., and K. Sandhoff. 1999. Sphingolipids—Their Metabolic Pathways and the Pathobiochemistry of Neurodegenerative Diseases. *Angew. Chem. Int. Ed.* **38**: 1532-1568.
56. Schulze, H., and K. Sandhoff. 2014. Sphingolipids and lysosomal pathologies. *Biochim. Biophys. Acta* **1841**: 799-810.
57. Walkley, S. U. 2004. Secondary accumulation of gangliosides in lysosomal storage disorders. *Semin. Cell Dev. Biol.* **15**: 433-444.
58. Dass, C. 2006. Quantitative Analysis. *In* Fundamentals of Contemporary Mass Spectrometry. John Wiley & Sons, Inc. 485-499.
59. Farwanah, H., and T. Kolter. 2012. Lipidomics of Glycosphingolipids. *Metabolites* **2**: 134-164.
60. Garrett, R. H., and C. M. Grisham. 2010. Biochemistry. 4. ed. Brooks/Cole, Australia [u.a.].
61. Domon, B., and R. Aebersold. 2006. Mass spectrometry and protein analysis. *Science* **312**: 212-217.
62. Cuadros-Rodriguez, L., M. G. Bagur-Gonzalez, M. Sanchez-Vinas, A. Gonzalez-Casado, and A. M. Gomez-Saez. 2007. Principles of analytical calibration/quantification for the separation sciences. *J. Chromatogr. A* **1158**: 33-46.
63. Fong, B., C. Norris, E. Lowe, and P. McJarrow. 2009. Liquid chromatography-high-resolution mass spectrometry for quantitative analysis of gangliosides. *Lipids* **44**: 867-874.

64. Fong, B., C. Norris, and P. McJarrow. 2011. Liquid chromatography–high-resolution electrostatic ion-trap mass spectrometric analysis of GD3 ganglioside in dairy products. *Int. Dairy J.* **21**: 42-47.
65. Lee, H., J. B. German, R. Kjelden, C. B. Lebrilla, and D. Barile. 2013. Quantitative analysis of gangliosides in bovine milk and colostrum-based dairy products by ultrahigh performance liquid chromatography-tandem mass spectrometry. *J. Agric. Food Chem.* **61**: 9689-9696.
66. Pirman, D. A., R. F. Reich, A. Kiss, R. M. Heeren, and R. A. Yost. 2013. Quantitative MALDI tandem mass spectrometric imaging of cocaine from brain tissue with a deuterated internal standard. *Anal. Chem.* **85**: 1081-1089.
67. Lozano, M. M., Z. Liu, E. Sunnick, A. Janshoff, K. Kumar, and S. G. Boxer. 2013. Colocalization of the ganglioside G(M1) and cholesterol detected by secondary ion mass spectrometry. *J. Am. Chem. Soc.* **135**: 5620-5630.
68. Rosenbaum, A. I., and F. R. Maxfield. 2011. Niemann-Pick type C disease: molecular mechanisms and potential therapeutic approaches. *J. Neurochem.* **116**: 789-795.
69. Gu, J., C. J. Tifft, and S. J. Soldin. 2008. Simultaneous quantification of GM1 and GM2 gangliosides by isotope dilution tandem mass spectrometry. *Clin. Biochem.* **41**: 413-417.
70. Ginkel, C., D. Hartmann, K. vom Dorp, A. Zlomuzica, H. Farwanah, M. Eckhardt, R. Sandhoff, J. Degen, M. Rabionet, E. Dere, P. Dormann, K. Sandhoff, and K. Willecke. 2012. Ablation of neuronal ceramide synthase 1 in mice decreases ganglioside levels and expression of myelin-associated glycoprotein in oligodendrocytes. *J. Biol. Chem.* **287**: 41888-41902.
71. Zhao, L., S. D. Spassieva, T. J. Jucius, L. D. Shultz, H. E. Shick, W. B. Macklin, Y. A. Hannun, L. M. Obeid, and S. L. Ackerman. 2011. A deficiency of ceramide biosynthesis causes cerebellar purkinje cell neurodegeneration and lipofuscin accumulation. *PLoS Genet.* **7**: e1002063.
72. Park, J. W., W. J. Park, and A. H. Futerman. 2013. Ceramide synthases as potential targets for therapeutic intervention in human diseases. *Biochim. Biophys. Acta*.
73. Hoveyda, A. H., and A. R. Zhugralin. 2007. The remarkable metal-catalysed olefin metathesis reaction. *Nature* **450**: 243-251.
74. Ashworth, I. W., I. H. Hillier, D. J. Nelson, J. M. Percy, and M. A. Vincent. 2011. What is the initiation step of the Grubbs-Hoveyda olefin metathesis catalyst? *Chem. Commun. (Camb.)* **47**: 5428-5430.
75. Urbina-Blanco, C. A., A. Poater, T. Lebl, S. Manzini, A. M. Slawin, L. Cavallo, and S. P. Nolan. 2013. The activation mechanism of Ru-indenylidene complexes in olefin metathesis. *J. Am. Chem. Soc.* **135**: 7073-7079.
76. Adlhart, C., and P. Chen. 2004. Mechanism and activity of ruthenium olefin metathesis catalysts: the role of ligands and substrates from a theoretical perspective. *J. Am. Chem. Soc.* **126**: 3496-3510.
77. Chatterjee, A. K., T. L. Choi, D. P. Sanders, and R. H. Grubbs. 2003. A general model for selectivity in olefin cross metathesis. *J. Am. Chem. Soc.* **125**: 11360-11370.
78. Furstner, A. 2013. Teaching metathesis "simple" stereochemistry. *Science* **341**: 1229713.
79. Hong, S. H., D. P. Sanders, C. W. Lee, and R. H. Grubbs. 2005. Prevention of undesirable isomerization during olefin metathesis. *J. Am. Chem. Soc.* **127**: 17160-17161.

80. Hong, S. H., M. W. Day, and R. H. Grubbs. 2004. Decomposition of a key intermediate in ruthenium-catalyzed olefin metathesis reactions. *J. Am. Chem. Soc.* **126**: 7414-7415.
81. Schmidt, R. R., J. C. Castro-Palomino, and O. Retz. 1999. New aspects of glycoside bond formation. *Pure Appl. Chem.* **71**: 729-744.
82. Castro-Palomino, J. C., B. Simon, O. Speer, M. Leist, and R. R. Schmidt. 2001. Synthesis of ganglioside GD3 and its comparison with bovine GD3 with regard to oligodendrocyte apoptosis mitochondrial damage. *Chemistry* **7**: 2178-2184.
83. Greilich, U., R. Brescello, K.-H. Jung, and R. R. Schmidt. 1996. Glycosyl Imidates, 74. Synthesis of Ganglioside GM1 via a GM3 Intermediate. *Liebigs Ann.* **1996**: 663-672.
84. Stauch, T., U. Greilich, and R. R. Schmidt. 1995. Glycosyl imidates, 73. Synthesis of ganglioside gm1 via a GA1 intermediate. *Liebigs Ann.* **1995**: 2101-2111.
85. Imamura, A., H. Ando, H. Ishida, and M. Kiso. 2009. Ganglioside GQ1b: efficient total synthesis and the expansion to synthetic derivatives to elucidate its biological roles. *J. Org. Chem.* **74**: 3009-3023.
86. Ishida, H., Y. Ohta, Y. Tsukada, M. Kiso, and A. Hasegawa. 1993. A synthetic approach to polysialogangliosides containing alpha-sialyl-(2-->8)-sialic acid: total synthesis of ganglioside GD3. *Carbohydr. Res.* **246**: 75-88.
87. Roy, R., and R. Pon. 1990. Efficient synthesis of α(2–8)-linkedN-acetyl andN-glycolylneuraminic acid disaccharides from colominic acid. *Glycoconjugate J.* **7**: 3-12.
88. McGuire, E. J., and S. B. Binkley. 1964. The Structure and Chemistry of Colominic Acid. *Biochemistry* **3**: 247-251.
89. Komba, S., H. Ishida, M. Kiso, and A. Hasegawa. 1996. Synthesis of deoxygalactose-containing sialyl LeX ganglioside analogues to elucidate the structure necessary for selectin recognition. *Glycoconjugate J.* **13**: 241-254.
90. Lipshutz, B. H., J. J. Pegram, and M. C. Morey. 1981. Chemistry of β-trimethylsilylethanol. II. A new method for protection of an anomeric center in pyranosides. *Tetrahedron Lett.* **22**: 4603-4606.
91. Murase, T., A. Kameyama, K. P. R. Kartha, H. Ishida, M. Kiso, and A. Hasegawa. 1989. Synthetic Studies on Sialoglycoconjugates. 5: A Facile, Regio and Stereoselective Synthesis of Ganglioside GM4 and Its Position Isomer1. *J. Carbohydr. Chem.* **8**: 265-283.
92. Dullenkopf, W., J. C. Castro-Palomino, L. Manzoni, and R. R. Schmidt. 1996. N-trichloroethoxycarbonyl-glucosamine derivatives as glycosyl donors. *Carbohydr. Res.* **296**: 135-147.
93. Yan, F., S. Mehta, E. Eichler, W. W. Wakarchuk, M. Gilbert, M. J. Schur, and D. M. Whitfield. 2003. Simplifying oligosaccharide synthesis: efficient synthesis of lactosamine and siaylated lactosamine oligosaccharide donors. *J. Org. Chem.* **68**: 2426-2431.
94. Aspinall, G. O., D. W. Gammon, R. K. Sood, D. Chatterjee, B. Rivoire, and P. J. Brennan. 1992. Structures of the glycopeptidolipid antigens of serovars 25 and 26 of the Mycobacterium avium serocomplex, synthesis of allyl glycosides of the outer disaccharide units and serology of the derived neoglycoproteins. *Carbohydr. Res.* **237**: 57-77.
95. Lee, R. T., and Y. C. Lee. 1974. Synthesis of 3-(2-aminoethylthio)propyl glycosides. *Carbohydr. Res.* **37**: 193-201.

96. Kiso, M., and A. Hasegawa. 1976. Acetonation of some pentoses with 2,2-dimethoxypropane-N,N-dimethylformamide-p-toluenesulfonic acid. *Carbohydr. Res.* **52**: 95-101.
97. Kiso, M., A. Nakamura, Y. Tomita, and A. Hasegawa. 1986. A novel route to d-erythro-sphingosine and related compounds from mono-O-isopropylidene-d-xylose or -d- galactose. *Carbohydr. Res.* **158**: 101-111.
98. Zimmermann, P., R. Sommer, T. Bär, and R. R. Schmidt. 1988. Azidosphingosine Glycosylation in Glycosphingolipid Synthesis. *J. Carbohydr. Chem.* **7**: 435-452.
99. Clasen, K. 1994. Dissertation: Synthese von Sphingosin und Sphingosinderivaten. Rheinische Friedrich-Wilhelms-Universität, Bonn.
100. Schwarzmann, G., P. Hofmann, and U. Putz. 1997. Synthesis of ganglioside GM1 containing a thioglycosidic bond to its labeled ceramide(s). A facile synthesis starting from natural gangliosides. *Carbohydr. Res.* **304**: 43-52.
101. Schwarzmann, G., C. Arenz, and K. Sandhoff. 2013. Labeled chemical biology tools for investigating sphingolipid metabolism, trafficking and interaction with lipids and proteins. *Biochim. Biophys. Acta*.
102. Wiegandt, H., and G. Baschang. 1965. [the Isolation of the Sugar Portion of Glycosphingolipids by Ozonolysis and Fragmentation]. *Z. Naturforsch. B.* **20**: 164-166.
103. Rasmussen, J. A., and A. Hermetter. 2008. Chemical synthesis of fluorescent glycero- and sphingolipids. *Prog. Lipid Res.* **47**: 436-460.
104. Schwarzmann, G., and K. Sandhoff. 1987. Lysogangliosides: synthesis and use in preparing labeled gangliosides. *Methods Enzymol.* **138**: 319-341.
105. Sonnino, S., D. Acquotti, G. Kirschner, A. Uguaglianza, L. Zecca, F. Rubino, and G. Tettamanti. 1992. Preparation of lyso-GM1 (II3Neu5AcGgOse4-long chain bases) by a one-pot reaction. *J. Lipid Res.* **33**: 1221-1226.
106. Neuenhofer, S., G. Schwarzmann, H. Egge, and K. Sandhoff. 1985. Synthesis of lysogangliosides. *Biochemistry* **24**: 525-532.
107. Kurita, T., H. Izu, M. Sano, M. Ito, and I. Kato. 2000. Enhancement of hydrolytic activity of sphingolipid ceramide N-deacylase in the aqueous-organic biphasic system. *J. Lipid Res.* **41**: 846-851.
108. Ito, M., K. Kita, T. Kurita, N. Sueyoshi, and H. Izu. 2000. Enzymatic N-deacylation of sphingolipids. *Methods Enzymol.* **311**: 297-303.
109. Zamfir, A., Z. Vukelic, and J. Peter-Katalinic. 2002. A capillary electrophoresis and off-line capillary electrophoresis/electrospray ionization-quadrupole time of flight-tandem mass spectrometry approach for ganglioside analysis. *Electrophoresis* **23**: 2894-2903.
110. Momoi, T., S. Ando, and Y. Magai. 1976. High resolution preparative column chromatographic system for gangliosides using DEAE-Sephadex and a new porus silica, Iatrobeads. *Biochim. Biophys. Acta* **441**: 488-497.
111. Distler, J. J., and G. W. Jourdian. 1973. The purification and properties of beta-galactosidase from bovine testes. *J. Biol. Chem.* **248**: 6772-6780.
112. Larsson, E. A., U. Olsson, C. D. Whitmore, R. Martins, G. Tettamanti, R. L. Schnaar, N. J. Dovichi, M. M. Palcic, and O. Hindsgaul. 2007. Synthesis of reference standards to enable single cell metabolomic studies of tetramethylrhodamine-labeled ganglioside GM1. *Carbohydr. Res.* **342**: 482-489.
113. Wiegandt, H. 1968. The structure and the function of gangliosides. *Angew. Chem. Int. Ed. Engl.* **7**: 87-96.

114. Nagahori, N., M. Abe, and S. Nishimura. 2009. Structural and functional glycosphingolipidomics by glycoblotting with an aminooxy-functionalized gold nanoparticle. *Biochemistry* **48**: 583-594.
115. Wiegandt, H., and H. W. Bucking. 1970. Carbohydrate components of extraneuronal gangliosides from bovine and human spleen, and bovine kidney. *Eur. J. Biochem.* **15**: 287-292.
116. Hakomori, S. I. 1966. Release of carbohydrates from sphingoglycolipid by osmium-catalyzed periodate oxidation followed by treatment with mild alkali. *J. Lipid Res.* **7**: 789-792.
117. Anderson, D. R., T. Ung, G. Mkrtumyan, G. Bertrand, R. H. Grubbs, and Y. Schrodi. 2008. Kinetic Selectivity of Olefin Metathesis Catalysts Bearing Cyclic (Alkyl)(Amino)Carbenes. *Organometallics* **27**: 563-566.
118. Nickel, A., T. Ung, G. Mkrtumyan, J. Uy, C. Lee, D. Stoianova, J. Papazian, W.-H. Wei, A. Mallari, Y. Schrodi, and R. Pederson. 2012. A Highly Efficient Olefin Metathesis Process for the Synthesis of Terminal Alkenes from Fatty Acid Esters. *Top. Catal.* **55**: 518-523.
119. Marinescu, S. C., D. S. Levine, Y. Zhao, R. R. Schrock, and A. H. Hoveyda. 2011. Isolation of pure disubstituted E olefins through Mo-catalyzed Z-selective ethenolysis of stereoisomeric mixtures. *J. Am. Chem. Soc.* **133**: 11512-11514.
120. Miyazaki, H., M. B. Herbert, P. Liu, X. Dong, X. Xu, B. K. Keitz, T. Ung, G. Mkrtumyan, K. N. Houk, and R. H. Grubbs. 2013. Z-Selective ethenolysis with a ruthenium metathesis catalyst: experiment and theory. *J. Am. Chem. Soc.* **135**: 5848-5858.
121. Patel, J., S. Mujcinovic, W. R. Jackson, A. J. Robinson, A. K. Serelis, and C. Such. 2006. High conversion and productive catalyst turnovers in cross-metathesis reactions of natural oils with 2-butene. *Green Chem.* **8**: 450-454.
122. van den Eijnden, D. H. 1971. Chromatographic separation of gangliosides on precoated silicagel thin-layer plates. *Hoppe Seylers Z. Physiol. Chem.* **352**: 1601-1602.
123. Ando, S., H. Waki, and K. Kon. 1987. New solvent system for high-performance thin-layer chromatography and high-performance liquid chromatography of gangliosides. *J. Chromatogr.* **405**: 125-134.
124. Acquotti, D., L. Poppe, J. Dabrowski, C. W. Von der Lieth, S. Sonnino, and G. Tettamanti. 1990. Three-dimensional structure of the oligosaccharide chain of GM1 ganglioside revealed by a distance-mapping procedure: a rotating and laboratory frame nuclear overhauser enhancement investigation of native glycolipid in dimethyl sulfoxide and in water-dodecylphosphocholine solutions. *J. Am. Chem. Soc.* **112**: 7772-7778.
125. Scarsdale, J. N., J. H. Prestegard, and R. K. Yu. 1990. NMR and computational studies of interactions between remote residues in gangliosides. *Biochemistry* **29**: 9843-9855.
126. Clayden, J., N. Greeves, and S. Warren. 2012. Organic Chemistry. *In*. OUP Oxford, Oxford.
127. Valiente, O., L. Mauri, R. Casellato, L. E. Fernandez, and S. Sonnino. 2001. Preparation of deacetyl-, lyso-, and deacetyl-lyso-GM(3) by selective alkaline hydrolysis of GM3 ganglioside. *J. Lipid Res.* **42**: 1318-1324.
128. Kita, K., T. Kurita, and M. Ito. 2001. Characterization of the reversible nature of the reaction catalyzed by sphingolipid ceramide N-deacylase. A novel form of reverse hydrolysis reaction. *Eur. J. Biochem.* **268**: 592-602.

129. Moss, G. P. April 29, 2014. Recommendations of the Nomenclature Committee of the International Union of Biochemistry and Molecular Biology on the Nomenclature and Classification of Enzymes by the Reactions they Catalyse. *In*. http://www.chem.qmul.ac.uk/iubmb/enzyme/.
130. Lapidot, Y., S. Rappoport, and Y. Wolman. 1967. Use of esters of N-hydroxysuccinimide in the synthesis of N-acylamino acids. *J. Lipid Res.* **8**: 142-145.
131. Brückner, R. 2004. Reaktionsmechanismen : organische Reaktionen, Stereochemie, moderne Synthesemethoden. 3. Aufl., aktualisiert und überarb. ed. Elsevier, München.
132. van Rantwijk, F., M. Woudenberg-van Oosterom, and R. A. Sheldon. 1999. Glycosidase-catalysed synthesis of alkyl glycosides. *J. Mol. Catal. B: Enzym.* **6**: 511-532.
133. Zechel, D. L., and S. G. Withers. 2000. Glycosidase mechanisms: anatomy of a finely tuned catalyst. *Acc. Chem. Res.* **33**: 11-18.
134. Stewart, I. C., C. J. Douglas, and R. H. Grubbs. 2008. Increased efficiency in cross-metathesis reactions of sterically hindered olefins. *Org. Lett.* **10**: 441-444.
135. Sugahara, K., K. Sugimoto, O. Nomura, and T. Usui. 1980. Enzymatic assay of serum sialic acid. *Clin. Chim. Acta* **108**: 493-498.
136. Miettinen, T., and I. T. Takkiluukkainen. 1959. Use of Butyl Acetate in Determination of Sialic Acid. *Acta Chem. Scand.* **13**: 856-858.
137. Svennerholm, L. 1957. Quantitative estimation of sialic acids. II. A colorimetric resorcinol-hydrochloric acid method. *Biochim. Biophys. Acta* **24**: 604-611.
138. Kobayashi, T., and I. Goto. 1991. A sensitive assay of lysogangliosides using high-performance liquid chromatography. *Biochim. Biophys. Acta, Lipids Lipid Metab.* **1081**: 159-166.
139. Chigorno, V., S. Sonnino, R. Ghidoni, and G. Tettamanti. 1982. Densitometric quantification of brain gangliosides separated by two-dimensional thin layer chromatography. *Neurochem. Int.* **4**: 397-404.
140. Ando, T., S. C. Li, M. Ito, and Y. T. Li. 2005. Facile method for the preparation of lyso-GM1 and lyso-GM2. *J. Chromatogr. A* **1078**: 193-195.
141. Ito, E., A. Tominaga, H. Waki, K. Miseki, A. Tomioka, K. Nakajima, K. Kakehi, M. Suzuki, N. Taniguchi, and A. Suzuki. 2012. Structural characterization of monosialo-, disialo- and trisialo-gangliosides by negative ion AP-MALDI-QIT-TOF mass spectrometry with MS(n) switching. *Neurochem. Res.* **37**: 1315-1324.
142. Georgiades, S. N., and J. Clardy. 2008. Synthetic libraries of tyrosine-derived bacterial metabolites. *Bioorg. Med. Chem. Lett.* **18**: 3117-3121.
143. Schlosser, M., and K. F. Christmann. 1966. Trans-Selective Olefin Syntheses. *Angew. Chem. Int. Ed. Engl.* **5**: 126-126.
144. Ikeda, K., and R. Taguchi. 2010. Highly sensitive localization analysis of gangliosides and sulfatides including structural isomers in mouse cerebellum sections by combination of laser microdissection and hydrophilic interaction liquid chromatography/electrospray ionization mass spectrometry with theoretically expanded multiple reaction monitoring. *Rapid Commun. Mass Spectrom.* **24**: 2957-2965.
145. Nussbaumer, P., P. Ettmayer, C. Peters, D. Rosenbeiger, and K. Hogenauer. 2005. One-step labelling of sphingolipids via a scrambling cross-metathesis reaction. *Chem. Commun. (Camb.)*: 5086-5087.

146. Peters, C., A. Billich, M. Ghobrial, K. Hogenauer, T. Ullrich, and P. Nussbaumer. 2007. Synthesis of borondipyrromethene (BODIPY)-labeled sphingosine derivatives by cross-metathesis reaction. *J. Org. Chem.* **72**: 1842-1845.
147. Coleman, R. S., and A. J. Carpenter. 1992. Diastereoselective addition of vinyl organometallic reagents to l-serinal. *Tetrahedron Lett.* **33**: 1697-1700.
148. Antes, P., G. Schwarzmann, and K. Sandhoff. 1992. Distribution and metabolism of fluorescent sphingosines and corresponding ceramides bearing the diphenylhexatrienyl (DPH) fluorophore in cultured human fibroblasts. *Eur. J. Cell Biol.* **59**: 27-36.
149. Bhabak, K. P., D. Proksch, S. Redmer, and C. Arenz. 2012. Novel fluorescent ceramide derivatives for probing ceramidase substrate specificity. *Bioorg. Med. Chem.* **20**: 6154-6161.
150. Bhabak, K. P., A. Hauser, S. Redmer, S. Banhart, D. Heuer, and C. Arenz. 2013. Development of a novel FRET probe for the real-time determination of ceramidase activity. *Chembiochem* **14**: 1049-1052.
151. Williams, M. A., and R. H. McCluer. 1980. The use of Sep-Pak C18 cartridges during the isolation of gangliosides. *J. Neurochem.* **35**: 266-269.
152. Touchstone, J. C., S. S. Levin, M. F. Dobbins, and P. J. Carter. 1981. Differentiation of saturated and unsaturated phospholipids on thin layer chromatograms. *J. High Res. Chromatog.* **4**: 423-424.
153. Stahl, E., and U. Kaltenbach. 1961. Dünnschicht-chromatographie: VI. Mitteilung. spurenanalyse von zuckergemischen auf kieselgur G-schichten. *J. Chromatogr. A* **5**: 351-355.
154. Domon, B., and C. Costello. 1988. A systematic nomenclature for carbohydrate fragmentations in FAB-MS/MS spectra of glycoconjugates. *Glycoconjugate J.* **5**: 397-409.

Eigenständigkeitserklärung

Hiermit erkläre ich, dass ich die vorliegende Arbeit ohne fremde Hilfe angefertigt und keine anderen als die in der Dissertation angegebenen Hilfsmittel und Quellen benutzt habe. Wörtlich oder sinngemäß aus Veröffentlichungen entnommene Stellen habe ich als solche kenntlich gemacht. Weiterhin habe ich die Dissertation an keiner anderen Universität eingereicht.

_____